CALCITE REACTION KINETICS IN SALINE WATERS

A Dissertation

by

DAVID WALLACE FINNERAN

Submitted to the Office of Graduate Studies of
Texas A&M University
in partial fulfillment of the requirements for the degree of

DOCTOR OF PHILOSOPHY

December 2010

Major Subject: Oceanography

CALCITE REACTION KINETICS IN SALINE WATERS

A Dissertation

by

DAVID WALLACE FINNERAN

Submitted to the Office of Graduate Studies of
Texas A&M University
in partial fulfillment of the requirements for the degree of

DOCTOR OF PHILOSOPHY

Approved by:

Co-Chairs of Committee,	John W. Morse
	Shari A. Yvon-Lewis
Committee Members,	Piers Chapman
	George A. Jackson
	Emile A. Schweikert
Head of Department,	Piers Chapman

December 2010

Major Subject: Oceanography

ABSTRACT

Calcite Reaction Kinetics in Saline Waters. (December 2010)

David Wallace Finneran, B.Sci., University of Delaware;

M.Sci., University of Delaware

Co-Chairs of Advisory Committee: Dr. John W. Morse
Dr. Shari A. Yvon-Lewis

The effect of ionic strength (I), pCO_2, and temperature on the reaction kinetics of calcite was investigated in magnesium-free, phosphate-free, low calcium ($m_{Ca^{2+}} \approx 0.01 – 0.02$ molal) simple KCl and NaCl solutions from both undersaturated and oversaturated conditions. First order kinetics were found sufficient to describe the dissolution rate data. Dissolution rates decreased with increasing I and were faster in KCl than NaCl solutions at the same I indicating that Na^+ interacts more strongly with the calcite surface than K^+ or that water is less available in NaCl solutions. Rates increased with increasing pCO_2 and temperature, and their influence diminished at high I. Arrhenius plots yielded a relatively high activation energy ($E_a \approx 20 \pm 2$ kJ mol-1) which indicated that dissolution was dominated by surface controlled processes. These results are consistent with the hypothesis that the mole fraction of "free" solvent plays a significant role in the dissolution kinetics of calcite with a minimum value of ~45-50% required for dissolution to proceed in undersaturated solutions at 25-55 °C and $pCO_2 = 0.1 – 1$ atm.

Precipitation rates were modeled using the general and Davies and Jones rate equations yielding similar results. Reaction orders were found to typically range between 0.8 and 2.5 for both rate equations regardless of electrolyte. For both solutions, rate constants were found to range between $10^{0.8}$ and $10^{1.7}$ mmole m^{-2} hr^{-1} (general rate equation) and $10^{1.5}$ and $10^{2.2}$ mmole m^{-2} hr^{-1} (Davies and Jones rate equation). Under the experimental conditions employed and the resultant precision (~20-25%), I and pCO_2 do not have a significant influence on the precipitation rate of calcite. Precipitation rates increased with temperature although Arrhenius plots yield a broad range of activation energies (E_a ≈ 15 – 28 kJ mol-1, $R^2 = 0.72$). The relatively low calculated activation energies coupled with the precision of the results suggest the possibility of surface nucleation in the present results.

Overall, these findings may be useful in understanding and predicting the interaction and reactivity of the host carbonate minerals in subsurface reservoirs to the injection of CO_2 although much work needs to be completed at elevated temperatures and pressures.

DEDICATION

This dissertation is dedicated to my loving wife and our wonderful children. Throughout my graduate studies, she has offered me unconditional patience and support. She never complained about the long evenings or early mornings that I had to devote to research. Instead, she has given me words of encouragement continually throughout the evolution of this dissertation. More importantly, she is the foundation of our family and words cannot express the love and admiration I have for her. Through their joy in exploring the most mundane things, my children have reminded me of what is truly important. May they never lose their sense of wonder of the world.

ACKNOWLEDGEMENTS

I would like to extend my sincere appreciation and gratitude to Dr. John W. Morse for providing me the opportunity to join his research group. Under his tutelage, I have gained an extensive amount of knowledge of both metal sulfides and metal carbonates in the marine and sedimentary environments. Dr. Morse has been a terrific mentor and his generosity, patience and frank discussion are much appreciated and will never be forgotten. I would also like to offer my gratitude to my committee members, Dr. George A. Jackson, Dr. Emile A. Schweikert, and Dr. Shari A. Yvon-Lewis, for their thoughtful suggestions and support throughout the course of this research. Furthermore, I would like to offer my sincerest thanks to Dr. Yvon-Lewis for becoming my co-chair after the untimely passing of Dr. Morse. I would like to acknowledge Dr. John H. Wormuth, with whom I have had many discussions on a myriad of topics which has ultimately assisted me in choosing my current career path.

I would like to acknowledge the past and present members of the Morse Research Group that have helped me through the research process both with laboratory assistance and/or frank discussion and analyses, particularly: Dr. Rolf S. Arvidson, Dr. Andrew Hebert, Dr. Dwight K. Gledhill, Ms. Janie Lee, Ms. Brandi Reese, Ms. Luz Romero, and Ms. Katherine Walton. I would also like to thank all of OGC, especially Dr. Daniel Marshalonis, Mr. Sharath Ravula and Mrs. Christine Wiederwohl. Finally, I would like to thank my family for their encouragement and unconditional love.

This research was supported by the U.S. Department of Energy (DOE) Basic Research Program Grant No. DE-FR02-06ER15816 and by the Louis and Elizabeth Scherck Endowed Chair in Oceanography.

TABLE OF CONTENTS

Page

ABSTRACT iii

DEDICATION v

ACKNOWLEDGEMENTS vi

TABLE OF CONTENTS viii

LIST OF FIGURES x

LIST OF TABLES xvii

1. INTRODUCTION 1

    1.1 Importance of Calcite-Water Reactions 1
    1.2 Carbonic Acid System Overview 4
    1.3 Calcite Solubility and Reaction Kinetics 7
    1.4 Dissolution 10
    1.5 Precipitation 14
    1.6 Experimental Objective 17

2. CALCITE DISSOLUTION KINETICS IN SALINE WATERS 18

    2.1 Introduction 19
    2.2 Materials and Methods 21
    2.3 Calculations 26
    2.4 Results 28
    2.5 Discussion 32
        2.5.1 I 32
        2.5.2 pCO_2 43
        2.5.3 Temperature 49
        2.5.4 Mole Fraction of “Free” Water 52
        2.5.5 Multiple Regression Model $X_{\text{“free”}H_2O}$ 57
    2.6 Conclusions 61

Page

3. HYDRATION NUMBERS OF NaCl, KCl, $CaCl_2$ and $MgCl_2$ DETERMINED FROM THE ANALYSIS OF COLLIGATIVE PROPERTY DATA 63

3.1 Introduction 63
3.2 Colligative Properties 66
3.3 Analysis of Colligative Property Data 69
3.4 Results 72
3.5 Discussion 81
3.5.1 NaCl 81
3.5.2 KCl 84
3.5.3 $MgCl_2$ 86
3.5.4 $CaCl_2$ 88
3.6 Temperature Effect 91
3.7 Effect of Concentration 96
3.8 Predictive Capability of Calculated Hydration Numbers 141
3.9 Future Direction 146
3.10 Conclusions 149

4. CALCITE PRECIPITATION KINETICS IN SALINE WATERS 151

4.1 Introduction 152
4.2 Materials and Methods 154
4.3 Calculations 159
4.4 Results 161
4.5 Discussion 168
4.6 Conclusions 174

5. CONCLUSIONS 176

REFERENCES 181

VITA 208

LIST OF FIGURES

FIGURE		Page
2.1	Schematic diagram of the experimental pH free drift reactor system used in this study.	21
2.2	k (mmole m^{-2} hr^{-1}) as a function of I (molal scale) for KCl (●) and NaCl (□).	30
2.3	k (mmole m^{-2} hr^{-1}) as a function of pCO_2 for KCl 2.0 (●), NaCl 2.0 (□) and NaCl 5.0 (◊) solutions	31
2.4	k (mmole m^{-2} hr^{-1}) as a function of I (molal scale) for KCl (●), NaCl (□) and predicted values from the MR model of Gledhill and Morse (2006a) where the solid line is used over I investigated in their work and dashed line indicates extrapolation	35
2.5	k (mmole m^{-2} hr^{-1}) as a function of a_{H_2O}, calculated from EQPITZER (He and Morse, 1993) for KCl (●) and NaCl (□).	37
2.6	Experimental and predicted k values (mmole m^{-2} hr^{-1}) as a function of a_{H_2O} for KCl (●) and NaCl (□) solutions with predicted values (solid line) where $k_{predicted} = k_0\, a_{H_2O}$.	38
2.7	k (mmole m^{-2} hr^{-1}) as a function of $X_{"free"\ H_2O}$ in KCl (●) and NaCl (□) solutions.	42
2.8	k (mmole m^{-2} hr^{-1}) as a function of pCO_2 for KCl 2.0 (●), NaCl 2.0 (□), NaCl 5.0 (◊) solutions and the solid line indicates predicted values from the MR model of Gledhill and Morse (2006a)	45
2.9	k (mmole m^{-2} hr^{-1}) as a function of $X_{"free"\ H_2O}$ for the four pCO_2 values investigated at 25 °C: 1 (●), 0.6 (□), 0.3 (◊) and 0.1 (*) atm pCO_2.	47
2.10	k (mmole m^{-2} hr^{-1}) as a function of $X_{"free"\ H_2O}$ for data at 25 °C from Gledhill and Morse (2006a) with pCO_2 values: 1 (●), 0.5 (□), 1 (with $SO_4^{2-} \approx 0.01$m) (◊) and 0.1 (*) atm pCO_2.	49

FIGURE Page

2.11 k (mmole m^{-2} hr^{-1}) at pCO_2 = 1 atm as a function of $X_{"free" H_2O}$ for three temperature values investigated, 25 (●), 40 (□), and 55 (◊) °C. 52

2.12 Predicted $X_{"free" H_2O}$ as a function of TDS (g L^{-1}) assuming salt concentrations (mol L^{-1}) predicted by Morse et al. (1997) are equivalent to molality $X_{"free" H_2O}$ (which is an underestimate of the true molality) 57

2.13 The predictive capability of the MR model (equation 2.12) with an adjusted R^2 = 0.862. 59

3.1A Freezing point depression data of Hall et al. (1998) plotted according to equation 3.10 where X_{sp} is determined from conventional stoichiometry (●) and determined from equation 3.2 with h = 4.0 (□). 80

3.1B Boiling point elevation data of Zaytsev and Aseyev (1992) plotted according to equation 3.10 where X_{sp} is determined from conventional stoichiometry (●) and determined from equation 3.2 with h = 2.0 (□). 81

3.2A h_{NaCl} as a function of temperature for Bousfield and Bousfield (♦), Frazer (□), Pearce and Nelson (◊), Gibson and Adams (○), Olynk and Gordon (x), Washburn (Δ,▲), Forsythe (+), Zaytsev and Aseyev (-). 92

3.2B h_{KCl} as a function of temperature for Lovelace et al. (◊), Lovelace et al. (♦), Pearce and Snow (■), Brown and Delaney (x), Apelblat (○), Washburn (Δ), Zaytsev and Aseyev (-). 93

3.2C h_{MgCl_2} as a function of temperature for Lovelace et al. (◊), Lovelace et al. (♦), Sako et al. (□) Washburn (Δ), Zaytsev and Aseyev (-). 94

3.2D h_{CaCl_2} as a function of temperature for Lovelace et al. (◊), Lovelace et al. (♦), Sako et al. (□) Washburn (Δ),Forsythe (+), Zaytsev and Aseyev (-). 95

3.3 Plot of $CaCl_2$ freezing point depression data of Haghighi et al. (2008) as the maximum ion concentration investigated is reduced 97

FIGURE Page

3.4A h_{NaCl} as a function of the ion concentration from freezing point depression data of Rodebush (●), Momicchioli et al. (x), Gibbard and Gossman (□), Potter et al. (■), Hall et al. (○), Oakes et al. (▲), Haghighi et al. (♦), Lide (*), Washburn (-)..... 99

3.4B h_{KCl} as a function of the ion concentration from freezing point depression data of for Rodebush (●), Roloff (□),Spencer (♦), Chiorboli et al. (▲), Momicchioli et al. (x), Hall et al. (○), Lide (*), Washburn (-), Forsythe (+)..... 100

3.4C h_{MgCl_2} as a function of the ion concentration from freezing point depression data of for Jones and Bassett (▲), Rodebush (●), Gibbard and Fong (♦), Gibbard and Gossman (□), Haghighi et al. (♦), Washburn (-). 101

3.4D h_{CaCl_2} as a function of the ion concentration from freezing point depression data of for Jones and Bassett (▲), Rodebush (●), Oakes et al. (▲), Haghighi et al. (♦), Lide (*), Washburn (-)..... 102

3.5A h_{NaCl} a as a function of the ion concentration from boiling point elevation data of Hass (●), Washburn (Δ,▲), Forsythe (+), Zaytsev and Aseyev (-). 103

3.5B h_{KCl} as a function the ion concentration from boiling point elevation data of Saxton and Smith (●), Washburn (Δ), Forsythe (+), Zaytsev and Aseyev (-). 104

3.5C h_{MgCl_2} as a function of the ion concentration from boiling point elevation data of Washburn (Δ), Forsythe (+), Zaytsev and Aseyev (-) 105

3.5D h_{CaCl_2} as a function of the ion concentration from boiling point elevation data of Washburn (Δ), Forsythe (+), Zaytsev and Aseyev (-) ... 106

3.6A h_{NaCl} a as a function of the ion concentration from vapor pressure depression data of Bousfield and Bousfield (♦), Frazer (20°C = □, 25°C = ■), Pearce and Nelson (◊), Gibson and Adams (○), Olynk and Gordon (20°C = x, 25°C = ■, 30°C = *), Washburn (Δ,▲), Forsythe (+). 107

FIGURE Page

3.6B h_{NaCl} a as a function of the ion concentration from vapor pressure depression data of Zaytsev and Aseyev at 5°C (□), 15°C (■), 25°C (◊), 35°C (♦), 45°C (Δ), 55°C (▲), 65°C (x), 75°C (x), 85°C (*), 95°C (*), 105°C (-), 115°C (-), 125°C (-), 135°C (-), 145°C (○), 155°C (●), 165°C (+), 175°C (+)..... 108

3.6C h_{KCl} a as a function of the ion concentration from vapor pressure depression data of Lovelace et al. (◊), Lovelace et al. (X), Brown and Delaney (*), Pearce and Snow (■), Apelblat (+), Washburn (♦)..... 109

3.6D h_{KCl} a as a function of the ion concentration from vapor pressure depression data of Zaytsev and Aseyev at 0°C (□), 10°C (■), 20°C (◊), 30°C (♦), 40°C (Δ), 50°C (▲), 60°C (x), 70°C (x), 80°C (*), 90°C (*), 100°C (-), 150°C (-), 200°C (-), 250°C (-), 300°C (○), 350°C (●)..... 110

3.6E h_{MgCl_2} a as a function of the ion concentration from vapor pressure depression data of Sako et al. at 60°C (□), 70°C (■), 80°C (◊), 90°C (♦), 100°C (Δ), 100°C (▲), 120°C (x) and Washburn for 0°C (x) and 100°C (*). 111

3.6F h_{MgCl_2} a as a function of the ion concentration from vapor pressure depression data of Zaytsev and Aseyev at 0°C (□), 10°C (■), 20°C (◊), 30°C (♦), 40°C (Δ), 50°C (▲), 60°C (x), 70°C (x), 80°C (*), 90°C (*), 100°C (-), 125°C (-), 150°C (-), 175°C (-), 200°C (○), 225°C (●), 250°C (+), 275°C (+)..... 112

3.6G h_{CaCl_2} as a function of the ion concentration from vapor pressure depression data of Sako et al. at 60°C (□), 70°C (■), 80°C (◊), 90°C (♦), 100°C (Δ), 110°C (▲), 120°C (x); data of Washburn at 0°C (x), 40°C (*), 70°C (*), 90°C (-), 100°C (-), 110°C (-), 120°C (-), 130°C (○), 140°C (●); data of Forsythe at 100°C (+)..... 113

3.6H h_{CaCl_2} a as a function of the ion concentration from vapor pressure depression data of Zaytsev and Aseyev at 0°C (□), 0°C (■), 10°C (◊), 20°C (♦), 30°C (Δ), 40°C (▲), 50°C (x), 60°C (x), 70°C (*), 80°C (*), 90°C (-), 100°C (-), 150°C (-), 200°C (-), 250°C (○), 300°C (●), 350°C (+)..... 114

FIGURE Page

3.7A $\Delta H_{fus(NaCl)}$ (kJ mol^{-1}) as a function of the ion concentration for the freezing point depression data of Rodebush (●), Momicchioli et al. (x), Gibbard and Gossman (□), Potter et al. (■), Hall et al. (○), Oakes et al. (▲), Haghighi et al. (♦), Lide (*), Washburn (-). 118

3.7B $\Delta H_{fus(KCl)}$ (kJ mol^{-1}) as a function of the ion concentration for the freezing point depression data of Rodebush (●), Roloff (□),Spencer (♦), Chiorboli et al. (▲), Momicchioli et al. (x), Hall et al. (○), Lide (*), Washburn (-), Forsythe (+)..... 119

3.7C $\Delta H_{fus(MgCl_2)}$ (kJ mol^{-1}) as a function of the ion concentration for the freezing point depression data of Jones and Bassett (▲), Rodebush (●), Gibbard and Fong (♦), Gibbard and Gossman (□), Haghighi et al. (♦), Washburn (-). 120

3.7D $\Delta H_{fus(CaCl_2)}$ (kJ mol^{-1}) as a function of the ion concentration for the freezing point depression data of Jones and Bassett (▲), Rodebush (●), Oakes et al. (▲), Haghighi et al. (♦), Lide (*), Washburn (-). 121

3.8A $\Delta H_{vap(NaCl)}$ (kJ mol^{-1}) as a function of the ion concentration for the boiling point elevation data of Hass (●), Washburn (Δ,▲), Forsythe (+), Zaytsev and Aseyev (-). 122

3.8B $\Delta H_{vap(KCl)}$ (kJ mol^{-1}) as a function of the ion concentration for the boiling point elevation data of Saxton and Smith (●), Washburn (Δ), Forsythe (+), Zaytsev and Aseyev (-)..... 123

3.8C $\Delta H_{vap(MgCl_2)}$ (kJ mol^{-1}) as a function of the ion concentration for the boiling point elevation data of Washburn (Δ), Forsythe (+), Zaytsev and Aseyev (-) 124

3.8D $\Delta H_{vap(CaCl_2)}$ (kJ mol^{-1}) as a function of the ion concentration for the boiling point elevation data of Washburn (Δ), Forsythe (+), Zaytsev and Aseyev (-) 125

3.9A $\Delta H_{vap(NaCl)}$ (kJ mol^{-1}) as a function of temperature for the boiling point elevation data of Hass (●), Washburn (Δ,▲), Forsythe (+), Zaytsev and Aseyev (-) with the solid curve generated from the data of Marsh, 1987. 130

FIGURE Page

3.9B $\Delta H_{vap(KCl)}$ (kJ mol^{-1}) as a function of temperature for the boiling point elevation data of Saxton and Smith (●), Washburn (Δ), Forsythe (+), Zaytsev and Aseyev (-) with the solid curve generated from the data of Marsh, 1987. 131

3.9C $\Delta H_{vap(MgCl_2)}$ (kJ mol^{-1}) as a function of temperature for the boiling point elevation data of Washburn (Δ), Forsythe (+), Zaytsev and Aseyev (-) with the solid curve generated from the data of Marsh, 1987 132

3.9D $\Delta H_{vap(CaCl_2)}$ (kJ mol^{-1}) as a function of temperature for the boiling point elevation data of Washburn (Δ), Forsythe (+), Zaytsev and Aseyev (-) with the solid curve generated from the data of Marsh, 1987 133

3.10A $\Delta H_{fus(NaCl)}$ (kJ mol^{-1}) as a function of h_{NaCl} for Rodebush (●), Momicchioli et al. (x), Gibbard and Gossman (□), Potter et al. (■), Hall et al. (○), Oakes et al. (▲), Haghighi et al. (♦), Lide (*), Washburn (-). 134

3.10B $\Delta H_{fus(KCl)}$ (kJ mol^{-1}) as a function of h_{KCl} for Rodebush (●), Roloff (□), Spencer (♦), Chiorboli et al. (▲), Momicchioli et al. (x), Hall et al. (○), Lide (*), Washburn (-), Forsythe (+). 135

3.10C $\Delta H_{fus(MgCl_2)}$ (kJ mol^{-1}) as a function of h_{MgCl_2} for Jones and Bassett (▲), Rodebush (●), Gibbard and Fong (♦), Gibbard and Gossman (□), Haghighi et al. (♦), Washburn (-). 136

3.10D $\Delta H_{fus(CaCl_2)}$ (kJ mol^{-1}) as a function of h_{CaCl_2} for Jones and Bassett (▲), Rodebush (●), Oakes et al. (▲), Haghighi et al. (♦), Lide (*), Washburn (-). 137

3.11A $\Delta H_{vap(NaCl)}$ (kJ mol^{-1}) as a function of h_{NaCl} for Hass (●), Washburn (Δ,▲), Forsythe (+), Zaytsev and Aseyev (-). 138

3.11B $\Delta H_{vap(KCl)}$ (kJ mol^{-1}) as a function of h_{KCl} for Saxton and Smith (●), Washburn (Δ), Forsythe (+), Zaytsev and Aseyev (-). 139

3.11C $\Delta H_{vap(MgCl_2)}$ (kJ mol^{-1}) as a function of h_{MgCl_2} for Washburn (Δ), Forsythe (+), Zaytsev and Aseyev (-). 140

FIGURE Page

3.11D $\Delta H_{vap(CaCl_2)}$ (kJ mol^{-1}) as a function of h_{CaCl_2} for Washburn (Δ), Forsythe (+), Zaytsev and Aseyev (-)..... 141

3.12 Predicted freezing point as a function of the actual freezing point (Haghighi et al., 2008) for ternary systems of H_2O and NaCl, $CaCl_2$ (●); NaCl, KCl (□), $CaCl_2$, KCl (*); $MgCl_2$, NaCl (◊). 142

3.13 Hydration number as a function of charge density for Li^+, Na^+, K^+ (○), Mg^{2+}, Ca^{2+}, Sr^{2+}, (Δ), Al^{3+}, Fe^{3+} (□) with radius of ion given by Marcus (1988) 147

3.14 h_{NaCl} as a function of ion concentration from the combined osmotic pressure data of Smith (1932) and Smith and Hirtle (1932) at 60°C (□), 70°C (■), 80°C (◊), 90°C (♦), 100°C (Δ). 148

4.1 Schematic diagram of the experimental pH free drift reactor system used in this study. 155

4.2 n and log k (mmole m^{-2} hr^{-1}) as a function of I (molal scale) for KCl (●) and NaCl (□). 165

4.3 n and log k (mmole m^{-2} hr^{-1}) as a function of pCO_2 (atm) for KCl 2.0 (●), NaCl 2.0 (□) and NaCl 5.0 (◊) solutions. 166

4.4 n and log k (mmole m^{-2} hr^{-1}) as a function of T (°C) for KCl 2.0 (●), NaCl 2.0 (□) and NaCl 5.0 (◊) solutions. 167

LIST OF TABLES

TABLE		Page
1.1	Water inventory near the Earth's surface (modified from Berner and Berner, 1987, with comments added.	2
2.1	Initial and final experimental dissolution conditions	29
2.2	The coefficients derived from the MR analysis	59
3.1A	Freezing point depression of NaCl solutions	73
3.1B	Freezing point depression of KCl solutions	73
3.1C	Freezing point depression of $MgCl_2$ solutions	74
3.1D	Freezing point depression of $CaCl_2$ solutions	74
3.2A	Boiling point elevation of NaCl solutions	74
3.2B	Boiling point elevation of KCl solutions	75
3.2C	Boiling point elevation of $MgCl_2$ solutions	75
3.2D	Boiling point elevation of $CaCl_2$ solutions	75
3.3A	Vapor pressure depression of NaCl solutions	76
3.3B	Vapor pressure depression of KCl solutions	77
3.3C	Vapor pressure depression of $MgCl_2$ solutions	78
3.3D	Vapor pressure depression of $CaCl_2$ solutions	79
3.4	Change in h and ΔH_{fus} for the $CaCl_2$ freezing point depression data of Haghighi et al. (2008) as the maximum ion concentration is reduced	97
3.5	Data of Han et al. (2006).	127
3.6	The coefficients derived from the MR analysis.	146

TABLE Page

3.7 Hydration numbers normalized to h_{Mg2+}. 146

4.1 Initial and final experimental precipitation conditions 162

4.2 Experimentally determined rate constant and reaction order 164

1. INTRODUCTION

1.1 Importance of Calcite-Water Reactions

Water of the Earth's near surface environment is present as one of three phases - solid (ice), liquid, or gas (water vapor) - although it is primarily present as a liquid of highly variable composition distributed in different environments (Table 1.1). Reactions between minerals and natural waters are important in controlling water composition and the cycling of most components on the Earth's surface (e.g. Garrels and Thompson, 1962). Among the most important of these minerals is calcite (hexagonal $CaCO_3$), which along with dolomite ($CaMg(CO_3)_2$) makes up close to 20% of Phanerozoic sedimentary rocks (e.g. Morse and Mackenzie, 1990).

The dissolution and precipitation of carbonate minerals in natural waters are controlled by a variety of biotic and abiotic processes in which the reaction kinetics between water and mineral play an important role in controlling fluxes, composition, and the relative rates at which different carbonate minerals are formed or dissolved. Understanding of carbonate reaction kinetics is important for a wide range of reasons, which include weathering of carbonate rocks, deposition of calcium carbonate in the world's oceans, surface diagenesis and mass transport of carbonates, characteristics of carbonate-hosted gas and petroleum reservoirs (at least 60% of the world's known petroleum reserves occur in carbonate reservoirs - e.g. Morse and Mackenzie, 1990), and more recently in understanding the impact of and possibilities for sequestration of

---

This dissertation follows the style and format of Chemical Geology.

Table 1.1. Water inventory near the Earth's surface (modified from Berner and Berner, 1987, with comments added.

Reservoir	Volume (10^{-6} km^3)	Percent of Total (%)	Comments
Oceans	1370	97.25	Fixed major ion ratios, majority ~35 g salt kg^{-1}
Ice caps and glaciers	29	2.05	Solid, melts to ~pure water
Deep groundwater (750-4000m)	5.3	0.38	Highly variable but most highly saline with NaCl as major salt
Shallow ground water	4.2 (<750)	0.3	Highly variable but majority is dilute brackish
Lakes	0.125	0.01	Dominantly dilute but can reach very saline conditions
TOTAL	1408.625	99.99	All others: soil moisture, atmosphere, rivers, biosphere contribute ~0.01% of the total volume

anthropogenically produced carbon dioxide (see volume 217 of Chemical Geology, 2005, for a recent overview of this field).

Given that seawater is by far the most abundant form of water on the Earth's surface it is not surprising that most research has been conducted on carbonate mineral formation and dissolution in this "constant" ionic medium (Marcet's Principle). Most non-seawater studies have been conducted in relatively simple dilute solutions (see reviews of Burton, 1993; Morse 1983; Morse and Arvidson, 2002; Morse et al., 2007; Plummer et al., 1979; Sjöberg, 1978; Sjöberg and Rickard, 1983). However, the ability

to predict and understand carbonate mineral reaction kinetics with waters of a wider range of composition under conditions extending to at least modest depths below the Earth's surface is clearly important and development of kinetic equations of a more universally applicable nature is needed.

The interaction of carbonate minerals with formation waters are of particular importance in the storage of carbon dioxide and other waste fluids injected into depleted oil/gas reservoirs and/or saline formations (see reviews of Gozalpour et al., 2005; Riahi et al., 2004; Voormeij and Simandl, 2004; White et al., 2003; Yamasaki, 2003). In particular, the carbonate mineral-water-waste interactions will greatly influence the physical properties (e.g. porosity, permeability) of the subsurface. In order to accurately predict formation response to injection of carbon dioxide (or some other fluid), the factors affecting the reactivity of carbonate minerals in solutions typical of these formations must be understood.

The salinities of most subsurface formation waters are quite varied ranging from about five to three hundred (gram salt kilogram^{-1} solution) (Kharaka and Hanor, 2004) although the largest published salinity is over six hundred (Case, 1945) . Despite this wide range, it has been demonstrated that the composition is not completely random as there is a systematic variation of the major dissolved cations (Na^+, K^+, Mg^{2+}, Ca^{2+}) with chloride (Cl^-) in southwest Louisiana Gulf Coast reservoirs (Hanor, 1994). As in seawater, sodium and chloride are the dominant cation and anion respectively in subsurface waters. However, unlike present day seawater, where the amount of magnesium is at least five times that of calcium, calcium is typically found in greater

relative abundance in subsurface waters. At extremely high salinities, the amount of calcium may even exceed that of sodium (Davisson and Criss, 1996; Hanor, 1987; Wilson and Long, 1993). Sulfate, the second most abundant anion in seawater, is highly variable in subsurface brines where it is often absent as a result of sulfate reduction.

Modeling carbonate mineral dissolution as a function of saturation state requires accurate calculations of the carbonic acid system species distributions. However, accurate determination of the activities of these species in high ionic strength solutions continues to be problematic. Investigations of the solubility of calcite coupled with the Pitzer parameterizations of the carbonic acid system in synthetic brines (He and Morse, 1993) have made such calculations more reliable. (For further discussion of modeling ionic interactions for the carbonate system in natural waters, see Millero, 2007). Also, there is little reliable data on subsurface brine pCO_2 values and alkalinity values. These alkalinity values are usually interpreted as HCO_3^- although they may be significantly to dominantly due to the presence of organic acid anions.

1.2 Carbonic Acid System Overview

Before beginning a meaningful discussion of any carbonate mineral reactivity in solution, the carbonic acid system must be well understood. (A thorough discussion of the carbonic acid system in seawater has recently been provided by Millero, 2007). The speciation of carbon dioxide dissolved in water is controlled by the following equilibrium equations.

$$CO_{2(g)} \rightleftharpoons CO_{2(aq)} \qquad (1.1)$$

$$CO_{2(aq)} + H_2O \rightleftharpoons H_2CO_{3(aq)} \quad (1.2)$$

$$H_2CO_{3(aq)} \rightleftharpoons HCO_3^-{}_{(aq)} + H^+{}_{(aq)} \quad (1.3)$$

$$HCO_3^-{}_{(aq)} \rightleftharpoons CO_3^{2-}{}_{(aq)} + H^+{}_{(aq)} \quad (1.4)$$

Using the conventions of Plummer and Busenberg (1982), equations 1.2 and 1.3 may be combined:

$$CO_{2(aq)} + H_2O \rightleftharpoons HCO_3^-{}_{(aq)} + H^+{}_{(aq)} \quad (1.5)$$

The thermodynamic equilibrium constants may then be written as:

$$K_H = \frac{a_{CO_2(aq)}}{f_{CO_2(g)}} \cong \frac{a_{CO_2(aq)}}{pCO_{2(g)}} \quad (1.6)$$

$$K_1 = \frac{a_{HCO_3^-(aq)} a_{H^+(aq)}}{a_{CO_2(aq)} a_{H_2O}} \quad (1.7)$$

$$K_2 = \frac{a_{CO_3^{2-}(aq)} a_{H^+(aq)}}{a_{HCO_3^-(aq)}} \quad (1.8)$$

where the activity (a) of a species is equal to its concentration (m) multiplied by its total ion activity coefficient (γ):

$$a_i = m_i \gamma_i \quad (1.9)$$

In equation 1.6, pCO_2 may be substituted for the fugacity coefficient, as it is greater than 0.999 under these conditions (Morse and Mackenzie, 1990) and is proportional to its

mole fraction (MacInnes and Belcher, 1933). It should be noted that values of these constants are both temperature and pressure dependent.

There are four fundamental parameters to describe the carbonic acid system: total alkalinity (At), total inorganic carbon (TCO_2 or ΣCO_2), partial pressure of carbon dioxide (pCO_2), and pH. Any two (2) of these parameters may be calculated if the complementary two (2) are known.

Alkalinity refers to the solution's ability to neutralize acid disregarding the contribution from the dissolution of any solid phases. Total alkalinity may be given as the alkalinity contributed by the carbonic acid system, or carbonate alkalinity (A_c), and that contributed by all other solution components:

$$A_t = A_c + \sum A_i = m_{HCO_3^-} + 2m_{CO_3^{2-}} + \sum A_i \quad (1.10)$$

In the synthetic solutions to be investigated, the only alkalinity contributing species are from the carbonic acid system and water (A_w), which can simplify the above equation to:

$$A_t = A_c + \sum A_i = A_c + A_w = m_{HCO_3^-} + 2m_{CO_3^{2-}} + m_{OH^-} - m_{H^+} \quad (1.11)$$

From these equations, it may be shown that as the pCO_2 changes, there will be a change in carbonate alkalinity but not total alkalinity.

Total inorganic carbon is defined as the amount of carbon dioxide gas that results when the solution is acidified:

$$\sum CO_2 = m_{CO_2} + m_{H_2CO_3} + m_{HCO_3^-} + m_{CO_3^{2-}} \quad (1.12)$$

pCO_2 is the mole fraction of carbon dioxide of the total gas mixture. Finally, pH is the negative logarithm of the activity of hydrogen ions in solution.

1.3 Calcite Solubility and Reaction Kinetics

With an understanding of the carbonic acid system, a discussion of carbonate mineral behavior in solution may begin. The destruction (dissolution) and formation (precipitation) of pure calcite in water may be simply given as the following equilibrium:

$$CaCO_{3(s)} \underset{k_r}{\overset{k_f}{\rightleftharpoons}} Ca^{2+}{}_{(aq)} + CO_3^{2-}{}_{(aq)} \tag{1.13}$$

where the forward reaction is dissolution, the reverse is precipitation and k_f and k_r are the forward and reverse rate constants respectively. The forward reaction rate may be given as (assuming the activity of the solid is one):

$$R_f = k_f a_{CaCO_3} = k_f \tag{1.14}$$

whereas the reverse reaction may be written as:

$$R_r = k_f a_{Ca^{2+}} a_{CO_3{}^{2-}} \tag{1.15}$$

This reaction yields a solubility product ($K_{sp_{calcite}}$) which is independent of the amount of solid present (assuming the activity of the solid is one):

$$K_{sp_{calcite}} = \frac{a_{Ca^{2+}} a_{CO_3{}^{2-}}}{a_{CaCO_3}} = a_{Ca^{2+}} a_{CO_3{}^{2-}} \tag{1.16}$$

In practice, an apparent stoichiometric solubility product, $K^*_{sp_{calcite}}$, is usually determined:

$$K^*_{sp_{calcite}} = m_{Ca^{2+}} m_{CO_3^{2-}} \tag{1.17}$$

where the stoichiometric solubility product is related to the thermodynamic solubility product:

$$K_{sp_{calcite}} = a_{Ca^{2+}} a_{CO_3^{2-}} = K^*_{sp_{calcite}} \gamma_{Ca^{2+}} \gamma_{CO_3^{2-}} \tag{1.18}$$

The saturation state of a solution (Ω) is simply calculated as the ratio of the ion activity product (IAP) to the solubility product:

$$\Omega = \frac{a_{Ca^{2+}} a_{CO_3^{2-}}}{K_{sp_{calcite}}} = \frac{m_{Ca^{2+}} \gamma_{Ca^{2+}} m_{CO_3^{2-}} \gamma_{CO_3^{2-}}}{K_{sp_{calcite}}} = \frac{IAP}{K_{sp_{calcite}}} \tag{1.19}$$

At equilibrium, $\Omega = 1$, and the forward and reverse reactions in equation 1.13 are equal. That is, the change in free energy is zero. This may be more easily understood if the Gibbs free energy of reaction is shown in terms of Ω:

$$\Delta G = \Delta G^o + RT\ln Q = RT\ln\left(\frac{IAP}{K_{sp_{calcite}}}\right) = RT\ln\Omega \tag{1.20}$$

where ΔG is the Gibbs free energy of reaction, ΔG^o is the standard free energy change, R is the gas constant, T is temperature, and Q is the reaction quotient. In undersaturated solutions, $\Omega < 1$ ($\Delta G < 0$) and dissolution may occur (the forward reaction is favored); $\Omega > 1$ ($\Delta G > 0$) and precipitation should thermodynamically occur in supersaturated solutions (the reverse reaction is favored). However, in natural waters the behavior is

much more complex and supersaturated solutions may persist (e.g. present day surface seawater has a typical $\Omega_{calcite}$ of approximately six).

The active field of experimental determination of carbonate mineral kinetics as a function of solution composition really took off about half a century ago (e.g. Akin and Lagerwerff, 1965a; Akin and Lagerwerff, 1965b; Berner, 1967; Schmalz, 1967; Terjesen et al., 1961; Weyl, 1958). Since that time, a large number of investigations have examined the influences of "foreign" ions, , total pressure, temperature, and other variables on calcite dissolution rates (see reviews of Burton, 1993; Morse, 1983; Morse and Arvidson, 2002; Morse et al., 2007; Plummer et al., 1979; Sjöberg, 1978; Sjöberg and Rickard, 1983). Typically these investigations have focused on dissolution rates in solutions with ionic strengths similar to or less than that of seawater. Meaningful results from precipitation of pure calcite in solutions of complex composition are more difficult to obtain due to adsorption, co-precipitation and inhibition by "foreign" ions. Little work has been published on calcite dissolution (Gledhill and Morse, 2004; Gledhill and Morse, 2006a; Pokrovsky et al., 2005) or precipitation rates (Zhang and Dawe, 1998) from high ionic strength solutions ($I > 1$).

The specific effect of ionic strength on calcite solubility or reaction kinetics has been reported by a few investigators. In solubility experiments, both Millero et al. (1984) and Wolf et al (1989) extrapolated rather consistent thermodynamic pKsp values for calcite regardless of ionic strength. Reaction rates however were found to be dependent on ionic strength by a number of researchers. Bischoff (1968) found that nucleation rate of calcite increased proportional to the square root of ionic strength.

Zhang and Dawe (1998) found that in high salinity waters the precipitation rate of calcite increased as a function of the square root of ionic strength. Gledhill and Morse (2004) found the dissolution rate was moderately inhibited as a function of ionic strength in complex (Na-Ca-Mg-Cl) brines.

1.4 Dissolution

The general dissolution rate of calcium carbonate for near-equilibrium dissolution has been given as (Berner and Morse, 1974; Sjöberg, 1978):

$$R = k(1 - \Omega)^n \tag{1.21}$$

where R is the dissolution rate normalized to the reacting surface area, k is the rate constant that is dependent on pressure, temperature and overall solution composition, Ω is the saturation state, and n is the order of the reaction, which in phosphate-free seawater is approximately three (3). Sjöberg (1978) also found that the kinetics could be described by:

$$R = kA\left(1 - \sqrt{\Omega}\right)^n \tag{1.22}$$

where the reaction order is two in phosphate-free seawater. A similar, although not simply related empirical model given by Sjöberg (1978) describes the rate as:

$$R = K_{sp}^n(1 - \Omega^n) \tag{1.23}$$

where n was found to be ½ for calcite in a pure ionic media (also see Lasaga, 1998).

Dissolution has been described by three simultaneous mechanisms (Chou et al., 1988; Plummer et al., 1978; Wollast, 1989):

$$CaCO_{3(s)} + H^{+}_{(aq)} \overset{k_1}{\rightarrow} Ca^{2+}_{(aq)} + HCO^{-}_{3\,(aq)} \tag{1.24}$$

$$CaCO_{3(s)} + H_2CO_{3(aq)} \overset{k_2}{\rightarrow} Ca^{2+}_{(aq)} + 2HCO^{-}_{3\,(aq)} \tag{1.25}$$

$$CaCO_{3(s)} + H_2O \underset{k_{-3}}{\overset{k_3}{\rightleftharpoons}} Ca^{2+}_{(aq)} + HCO^{-}_{3\,(aq)} + OH^{-}_{(aq)} \tag{1.26}$$

in which the net rate of dissolution was given by the semi-empirical equation:

$$\begin{aligned} R = -\frac{dm_{calcite}}{dt} \\ = k_1 a_{H^+} + k_2 a_{H_2CO_3{}^+} + k_3 a_{H_2O} \\ - k_{-3} a_{Ca^{2+}} a_{HCO_3{}^-} \end{aligned} \tag{1.27}$$

where k_1, k_2, k_3 are the forward rate constants and k_{-3} is the is the reverse rate constant that is dependent.

A more sophisticated mechanistic model, based on surface complexation theory, was presented by Van Cappellen et al. (1993). It postulates the formation of the hydration species $>CO_3H^0$ and $>CaOH^0$ (where > denotes a surface bond) at the calcite surface that govern the reactivity of the carbonate-water interface. The model proposes the following surface species:

$$> CO_3H^0 \rightarrow > CO_3{}^- + H^+ \tag{1.28}$$

$$> CO_3H^0 + Ca^{2+} \rightarrow > CO_3Ca^+ + H^+ \tag{1.29}$$

$$> CaOH_2^+ \rightarrow > CaOH^0 + H^+ \quad (1.30)$$

$$> CaOH^0 \rightarrow > CaO^- + H^+ \quad (1.31)$$

$$> CaOH^0 + CO_2 \rightarrow > CaHCO_3^0 \quad (1.32)$$

$$> CaOH^0 + CO_2 \rightarrow > CaCO_3^- + H^+ \quad (1.33)$$

Arakaki and Mucci (1995) combined the semi-empirical model of Plummer et. al. (1978) with the surface complexation model of Van Cappellen et. al. (1993) to describe the dissolution of calcite in deionized water. This yielded an overall reaction rate given by:

$$\begin{aligned} R = k_1 > CO_3^-(a_{H^+})^2 + (k_2 - k_5) \\ > Ca^{2+}a_{H_2CO_3} + k_4 - (k_6 - k_3) \\ > CO_3H^0a_{CaHCO_3^+} - k_7 \\ > Ca^+a_{H_2CO_3}a_{CaCO_3^0} - k_8a_{CaCO_3^0} \end{aligned} \quad (1.34)$$

Although these mechanistic models are intriguing, they are largely theoretical resting on unverified correlations rather than direct observations of surface species and mechanisms. They require the use of intrinsic stability constants for the surface complexation reactions that are not currently available in complex solutions causing them to have no predictive utility for natural waters. As such, this dissertation will focus on the general rate equation.

The general dissolution rate equation has typically yielded orders between three and four when applied to calcite dissolution in seawater (Morse and Arvidson, 2002). (It should be noted that small uncertainties in the IAP used to calculate W can have a pronounced effect on the interpreted reaction order (n) and rate constant (k) using the

general equation (Jeschke and Dreybrodt, 2002). The presence of other ions may dramatically affect the reaction order (n) and/or rate constant (k). For example, DeKanel and Morse (1978) found trace levels (10 μM) of phosphate (PO_4^{3-}) to have a tremendous effect on the reaction order (n ~ 16) with minimal effect on the rate constant. Trace metals have also been shown to act as inhibitors on calcite dissolution (Terjesen et al., 1961). The specific effect of magnesium ion on calcite dissolution kinetics is one of controversy. At neutral to basic pH, Weyl (1958) and Berner (1967) found magnesium ions to inhibit calcite dissolution whereas Gutjahr (1996b) found no significant effect. The presence of calcium ions has been found to both inhibit (Sjöberg, 1978; Sjöberg and Rickard, 1985) and promote (Gutjahr et al., 1996a) calcite dissolution.

In contrast to the typical reaction order of three to four, first order (n = 1) dissolution kinetics have also been reported in the literature. First order dissolution kinetics were predicted by the mechanistic model of calcite dissolution rates near saturation ($0.1 < \Omega < 0.8$) (Arakaki and Mucci, 1995). When Hales and Emerson (1997) applied an apparent kinetic solubility product to experimental data (which originally yielded a reaction order of ~4.5), they concluded that the dissolution rate could be described by first order kinetics. In using an open system pH-free-drift method to measure calcite dissolution in geologically relevant Na-Ca-Mg-Cl synthetic brines, Gledhill and Morse (2004) found dissolution rates to be composition dependent assuming a first order reaction (n = 1) using the general dissolution rate equation. They found that the rate constant could be estimated from a multiple regression model of the form:

$$k = \beta_0 + \beta_1(T) + \beta_2\left(p_{CO_2}\right) + \beta_3(I) + \beta_4(a_{Ca^{2+}}) + \beta_5(a_{Mg^{2+}}) \quad (1.35)$$

where k is the rate constant, T is temperature, is the partial pressure of carbon dioxide, I is the ionic strength, and a_i is the activity of the i^{th} species. In addition, they found that inhibition of dissolution rate was dependent on the ionic strength of the solution.

Experimental results on the effect of the partial pressure of carbon dioxide on dissolution rates have been mixed. Berner and Morse (1974) found calcite dissolution rates at 4 < pH < 6.8 in NaCl-$CaCl_2$ solutions of ionic strength approximately that of seawater (I ~ 0.7 mol kg-1 solvent) to be independent of pCO_2 in the range 0.003 – 1 atm. Pokrovsky et al. (Pokrovsky et al., 2005), found at ~pH 4, calcite dissolution rates increase by a factor of 3 from 1 - ~20 atm pCO_2. In brines of ionic strength ranging from 0.1 to 1, Zuddas and co-workers also found pCO_2 to increase calcite dissolution rates (Charara et al., 2005) (O. Lopez, 2007 personal communication).

1.5 Precipitation

Rate date for precipitation has been commonly fit to the general equation (Berner and Morse, 1974; Morse, 1983; Nancollas and Reddy, 1971):

$$R = k(\Omega - 1)^n \quad (1.36)$$

where R is the precipitation rate normalized to the reacting surface area, k is the rate constant, and n is the reaction order and is approximately three in seawater. In addition to the general equation, the precipitation rate has been determined by Zhang and Dawe

(1998) to fit the Burton-Cabrera-Frank (BCF) rate law (Burton et al., 1951) and the Davies and Jones' (DJ) rate equation (1955) as well:

$$R_{BCF} = \frac{k\left(\sqrt{\Omega} - 1\right)^{n}}{Bstanh\left(\frac{Bs}{\left(\sqrt{\Omega} - 1\right)}\right)} \tag{1.37}$$

$$R_{DJ} = k\left(\sqrt{\Omega} - 1\right)^{n} \tag{1.38}$$

where R is the precipitation rate, k is the precipitation rate constant which is dependent on temperature, crystal surface area, and inhibitors, Bs is a BCF constant dependent on diffusion and temperature and the reaction order is two (n = 2) for both the BCF and the DJ rate equations.

As stated previously, meaningful results from precipitation of pure calcite in solutions of complex composition are more difficult to obtain due to adsorption, co-precipitation and inhibition by "foreign" ions. The general rate equation has typically yielded a reaction order of approximately three when applied to calcite precipitation in seawater. The presence of other ions may dramatically affect the reaction order (n) and/or rate constant (k). Sulfate was found to significantly reduce the precipitation rate (Busenberg and Plummer, 1985). Likewise, phosphate was found to be a strong inhibitor increasing the reaction order from n = 2.8 in phosphate free seawater to n = 3.4 in the presence of phosphate (Mucci, 1986). He also found that increasing levels of phosphate decrease the rate constant (although the reaction order of n = 3.4 remains constant). Many divalent metals, particularly magnesium are incorporated into the lattice structure. The solution ratio of magnesium to calcium controls the composition of

magnesian calcite ($Ca_{(1-x)}Mg_{(x)}CO_3$) overgrowths (Mucci and Morse, 1983; Mucci et al., 1985).

On the other hand, salinity (and thus indirectly, ionic strength), over the range S = 5 – 44, was found to have little effect on calcite precipitation rates (Zhong and Mucci, 1989). When using the Davies and Jones rate equation, Zhang and Dawe (1998) suggest that the rate constant is dependent on the square root of ionic strength in a closed system pH-free-drift precipitation experiment. Zuddas and Mucci (1998) used the net precipitation rate:

$$r = k_f(a_{Ca^{2+}})^{n_1}\left(a_{CO_3{}^{2-}}\right)^{n_2} - k_r \tag{1.39}$$

to formulate a rate expression as a function of carbonate ion concentration only:

$$\log(r + k_r) = \log K_f + n_2 \log\left[CO_3{}^{2-}\right] \tag{1.40}$$

where K_f is:

$$K_f = k_f(a_{Ca^{2+}})^{n_1}\left(\gamma_{CO_3{}^{2-}}\right)^{n_2} \tag{1.41}$$

As ionic strength is varied ($0.1 \leq I \leq 0.93$), both the reaction order with respect to carbonate (n_2) and the forward reaction rate (k_f) were found to increase which they suggested was a result of change in the precipitation mechanism as well as catalysis provided by the additional electrolyte.

1.6 Experimental Objective

From the preceding discussion, it is apparent that there are many components in natural waters that influence the reaction kinetics of calcite. In order to elucidate the specific effect of I on calcite reaction kinetics while attempting to minimize the influence of various ions, a series of classical free-drift pH experiments were conducted in magnesium-free, phosphate-free, low calcium (~0.01- 0.02 molal) simple electrolyte solutions. Both KCl and NaCl solutions were investigated because KCl is not believed to strongly interact with carbonic acid system components (Davis and Oliver, 1972; Frantz, 1998; Oliver and Davis, 1973). The influence of temperature and pCO_2 on the reaction kinetics of calcite were also investigated in these same solutions. The effect of I, pCO_2 and temperature on calcite dissolution in undersaturated solutions are reported in Section 2 whereas the influence of these same variables on precipitation kinetics of calcite are reported in Section 4. As the amount of "free" water was found to play a significant roles in the dissolution kinetics of calcite, the hydration characteristics of the cations are analyzed from existing literature data in Section 3. Finally, Section 5 draws some general conclusions from the two separate, yet complementary, sections on reaction kinetics as well as from the section on hydration.

2. CALCITE DISSOLUTION KINETICS IN SALINE WATERS

The effect of ionic strength (I), pCO_2, and temperature on the dissolution rate of calcite was investigated in magnesium-free, phosphate-free, low calcium ($m_{Ca^{2+}} \approx 0.01$ molal) simple KCl and NaCl solutions over the undersaturation range of $0.4 \leq \Omega_{calcite} \leq 0.8$. First-order kinetics were found sufficient to describe the rate data where the rate constant (k) is dependent on the solution composition. Rates decreased with increasing I and were faster in KCl than NaCl solutions at the same I indicating that Na^+ interacts more strongly with the calcite surface than K^+ or that water is less available in NaCl solutions. Rates increased with increasing pCO_2 and temperature, and their influences diminished at high I. Arrhenius plots yielded a relatively high activation energy ($E_a \approx 20 \pm 2$ kJ mol^{-1}) which indicated that dissolution was dominated by surface controlled processes. The multiple regression model (MR) of Gledhill and Morse (2006a) was found to adequately describe the results at high I in NaCl solutions, but caution must be used when extrapolating to low I or pCO_2 values. These results are consistent with the hypothesis that the mole fraction of "free" solvent ($X_{"free"H_2O}$) plays a significant role in the dissolution kinetics of calcite with a minimum value of ~45-55% required for dissolution to proceed in undersaturated solutions at 25-55 °C and $pCO_2 = 0.1 – 1$ atm. This hypothesis has been incorporated into a modified version of the MR model of Gledhill and Morse (2006a) where $X_{"free"H2O}$ has replaced I and the Ca^{2+} and Mg^{2+} terms have been dropped:

$$k_{pred} = \beta_0 + \beta_1 T + \beta_2 pCO_2 + \beta_3 X_{"free"H_2O}$$

2.1. Introduction

The dissolution and precipitation of carbonate minerals in natural waters are controlled by a variety of biotic and abiotic processes in which the reaction kinetics between water and mineral play an important role in controlling fluxes, composition, and the relative rates at which different carbonate minerals are formed or dissolved. Understanding of carbonate mineral reaction kinetics is important for a wide range of reasons. These include the weathering of carbonate rocks, deposition of calcium carbonate in the world's ocean, early diagenesis and mass transport of carbonates, characteristics of carbonate-hosted gas and petroleum reservoirs, and more recently in understanding the impact of and possibilities for sequestration of anthropogenically produced carbon dioxide (see volume 217 of Chemical Geology, 2005, for a recent overview of this field).

Given that seawater is by far the most abundant form of water on the Earth's surface (Table 1.1), it is not surprising that most research has been conducted on carbonate mineral formation and dissolution in seawater. Most non-seawater studies have been conducted in relatively simple dilute solutions (see reviews of Plummer et al., 1979; Sjöberg, 1978; Morse, 1983; Sjöberg and Rickard, 1983; Burton, 1993; Morse and Arvidson, 2002; Morse et al., 2007). However, the ability to predict and understand carbonate mineral reaction kinetics in aqueous solutions over a wider range of composition under conditions extending to at least modest depths below the Earth's surface is clearly important and development of kinetic equations of a more universally applicable nature is needed.

In using an open system pH-free-drift method to measure calcite dissolution in geologically relevant Na-Ca-Mg-Cl synthetic brines, Gledhill and Morse (2006a) found dissolution rates to be composition dependent assuming a first order reaction using the general dissolution rate equation (Berner and Morse, 1974; Sjöberg, 1978):

$$R = k(1 - \Omega_{calcite})^n \quad (2.1)$$

where R is the dissolution rate normalized to the reacting surface area, k is the dissolution rate constant that is dependent on temperature and overall solution composition, $\Omega_{calcite}$ is the saturation state with respect to calcite and n is the reaction order. They found that k could be estimated from a multiple regression (MR) model and that the moderate inhibitory effect of I was reported to be approximately equivalent (in standardized coefficients) and opposite in nature, to the effect of pCO_2.

In this study, their observation of the influence of I was further investigated in a series of classical free-drift pH experiments that were conducted in magnesium-free, phosphate-free, low calcium (~0.01 molal) simple electrolyte solutions in order to further elucidate the specific effect that I has on the dissolution kinetics of calcite. Both KCl and NaCl solutions were investigated because KCl is not believed to strongly interact with carbonic acid system components (Davis and Oliver, 1972; Frantz, 1998; Oliver and Davis, 1973).

2.2. Materials and Methods

A schematic diagram of the experimental system is shown in Figure 2.1.

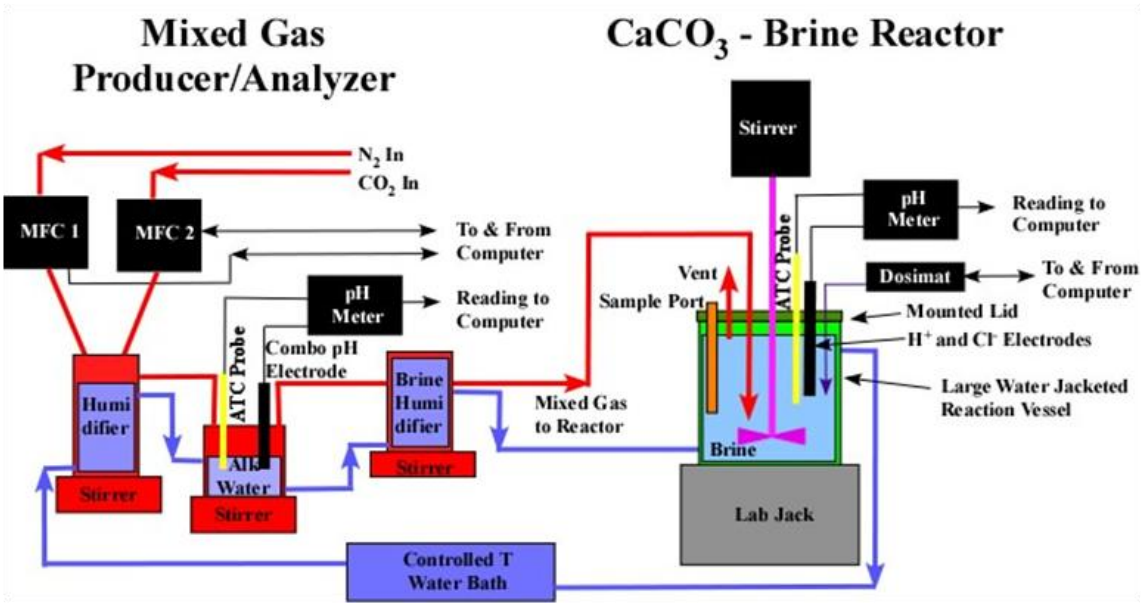

Figure 2.1. Schematic diagram of the experimental pH free drift reactor system used in this study.

Commercially purified high grade CO_2 and ultra-high purity N_2 were precisely controlled using dual MKS® Type 1479A Mass-Flo® mass-flow controllers that were controlled by a computer running LabVIEW® software. Both gases flowed individually through NO-OX® tubing into a vigorously stirred ~230 mL water jacketed humidifier containing deionized MilliQ® (18.2 MΩ) water thoroughly mixing the humidified gases. The mixed gas outflow then flowed (2 L min^{-1}) through NO-OX® tubing into a ~100 mL water jacketed vessel containing a solution of known alkalinity. The temperature and pH of the solution was monitored with an Orion ATC probe and Orion Ross

combination electrode coupled to an Orion 720A potentiometer. These measurements allowed for the independent determination of the partial pressure of CO_2 in the mixed gas to be compared with the flow set by the mass-flow controllers. The gas outflow then passed through NO-OX® tubing into a stirred ~230 mL water jacketed humidifier containing water of the same I as the solution being investigated. The mixed gas outflow then encountered a "T" thereby creating two (2) gas outflows through NO-OX® tubing, which were placed at the bottom of the approximately 2 L water jacketed reaction vessel. Gas dispersion tubing was not used as it has been shown that calcite can be caught in the sintered glass which also can exhibit "memory" effects from slow exchange with liquid in the micropores (Morse and Berner, 1972).

The solution was well stirred at a constant rate (500 rpm) using an electronically controlled IKA Works overhead stirrer to prevent the grinding action a magnetic stirrer may provide while ensuring suspension of the solid in solution as well as thorough mixing of the gas and solution. The temperature of all vessels was held constant (±0.1 °C) using a Neslab constant temperature bath controlled by a computer running LabVIEW® software. Temperature of the solution in the reaction vessel was measured with an Orion ATC probe coupled to an Orion 720A potentiometer. Electrode potential (electromotive force) was measured using a Ross® H+ selective electrode referenced to a Single Refex® solid-state reference electrode thereby avoiding a porous liquid-junction (Knauss et al., 1990). The potential of the solution was converted to a "Pitzer scale" pH for rate determination following the methodology of Gledhill and Morse (2006a). Total

alkalinity (TA) and total CO_2 (DIC) were used to calculate the pH and pCO_2 in solution serving as a check on the internal consistency of the system.

Concentrated stock solutions close to saturation of ACS reagent grade KCl, NaCl, and $CaCl_2 \cdot 2H_2O$ were prepared and passed through individual columns of reagent grade calcium carbonate powder and filtered to remove any "foreign" surface active ions (e.g. phosphate and metals) that may have been present at trace levels. Experimental solutions were prepared gravimetrically on the molal scale (m) from these separate concentrated stock solutions and diluted with deionized MilliQ® (18.2 MΩ) water for the appropriate concentration. The initial salt concentrations were verified by analytical determination of calcium and chloride concentrations.

The experimental solution was added to the reaction vessel and allowed to equilibrate with the constant temperature bath and mixed gas bubbling through the solution. Next, the initial calcite saturation state was poised at ~10% saturation by the addition of a concentrated potassium or sodium (depending on supporting electrolyte used) carbonate solution. Once the solution had equilibrated, several aliquots were withdrawn for analysis (TA, Ca^{2+}, Cl^-, DIC) of the initial state. Experimental solutions were reacted with crushed rhombic Iceland spar calcite from Creel, Chihuahua, Mexico that had been obtained from Ward's Scientific Inc. (Rochester, NY). Large calcite pieces were manually crushed with mortar and pestle, wet sieved, sonicated, re-sieved, cured in water, and finally dried for 48 hours. The resultant 63–125 μm size fraction was estimated to have a specific surface area of 0.016 $m^2\ g^{-1}$ from a geometric

determination using scanning electron micrograph (SEM) imaging. The mineralogy was verified by powder X-ray diffraction as being >99% calcite.

TA was determined by a modified Gran-type titration (Gran, 1952) using a Metrohm 755 Dosimat and an Orion 720A pH meter interfaced with a computer controlled by LabVIEW® software as described in Gledhill and Morse (2006a), although six point calibration curves were employed rather than five. Briefly, HCl titrant and K_2CO_3 or Na_2CO_3 standards were prepared in KCl and NaCl solutions respectively at I specific to each experimental solution. The carbonate standards were prepared gravimetrically under a nitrogen environment and their concentrations verified by DIC coulometric measurement. Titrations were conducted at 25 ± 0.1 °C in a water-jacketed open cell into which CO_2 was continuously bubbled to prevent the solution from becoming supersaturated with respect to $CaCO_3$ mineral phases prior to the initial addition of acid in a modification (Gledhill and Morse, 2006a; Finneran and Morse, unpublished data) of the open cell titration as described in the Guide to Best Practices for Ocean CO_2 Measurements (Dickson et al., 2007).

DIC was determined according to the method of Dickson and Goyet (2005) with a UIC Incorporated Model 5011 CO_2 coulometer with a typical precision of 1%. The Ca^{2+} concentration was determined by EGTA titration with the calcium indicator hydroxynapthol blue deposited on sodium chloride sold under the name Cal/Ver II®. Endpoint detection was facilitated using a Brinkmann PC 800 colorimeter interfaced with a computer controlled by LabVIEW® software yielding a precision of 2%. The Cl^- concentration was determined by $AgNO_3$ titration using a Metrohm 755 Dosimat and an

Orion silver ion selective electrode, and an Orion 720A pH meter interfaced with a computer controlled by LabVIEW® software with a precision of 1.5%. The concentration of the supporting cation (K^+ or Na^+) was calculated from charge balance.

The pCO_2 in the gas feed was first estimated by the ratio of the CO_2 flow rate to the total gas flow rate of 2 L min^{-1} (flow was balanced with ultra-high purity N_2) and more precisely determined by the pH of the solution of known TA. Three point calibration curves were made using 100% (BOTCO), 10% (Scott Specialty Gases) and 1% (Scott Specialty Gases) CO_2 and solutions of known TA.

It should be noted that gas phase disequilibrium in the experimental solution can occur in which there is an excess consumption of CO_2 relative to supply in the solution if the initial rate of dissolution is too rapid relative to the supply of CO_2 (e.g., Arakaki and Mucci, 1995). This can be prevented by: (1) conducting the dissolutions at high pCO_2 where appropriate; (2) reducing the available calcite surface area; and (3) avoiding initiating the experiments at extreme degrees of disequilibrium. These experiments were conducted near 0.1 atm pCO_2 or greater and the calcite used had a relatively low specific surface area (0.016 m^2 g^{-1}). The low specific surface area also produced considerably slower initial rates allowing for significant amounts of calcite to be added (5 g L^{-1}), thus minimizing the change in surface area during the experiments. Finally, a concentrated carbonate solution, K_2CO_3 or Na_2CO_3 depending on the electrolyte being investigated, was added to set approximately 10% saturation with respect to calcite. These precautions resulted in little variation between initial and final calculated pCO_2 values.

Prior to calcite addition, samples were drawn and filtered using an in-line 0.45μm Acrodisk filter for initial solution analysis. Although unnecessary, a filter was employed so that the withdrawal of the initial and final samples was subjected to the same experimental protocol. The calcite was then allowed to react with the solution while changes in electrode potential were monitored at 5 second intervals. After 5 hours, experiments were terminated as changes in solution chemistry were within the measurement precision of the analytical procedure for each desired analyte. Samples were drawn and filtered using an in-line 0.45 μm Acrodisk filter for final solution analysis. Remaining calcite was collected by vacuum filtration and briefly rinsed with MilliQ® (18.2 MΩ) water. The filtered material was dried and stored in a vacuum desiccator for later SEM imaging which confirmed that there was no excessive alteration to the specific surface area.

2.3. Calculations

The dissolution and precipitation of calcite can be written in classic form as:

$$CaCO_{3(s)} \underset{k_r}{\overset{k_f}{\rightleftharpoons}} Ca^{2+}{}_{(aq)} + CO_3^{2-}{}_{(aq)} \tag{2.2}$$

where the forward reaction is dissolution and k_f is the forward rate constant, and precipitation is the reverse reaction with the reverse rate constant k_r. If the reaction is rewritten in terms of carbonic acid system components:

$$CaCO_{3(s)} + H_2O + CO_2 \underset{k_r}{\overset{k_f}{\rightleftharpoons}} Ca^{2+}{}_{(aq)} + 2HCO_3^{-}{}_{(aq)} \tag{2.3}$$

and given the definition of TA

$$TA = m_{HCO_3^-} + 2m_{CO_3^-} + m_{OH^-} - m_{H^+} \quad (2.4)$$

it is apparent that the dissolution of one mole of calcite yields two moles of TA. Thus, the dissolution rate may be defined from the time dependent rate of change in TA:

$$R = -\frac{dm_{CaCO_{3(s)}}}{dt} = \frac{dm_{Ca^{2+}(aq)}}{dt} = \frac{dm_{CO_3^{2-}(aq)}}{dt} = \frac{1}{2}\left(\frac{dTA}{dt}\right) \quad (2.5)$$

which must be normalized to both the mass of solvent and surface area of calcite used. Geometric surface area was used as a proxy for the reactive surface area rather than BET surface area (e.g. Keir, 1980; Walter, 1985; Cubillas et al., 2005a, 2005b; Gledhill and Morse, 2006a;). As pCO_2 was constant throughout each experimental run and electrode potential monitored continuously, the observed electrode potential was first converted to a Pitzer scale pH which was subsequently converted to TA using the Pitzer formalism incorporated into the software program EQPITZER (He and Morse, 1993) following the methodology of Gledhill and Morse (2006a). The rate was then determined by the change in TA with respect to time (Gledhill and Morse, 2006a)

The experimental rate data were modeled using the general rate equation over the range of $0.4 \leq \Omega_{calcite} \leq 0.8$. The upper limit of $\Omega_{calcite}$ was chosen as the small voltage change with respect to time and the analytical uncertainty of the final solution chemistry may lead to erratic rate measurements at higher $\Omega_{calcite}$ as demonstrated by Gledhill and Morse (2004). Three kinetic experiments comprised of KCl 2.0 (I ≈ 2.2 m), NaCl 2.0 (I

≈ 2.2 m) and NaCl 5.0 (I ≈ 5.5 m) solutions were repeated (individual batches of solution) under the same initial conditions (pCO_2 = 1 atm, T = 25 °C, $m_{Ca^{2+}} \approx 0.01$ molal). This Ca^{2+} concentration was chosen as it is approximately equivalent to that found in modern seawater with salinity of 35. Additionally, this low Ca^{2+} concentration does not result in erroneously high calculated saturation states using EQPITZER (He and Morse, 1993) that calcium rich brines do (Gledhill and Morse, 2006b). The first two sets of solutions (KCl 2.0 and NaCl 2.0 with I ≈ 2.2 m) yielded dissolution rate constants with a precision (RSD) of better than 6%. The NaCl 5.0 (I ≈ 5.5) had a much lower precision of 25%. Additionally, five replicates of the same batch of solution (I ~ 2.5) were reacted (though no analyses of the solution conditions were performed) yielding a precision (RSD) better than 7%. Therefore, 7% precision (RSD) has been assumed for solutions of I ≤ 2.2 m whereas for solutions with I > 2.2 m, precision was assumed to vary linearly from 7 – 25% as a function of I from 2.2 to 5.5 m.

2.4. Results

Initial experimental conditions prior to reaction with calcite and final (steady state) conditions after reaction with calcite are presented in Table 2.1, where pH values are Pitzer scale values obtained from EQPITZER (He and Morse, 1993).

Table 2.1. Initial and final experimental dissolution conditions.

Experimental ID	Ca^{2+}_i (m)	K^+ (m)	Na^+ (m)	Cl^- (m)	TA_i (eq kg^{-1} H_2O)	pH_i	Ionic Strength (m)	Temperature (°C)	X_{CO2}	Ca^{2+}_f (m)	TA_f (eq kg^{-1} H_2O)	pH_f	k (millimoles m^{-2} hr^{-1})
KCl 0.05	0.011	0.03		0.05	0.009	5.72	0.07	25.0	1.0	0.014	0.017	5.99	120
KCl 0.1	0.010	0.09		0.10	0.009	5.68	0.13	25.0	1.0	0.017	0.019	5.99	117
KCl 0.5	0.010	0.53		0.54	0.010	5.73	0.57	25.0	1.0	0.017	0.024	6.10	114
KCl 1.0	0.010	1.09		1.10	0.011	5.68	1.12	25.0	1.0	0.018	0.028	6.07	109
KCl 2.0	0.010	2.16		2.17	0.011	5.59	2.20	25.0	1.0	0.019	0.029	6.00	91
KCl 2.0 rep	0.010	2.25		2.26	0.014	5.66	2.29	25.0	1.0	0.018	0.030	5.99	85
KCl 3.0	0.010	3.77		3.77	0.013	5.52	3.80	25.0	1.0	0.019	0.030	5.87	78
NaCl 0.05	0.010		0.04	0.05	0.010	5.71	0.07	25.0	1.0	0.014	0.018	5.95	114
NaCl 0.1	0.011		0.09	0.10	0.010	5.67	0.13	25.0	1.0	0.015	0.019	6.03	104
NaCl 0.5	0.010		0.55	0.56	0.009	5.73	0.59	25.0	1.0	0.017	0.022	6.15	103
NaCl 1.0	0.010		1.12	1.13	0.011	5.69	1.15	25.0	1.0	0.018	0.027	6.10	99
NaCl 2.0	0.010		2.24	2.25	0.011	5.73	2.27	25.0	1.0	0.017	0.025	6.08	69
NaCl 2.0 rep	0.010		2.22	2.23	0.014	5.77	2.26	25.0	1.0	0.017	0.028	6.06	75
NaCl 3.0	0.010		3.35	3.36	0.008	5.65	3.38	25.0	1.0	0.016	0.021	6.06	51
NaCl 4.0	0.010		4.55	4.56	0.011	5.80	4.59	25.0	1.0	0.012	0.019	6.06	45
NaCl 5.0	0.010		5.51	5.52	0.010	5.76	5.55	25.0	1.0	0.013	0.016	5.96	28
NaCl 5.0 rep	0.010		5.53	5.53	0.014	5.68	5.57	25.0	1.0	0.012	0.018	5.77	19
KCl 2.0 T40	0.010	2.21		2.22	0.009	5.54	2.25	40.0	1.0	0.017	0.022	5.95	123
KCl 2.0 T55	0.010	2.23		2.24	0.006	5.56	2.26	55.0	1.0	0.015	0.016	5.97	185
KCl 2.0 p06	0.011	2.24		2.25	0.010	5.74	2.28	25.0	0.6	0.017	0.023	6.12	68
KCl 2.0 p03	0.011	2.24		2.25	0.006	5.87	2.27	25.0	0.3	0.015	0.017	6.30	41
KCl 2.0 p01	0.010	2.25		2.27	0.004	6.13	2.28	25.0	0.1	0.013	0.011	6.56	21
NaCl 2.0 T40	0.010		2.20	2.22	0.009	5.68	2.24	40.0	1.0	0.016	0.021	6.02	73
NaCl 2.0 T55	0.010		2.22	2.23	0.008	5.73	2.25	55.0	1.0	0.014	0.016	6.05	123
NaCl 2.0 T70	0.010		2.23	2.24	0.007	5.77	2.26	70.0	1.0	0.013	0.013	6.04	174
NaCl 2.0 T85	0.012		2.24	2.26	0.006	5.90	2.28	85.0	1.0	0.013	0.009	6.08	313
NaCl 2.0 p06	0.010		2.20	2.21	0.010	5.90	2.24	25.0	0.6	0.015	0.021	6.22	43
NaCl 2.0 p03	0.010		2.20	2.21	0.008	6.06	2.24	25.0	0.3	0.014	0.016	6.37	30
NaCl 2.0 p01	0.009		2.21	2.22	0.005	6.28	2.24	25.0	0.1	0.013	0.011	6.58	22
NaCl 5.0 T40	0.007		5.51	5.51	0.009	5.66	5.53	40.0	1.0	0.014	0.013	5.84	30
NaCl 5.0 T55	0.007		5.42	5.43	0.006	5.81	5.45	55.0	1.0	0.011	0.010	5.98	47
NaCl 5.0 p06	0.010		5.42	5.44	0.006	5.82	5.45	25.0	0.6	0.013	0.012	6.10	17
NaCl 5.0 p03	0.010		5.46	5.48	0.004	5.96	5.49	25.0	0.3	0.012	0.009	6.26	12
NaCl 5.0 p01	0.010		5.47	5.49	0.003	6.28	5.50	25.0	0.1	0.011	0.005	6.53	8

Linear least squares fits of the rate as a function of $(1-\Omega_{calcite})$ typically yielded R^2 values of 0.98 or greater over the undersaturation range investigated although k may not be first order over a wider range of undersaturation. At constant pCO_2 (1 atm), T (25 °C) and initial $m_{Ca^{2+}}$ (~0.01 molal) increased I served to depress k in both KCl and NaCl solutions (Figure 2.2).

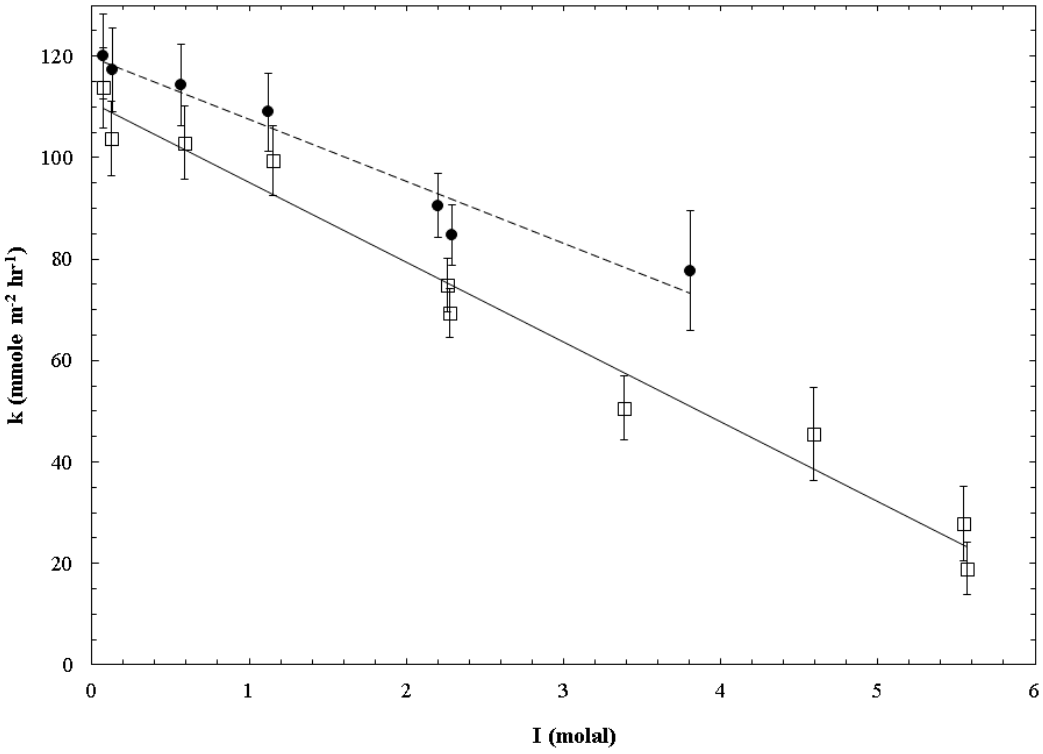

Figure 2.2. k (mmole m^{-2} hr^{-1}) as a function of I (molal scale) for KCl (●) and NaCl (□). As I increases, the experimental and predicted dissolution k decreases for both solutions.

The effect of pCO_2 (Figure 2.3) on the dissolution kinetics of calcite was investigated by measuring the dissolution rate of calcite in three sets of solutions (KCl 2.0 and NaCl 2.0 with I ≈ 2.2m and NaCl 5.0 with I ≈ 5.5m) at constant T (25 °C) and

initial $m_{Ca^{2+}}$ (~ 0.01 m) at four different approximate pCO_2: 0.1, 0.3, 0.6 and 1 atm. As pCO_2 was decreased, observed dissolution rates also decreased for both KCl and NaCl solutions although the influence of pCO_2 on dissolution decreased with increasing I.

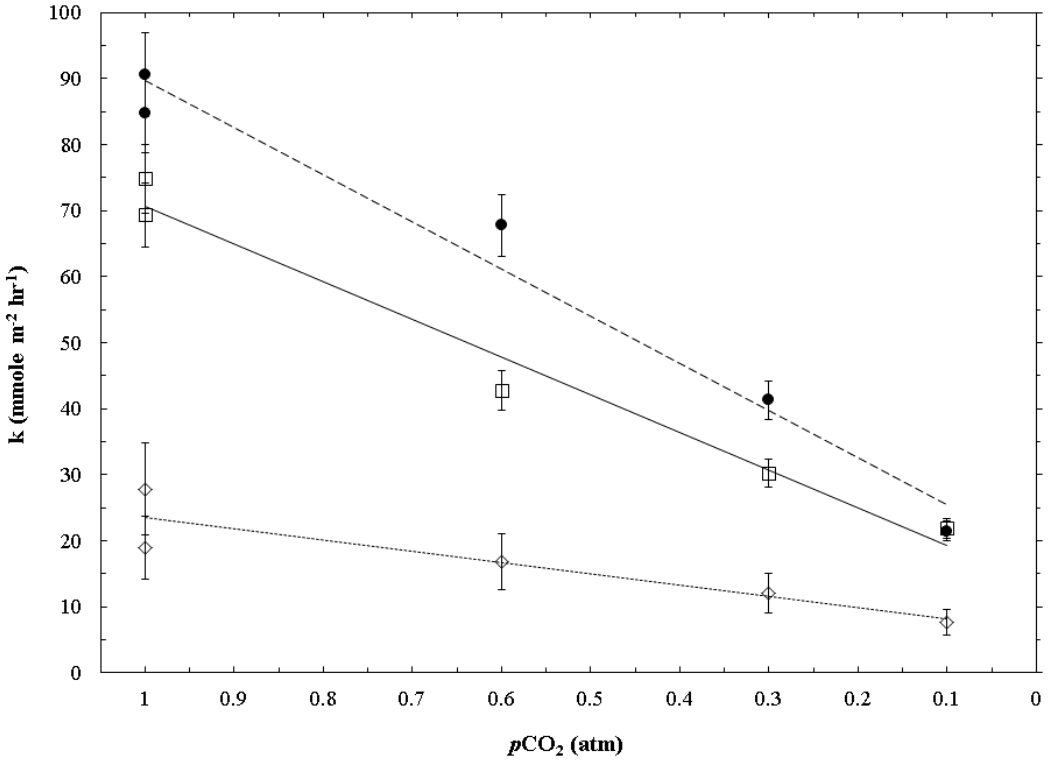

Figure 2.3. k (mmole m^{-2} hr^{-1}) as a function of pCO_2 for KCl 2.0 (●), NaCl 2.0 (□) and NaCl 5.0 (◊) solutions. Rates decrease concomitantly with pCO_2 although this effect seems to be more pronounced at the higher pCO_2 values.

The effect of T on the dissolution kinetics of calcite was investigated by measuring the dissolution rate of calcite in three sets of solutions (KCl 2.0 and NaCl 2.0 with I ≈ 2.2m and NaCl 5.0 with I ≈ 5.5m) at constant pCO_2 (1 atm) and initial $m_{Ca^{2+}}$ (~

0.01 m) at three different T: 25, 40 and 55 °C. Two additional temperatures, 70 and 85 °C were investigated in NaCl 2.0 (I ≈ 2.2m) solutions. Arrhenius plots yielded an activation energy of ~20 ± 2 kJ mol^{-1} with the pre-exponential factor (frequency factor) ranging from 47 to 285 millimole m^2 hr^{-1} depending upon the solution being investigated.

2.5. Discussion

2.5.1 I

Much of the literature available on high I saline waters has been published by the petroleum engineering community and in conventional terminology (Kharaka and Hanor, 2004) results are typically reported in units of total dissolved solids (TDS) as g L^{-1} or g mL^{-1}, which is considered to be synonymous with "salinity". This should not be confused with the formal definition of the practical salinity scale for seawater, where salinity is in fact a unitless ratio but approximates TDS x 10^3. (It should be noted that this is different from the practical salinity scale which is valid for $2 \leq S \leq 42$ UNESCO, 1981a; 1981b). Although this is a convenient unit of measurement, it does not take into account pressure or temperature effects. It should also be remembered that TDS is not precisely linked to I since the ratios of major ions can vary significantly and so does not have much, if any, chemical meaning.

Therefore, results were expressed as a function of I (molal scale) of the reactant solution for both electrolyte solutions (Figure 2.2). At constant pCO_2, T and initial $m_{Ca^{2+}}$, increased I served to depress k in both KCl and NaCl solutions (k_{KCl} = -12.2I +

119.7, $R^2 = 0.951$; $k_{NaCl} = -15.7I + 110.9$, $R^2 = 0.976$). Rates were found to be slower in NaCl solutions although k appears to converge (as should be expected) at low I within experimental error. The offset between the two electrolytes at higher I may be due to the greater interaction of the sodium cation with the calcite surface as implied from sodium ion pairing with carbonate and bicarbonate (e.g. Butler and Huston, 1970; Capewell et al.; 1998; Capewell et al., 1999; Pytkowicz and Hawley, 1974). This is not unexpected for a kinetic electrolyte effect (kinetic ionic-strength effect) as the chemical identity of the supporting electrolyte does not matter at low concentrations since only long-range coulombic forces need to be considered (Muller, 1994).

The specific effect of I on calcite solubility or reaction kinetics has been reported by few investigators. In solubility experiments, both Millero et al. (1984) and Wolf et al. (1989) extrapolated rather consistent thermodynamic pKsp values for calcite regardless of I. Buhmann and Dreybrodt (1987) found that I was only of minor importance in very dilute solutions (<2 mM). In the transport-controlled region far from equilibrium, rates were independent of I in NaCl solutions up to 1m (Pokrovsky et al. 2005). Likewise, salinity (and thus indirectly, I), over the range S = 5 – 44, was found to have little effect on calcite precipitation rates by Zhong and Mucci (1989). Bischoff (1968) found that nucleation rate of calcite increased proportional to $\sqrt{I}$ and Bischoff and Fyfe (1968) found the transformation rate of aragonite to calcite increased with I. Zuddas and Mucci (1998) formulated a precipitation rate expression as a function of carbonate ion concentration only and found that as I was varied ($0.1 \leq I \leq 0.93$), both the reaction order with respect to carbonate (n_2) and the forward reaction rate (k_f) increased. They

suggested this was a result of change in the precipitation mechanism as well as catalysis provided by the additional electrolyte in a similar fashion to flocculation induced by increasing salt concentration. Furthermore, Zuddas and Mucci (1998) reported that both the reaction order with respect to carbonate (n_2) and the forward reaction rate (k_f) increased when the precipitation rates observed by Zhong and Mucci (1989) were expressed as a function of carbonate ion concentration.

Little work has been published on calcite dissolution (Gledhill and Morse, 2006a) or precipitation rates (Zhang and Dawe, 1998) from solutions with I > 1. Zhang and Dawe (1998) suggest that in high salinity waters the precipitation rate of calcite is dependent on $\sqrt{I}$ in a closed system pH-free-drift precipitation experiment when modeled using the Davies and Jones rate equation

$$R_{DJ} = k\left(\sqrt{\Omega} - 1\right)^n \tag{2.6}$$

where R_{DJ} is the precipitation rate normalized to the reacting surface area, k is the precipitation rate constant that is dependent on temperature and overall solution composition, $\Omega_{calcite}$ is the saturation state with respect to calcite and n is the reaction order. In using an open system pH-free-drift method to measure calcite dissolution in geologically relevant Na-Ca-Mg-Cl synthetic brines, Gledhill and Morse (2006a) found dissolution rates to be composition dependent with first order reaction (n = 1) using the general dissolution rate equation. They found that the k could be estimated from a MR model of the form:

$$k = \beta_0 + \beta_1(T) + \beta_2\left(p_{CO_2}\right) + \beta_3(I) + \beta_4(a_{Ca^{2+}}) + \beta_5(a_{Mg^{2+}}) \tag{2.7}$$

where k is the dissolution rate constant, T is temperature, pCO_2 is the partial pressure of carbon dioxide, I is the ionic strength, a_i is the activity of the i^{th} species, and β_i is the coefficient of the i^{th} term. Predicted values from this model for k at 25 °C and 1 atm pCO_2, assuming $a_{Ca^{2+}} = 0.01$, are presented in Figure 2.4 with the previously presented experimental data.

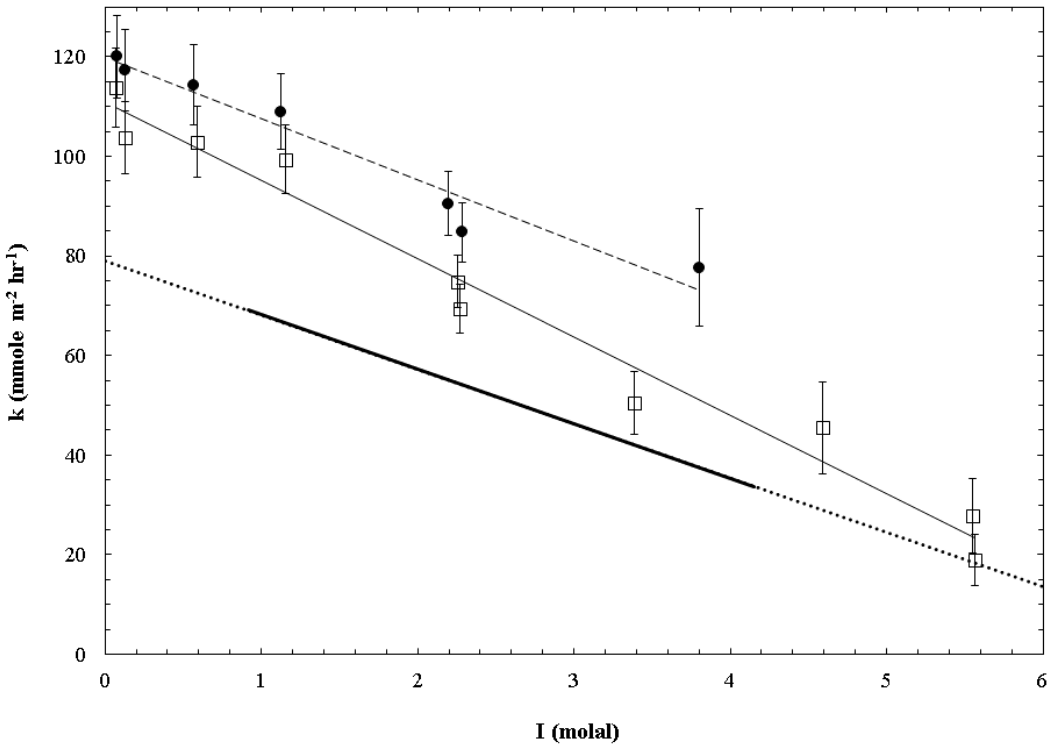

Figure 2.4. k (mmole m^{-2} hr^{-1}) as a function of I (molal scale) for KCl (●), NaCl (□) and predicted values from the MR model of Gledhill and Morse (2006a) where the solid line is used over I investigated in their work and dashed line indicates extrapolation. It should be noted that the $m_{Ca^{2+}}$ concentration investigated in Gledhill and Morse (2006a) was at least four times that of the present study. As I increases, the experimental and predicted dissolution k decreases for all solutions.

The MR model underestimates the experimentally determined values found in the present study for low I although it does appear to converge at higher I with the experimental NaCl data. This concurrence is remarkable because the solutions examined in their investigation were complex Na-Ca-Mg-Cl brines with initial calcium concentrations at least four times that of the present study. The underestimation of the model suggests that doubly charged cations (e.g. Ca^{2+}, Mg^{2+}) have a greater influence at lower I. That is, the range of I in which only the long-range coulombic forces need to be considered is diminished as the amount of doubly charged cations increases.

The seemingly conflicting results of the dissolution studies of Gledhill and Morse (2006a) and the precipitation studies of Zhang and Dawe (1998) and Zuddas and Mucci (1998) may be due to the lowered activity of water (a_{H_2O}) in high I solutions and its effect on the hydration of ions as first suggested by Sjöberg (1978). The dehydration of reactants on the surface of a growing crystal is often a rate controlling step in the crystallization processes (Nancollas and Purdie, 1964) and if dehydration of the cation is an energetic barrier to precipitation (Lippmann, 1973; Arvidson and Mackenzie, 1999) then the dissolution rate may be dependent on the hydration of the calcium ion. This is further supported by Pokrovsky et al. (2002) who argue that carbonate dissolution is controlled by the hydration of surface metal sites at neutral to alkaline conditions (also see Villegas-Jiménez et al., 2009). As I is increased, a_{H_2O} decreases ($a_{H_2O_{KCl}} = -0.029I$; $a_{H_2O_{NaCl}} = -0.040I$) thereby inhibiting the dissolution rate. k was found to decrease as a_{H_2O} decreased with increasing I for both KCl ($k_{KCl} = 428.9a_{H_2O} - 308.3$, $R^2 = 0.975$) and NaCl ($k_{NaCl} = 396.4a_{H_2O} - 288.2$, $R^2 = 0.968$) solutions (Figure 2.5), but this decrease was

not directly proportional to a_{H_2O} (i.e. $k_I = k_{I=0}a_{H_2O}$) and differed for KCl and NaCl solutions (Figure 2.6).

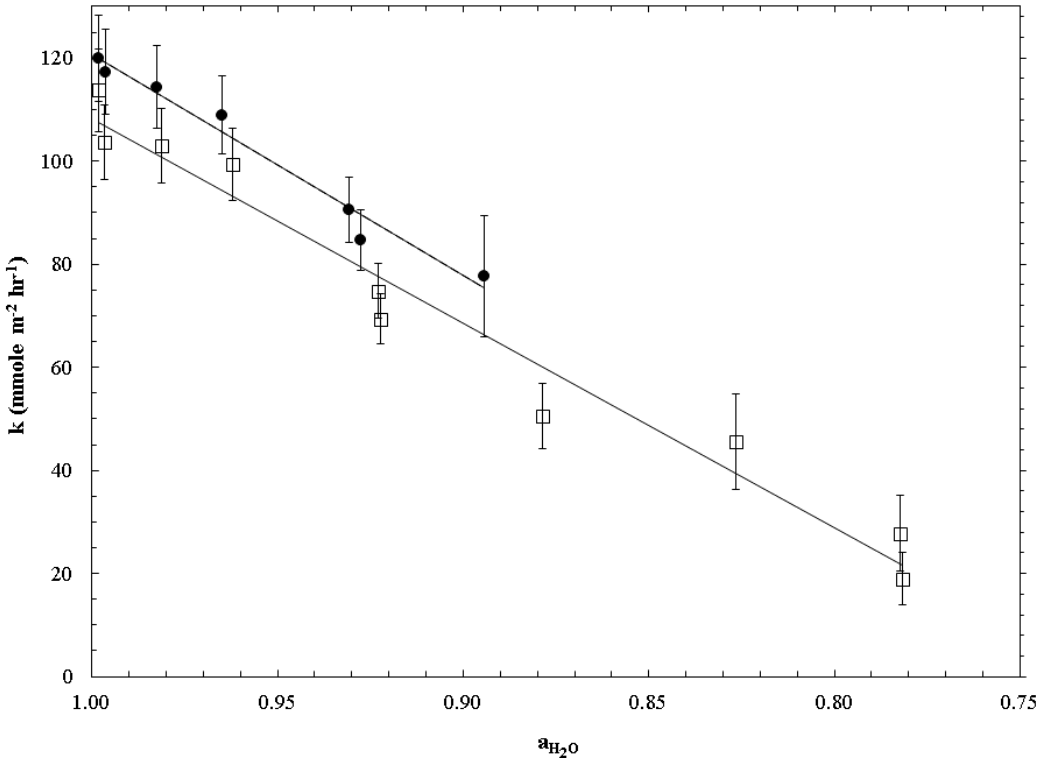

Figure 2.5. k (mmole m^{-2} hr^{-1}) as a function of a_{H_2O}, calculated from EQPITZER (He and Morse, 1993) for KCl (●) and NaCl (□). As a_{H_2O} decreases, k decreases for both solutions.

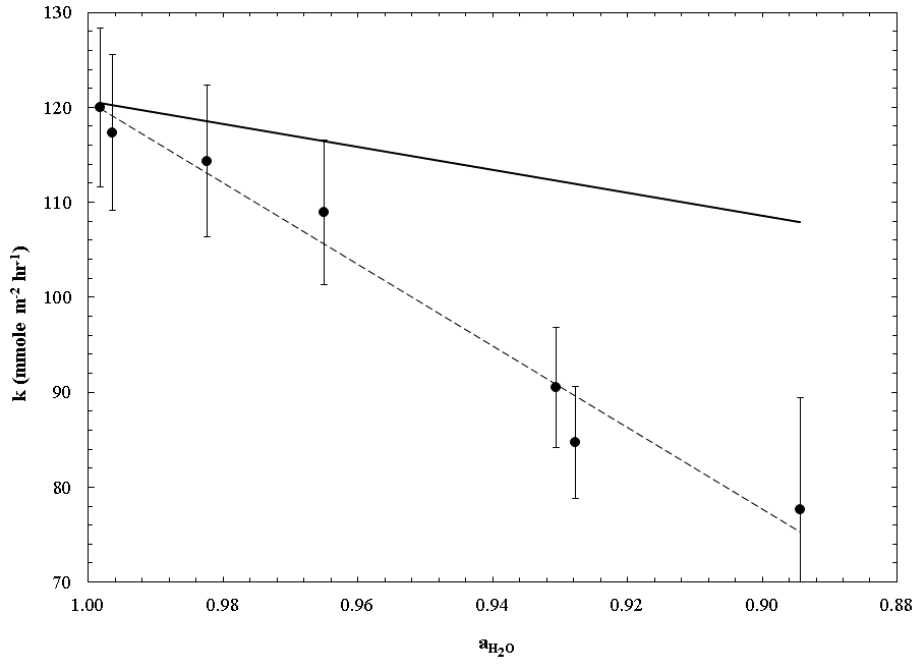

(a)

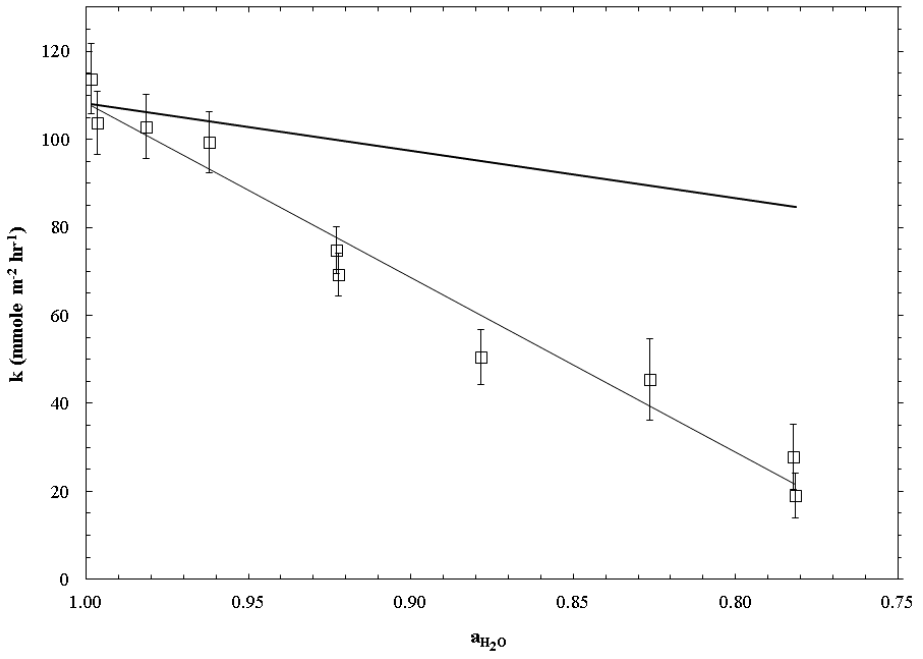

(b)

Figure 2.6. Experimental and predicted k values (mmole m^{-2} hr^{-1}) as a function of a_{H_2O} for KCl (●) and NaCl (□) solutions with predicted values (solid line) where $k_{predicted} = k_0 a_{H_2O}$. Note the different scale for k.

Even though the size of the ions (r_{K^+} = 1.33Å, r_{Na^+} = 0.97Å from Lide, 2007) differs by less than a factor of two, the charge densities ($z\ r^{-3}$) differ by more than 2.5. Consequently, solvent molecules will be bound much more strongly to Na^+ than K^+. This is also supported by the differences in the enthalpies of hydration, $\Delta_{hyd}H^0_{K+}$ = -308 kJ mol^{-1}, $\Delta_{hyd}H^0_{Na+}$ = -391 kJ mol^{-1} (Schmid et al., 2000). This means it is easier for a solvent molecule associated with K^+ to hydrate the calcite surface than one associated with Na^+. However, the change in k for the dissolution of calcite in these solutions is not directly proportional to a_{H_2O}, but decreases about three times as fast as a_{H_2O} decreases (Figure 2.6). This suggests that the fraction of "free" solvent molecules that can hydrate the calcite surface is not simply proportional to a_{H_2O} but rather depends on the number of water molecules associated, both temporarily and permanently, with each ion in solution. As tabulated in Burgess (p.34, 1999), a wide range of hydration numbers are reported in the literature for Na^+ (2-13) and K^+ (1-7). Complicating matters is that reported hydration numbers may include water molecules in both the primary (first layer) and secondary solvent shells (e.g. Di Leo and Marañón, 2005; Mel'nichenko, 2007). Furthermore, it has been suggested that the innermost four water molecules stay in the solvation shell on a longer time scale for K^+ then do eight other water molecules which exchange between the first and second shells (Ramaniah, et al, 1999). Therefore, it is not an easy task to determine the overall number of water molecules "removed" from the bulk solution for each cation.

In a classic paper, Stokes and Robinson (1948) determined hydration numbers for the average effect of all ion-solvent interactions for a number of electrolytes and

found NaCl to be more highly hydrated (3.5) than KCl (1.9) which supports the earlier suggestion that there are less "free" solvent molecules in NaCl solutions compared with KCl solutions of equivalent concentration. This is further supported by the results of Kowacz and Putnis (2008) who found that solvent structure dynamics decreased from KCl to NaCl solutions. For colligative properties of a variety of electrolyte and non-electrolyte solutions, Zavitsas (2001) noted that deviations from ideal behavior in concentrated solutions are removed if the calculated mole fraction of solute is corrected for bound waters. Adapting that argument to the present results, if the mole fraction of total water is:

$$X_{H_2O} = \frac{\text{mole } H_2O}{\text{mole } H_2O + \sum \text{mole solute}_i} \tag{2.8}$$

then the mole fraction of "free" water ($X_{\text{"free" } H_2O}$)is:

$$X_{\text{free } H_2O} = \frac{\text{mole } H_2O - \sum n_i(\text{mole solute}_i)}{\text{mole } H_2O + \sum \text{mole solute}_i} \tag{2.9}$$

and the mole fraction of "bound" water ($X_{\text{"bound" } H_2O}$) is:

$$X_{\text{bound } H_2O} = \frac{\sum h_i(\text{mole solute}_i)}{\text{mole } H_2O + \sum \text{mole solute}_i} \tag{2.10}$$

where h_i is the hydration number of each salt, and X_{H_2O} is the sum of $X_{\text{"free" } H_2O}$ and $X_{\text{"bound" } H_2O}$. For the purposes of this manuscript, mole solute was considered to be the mole of each individual chloride salt (e.g. $CaCl_2$, KCl, NaCl). Using freezing point depression data, Zavitsas (2001) found hydration values of $h_{Na^+} = 3.9 \pm 0.5$; $h_{K^+} = 1.7 \pm$

0.5; $h_{Mg^{2+}} = 13 \pm 2$; $h_{Ca^{2+}} = 12 \pm 2$ which was further refined to 12 ± 0.8 (Zavitsas, 2005) all of which agree relatively well with those postulated by Stokes and Robinson (1948). h was assumed to be predominantly due to the cation and thus h_{Na^+} and h_{K^+} values given above are the results of combination of three different halide (Cl^-, Br^-, I^-) solution sets respectively (Zavitsas, 2001). Although some investigators have reported a dependency of the hydration number on concentration (e.g. Driesner, et al., 1998; Soper and Weckström, 2006; Du et al., 2007), for the purposes of this manuscript the hydration numbers employed have been assumed to remain constant regardless of concentration or temperature. Furthermore, calcium values were ignored as they are one to two orders of magnitude less than the concentration of the supporting electrolyte and any contribution is negligible. In addition, as the initial calcium concentrations are all approximately 0.01 molal, any error by their lack of inclusion would be a relatively systematic error and not affect the comparative results.

Using the values of Zavitsas (2001; 2005) to calculate $X_{"free" H_2O}$ removes the offset between the two electrolyte solutions within experimental uncertainty (Figure 2.7) where $k_{KCl} = 268.7X_{"free" H_2O} - 148.5$, $R^2 = 0.955$ and $k_{NaCl} = 196.4\ X_{"free" H_2O} - 84.6$, $R^2 = 0.977$. Furthermore, the standard error of the constant, coefficient and y estimate are all reduced when k is expressed as a function of $X_{"free" H_2O}$ as opposed to a_{H_2O}. It should be noted that the uncertainty in $X_{"free" H_2O}$ increases with increasing I.

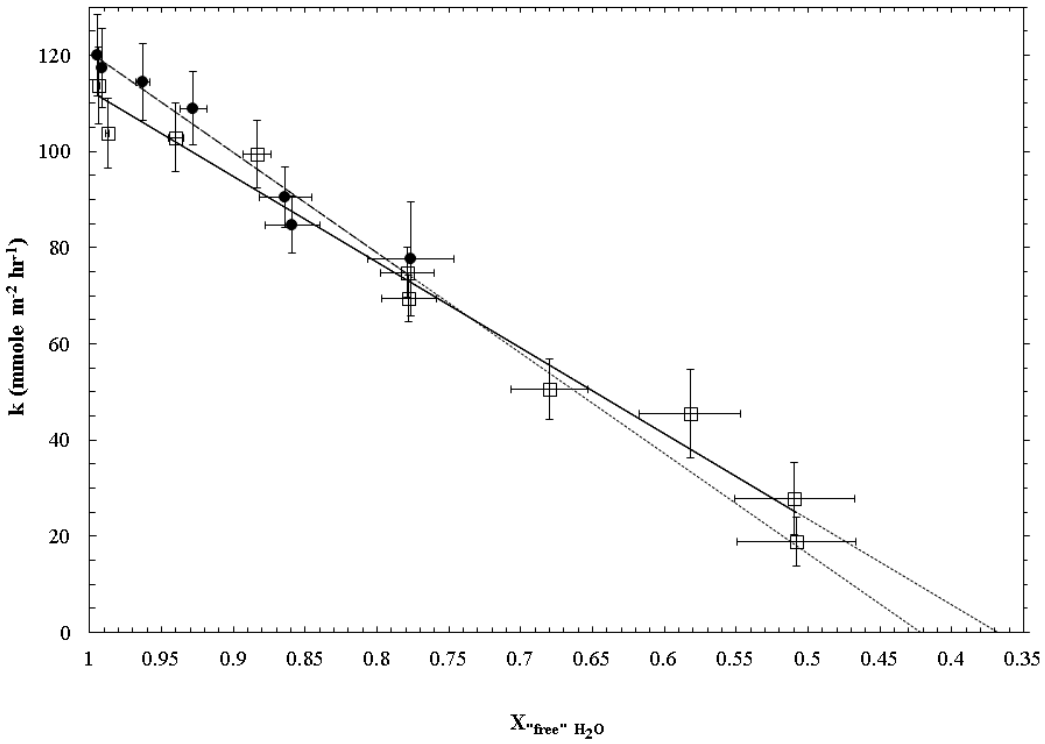

Figure 2.7. k (mmole m^{-2} hr^{-1}) as a function of $X_{"free" H_2O}$ in KCl (●) and NaCl (□) solutions.

This data (Figure 2.7) indicates that the proportion of "free" solvent has a major influence on calcite mineral dissolution. The intercept of the x-axis (k = 0) is calculated to be 0.55 for KCl and 0.43 for NaCl which presents a problem for the model in that under the present conditions (low calcium, inhibitor-free, pCO_2 = 1 atm electrolyte solutions at 25 °C), dissolution could not occur in undersaturated solutions when $X_{"free" H_2O} < \sim$ 45-55%. If true, then under these experimental conditions dissolution could be prevented (or at least greatly depressed) by the addition of inert salts to undersaturated solutions (e.g. Kowacz and Putnis, 2008). Consequently, it must be stressed that this is a

prediction based on extrapolated data that cannot be tested in the present solutions because KCl and NaCl are not soluble enough to reach the required I. The larger hydration numbers of $CaCl_2$ (12.0; 12 ± 0.8) and $MgCl_2$ (13.7; 13 ± 2) reported by Stokes and Robinson (1948) and Zavitsas (2001; 2005) lend further support to the earlier idea that doubly charged ions have a more significant influence at lower I which may help to explain the underestimation of the MR model of Gledhill and Morse (2006a). Data in other simple electrolyte solutions (e.g. LiCl, RbCl, etc.) will need to be obtained to test the hypothesis that (at constant T and pCO_2) the overall rate may be controlled by the fraction of "free" solvent.

2.5.2 pCO_2

A strong pCO_2 dependence was observed ($k_{KCl\ 2.0} = 71.2pCO_2 + 18.4$, $R^2 = 0.975$; $k_{NaCl2.0} = 57.0pCO_2 + 13.6$, $R^2 = 0.977$; $k_{NaCl\ 5.0} = 17.1pCO_2 + 6.4$, $R^2 = 0.829$), where a three to four fold decrease in k was measured when pCO_2 was reduced from 1 to ~ 0.1 atm regardless of the supporting electrolyte (Figure 2.3). Again, there is a slight offset between the potassium and sodium solutions of similar I (I ≈ 2.2 m). The inhibitory effects of the salts also appear to exhibit CO_2 dependence as dissolution rates became progressively more depressed with increasing I. The effect of I on the absolute value of k was more pronounced at the higher partial pressures and was inconsequential at 0.1 atm.

Previous experimental results on the effect of pCO_2 on dissolution rates have been mixed. Berner and Morse (1974) found calcite dissolution rates at $4 < pH < 6.8$ in

$NaCl$-$CaCl_2$ solutions of I approximately that of seawater (I ~ 0.7 mol kg^{-1} solvent) to be independent of pCO_2 in the range 0.003 – 1 atm. Other investigators (e.g., Sjöberg, 1978; Busenberg and Plummer, 1986;) have demonstrated a rate dependence on CO_2 for partial pressures above 0.1 atm and for pH values greater than about 4.5 when the rate is dominated by surface control reactions. Pokrovsky et al. (2005) found that, in the transport-controlled region far from equilibrium, solutions of up to 1 M NaCl also showed pCO_2 dependence with dissolution rates increasing by a factor of 3 from 1 - ~20 atm pCO_2. In solutions of I ranging from 0.1 to 1, Zuddas and co-workers also found pCO_2 to increase calcite dissolution rates (Charara et al., 2005; O. Lopez, 2007 personal communication). Van Cappellen et al. (1993) attributed a dissolution rate CO_2 dependence to the formation of carbonate complexes with surface lattice calcium ions. According to their surface complexation model, the CO_2-promoted dissolution rate is directly proportional to the concentration of sites and is an example of ligand promoted dissolution in which the formation of the bicarbonate surface complex increases the rate of detachment of Ca^{2+} from surface positions. Gledhill and Morse (2006a) found the effect of pCO_2 to be approximately equivalent (in standardized coefficients) and opposite in nature to the moderate inhibitory effect of I in their MR model. Despite assuming relatively high I, in which earlier predicted k values were in close agreement with present NaCl experimental values at pCO_2 = 1 atm (Figure 2.4), the MR model fails at lower pCO_2 values (Figure 2.8) predicting negative values for k and illustrates the danger of extrapolating far from the experimental domain in which the model was devised. On the other hand, the predicted negative values by the MR model may be an

indication that k is no longer linear with respect to pCO_2 at high I and low pCO_2 for solutions with similar makeup to their complex solutions.

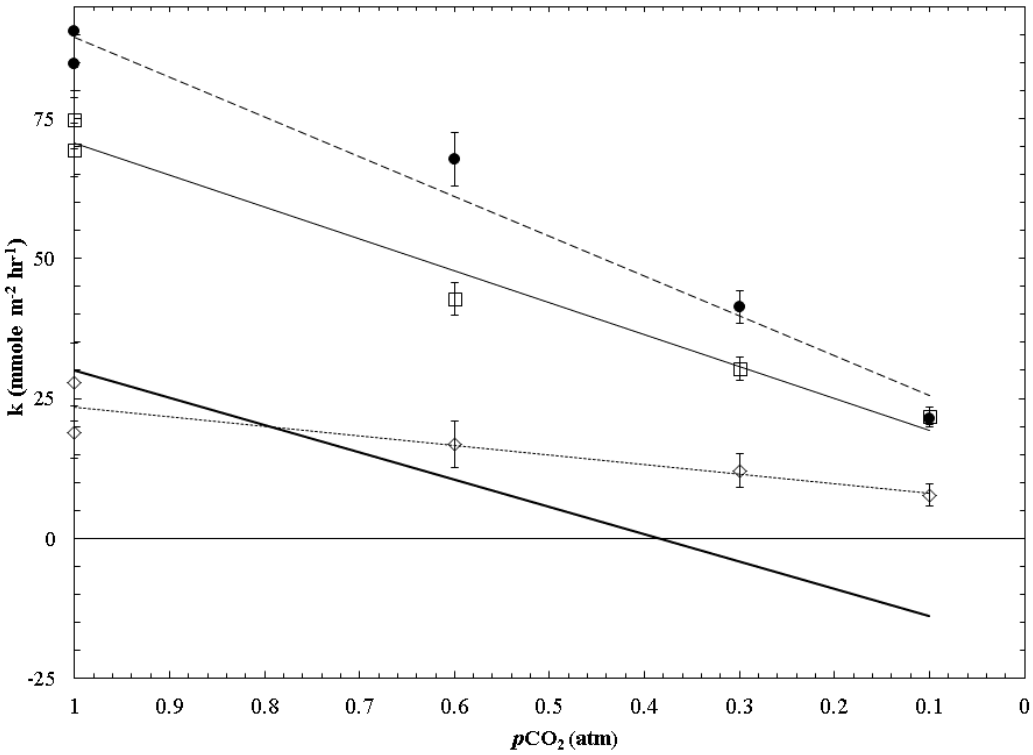

Figure 2.8. k (mmole m^{-2} hr^{-1}) as a function of pCO_2 for KCl 2.0 (●), NaCl 2.0 (□), NaCl 5.0 (◊) solutions and the solid line indicates predicted values from the MR model of Gledhill and Morse (2006a). It should be noted that the $m_{Ca^{2+}}$ concentration investigated in Gledhill and Morse (2006a) was at least four times that of the present study. As I increases, the experimental and predicted dissolution k decreases for all solutions although the MR model fails at low of pCO_2 predicting negative values for k.

Following up on the earlier proposed importance of the fraction of "free" solvent, k is expressed as a function of $X_{\text{"free"}\ H_2O}$ for the four different approximate pCO_2 values investigated in this work (Figure 2.9). Rates increase concomitantly with experimental pCO_2 over the range investigated ($k_{1atm} = 189.8X_{\text{"free"}H_2O} - 81.8$, $R^2 = 0.986$; $k_{0.6atm} = 142.3X_{\text{"free"}H_2O} - 65.0$, $R^2 = 0.928$; $k_{0.3atm} = 84.1X_{\text{"free"}H_2O} - 35.5$, $R^2 = 0.980$; $k_{0.1atm} = 44.6X_{\text{"free"}H_2O} - 16.6$, $R^2 = 0.931$), with k values converging as $X_{\text{"free"}\ H_2O}$ is depressed, and perhaps more intriguing, the range (0.42 – 0.46) of the $X_{\text{"free"}H_2O}$ intercept (k = 0), for the three greatest pCO_2 values investigated (0.3, 0.6, 1atm), lies within the range (0.43-0.55) found earlier. The results at pCO_2 = 0.1atm return a value for the intercept of the $X_{\text{"free"}H_2O}$ of approximately 0.37. Again, this indicates that there is a minimum critical threshold for $X_{\text{"free"}H_2O}$ in undersaturated inhibitor-free solutions over the pCO_2 range of 0.1 – 1 atm at 25 °C.

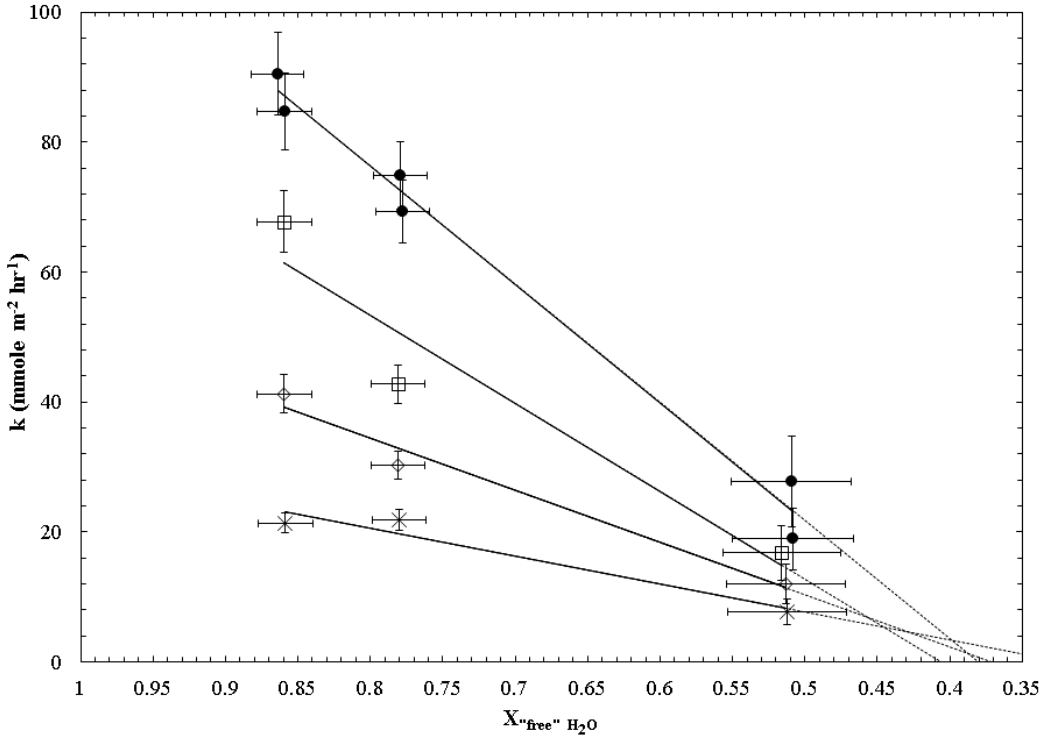

Figure 2.9. k (mmole m^{-2} hr^{-1}) as a function of $X_{"free" H_2O}$ for the four pCO_2 values investigated at 25 °C: 1 (●), 0.6 (□), 0.3 (◊) and 0.1 (*) atm pCO_2. For each series, the data points, from left to right, are from KCl 2.0 ($X_{"free" H_2O} \approx 0.88$), NaCl 2.0 ($X_{"free" H_2O} \approx 0.82$) and NaCl 5.0 ($X_{"free" H_2O} \approx 0.59$) solutions. As $X_{"free" H_2O}$ decreases, the k range ($k_{0.1atm} - k_{1atm}$) decreases.

The same treatment was applied to the experimental data of Gledhill and Morse (2006a) where all data, with the exception of two runs at elevated temperatures, were used resulting in four series, pCO_2 = 1atm, pCO_2 = 1atm with SO_4^{2-} (~0.01 m), pCO_2 = 0.5atm and pCO_2 = 0.1atm (Figure 2.10). The intercept of the $X_{"free"H_2O}$ was approximately 0.46 for results at 25 °C under pCO_2 = 0.5 and 1atm, even in the presence

of the potent inhibitor sulfate (($k_{1atm\text{-}GM} = 152.6X_{"free"H_2O} - 69.3$, $R^2 = 0.980$; $k_{1atm\text{-}SO_4^{2-}\text{-}GM} = 107.7X_{"free"H_2O} - 49.3$, $R^2 = 0.997$; $k_{0.5atm\text{-}GM} = 91.1X_{"free"H_2O} - 41.9$, $R^2 = 0.896$). The pCO_2 = 0.1 atm results return a value close to zero for the $X_{"free"H_2O}$ intercept although the correlation coefficient is much less ($k_{0.1atm\text{-}GM} = 15.9X_{"free"H_2O} + 0.7$, R^2 = 0.741) than the other series. Despite the complexity of their solutions ($m_{Ca^{2+}} \approx 0.04 - 0.36$ m, $m_{Mg^{2+}} \approx 0.02 - 0.13$ m), the same approximate value for the intercept of the $X_{"free"H_2O}$ was obtained as was observed with the present experimental data. This further supports the hypothesis that some sort of critical threshold has been crossed once $X_{"free"H_2O}$ is less than ~45-55%. The present results clearly show that at constant T, pCO_2 positively influences the dissolution rate from 0.1-1atm pCO_2, although I becomes the dominant control on the dissolution kinetics of calcite at high I.

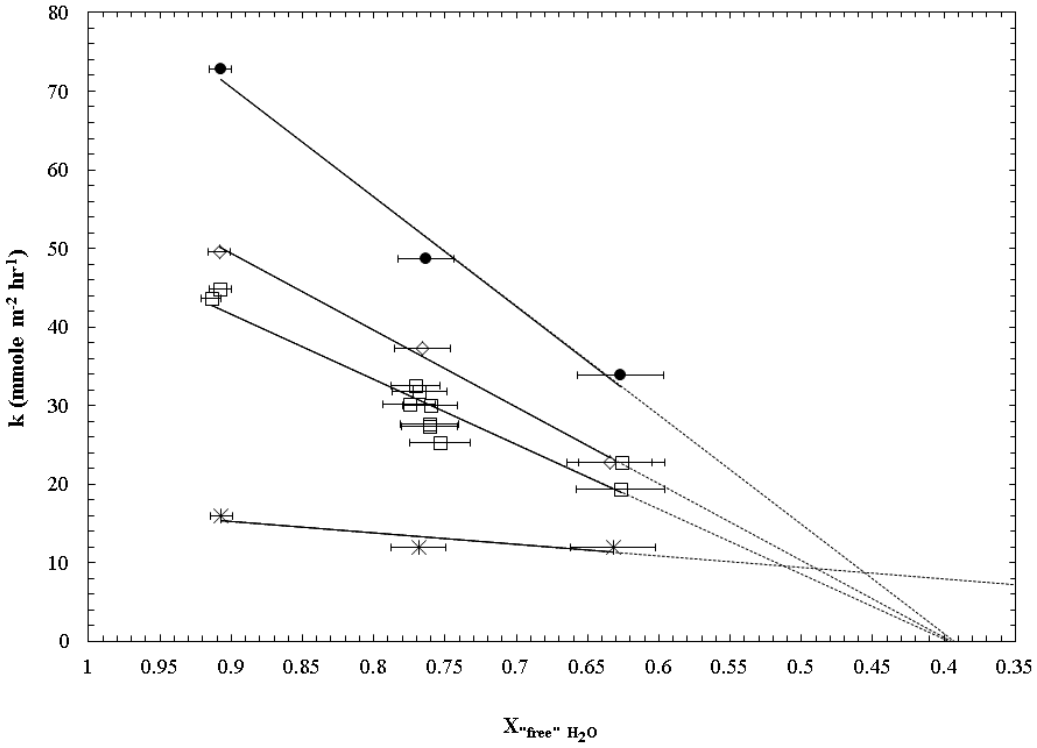

Figure 2.10. k (mmole m^{-2} hr^{-1}) as a function of $X_{"free" H_2O}$ for data at 25 °C from Gledhill and Morse (2006a) with pCO_2 values: 1 (●), 0.5 (□), 1 (with SO42- ≈ 0.01m) (◊) and 0.1 (*) atm pCO_2. As $X_{"free" H_2O}$ decreases, the range of k values (k0.1atm – k1atm) decreases.

2.5.3 Temperature

Temperature was found to positively influence the dissolution rate. Rates were found again to be faster in KCl than NaCl solutions. The temperature dependence of the reaction rate is often assumed to follow the classic Arrhenius equation:

$$k = Ae^{-\frac{E_a}{RT}} \tag{2.11}$$

where k is the rate constant, A is the preexponential (or frequency) factor, Ea is the Arrhenius activation energy, R is the gas constant and T is the thermodynamic (K) temperature. This equation also may be rearranged in to the more familiar linear equation of a line:

$$\ln(k) = \ln(A) - \frac{E_a}{RT} \tag{2.12}$$

where the Arrhenius factors (A and E_a) may be easily determined from a least squares regression line of a plot of ln(k) versus T^{-1}. Arrhenius plots of the data yielded an activation energy of ~20 ± 2 kJ mol^{-1} independent of the cation or I of the solution being investigated. There are a wide range of activation energies reported for calcite dissolution (about 8–60 kJ mol^{-1}; see Morse and Arvidson, 2002 for review). In dilute solutions far from equilibrium where diffusion-controlled processes dominate, most reported values are close to 10 kJ mol^{-1} (e.g., Plummer et al., 1978; Sjöberg, 1978; Salem, 1994). However, larger values are believed to be typical of surface-controlled processes (Lasaga, 1998). The value determined in this study is in excellent agreement with previously reported data of E_a = 19 ± 4 kJ mol^{-1} (Alkattan et al., 1998) and 20 ± 1 kJ mol^{-1} (Gledhill and Morse, 2006a). The pre-exponential factor (frequency factor) was found to range from 47 to 285 mmole m^2 hr^{-1} and decreased with an increase in I. These results clearly show that the influence of temperature is diminished as I is increased.

Although the determination of the activation energy is relatively straightforward, its chemical meaning is somewhat ambiguous as the mechanism that dominates the

dissolution process may vary somewhat with temperature (Lasaga and Lüttge, 2004). That is, the activation energy experimentally determined "most likely does not reflect the activation energy for the breaking of one particular bond or a suite of bonds" (Lüttge, 2006), but is some statistical average of all of the activation energies over the temperature range investigated. Despite the ongoing discussion in the literature, the temperature results presented clearly show that the influence of temperature wanes as I is increased. This could indicate that there may be some I threshold above which increases in temperature will have a negligible impact on the dissolution rate.

Temperature results were also expressed as a function of $X_{"free"\ H_2O}$ for 25, 40 and 55 °C results (Figure 2.11). k increased concurrently with temperature although the influence diminishes as $X_{"free"H_2O}$ decreases ($k_{25°C} = 189.8X_{"free"H_2O} - 81.8$, $R^2 = 0.986$; $k_{40°C} = 252.0X_{"free"H_2O} - 114.4$, $R^2 = 0.897$; $k_{55°C} = 392.1X_{"free"H_2O} - 177.5$, $R^2 = 0.952$). Additionally, the intercept of $X_{"free"H_2O}$ (k = 0) of each temperature series was found to range from 0.43 – 0.45 which agrees well with the values found previously. This again suggests that ~45-55% $X_{"free"H_2O}$ is some sort of threshold required in undersaturated inhibitor-free solutions over the temperature range of 25-55 °C at pCO_2 of 1 atm.

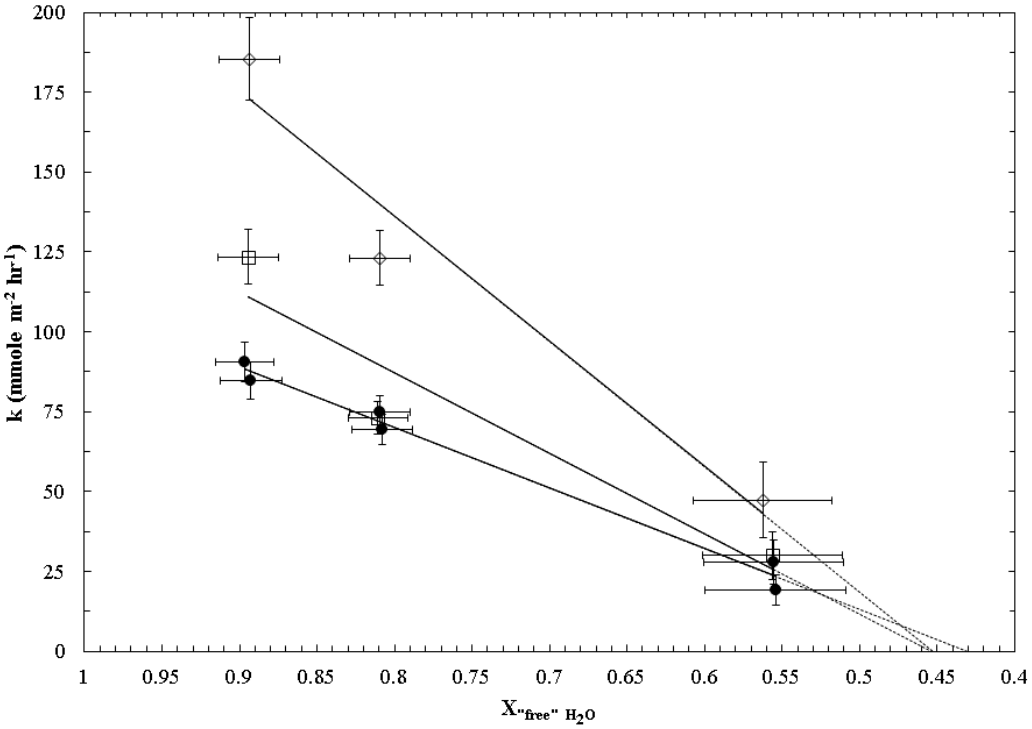

Figure 2.11. k (mmole m^{-2} hr^{-1}) at pCO_2 = 1 atm as a function of $X_{"free" H_2O}$ for three temperature values investigated, 25 (●), 40 (□), and 55 (◊) °C. For each series, the data points, from left to right, are from KCl 2.0 ($X_{"free" H_2O} \approx 0.88$), NaCl 2.0 ($X_{"free" H_2O} \approx 0.82$) and NaCl 5.0 ($X_{"free" H_2O} \approx 0.59$) solutions. As $X_{"free" H_2O}$ decreases, the range of k values (k25 °C – k55 °C) decreases.

2.5.4 Mole Fraction of "Free" Water

$X_{"free" H_2O}$ has been postulated to play a significant role in the dissolution kinetics of calcite as water becomes limiting regardless of the temperature (25-55 °C) or the pCO_2 (0.1-1 atm) examined in this study. This is an unforeseen result as only the rate equation of Plummer et al. (1978) has an explicit water term (although other rate

equations indirectly account for water through the use of activities rather than concentrations). As previously discussed, there appears to be a critical minimum $X_{"free"H_2O}$ (~45-50%) needed in order for dissolution to proceed in undersaturated solutions. Thermodynamically, this may imply that in very concentrated solutions, the Gibbs free energy of the system with separate components (dissolved salts, water and solid calcite) is lower than that of the solution (dissolved salts, water, dissolved calcite, and remaining solid calcite). That is, the energy cost to hydrate the calcite surface and solvate the resultant ions released into solution in these highly saline waters is too great for dissolution to occur. It may be in these highly concentrated (and thus highly ordered) salt solutions that the decrease in entropy from calcite dissolution is too large and thus, the dissolution process is entropy forbidden. Computational calculations demonstrate an ordering of the solvent near the calcite surface limiting water diffusion (e.g. Kerisit, and Parker, 2004) suggesting the importance of the entropy term. From a kinetic viewpoint, the mobility of the solvent molecules is hampered with increasing salt concentration particularly for smaller ions (e.g. Du et al., 2007). As the amount of "free" solvent decreases, the interactions between "free" water molecules and the calcite surface will become less frequent slowing the rate of dissolution. This may mean that highly concentrated solutions are no longer in the surface controlled regime but in the transport regime and thus reactions need to be carried out on much longer time scales since diffusion will be hindered.

An alternate simple explanation is that the extrapolated critical minimum could simply be an artifact of the data as it has been assumed that the k is linearly correlated

with the various independent variables. Quite possibly, the k may exponentially decay with respect to the independent variables which would explain the convergence of the temperature and pCO_2 data at high I. As most previous experimental investigations have occurred in solutions with I < 1, it could be that a majority of data reported in the literature has occurred in the linear portion of the exponential decay curve. If this were the case, a minimum (albeit slow) dissolution rate in inhibitor free, low calcium solutions would be expected rather than no dissolution whatsoever.

It has been demonstrated that the extent and rate of restructuring (etch pits, islands) of the calcite surface is directly dependent on relative humidity (RH) (e.g. Hausner et al., 2007; Kendall and Martin, 2007; Stipp et al., 1996; Stipp, 1999) which may be due to the inverse relationship of RH and calculated surface energies (de Leeuw and Parker, 1997). Using scanning polarization microscopy (SPM), Kendall and Martin (2005) observed a transition from a structured 2-dimensional heteroepitaxial water layer (RH < 55%) to a 3-dimensional water layer with complete solvation shells (RH > 55%) on the calcite surface. Infrared spectroscopy, specifically ATR-FTIR, was used to infer such a transition at RH ~55% due to observed changes in the O-H stretching region as RH was increased (Al-Abadleh et al., 2005). Hausner et al., (2007) reported a sharp increase in the adhesion of the AFM tip to the calcite surface between RH = 40-45%, which was attributed to the transition from a 2- to 3-dimensional water layer. These independent observations of the calcite-water surface all suppose a transition from a 2- to 3-dimensional water layer at RH (40-55%) which is in rather good agreement with the critical minimum $X_{"free"H_2O}$ (~45-55%) postulated in this study. Assuming that

$X_{"free"H_2O}$ is the bulk solution equivalent to RH, the concurrence of results suggests that the critical minimum $X_{"free"H_2O}$ postulated in this work may be related to the calcite-water interface where surface ion density and mobility is likely to be low. It may be that the extrapolated critical minimum $X_{"free" H_2O}$ indicates a transition from an adsorbed water layer on the calcite surface more than one monolayer thick (3-dimensional) to one where the calcite surface may have only one complete monolayer of adsorbed water or less (2-dimensional). Furthermore, the qualitative observations of calcite surface restructuring as a function of RH suggests that the slower rates observed in this study at lower $X_{"free" H_2O}$ may be due to the decreased surface ion mobility and/or density. Coupled together, this suggests that the microscopic observations of the calcite-water interface are manifested in the macroscopic bulk solution properties observed in this study.

Regardless of the true cause, results from the present work, as well as data from Gledhill and Morse (2006a), indicate that a critical minimum lies in the approximate range of $X_{"free"H_2O}$ = 45-55%. Although this postulate cannot be tested in the present solutions as KCl and NaCl are not soluble enough, it should be possible with the use of the more soluble, highly hydrated LiCl salt. Rearrangement of equation 2.9 and substitution of n = 6.6 ± 0.6 (Zavitsas, 2001) to solve for the required molality of LiCl to give $X_{"free"H_2O}$ = 45-55% yields 3.5-4.4 m which is much less than that of a saturated solution ($m_{LiCl_{saturated}}$ = 19.2 from Hamer and Wu, 1972).

Although this discussion is interesting from a purely theoretical viewpoint, if true, this limit may also apply in natural waters. Hanor (1994) reported that the major dissolved cations (Na^+, K^+, Mg^{2+}, Ca^{2+}) in southwest Louisiana Gulf Coast reservoirs varies systematically with chloride (Cl^-). Morse et al. (1997) provided polynomial equations to predict ion concentrations (mol L^{-1}) as a function of TDS (mg L^{-1}). Assuming the calculated concentration of each cation is equivalent to the molality of the respective chloride salt (which is an underestimation of the true molality), $X_{"free"\ H_2O}$ was determined using the hydration numbers of Zavitsas (2001; 2005) and if the minimum $X_{"free"H_2O}$ postulated in this study is correct, then undersaturated conditions should persist (or dissolution should be greatly slowed) once the TDS has surpassed ~280-330 g L^{-1} in the temperature range 25-55 °C and pCO_2 range 0.1 – 1atm (Figure 2.12). This may be useful in understanding and predicting the interaction and reactivity of the host carbonate minerals in subsurface reservoirs to the injection of CO_2 although much work needs to be completed at elevated temperatures and pressures.

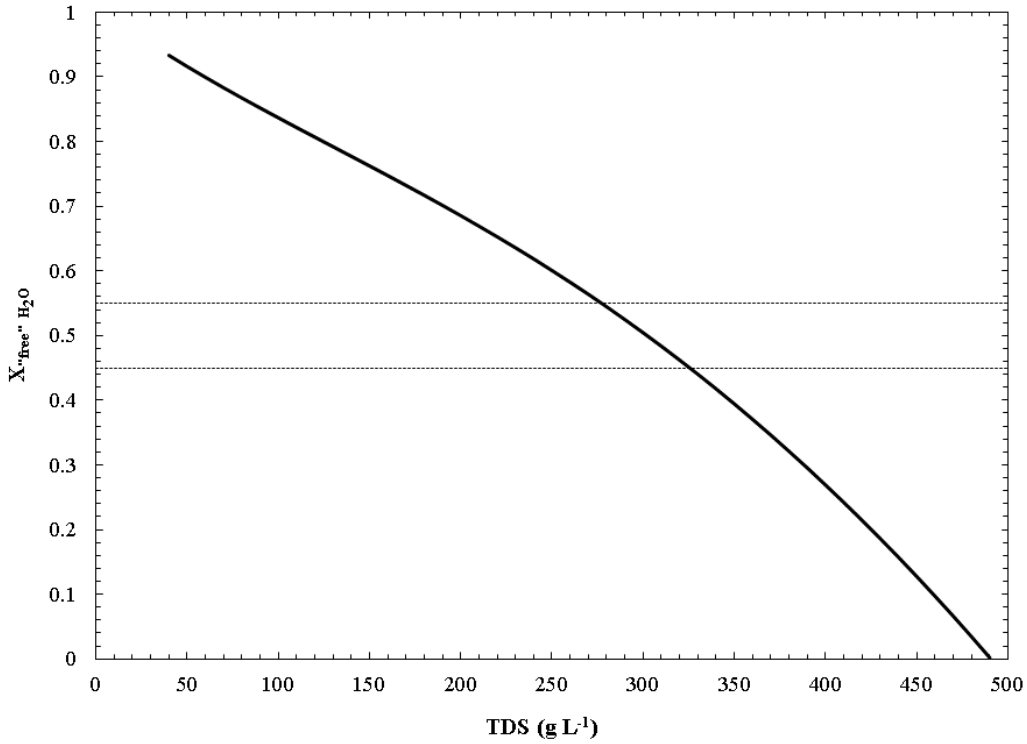

Figure 2.12. Predicted $X_{"free"\ H_2O}$ as a function of TDS (g L^{-1}) assuming salt concentrations (mol L^{-1}) predicted by Morse et al. (1997) are equivalent to molality $X_{"free"\ H_2O}$ (which is an underestimate of the true molality). Dashed lines are provided for $X_{"free"\ H_2O}$ = 0.45 and 0.5.

2.5.5 Multiple Regression Model $X_{"free"\ H_2O}$

As k has been shown to be composition and temperature dependent, an attempt was made to elucidate the primary variables most responsible for determining k. A stepwise MR analysis was performed using the statistical software SPSS® v. 16.0 for Windows® in which all possible combinations of independent variables (I, $m_{Ca^{2+}}$, m_{Cl^-},

m_{K^+}, $m_{Mg^{2+}}$, m_{Na^+}, pCO_2, T, $X_{"free" H_2O}$) were considered. All data in the present study as well as data used in the MR model of Gledhill and Morse (2006a) were initially included in the MR analysis. Outliers, NaCl 2.0 T85 and KCl 2.0 T55, were identified as having standardized residuals outside the range of ± 3, and were thus removed from the analysis. A slight positive autocorrelation of the regression was indicated by the calculated Durbin-Watson coefficient (1.307). The t-test statistics were found to be significant (<0.001), condition indices for collinearity were less than 20 and the variance inflation factors (VIF) less than 1.05 for each predictor, indicating that severe collinearity was not a factor (Belsley et al., 2005). Removal of these outliers yielded (adjusted $R^2 = 0.862$, $p < 0.001$) a predictive equation for k:

$$k_{pred} = \beta_0 + \beta_1 T + \beta_2 pCO_2 + \beta_3 X_{"free" H_2O} \quad (2.13)$$

where k is the predicted dissolution rate constant, T is the temperature, pCO_2 is the partial pressure of carbon dioxide, $X_{"free" H_2O}$ is the mole fraction of free water calculated according to equation 9, and β_i is the coefficient of the i^{th} term. β values (unstandardized coefficients) for predicting k (Figure 2.13) are provided (Table 2.2). As the units of the predictors are different, standardized coefficients are typically used to determine the relative importance of the individual predictors on the dependent variable and are provided (Table 2.2). Using the standardized coefficients for the direct comparison of the predictors, indicate the relative effects on k are $X_{"free" H_2O} > pCO_2 >$ T. However, it should be noted that there is some debate as to the usefulness of standardized

coefficients (e.g. Bring, 1994; Kim and Ferree, 1981; Kim and Mueller, 1976) so the

Table 2.2.The coefficients derived from the MR analysis.

Predictor	Coefficient	Unstandardized	Standardized	Unstandardized	Standardized
constant	β_0	-179.98		-118.60	
T (°C)	β_1	1.38	0.42		
$p\,CO_2$ (atm)	β_2	61.42	0.52	58.48	0.57
$X_{"free"H2O}$	β_3	190.07	0.58	164.11	0.57
m_{Mg2+}	β_4			-114.32	-0.13

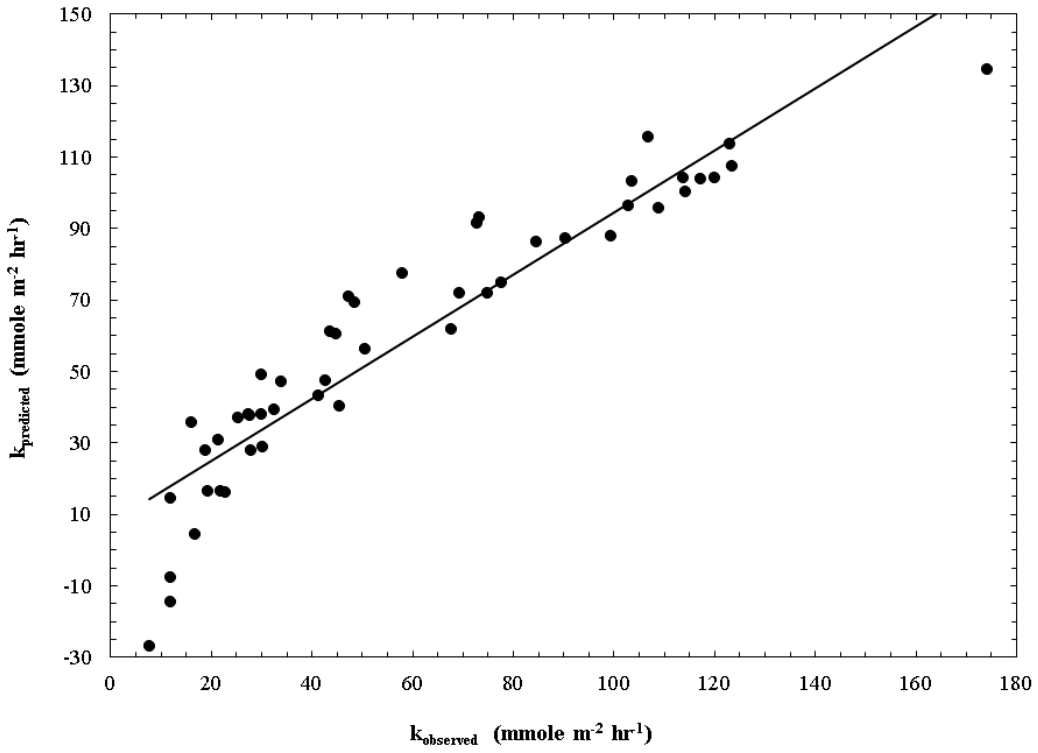

Figure 2.13. The predictive capability of the MR model (equation 2.12) with an adjusted $R^2 = 0.862$.

true relative importance of these variables may be different although it is clear that each has a direct impact on the observed rate. Although rates were found to be different in

KCl and NaCl solutions of equivalent ionic strength, the MR model (equation 2.13) shows no cation dependency as the "cation effect" is assumed to be incorporated into the $X_{"free" H_2O}$ term due to the different hydration numbers for KCl and NaCl used in the calculation. Interestingly, despite the well-known inhibitory effect of Mg^{2+} on calcite dissolution, there is no direct Mg^{2+} dependency of k in the present MR model (equation 2.13). As a majority of the data analyzed (both from the present study and that of Gledhill and Morse, 2006a) was obtained at 25 °C and two of the elevated temperatures were found to be outliers, the MR analysis was performed again using only data obtained at 25 °C. This analysis revealed a small dependence on Mg^{2+} (adjusted $R^2 = 0.888$, $p < 0.001$)

$$k_{pred_{25°C}} = \beta_0 + \beta_1 T + \beta_2 pCO_2 + \beta_3 X_{"free"H_2O} + \beta_4 m_{Mg^{2+}} \qquad (2.14)$$

where the variables are the same as before with the addition of the molality of Mg^{2+} ($m_{Mg^{2+}}$) term and the T term being neglected as it is incorporated into the constant. Both unstandardized and standardized β values are provided (Table 2.2) which indicate the relative effects on k are $X_{"free"H_2O} \approx pCO_2 > m_{Mg^{2+}}$. It is not surprising to find that Mg^{2+} has an inhibitory effect on the dissolution kinetics of calcite but demonstrates the need to obtain more data both in the presence and absence of Mg^{2+} at elevated temperatures to improve the robustness of the model. A comparison of the present MR model results (equations 11, 12) with that of Gledhill and Morse (equation 7, 2006a) suggests that when $X_{"free"H_2O}$ is used in lieu of I, then molalities may be used instead of activities, thereby simplifying the calculation. More importantly, the comparison demonstrates the

significant influence $X_{"free"H_2O}$ has on k. However, more data will need to be obtained, particularly at elevated temperatures, to determine if $X_{"free"H_2O}$ and molalities, along with pCO_2 and T are sufficient in determining k in solutions containing inhibitory ions or if activities will ultimately need to be considered.

2.6. Conclusions

The dissolution rates of calcite in magnesium-free, phosphate-free, low calcium (~0.01 molal) simple electrolyte solutions of either KCl or NaCl were measured and it was found that the rates can be described using first-order kinetics by the general rate equation: $R = k(1 - \Omega)^n$, where n = 1 (first-order) and k is a function of temperature, partial pressure of CO_2, I, or perhaps more appropriately, a_{H_2O}. Additionally, the identity of the cation of the supporting electrolyte appears to play a minor role as rates were found to be faster in KCl than NaCl solutions under the same experimental conditions. From the data presented, it is quite clear that the influence of I on the dissolution kinetics of calcite clearly becomes more dominant (compared with pCO_2 and T), as I is increased. This does not appear to be simply due to a_{H_2O} but may in some complex and ion specific way involve hydration mechanisms on the calcite mineral surface. The underestimation of MR model of Gledhill and Morse (2006a) at low I or low pCO_2 illustrates the danger of extrapolating much beyond the experimental domain used in formulating the model. The most significant finding was $X_{"free" H_2O}$ has been postulated to play a significant role in the dissolution kinetics of calcite as water becomes limiting regardless of the temperature (25-55 °C) or the pCO_2 (0.1-1 atm) examined in this study.

In addition, it was extrapolated that approximately 45-50% $X_{"free" H_2O}$ may represent a critical threshold below which dissolution will not occur (or occur very slowly) in undersaturated solutions which may be related to the transition from a two-dimensional to three-dimensional water layer adsorbed on the calcite surface. This hypothesis clearly needs testing in other simple inert electrolyte solutions before investigating in more complex natural solutions. Finally, the MR model presented by Gledhill and Morse (2006a) has been modified slightly:

$$k_{pred} = \beta_0 + \beta_1 T + \beta_2 pCO_2 + \beta_3 X_{"free" H_2O} \quad (2.15)$$

where $X_{"free" H_2O}$ has been found to have the largest influence on k.

3. HYDRATION NUMBERS OF NaCl, KCl, $CaCl_2$ and $MgCl_2$ DETERMINED FROM THE ANALYSIS OF COLLIGATIVE PROPERTY DATA

The physical structure of water plays an important role in solution properties, particularly for seawater, but reported results are surprisingly variable. Here, the hydration numbers of simple electrolyte solutions (NaCl, KCl, $CaCl_2$ and $MgCl_2$) were calculated from colligative property data using the methodology of Zavitsas (2001). Published freezing point depression, boiling point elevation, and vapor pressure depression data sets were each analyzed to determine hydration numbers. The resulting hydration numbers of $h_{NaCl} = 2.8 \pm 0.9$; $h_{KCl} = 1.2 \pm 1.2$; $h_{MgCl_2} = 9.8 \pm 3.7$; $h_{CaCl_2} = 6.3 \pm 3.3$. ΔH results from freezing point depression and boiling point elevation data demonstrate the need for calorimeter research of simple electrolyte solutions to determine if ΔH does approach that of pure water at infinite dilution. Despite the lower absolute values and larger uncertainties of the hydration numbers, multiple regression analysis of the dissolution data results in similar coefficients for the predictive equation for k although there is a non-zero $m_{Mg^{2+}}$ term at all temperatures. These findings suggest that effect of solute bound solvent molecules must be included when determining "true" mole fraction of solute particles in aqueous systems.

3.1. Introduction

The results from the previous section show that the mole fraction of free water plays a significant role in controlling the dissolution rate of calcite in saline waters. As

salt concentration increases, the mole fraction of free water decreases as does the dissolution rate. It was suggested that water can become limiting in highly concentrated electrolyte solutions. This result is not just relevant to the previous investigation of the dissolution kinetics of calcite in saline waters since the interaction of solute particles and solvent affects reactions in all fields of chemistry with an aqueous phase. Therefore, it is no surprise that ionic hydration is a well investigated field summarized in a number of books (e.g. Burgess, 1978; Conway, 1981; Magini, et al., 1988; Marcus, 1986) and reviews (e.g. Bakker, 2008; Blandamer et al., 2005; Marcus, 1988; Marcus, 2009; Ohtaki and Radnai, 1993; Soper, 2000; Vinogradov, 2003). A wide variety of methods (see review of Ohtaki and Radnai, 1993) have been employed to investigate ion hydration. Not surprisingly, there is a large range of hydration numbers of the major seawater cations Na^+ (2-13), K^+ (1-7), Mg^{2+} (8-14), Ca^{2+} (7-12) (Burgess, 1999). Complicating matters is that reported hydration numbers may include water molecules in both the primary (first layer) and secondary solvent shells (e.g. Di Leo and Marañón, 2005; Mel'nichenko, 2007), as opposed to solvent molecules directly bound to the solute which is the reported value for some methods (see review of Ohtaki and Radnai, 1993).

Colligative properties are those properties of a solution that depend only on the number of solute particles in a given volume of solvent and not on the identity of the solute particles. These properties include boiling point elevation, freezing point depression, osmotic pressure and vapor pressure lowering. As the concentration of a solution is increased, colligative properties typically deviate from ideality. For the nonelectrolytes glucose, sucrose, glycerol and ethylene glycol, Fullerton et al. (1994)

found that ideal dilute expressions could be used for concentrations up to 2.5 molal when the mass of water was corrected for a constant hydration mass per solute molecule. Similarly, Zavitsas (2001) demonstrated that deviations of colligative properties from ideal behavior in concentrated solutions of a variety of both electrolytes and nonelectrolytes are removed if the calculated mole fraction of the solute is corrected for bound waters. The mole fraction of solute particles (X_{sp}) is typically defined as:

$$X_{sp} = \frac{in_s}{n_{H2O} + in_s} \tag{3.1}$$

where i is the number of ions of the dissolved solute (van't Hoff index), n_s is the mole number of solute, and n_{H_2O} is the mole number of water. Accounting for bound waters, the corrected mole fraction of solute particles ($X_{sp_{cor}}$) as defined by Zavitsas (2001; 2005) is:

$$X_{sp_{cor}} = \frac{in_s}{n_{H2O} + in_s - hn_s} \tag{3.2}$$

where h is the hydration number of the solute. Zavitsas (2001) found values of h_{Na^+} = 3.9 ± 0.5; h_{K^+} = 1.7 ± 0.5; $h_{Mg^{2+}}$ = 13 ± 2; $h_{Ca^{2+}}$ = 12 ± 2 using freezing point depression data. $h_{Ca^{2+}}$ has subsequently been further refined to 12 ± 0.8 (Zavitsas, 2005). The value of h was assumed to be controlled predominantly by the cation. For this reason, h_{Na^+} and h_{K^+}values given above were calculated by combining three different halide (Cl^-, Br^-, I^-) solution sets (Zavitsas, 2001).

The present study is an effort to further refine the h value only using chloride solutions, as only chloride solutions of the major seawater cations Na^+, K^+, Mg^{2+} and Ca^{2+} were used in the investigation of the dissolution kinetics of calcite in saline waters as discussed in the previous section. Furthermore, using only chloride solutions removes any differences that may be present for the hydration characteristics of the various halide anions. The majority of freezing point depression data analyzed by Zavitsas (2001) were obtained from compilations. For the present study, an extensive literature search has been undertaken in order to use all possible experimental freezing point depression data currently available. Finally, in order to investigate the effect of temperature on h, boiling point elevation data and vapor pressure depression data have also been analyzed.

3.2 Colligative Properties

In an equilibrium mixture of pure solid and liquid at the freezing (melting) point, the chemical potentials of the solid and liquid must be equal. In the case of water and ice, at the freezing (melting) point:

$$\mu_{H_2O_{(s)}} = \mu_{H_2O_{(l)}} \tag{3.3}$$

where $\mu_{H_2O_{(s)}}$ and $\mu_{H_2O_{(l)}}$ are the chemical potentials of the solid and liquid phases of water respectively. With the addition of solute, the chemical potential of the solution is reduced:

$$\mu_{soln} = \mu_{H_2O_{(l)}} + RT\ln\left(X_{H_2O}\right) \tag{3.4}$$

where R is the universal gas constant, T is the absolute temperature and X_{H_2O} is the mole fraction of water. There is a new freezing (melting) point where:

$$\mu_{H_2O_{(s)}} = \mu_{soln} = \mu_{H_2O_{(l)}} + RT\ln\left(X_{H_2O}\right) \tag{3.5}$$

Upon rearrangement, the activity of the solvent is:

$$\ln\left(X_{H_2O}\right) = \frac{\mu_{H_2O_{(s)}} - \mu_{H_2O_{(l)}}}{RT} = \frac{\Delta G_{fus}}{RT} \tag{3.6}$$

where ΔG_{fus} is the Gibbs Free Energy of fusion. Differentiation of the above equation with respect to temperature yields:

$$\frac{\partial \ln\left(X_{H_2O}\right)}{\partial T} = \frac{\partial \Delta G_{fus}}{\partial RT} = \frac{\Delta H_{fus}}{RT^2} \tag{3.7}$$

where ΔH_{fus} is the latent heat of fusion. Integration from the freezing point of the solution (T_f, $X_{H_2O} < 1$) to the freezing point of pure water (T_0, $X_{H_2O} = 1$):

$$\ln\left(X_{H_2O}\right) = \int_{T_f}^{T_0} \frac{\Delta H_{fus}}{RT^2} dT \tag{3.8}$$

and ignoring any temperature dependence of ΔH_{fusion} yields:

$$\ln\left(X_{H_2O}\right) = -\frac{\Delta H_{fus}}{R}\left(\frac{1}{T_f} - \frac{1}{T_0}\right) \tag{3.9}$$

As X_{H_2O} and X_{sp} must sum to unity, 1-X_{sp} may be substituted for X_{H_2O}. With this substitution and simple rearrangement, the familiar equation for a line emerges:

$$\left(\frac{1}{T_f} - \frac{1}{T_0}\right) = -\frac{R}{\Delta H_{fus}} \ln\left(1 - X_{sp}\right) \tag{3.10}$$

ΔH_{fus} may be easily be determined from the slope of a line fit to the data. If X_{sp} is small then:

$$\ln(1 - X_{sp}) \approx -X_{sp} \tag{3.11}$$

If T_f is close to T_0, then:

$$\left(\frac{1}{T_f} - \frac{1}{T_0}\right) = \left(\frac{T_0 - T_f}{T_f T_0}\right) \approx \frac{\Delta T}{{T_0}^2} \tag{3.12}$$

At low solute concentration, the mole fraction of solute particles can be approximated as:

$$X_{sp} \approx i m_s M_{H_2O} \tag{3.13}$$

where i is again the number of ions of the dissolved solute (van't Hoff index), m_s the molality of the solute, and M_{H_2O} the molar mass of water. Substituting these approximations yields the familiar cryoscopic equation:

$$\Delta T = K_f m_s i \tag{3.14}$$

where:

$$K_f = \frac{R{T_0}^2 M_{H_2O}}{\Delta H_{fus}} \tag{3.15}$$

and m_s is the molality of the solute. As demonstrated above, the cryoscopic equation is the result of a few approximations which are sufficient for dilute solutions. These approximations do not hold at higher concentrations such as the saline solutions investigated in the previous section.

Boiling point elevation can be derived in a similar fashion :

$$\left(\frac{1}{T_b} - \frac{1}{T_b + \Delta t}\right) = -\frac{R}{\Delta H_{vap}} \ln\left(1 - X_{sp}\right) \qquad (3.16)$$

where T_b is the boiling point of pure water (373.15 K), Δt is the observed boiling point elevation, and ΔH_{vap} is the heat of vaporization of water at the boiling point.

The vapor pressure of solvent over a solution is also considered a colligative property:

$$\frac{p}{p_0} = \left(1 - X_{sp}\right) \qquad (3.17)$$

where p_0 is the vapor pressure of pure water at a given temperature and p is the partial vapor pressure of the solvent over a solution of X mole fraction of solute at the same temperature.

3.3 Analysis of Colligative Property Data

No actual colligative property experiments were carried out for this work. This section is the result of the analysis of colligative property data that have been published. Published freezing point depression data were analyzed to refine further the h value of each of the chloride solutions investigated in the previous section (NaCl, KCl, $MgCl_2$, $CaCl_2$). Freezing point depression data were plotted according to equation 3.10 with $T_f^{-1} - T_0^{-1}$ as the y value and $\ln(1-X_{sp})$ as the x value. X_{sp} was determined according to equation 3.2. The value of h that produced an intercept of zero for the plot of $T_f^{-1} - T_0^{-1}$ as a function of $\ln(1-X_{sp})$ was determined using the Solver function of Microsoft Excel

2007. Reported values have been rounded to the nearest tenth. All reported experimental data available for each set of freezing point depression data down to and including the eutectic point was used in the initial analysis. All experimental data sets used in the analysis had a $\Delta T \geq 4°C$ as outlined by Zavitsas (2001). Only reported freezing point depression data were used. The freezing point of pure water ($T_f = T_0 =$ 273.15K) was not included as a data point in the analysis.

Concentrations reported as weight percent were converted to molality according to:

$$m = \frac{1000(Wt\%)}{100(M_i) - (M_i)(Wt\%)} \tag{3.18}$$

where Wt% is the reported weight percent and M_i is the molecular weight of the electrolyte. Freezing point depressions in terms of the j function of Lewis and Randall can be converted to freezing point depression:

$$\theta = (1 - j)(1.858im) \tag{3.19}$$

where θ is the freezing point depression, and j is the reported coefficient. Note that v is the symbol used by Scatchard (1925) in lieu of i in equation 3.19.

Published data showing the elevation of boiling point were analyzed in an effort to investigate the effect of temperature on the h value of each of the chloride solutions investigated in the previous section (NaCl, KCl, $MgCl_2$, $CaCl_2$). Boiling point elevation data were plotted according to equation 3.16 where $T_b^{-1} - (T_b^{-1}+\Delta t)$ as the y value and $\ln(1-X_{sp})$ as the x value. X_{sp} was determined according to equation 3.2. The value of h

that produced an intercept of zero for the plot of $T_b^{-1} - (T_b^{-1}+\Delta t)$ as a function of $\ln(1-X_{sp})$ was determined using the Solver function of Microsoft Excel 2007. Reported values have been rounded to the nearest tenth. All reported experimental data available for each set of boiling point elevation data down to and including the eutectic point was used in the initial analysis. All experimental data sets used in the analysis had a $\Delta T \geq 4°C$ as outlined by Zavitsas (2001). Only reported boiling point elevation data were used; the boiling point of pure water (373.15 K) was not used in the analysis.

Published data showing lowering of vapor pressure were also analyzed. These were for each of the chloride solutions investigated in the previous section (NaCl, KCl, $MgCl_2$, $CaCl_2$) . p/p_0 was plotted as a function of $1-X_{sp}$ according to equation 3.17. X_{sp} was determined according to equation 3.2. The value of h that produced an intercept of zero for the plot of p/p_0 versus $1-X_{sp}$ was determined using the Solver function of Microsoft Excel 2007. Reported values have been rounded to the nearest tenth. Some references reported vapor pressure depression ($p_0 - p$) only, without providing the actual measurement of p_0. If p_0 was not provided, p_0 was obtained from the table of vapor pressure of water given in the CRC Handbook of Chemistry and Physics (Lide, 2008). A best fit line was generated for the data of Sako et al. (1985) as reported vapor pressures were not at consistent temperatures throughout the concentration regime investigated. Vapor pressure was then calculated for the experimental concentrations at 10 degree intervals over the range $60°C \leq T \leq 120°C$.

Hydration numbers determined in this section, whether determined from analysis of freezing point depression data, boiling point elevation data, or vapor pressure

lowering data, refer to the mole number of water bound to the solute and thus "removed" from the bulk solvent for each mole number of solute. With the present analysis, there is no way to determine where these bound water molecules are in relation to solute particles. Therefore, reported h values could refer to all solvent molecules in both the primary and secondary solvent shells, some combination thereof, or some or all those present in the primary solvent shell.

3.4. Results

Results of the analysis of freezing point depression data are given in Table 3.1A (NaCl), Table 3.1B (KCl), Table 3.1C ($MgCl_2$) and Table 3.1D ($CaCl_2$). All tables list the reference, year, number of data points (n) of the freezing point depression, the maximum molality of solute particles (m), the largest freezing point depression (ΔT) obtained, the slope and R^2 value of the linear least squares fit line, the hydration number (h) and ΔH_{fus} (kJ mol^{-1}) calculated from the slope. The results listed before the break in each table refer to published works containing the data used here; the results after the break are compilations of "best" values from the International Critical Tables (Washburn, 1926-1930), the Smithsonian Tables (Forsythe, 1954), Properties of Aqueous Solutions (Zaytsev and Aseyev, 1992), and the CRC Handbook of Chemistry and Physics (Lide, 2008). Compilation data are included so that direct comparison may be made between the present analysis and that of Zavitsas (2001).

The analysis results of boiling point elevation data sets are given in Table 3.2A (NaCl), Table 3.2B (KCl), Table 3.2C ($MgCl_2$) and Table 3.2D ($CaCl_2$). The

organization is the same as for freezing point depression. For the $MgCl_2$ and $CaCl_2$ solutions, only compilation data of boiling point elevation measurements has been included.

Results of the analysis of vapor pressure depression data are given in Table 3.3A (NaCl), Table 3.3B (KCl), Table 3.3C ($MgCl_2$) and Table 3.3D ($CaCl_2$) with the same layout as before.

Table 3.1A. Freezing Point Depression of NaCl Solutions

Reference	Year	n	maximum m	ΔT (K)	slope	h	R^2	ΔH_{fus} (kJ mol^{-1})
Rivett	1912	8	2.46	4.21	12.64	1.8	0.999951	6.58
Rodebush	1918	12	10.40	21.12	11.67	4	0.999919	7.12
Scatchard & Prentiss	1933	28	2.55	4.35	12.69	1.3	0.999960	6.55
Vilcu & Stanciu	1965	7	4.00	7.01	12.33	3	0.999870	6.74
Momicchioli et al.	1970	21	6.15	11.21	12.37	3.1	0.999882	6.72
Gibbard & Fong	1972	13	3.89	6.75	12.52	2.4	0.999939	6.64
Gibbard & Gossmann	1974	19	7.25	13.63	12.10	3.6	0.999895	6.87
Potter et al.	1978	5	10.37	20.81	12.01	3.7	0.999989	6.92
Hall et al.	1988	21	10.34	21.21	11.85	4	0.999975	7.02
Oakes et al.	1990	13	10.42	21.48	11.85	4	0.999951	7.01
Haghigh et al.	2008	5	7.51	14.29	12.34	3.5	0.999836	6.74
Washburn	1926-1930	17	10.40	21.12	12.07	3.7	0.999877	6.89
Zaytsev & Aseyev	1992	39	10.22	20.86	12.00	3.8	0.999901	6.93
Lide	2008	17	9.65	19.18	12.01	3.7	0.999879	6.93

Table 3.1B. Freezing Point Depression of KCl Solutions

Reference	Year	n	maximum m	ΔT (K)	slope	h	R^2	ΔH_{fus} (kJ mol^{-1})
Rivett	1912	7	2.13	3.46	12.46	0.0	0.999992	6.67
Rodebush	1918	6	6.60	10.66	11.98	1.7	0.999984	6.94
ıd noyes/falk as cited in l	1921	16	6.60	10.75	12.42	1.1	0.999928	6.69
Spencer	1932	14	3.00	4.86	12.25	1.0	0.999979	6.79
Scatchard & Prentiss	1933	27	2.49	4.05	12.26	1.0	0.999967	6.78
Vilcu and Stanciu	1965	7	4.00	6.58	12.20	1.4	0.999343	6.81
Chiorboli et al.	1966	46	4.19	6.79	12.50	0.3	0.999745	6.65
Momicchioli et al.	1970	4	6.05	9.87	11.81	2.1	0.999991	7.04
Hall et al.	1988	12	6.52	10.69	12.11	1.7	0.999934	6.87
Washburn	1926-1930	14	6.60	10.69	12.24	1.3	0.999941	6.79
Forsythe	1954	10	6.00	9.77	12.41	1.1	0.999915	6.70
Zaytsev & Aseyev	1992	18	5.89	9.60	12.15	1.5	0.999301	6.85
Lide	2008	12	3.66	5.88	12.49	0.2	0.999972	6.65

Table 3.1C. Freezing Point Depression of $MgCl_2$ Solutions

Reference	Year	n	maximum m	ΔT (K)	slope	h	R^2	ΔH_{fus} (kJ mol^{-1})
Jones & Bassett	1905	12	7.40	27.00	12.50	14.7	0.999495	6.65
Rivett	1912	9	2.37	4.72	11.65	17.2	0.999937	7.14
Sluiter	1914	11	2.87	6.06	11.80	14.2	0.992238	7.04
Rodebush	1918	6	8.82	33.50	13.83	12.3	0.998508	6.01
Gibbard & Fong	1972	15	6.10	6.49	5.78	9.3	0.999982	14.38
Gibbard & Gossmann	1974	15	12.16	18.39	6.11	8.2	0.999819	13.60
Haghighi et al.	2008	5	5.56	15.58	12.64	14.4	0.999582	6.58
Washburn	1926-1930	9	8.82	33.52	13.25	12.6	0.999123	6.27
shburn (minus extrapolat	1926-1930	8	6.00	17.60	12.03	14.9	0.999955	6.91
Zaytsev & Aseyev	1992	20	7.88	29.01	12.25	14.3	0.999250	6.79
Lide	2008	6	1.66	3.01	11.74	15.2	0.999926	7.08

Table 3.1D. Freezing Point Depression of $CaCl_2$ Solutions

Reference	Year	n	maximum m	ΔT (K)	slope	h	R^2	ΔH_{fus} (kJ mol^{-1})
Jones and Bassett	1905	15	10.73	46.50	13.51	11.7	0.997106	6.15
Sluiter	1914	12	3.03	5.97	11.15	15.1	0.999680	7.46
Rodebush	1918	6	12.97	51.00	14.48	9.1	0.998381	5.74
Gibbard & Fong	1975	10	4.36	3.95	5.75	7.4	0.999935	14.46
Oakes et al.	1990	59	11.91	51.20	14.01	10.5	0.998064	5.94
Haghighi et al.	2008	5	8.30	25.90	12.95	11.4	0.999709	6.42
Washburn	1926-1930	12	12.98	50.99	13.89	9.3	0.998508	5.99
Forsythe	1954	10	9.00	28.08	13.20	10.5	0.999124	6.30
Zaytsev & Aseyev	1992	32	12.72	49.62	14.12	9.5	0.995245	5.89
Lide	2008	22	12.72	49.70	13.71	9.5	0.998425	6.07

Table 3.2A. Boiling Point Elevation of NaCl Solutions

Reference	Year	n	maximum m	ΔT (K)	slope	h	R^2	ΔH_{vap} (kJ mol^{-1})
Haas	1971	6	11.41	6.70	1.87	2.8	0.999879	44.49
Washburn	1926-1930	7	13.56	8.66	1.90	2.9	0.999810	43.86
		11	12.98	8.12	1.87	2.9	0.999752	44.42
Forsythe	1954	7	13.93	8.80	1.79	3.2	0.997709	46.45
Zaytsev and Aseyev	1992	38	13.31	8.57	1.87	3.2	0.999788	44.41

Table 3.2B. Boiling Point Elevation of KCl Solutions

Reference	Year	n	maximum m	ΔT (K)	slope	h	R^2	ΔH_{vap} (kJ mol^{-1})
Saxton & Smith	1932	20	15.60	8.62	1.83	2.1	0.999890	45.33
Washburn	1926-1930	7	15.64	8.59	1.87	1.9	0.999951	44.58
Forsythe	1954	7	15.40	8.50	1.71	2.5	0.998603	48.67
Zaytsev & Aseyev	1992	21	15.09	8.31	1.81	2.0	0.993790	45.94

Table 3.2C. Boiling Point Elevation of $MgCl_2$ Solutions

Reference	Year	n	maximum m	ΔT (K)	slope	h	R^2	ΔH_{vap} (kJ mol^{-1})
Washburn	1926-1930	7	18.00	25.56	2.33	6.6	0.995047	35.74
Forsythe	1954	10	105.40	25.00	1.27	0.6	0.997048	65.45
Zaytsev and Aseyev	1992	19	19.31	28.78	2.77	5.8	0.996760	29.97

Table 3.2D. Boiling Point Elevation of $CaCl_2$ Solutions

Reference	Year	n	maximum m	ΔT (K)	slope	h	R^2	ΔH_{vap} (kJ mol^{-1})
Washburn	1926-1930	8	82.50	78.18	4.20	0.6	0.994485	19.79
Forsythe	1954	13	84.88	80.00	3.84	0.8	0.989186	21.65
Zaytsev and Aseyev	1992	38	85.60	78.22	4.04	0.8	0.988325	20.56

Table 3.3A. Vapor Pressure Depression of NaCl Solutions

Reference	Year	T (°C)	n	maximum m	p/p_0	slope	h	R^2
Bousfield & Bousfield	1923	18	20	12.06	0.76	1.00	2.9	0.998951
Frazer	1927	20	18	11.66	0.77	1.00	2.7	0.998584
		25	20	9.92	0.81	1.00	2.5	0.998336
Pearce and Nelson	1932	25	16	12.28	0.75	1.00	3.0	0.998920
Gibson & Adams	1933	25	8	12.24	0.75	1.01	3.1	0.999741
Olynk & Gordon	1943	20	10	12.25	0.75	1.01	3.2	0.999883
		25	15	12.29	0.75	1.01	3.1	0.999888
		30	11	12.33	0.75	1.01	3.2	0.997410
Washburn	1926-1930	20/25	10	12.00	0.76	1.00	2.9	0.999185
		80	3	12.00	0.77	1.02	3.0	0.998012
		100	6	13.40	0.74	1.01	2.8	0.999603
		0	10	5.70	0.76	1.01	3.1	0.989238
		10	10	5.70	0.77	1.00	3.1	0.998462
		20	10	5.70	0.78	1.01	2.8	0.996955
		30	10	5.70	0.78	1.01	2.8	0.998300
		40	10	5.70	0.78	1.00	2.7	0.998179
		50	10	5.70	0.78	1.00	2.6	0.998635
		60	10	5.70	0.78	1.00	2.5	0.998781
		70	10	5.70	0.78	1.00	2.4	0.998857
		80	11	6.49	0.75	1.00	2.5	0.998589
		90	11	6.49	0.75	1.00	2.4	0.998599
		100	11	6.49	0.75	1.00	2.4	0.998290
		110	11	6.49	0.75	1.00	2.3	0.998617
Forsythe	1954	100	7	12.00	0.77	1.00	2.7	0.999217
Zaytsev & Aseyev	1992	5	12	10.81	0.79	1.01	3.0	0.998140
		10	12	10.81	0.79	1.01	3.0	0.995232
		15	12	10.81	0.79	1.01	3.1	0.993029
		20	12	10.81	0.79	1.01	3.1	0.993346
		25	12	10.81	0.79	1.01	3.1	0.993457
		30	12	10.81	0.78	1.01	3.1	0.993798
		35	12	10.81	0.78	1.01	3.1	0.993950
		40	12	10.81	0.78	1.00	2.8	0.986352
		45	12	10.81	0.78	1.00	2.9	0.991160
		50	12	10.81	0.78	1.00	3.1	0.994283
		55	12	10.81	0.78	1.00	3.0	0.999731
		60	12	10.81	0.78	1.00	2.9	0.999725
		65	12	10.81	0.79	1.00	2.9	0.999767
		70	12	10.81	0.79	1.00	2.9	0.999799
		75	12	10.81	0.79	1.00	2.9	0.999825
		80	12	10.81	0.79	1.00	2.8	0.999846
		85	12	10.81	0.79	1.00	2.8	0.999866
		90	12	10.81	0.79	1.00	2.8	0.999881
		95	12	10.81	0.79	1.00	2.7	0.999894
		100	12	10.81	0.79	1.00	2.7	0.999907
		105	13	12.02	0.76	1.00	2.8	0.999227
		110	13	12.02	0.76	1.00	2.8	0.999220
		115	13	12.02	0.76	1.00	2.8	0.999245
		120	13	12.02	0.76	1.00	2.7	0.999230

Table 3.3A Continued,

Reference	Year	T (°C)	n	maximum m	p/p_0	slope	h	R^2
Zaytsev & Aseyev	1992	125	13	12.02	0.77	1.00	2.6	0.999865
		130	14	13.31	0.75	0.28	8.4	0.012578
		135	14	13.31	0.75	1.00	2.4	0.999972
		140	14	13.31	0.75	1.00	2.4	0.999973
		145	14	13.31	0.75	1.00	2.4	0.999975
		150	14	13.31	0.75	1.00	2.3	0.999977
		155	14	13.31	0.75	1.00	2.3	0.999979
		160	14	13.31	0.75	1.00	2.2	0.999980
		165	14	13.31	0.75	1.00	2.2	0.999982
		170	14	13.31	0.76	1.00	2.2	0.999984
		175	14	13.31	0.76	1.00	1.8	0.994078

Table 3.3B. Vapor Pressure Depression of KCl Solutions

Reference	Year	T (°C)	n	maximum m	p/p_0	slope	h	R^2
Lovelace et al.	1916	20	9	4.00	0.94	1.00	-1.7	0.998501
Lovelace et al.	1921	20	20	8.01	0.87	1.00	0.1	0.997813
Pearce & Snow	1927	25	12	9.62	0.84	1.00	0.6	0.997795
Brown & Delaney	1954	~25	12	4.76	0.92	1.00	-1.3	0.998833
Apelblat	1998	25	5	8.04	0.87	1.01	1.0	0.999876
Washburn	1926-1930	20-100	10	15.00	0.79	0.86	5.1	0.775458
Zaytsev and Aseyev	1992	0	18	15.09	0.91	0.99	-0.6	0.780460
		10	18	15.09	0.75	1.01	1.4	0.998383
		20	18	15.09	0.75	1.00	0.6	0.935884
		30	18	15.09	0.75	1.01	1.4	0.998407
		40	18	15.09	0.75	1.01	1.4	0.998400
		50	18	15.09	0.75	1.01	1.4	0.998396
		60	18	15.09	0.75	1.01	1.4	0.998398
		70	18	15.09	0.75	1.01	1.4	0.998392
		80	18	15.09	0.75	1.01	1.4	0.998248
		90	18	15.09	0.75	1.01	1.4	0.998394
		100	18	15.09	0.75	1.01	1.5	0.990071
		150	11	9.43	0.86	1.01	0.2	0.988197
		200	11	9.43	0.86	1.01	-0.4	0.988762
		250	11	9.43	0.87	1.01	-1.1	0.988719
		300	11	9.43	0.88	1.01	-2.5	0.984074
		350	11	9.43	0.91	1.01	-6.5	0.979838

Table 3.3C. Vapor Pressure Depression of $MgCl_2$ Solutions

Reference	Year	T (°C)	n	maximum m	p/p_0	slope	h	R^2
Sako et al.	1985	60	4	12.31	0.62	0.99	8.8	0.992262
		70	4	12.31	0.61	0.98	8.7	0.994334
		80	4	12.31	0.62	0.98	8.6	0.996022
		90	4	12.31	0.62	0.99	8.6	0.997361
		100	4	12.31	0.62	0.99	8.5	0.998382
		110	4	12.31	0.63	1.00	8.4	0.999112
		120	4	12.31	0.64	1.01	8.4	0.999578
Washburn	1926-1930	0	16	15.75	0.38	0.99	9.2	0.983140
		100	20	22.06	0.24	0.98	7.1	0.976017
Forsythe	1954	100	6	15.00	0.58	1.00	7.2	0.996796
Zaytsev and Aseyev	1992	0	16	16.23	0.36	0.97	9.0	0.979051
		10	16	16.23	0.37	0.94	9.0	0.806324
		20	16	16.23	0.37	0.98	8.9	0.982388
		30	16	16.23	0.38	0.99	8.8	0.983170
		40	17	17.72	0.34	0.98	8.3	0.976608
		50	17	17.72	0.35	0.98	8.2	0.978236
		60	18	17.72	0.30	0.97	8.8	0.918504
		70	17	17.72	0.31	0.97	8.6	0.956751
		80	18	17.72	0.32	0.98	8.6	0.960794
		90	19	19.31	0.27	0.97	8.1	0.954582
		100	19	21.01	0.22	0.97	7.6	0.948152
		125	15	13.50	0.61	1.01	7.9	0.998490
		150	15	13.50	0.63	1.01	7.4	0.997405
		175	15	13.50	0.66	1.02	6.6	0.994951
		200	15	13.50	0.69	1.02	5.6	0.989770
		225	15	13.50	0.72	1.02	4.6	0.982911
		250	15	13.50	0.74	1.02	3.3	0.974904
		275	15	13.50	0.77	1.03	1.7	0.954311
		300	15	13.50	0.80	1.03	-0.4	0.935366
		325	15	13.50	0.82	1.02	-3.3	0.899960
		350	15	13.50	0.86	1.03	-8.2	0.855636

Table 3.3D. Vapor Pressure Depression of $CaCl_2$ Solutions

Reference	Year	T (°C)	n	maximum m	p/p_0	slope	h	R^2
Sako et al.	1985	60	5	15.01	0.54	1.00	7.8	0.990792
		70	5	15.01	0.54	0.99	7.7	0.991954
		80	5	15.01	0.55	0.98	7.5	0.992924
		90	5	15.01	0.56	0.98	7.4	0.993715
		100	5	15.01	0.57	0.99	7.2	0.994339
		110	5	15.01	0.58	0.99	7.0	0.994807
		120	5	15.01	0.60	1.00	6.9	0.995128
Washburn	1926-1930	0	7	33.00	0.11	0.80	5.0	0.842249
		40	9	36.00	0.14	0.86	4.7	0.851729
		70	4	36.00	0.19	0.92	4.1	0.926547
		90	5	42.00	0.18	0.91	3.6	0.907259
		100	6	42.00	0.20	0.94	3.6	0.922339
		110	4	42.00	0.21	0.72	2.9	0.961181
		120	4	42.00	0.22	0.74	2.9	0.971492
		130	3	42.00	0.23	0.73	2.7	0.991540
		140	3	42.00	0.24	0.77	2.9	0.959105
Forsythe	1954	100	6	15.00	0.58	1.00	7.2	0.996796
Zaytsev and Aseyev	1992	0	8	18.02	0.36	0.97	7.8	0.982162
		0	8	18.02	0.36	0.97	7.8	0.982162
		10	9	22.12	0.27	0.96	6.8	0.959440
		20	9	22.12	0.28	0.96	6.7	0.961987
		30	10	27.03	0.22	0.95	5.8	0.934172
		40	11	33.04	0.17	0.93	5.0	0.911185
		50	11	33.04	0.18	0.93	4.9	0.915585
		60	11	33.04	0.15	0.94	4.9	0.936790
		70	11	33.04	0.16	0.95	4.9	0.941180
		80	11	33.04	0.18	0.95	4.8	0.946069
		90	11	33.04	0.20	0.96	4.7	0.951427
		100	11	33.04	0.21	0.96	4.6	0.956516
		150	7	14.56	0.64	1.00	6.4	0.997732
		200	7	14.56	0.69	1.53	10.5	0.250943
		250	7	14.56	0.73	1.01	3.4	0.995610
		300	7	14.56	0.78	1.02	1.0	0.977097
		350	7	14.56	0.08	0.39	11.8	0.211856

When the mole fraction is corrected for bound solvent molecules and plotted as in Eq. 3.10, deviation from ideal behavior is removed (e.g., Figure 3.1A for NaCl freezing point depression data ; Hall et al., 1988; Figure 3.1B for boiling point elevation

data; Zaytsev and Aseyev, 1992) Here X_{sp} is determined from conventional stoichiometry (closed circles) and from equation 3.2 with h = 4.0 (open squares).

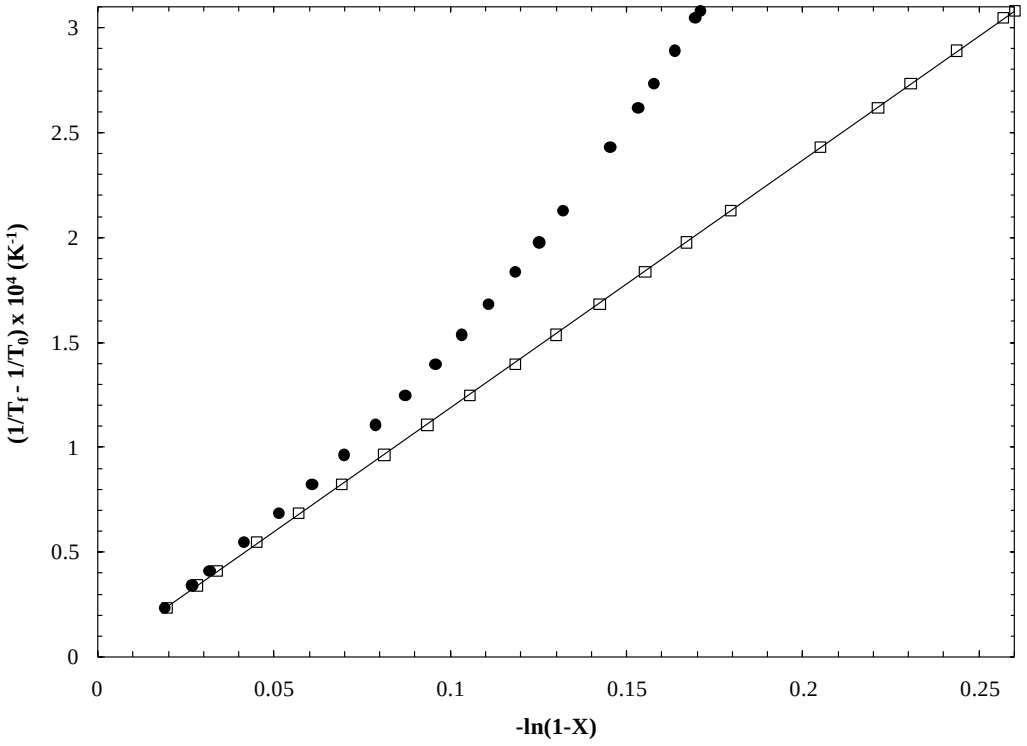

Figure 3.1A. Freezing point depression data of Hall et al. (1998) plotted according to equation 3.10 where X_{sp} is determined from conventional stoichiometry (●) and determined from equation 3.2 with h = 4.0 (□).

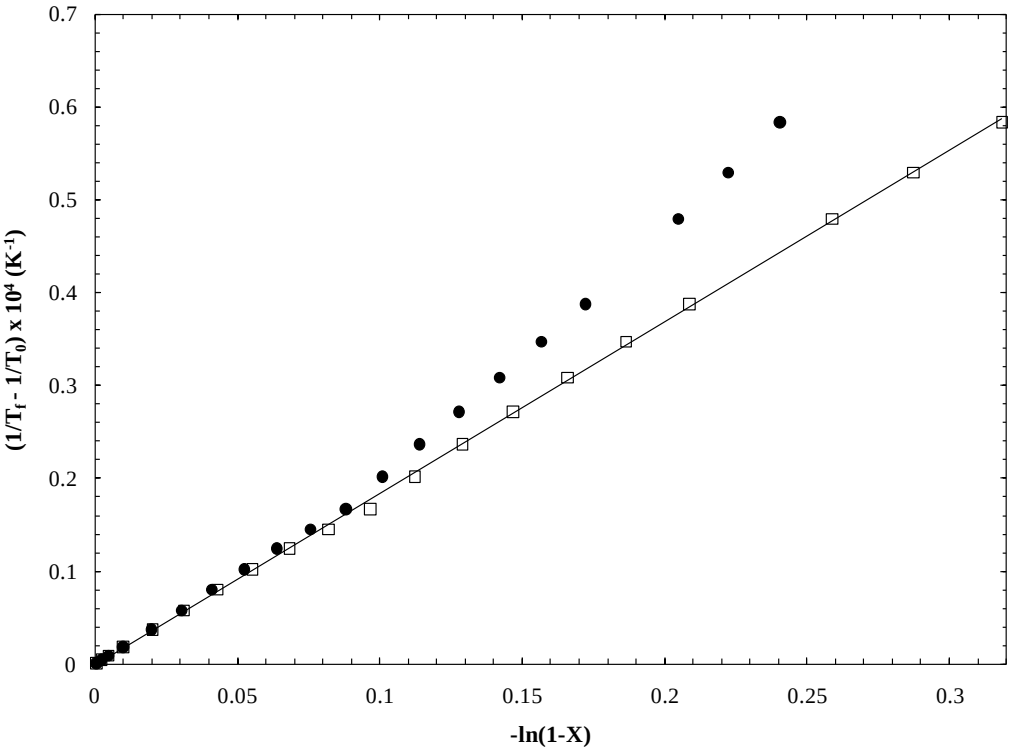

Figure 3.1B. Boiling point elevation data of Zaytsev and Aseyev plotted according to equation 3.10 where X_{sp} is determined from conventional stoichiometry (●) and determined from equation 3.2 with h = 2.0 (□).

3.5. Discussion

3.5.1 NaCl

Eleven data sets of freezing point depression of NaCl solutions were analyzed as were three compilations (Table 3.1A). The eleven independent studies yield $h_{NaCl} = 3.1 \pm 1.0$, with a range of 1.3- 4.0 and a median of 3.6; compilations give $h_{NaCl} = 3.7 \pm 0.1$. The average ΔH_{fus} value of the independent studies is 6.8 ± 0.2 kJ mol^{-1} whereas the literature value is $\Delta H_{fus} = 6.9 \pm 0.02$ kJ mol^{-1}. Although in close agreement with each

other, these values are about 15% greater than ΔH_{fus} of pure water at 0°C and 1atm, 6.00678 kJ mol^{-1} (Feistel and Wagner, 2006). As there may be some temperature dependence expected for ΔH_{fus} (see Dougherty and Howard, 1998), this gives some confidence to the analysis. The two independent studies (Rivett, 1912; Scatchard and Prentiss, 1933) with the lowest calculated h_{NaCl} also have the smallest depression. Removal of these two sets from the analysis of the freezing point depression data returns $h_{NaCl} = 3.5 \pm 0.6$. Only one paper (Hass, 1971) had a ΔT large enough reported for the boiling point elevation to be useful in the present study, yielding $h_{NaCl} = 2.8$, compared to literature value of 3.1 ± 0.2 (Table 3.2A); both values are about 80% of the values determined using the freezing point depression data. $\Delta H_{vap} = 44.5$ kJ mol^{-1} was calculated for the relevant paper, which is in good agreement with the average value returned from the literature values ($\Delta H_{vap} = 44.8 \pm 1.1$ kJ mol^{-1}). At 100°C, $\Delta H_{vap} =$ 40.657 kJ mol^{-1} for pure water (Marsh, 1987) which is about 10% lower than the present results. Eight sets of experimental vapor pressure depression of NaCl solutions ranging from $18°C \leq T \leq 30°C$ were analyzed as were fifty one sets of compilation data over the temperature range 0-175°C (Table 3.3A). The analysis of the individual papers returned $h_{NaCl} = 3.0 \pm 0.2$ whereas the analysis of the compilation data yielded $h_{NaCl} = 2.8 \pm 0.9$. If only the data at 100°C or less are included in the analysis of the vapor pressure depression compilation data, $h_{NaCl} = 2.8 \pm 0.2$. Regardless of experimental method analyzed, it appears that the hydration number of NaCl lies approximately between 2 and 4 over the approximate temperature range -20 to 120°C with $h_{NaCl} = 2.9 \pm 0.7$ overall.

According to a review (Ohtaki and Radnai, 1993), diffraction studies and computer simulations suggest that between 4 and 8 water molecules are coordinated with Na^+ . More recent work suggests values closer to the lower end of that range (and thus more similar to the presently found values) as Buchner et al., (1999) determined h_{Na^+} = 4.2 ± 0.3 from dielectric studies. Osakai, et al., (1997) found 3.8 ± 0.3 water molecules were co-extracted with Na^+ from water to nitrobenzene.

The current results also compare well with theoretical results. In a classic paper, Stokes and Robinson (1948) determined hydration numbers for the average effect of all ion-solvent interactions for a number of electrolytes and found 3.5 water molecules to be associated with NaCl. Using a semi-empirical hydration model (SEHM), Balomenos et al. (2006) were able to "estimate the overall distribution of water molecules between the solvent state and the ionic hydration state" as verified by the agreement of the predicted and experimental osmotic coefficients and predicted the maximum number of hydration sites for NaCl to be 3.9830. It should be noted that they also determined an average ionic hydration number for each electrolyte in which it was assumed that that each solute particle, regardless of charge, was surrounded by the same number of solvent molecules. That is, the number of waters associated with the Na^+ cation in a solution of NaCl was assumed to be the same as that bound to the Cl^- anion. Their model predicts a decrease of the average ionic hydration number from 1.99 – 1.7 with concentration of 0.02 – 12m ions for NaCl which suggests h_{NaCl} ranges from 3.4 – 4 which compares well with the present results. Max and Chapados (2001) determined h_{NaCl} = 5 from "pure salt-solvated water spectra" obtained from attenuated total reflection infrared spectra (ATR-IR) of

aqueous solutions which is greater than the present results. The present hydration numbers for NaCl are all lower than $h_{Na^+} = 3.9 \pm 0.5$ reported by Zavitsas (2001), although results from NaCl, NaBr, and NaI solutions are incorporated into that value.

3.5.2 KCl

Analysis of eight data sets of experimental freezing point depression in KCl solutions (Table 3.1B) yielded $h_{KCl} = 1.1 \pm 0.7$ with a range of 0.0 to 2.1 and median value of 1.1, whereas the four literature values average $h_{KCl} = 0.9 \pm 0.6$. The average ΔH_{fus} value of the independent studies is 6.8 ± 0.1 kJ mol^{-1} and the literature values are $\Delta H_{fus} = 6.7 \pm 0.1$ kJ mol^{-1}, both of which correspond well with that of the NaCl data but are greater than $\Delta H_{fus} = 6.00678$ kJ mol^{-1} of pure water at 0°C and 1 atm (Feistel and Wagner, 2006). Only one paper (Saxton and Smith, 1932) had a ΔT large enough in the boiling point elevation data to be used in the present study. The analysis yielded $h_{KCl} =$ 2.1, which also is the average of the literature values, $h_{KCl} = 2.1 \pm 0.3$ (Table 3.2B). Unlike the NaCl situation, h_{KCl} determined from boiling point elevation data was greater than that determined from freezing point depression. $\Delta H_{vap} = 45.3$ kJ mol^{-1} calculated for the independent paper is in good agreement with the average value returned by the compilation data ($\Delta H_{vap} = 46.4 \pm 2.1$ kJ mol^{-1}). Both values are slightly larger than that determined from the NaCl data and about 13% larger than $\Delta H_{vap} = 40.657$ kJ mol^{-1} of pure water at 100°C (Marsh, 1987). Five sets of experimental vapor pressure depression of room temperature (~20-25°C) KCl solutions were analyzed as were seventeen sets of literature values over the temperature range 0-350°C (Table 3.3B). Five sets of

experimental vapor pressure depression of KCl solutions ranging from 20°C≤T≤25°C were analyzed as were seventeen sets of compilation data over the temperature range 0-350°C (Table 3.3B). The independent papers returned $h_{KCl} = -0.3 \pm 1.2$ whereas the compilation data gave $h_{KCl} = 0.4 \pm 2.3$ with a marked decrease in the hydration number for temperatures greater than 100°C. If only the data at 100°C or less are included in the analysis of the vapor pressure depression compilation data, $h_{KCl} = 1.5 \pm 1.3$ with the value being skewed from the data of Washburn (1926-1930). In regards to the vapor pressure lowering, the text of Washburn states: "No apparent change with temperature". Over the temperature range of 0°C≤T≤100°C, the data of Zaytsev and Aseyev (1992) yields $h_{KCl} = 1.2 \pm 0.6$. Regardless of experimental method investigated, it appears that the hydration number of KCl is less than (and more uncertain than) that of NaCl and lies approximately between 0 and 2 over the approximate temperature range -10 to 110°C with $h_{KCl} = 1.2 \pm 1.2$ overall. At higher temperatures, the analysis returns negative hydration numbers.

Directly comparing h_{KCl} with h_{NaCl} the smaller charge density of K^+ compared with Na^+ leads to fewer bound solvent molecules as would be expected from first principles. From dielectric relaxation studies, Buchner et al., (1999) determined $h_{K^+} = 1.3$ whereas Osakai, et al., (1997) found 1.0 water molecules were co-extracted with K^+ from water to nitrobenzene. The present results also compare well with that calculated by Stokes and Robinson (1948) of 1.9. The SEHM model of Balomenos et al. (2006) predicts a value 2.2945 for the maximum number of hydration sites for KCl. The predicted average hydration number of KCl is 1.15 – 1.05 over the concentration range

of 0.02 – 9m ions, which implies h_{KCl} ranges 2.3 – 2 which agrees with the present results. Max and Chapados (2001) determined $h_{KCl} = 5$ using ATR-IR, which is also much greater than the present results. The present results are also less than that of Zavitsas, who reported $h_{K^+} = 1.8 \pm 0.5$. It should be noted that the CRC Handbook of Chemistry and Physics (Lide, 2008) freezing point depression data which gave $h_{KCl} = 0.2$ was included in the present analysis but not in the analysis by Zavitsas (2001) even though that reference was used for other electrolytes.

3.5.3 $MgCl_2$

Six sets of experimental freezing point depression in $MgCl_2$ solutions were analyzed as were four compilations (Table 3.1D). For the analysis of published data, $h_{MgCl_2} = 12.9 \pm 3.2$ with a range of 8.2 – 17.2 and median of 14.2. The datasets with the two lowest h_{MgCl_2} values (Gibbard and Fong, 1972; Gibbard and Gossman, 1974) have disparate ΔH_{fus} values (14.4, 13.6 kJ mol^{-1} respectively) compared with the others (6.7 ± 0.4 kJ mol^{-1}). Removal of these two sets from the analysis yields $h_{MgCl_2} = 14.6 \pm 1.8$ which agrees well with that of the compilation data, $h_{MgCl_2} = 14.2 \pm 1.4$. The calculated ΔH_{fus} values independent (6.7 ± 0.4 kJ mol^{-1}) and compilation data (6.9 ± 0.1 kJ mol^{-1}) agree well with that determined for the NaCl and KCl freezing point depression data although still larger than that of ΔH_{fus} of pure water at 0°C and 1atm (6.00678 kJ mol^{-1}; Feistel and Wagner, 2006). The compilation data for boiling point elevation gave h_{MgCl_2} = 4.3 ± 3.3 (Table 3.2C), which is a much lower hydration number and larger uncertainty

(± 77%). Although the calculated average value of ΔH_{vap} (43.7 ± 19.0 kJ mol^{-1}) agrees with pure water at 100°C (40.657 kJ mol^{-1}; Marsh, 1987), not one compilation set was close to the average as evidenced by the large standard deviation. However, the dataset from the International Critical Tables gives ΔH_{vap} = 35.7 kJ mol^{-1} which is about 90% of the value for pure water at 120°C (ΔH_{vap} = 39.684; Marsh, 1987). Overall, the large deviation suggests that the analysis using the boiling point elevation data is not as robust as the freezing point data which may be expected as the elevation for a given molality is much less than the depression. Seven sets of experimental vapor pressure depression of $MgCl_2$ solutions ranging from 60°C≤T≤120°C were analyzed as were twenty-four sets of compilation data over the temperature range 0-350°C (Table 3.3C). The independent papers returned h_{MgCl_2} = 8.6 ± 0.1 whereas the compilation data gave h_{MgCl_2} = 5.9 ± 4.4 with a marked decrease in the hydration number for temperatures greater than 100°C. If only the data at 100°C or less is included in the analysis of the vapor pressure depression compilation data, h_{MgCl_2} = 8.4 ± 0.7 The hydration number of $MgCl_2$ appears to be quite dependent on the colligative property investigated ranging from 4.3 (boiling point elevation data) to 14.6 (freezing point depression data). From all three investigations, over the approximate temperature range -30 to 130°C, h_{MgCl_2} = 9.8 ± 3.6 overall (excluding the boiling point data h_{MgCl_2} = 10.1 ± 2.8). There is a significant decrease in the determined hydration number at higher temperatures with negative hydration numbers at temperatures greater than 300°C.

These values presented here for the freezing point depression data correspond well with that found by Price et al. (1996) who reported a value of 12 on the basis of

diffusion coefficient of $MgCl_2$ assuming $h_{Cl^-} = 0$. The present results also compares well with that calculated by Stokes and Robinson (1948) of 13.7. However, the mean hydration number calculated from freezing point depression data is much larger than the maximum number of hydration sites predicted by the SEHM of Balomenos et al. (2006) of 9.1623 which is closer to the value predicted by analysis of the vapor pressure depression data. Their model also predicts a decrease of the average ionic hydration number with concentration from 4.57 – 3.08 (0.3 – 13.5m ions) for $MgCl_2$ which suggests h_{MgCl_2} ranges from 13.7 – 9.24 which is slightly less than h_{MgCl_2} obtained in the present results. In contrast, Max and Chapados (2001) determined $h_{MgCl_2} = 4$ using ATR-IR, which is less than $h_{NaCl} = 5$ that they determined. This does not correspond with what is expected simply based on charge densities, which raises a question as to the validity of their technique for determining hydration numbers. h_{MgCl_2} determined from the freezing point depression data compares very well with that previously reported by Zavitsas of $h_{Mg^{2+}} = 13 \pm 2$.

3.5.4 $CaCl_2$

Six sets of experimental freezing point depression in $CaCl_2$ solutions were analyzed (Table 3.1C) giving $h_{CaCl_2} = 10.9 \pm 2.6$ ranging from 7.4 to 15.1 with a median value of 11. The dataset with the lowest h_{CaCl_2} value (Gibbard and Fong, 1972) yields a much larger ΔH_{fus} value (14.5 kJ mol^{-1}) compared with the others (6.3 ± 0.7 kJ mol^{-1}). Removal of this dataset from the analysis yields $h_{CaCl_2} = 11.6 \pm 2.2$ which compares very

well with that $h_{Ca^{2+}} = 12 \pm 0.8$ obtained by Zavitsas (2005) for $CaCl_2$ solutions. Compilation data returns an even smaller $h_{CaCl_2} = 9.8 \pm 0.6$. ΔH_{fus} values for both the independent (6.3 ± 0.7 kJ mol^{-1}) and compilation data (6.1 ± 0.2 kJ mol^{-1}) are the closest to the ΔH_{fus} value of pure water at 0°C (6.00678 kJ mol^{-1}; Feistel and Wagner, 2006) and less than ΔH_{fus} values determined for the previous three electrolytes. The compilation data for boiling point elevation gave a much lower hydration number, $h_{CaCl_2} = 0.7 \pm 0.1$, than that determined from freezing point data (Table 3.2D). Furthermore, the calculated average value of ΔH_{vap} (20.7 ± 0.9 kJ mol^{-1}) is only about half of the true value of water at 100°C and less than 60% of ΔH_{vap} at 180°C (36.304 kJ mol^{-1}; Marsh, 1987). This complete lack of agreement between calculated and actual ΔH_{vap}, suggest that the boiling point elevation data is not as robust as the freezing point data as noted in the previous section. Seven sets of experimental vapor pressure depression of $CaCl_2$ solutions ranging from $60°C \leq T \leq 120°C$ were analyzed as were twenty-seven sets of compilation data over the temperature range 0-350°C (Table 3.3D). The independent papers returned $h_{CaCl_2} = 7.3 \pm 0.3$ whereas the compilation data gave $h_{CaCl_2} = 5.2 \pm 2.4$ with a marked decrease in the hydration number for temperatures greater than 100°C. If only the data at 100°C or less is included in the analysis of the vapor pressure depression compilation data, $h_{CaCl_2} = 5.4 \pm 1.3$. The hydration number of $CaCl_2$ appears to be quite dependent on the colligative property investigated ranging from 0.7 (boiling point elevation data) to 11.6 (freezing point depression data). From all three investigations, over the

approximate temperature range -50 to 180°C, $h_{CaCl_2} = 6.3 \pm 3.3$ overall (excluding the boiling point data where $h_{CaCl_2} = 6.7 \pm 3.0$).

The discrepancy between the present results and that of Zavitsas could arise from the maximum concentration investigated for each data set. The present analysis included all data up to and including the eutectic point whereas Zavitsas did not which will be addressed in the next section. As Ca^{2+} is larger than Mg^{2+} (and thus has a smaller charge density), it may be expected that less solvent molecules would be bound to Ca^{2+} as evidenced by $h_{CaCl_2} < h_{MgCl_2}$. Regardless of experimental method investigated, the results for h_{CaCl_2} were less than those determined for h_{MgCl_2}. In contrast, Max et al. (2007) determined $h_{CaCl_2} = 6$ using ATR-IR, which is less than $h_{Mg\,Cl_2} = 4$ that they determined which does not correspond with what is expected simply based on charge densities. The results of Max and co-workers (Max and Chapados, 2001; Max et al., 2007) suggest that their extrapolation technique may be of limited use when determining the number of bound solvent molecules in aqueous solutions. Osakai, et al., (1997) found 14 ± 2 water molecules were co-extracted with Ca^{2+} from water to nitrobenzene. This also compares well with $h_{CaCl_2} = 12.0$ as calculated by Stokes and Robinson (1948). The mean hydration number calculated from freezing point depression data is larger than maximum number of hydration sites of $CaCl_2$ predicted by the Balomenos et al. (2006) SEHM model of 7.8111. Their model also predicts a decrease of the average ionic hydration number with concentration from 3.89 – 2.65 (0.3 – 13.5m ions) for $CaCl_2$

which implies h_{CaCl_2} ranges from 11.6 – 8.0 which agrees well with the present results determined from freezing point depression data.

3.6 Temperature Effect

Intuitively, it may be assumed that as temperature is increased, the hydration number will decrease to the increased thermal energy of the system (e.g. as temperature increases the movement and collisions of the dissolved ions and water molecules will also increase leading to less bound solvent molecules). The discrepancy between hydration numbers calculated from freezing point depression data and those determined from boiling point elevation data suggest that temperature does have an effect. In order to investigate this possibility, the calculated hydration number for each electrolyte was plotted as a function of temperature for vapor pressure depression data of NaCl, KCl, $MgCl_2$, and $CaCl_2$ solutions (Figures 3.2A-D).

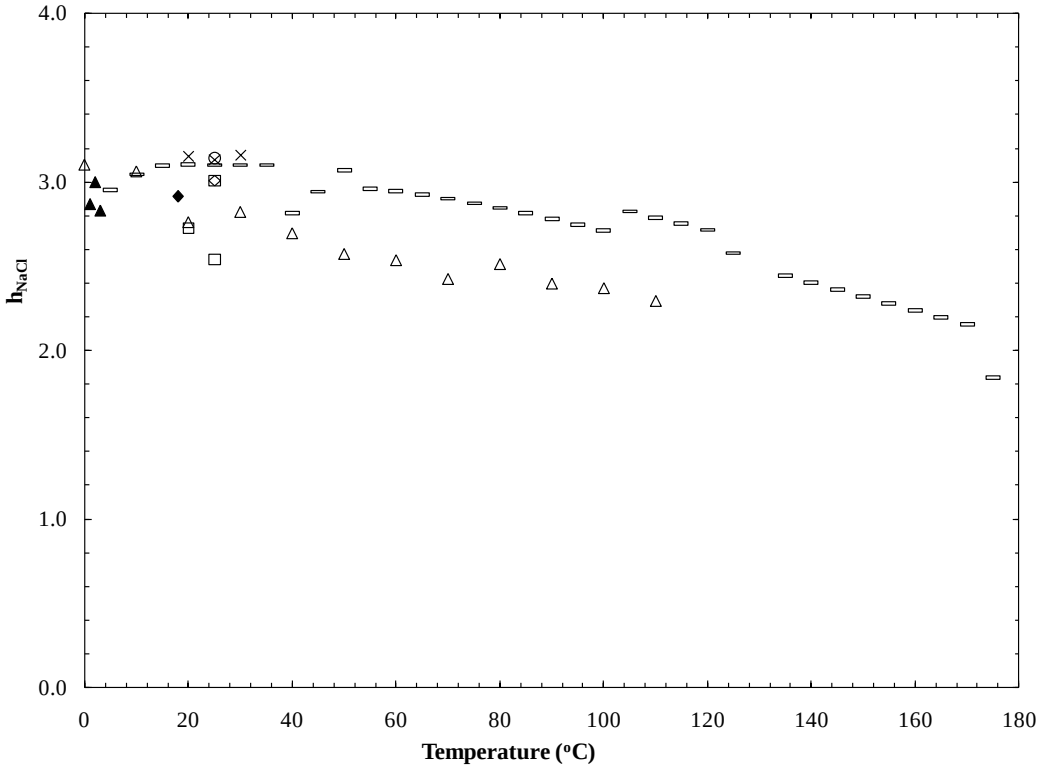

Figure 3.2A. h_{NaCl} as a function of temperature for Bousfield and Bousfield (♦), Frazer (□), Pearce and Nelson (◊), Gibson and Adams (○), Olynk and Gordon (x), Washburn (Δ,▲), Forsythe (+), Zaytsev and Aseyev (-).

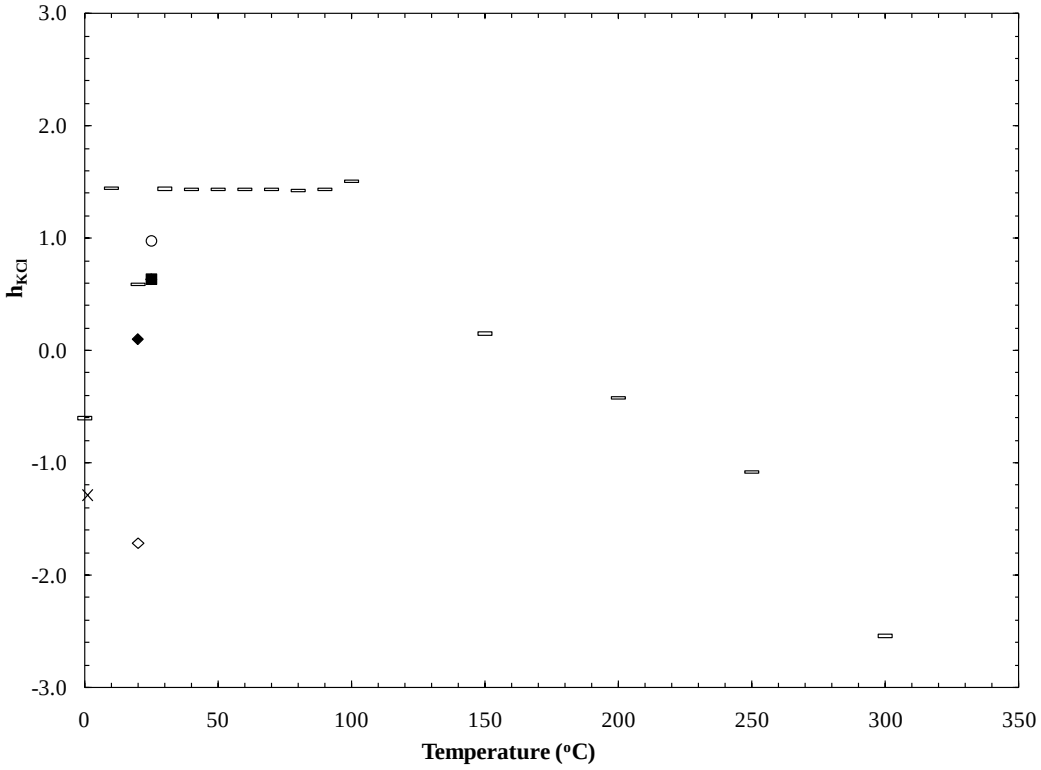

Figure 3.2B. h_{KCl} as a function of temperature for Lovelace et al. (◊), Lovelace et al. (♦), Pearce and Snow (■), Brown and Delaney (x), Apelblat (○), Washburn (Δ), Zaytsev and Aseyev (-).

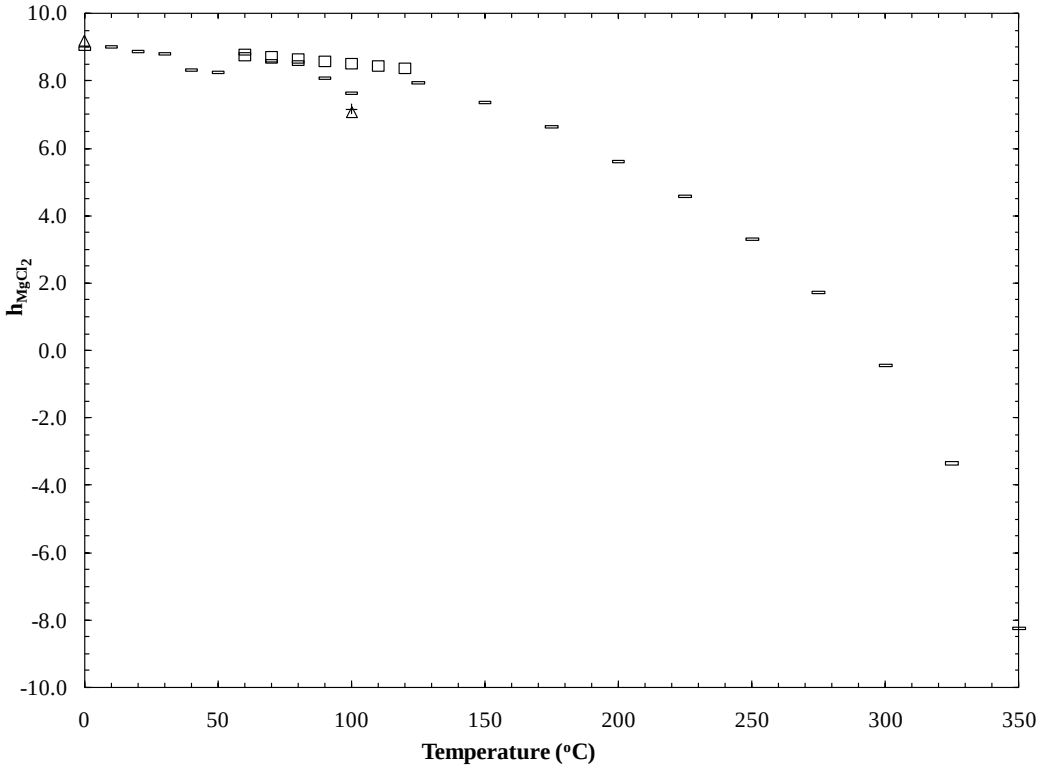

Figure 3.2C. h_{MgCl_2} as a function of temperature for Lovelace et al. (◊), Lovelace et al. (♦), Sako et al. (□) Washburn (Δ), Zaytsev and Aseyev (-).

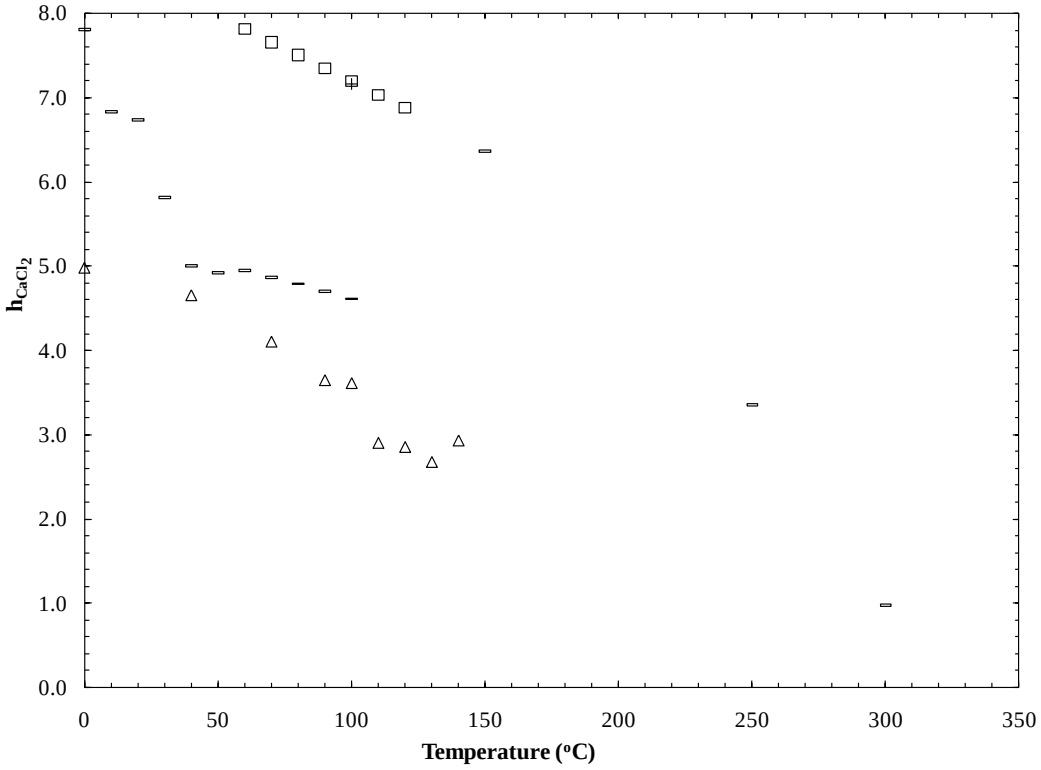

Figure 3.2D. h_{CaCl_2} as a function of temperature for Lovelace et al. (◊), Lovelace et al. (♦), Sako et al. (□) Washburn (Δ),Forsythe (+), Zaytsev and Aseyev (-).

All electrolytes show a decrease in the hydration number with increasing temperature for datasets with more than one temperature with the exception of the first data set for NaCl from the International Critical Tables (Washburn, 1926-1930). The decrease in hydration number for each electrolyte appears to be slight up to a temperature of 100°C after which the decreases are larger. Furthermore, this analysis predicts a negative hydration number for KCl and $MgCl_2$ solutions at high temperatures, which does raise some concerns as to the validity of the current analysis. However, the greatest temperature investigated in the dissolution (Section 2) and precipitation (Section

4) experiments was less than 100°C which is within the positive range of hydration numbers.

3.7 Effect of Concentration

The hydration number results presented in Tables 3.1A-D, 3.2A-D, and 3.3A-D assume that both h and ΔH_{fus} are constant regardless of solute concentration. However, some investigators have reported a dependency of the hydration number on concentration (e.g. Driesner, et al., 1998; Du et al., 2007; Soper and Weckström, 2006). For freezing point depression data, Zavitsas (2005) demonstrated downward curvature at high concentrations for highly hydrated salts which he attributed to " 'solvent-shared' ion pairs" which the anions form as the solvent becomes limiting (solvent approaches infinite dilution). As the most highly concentrated data points are removed from an analysis of one data set, both h and the slope of the linear least squares fit will change as well as exemplified by some subsets of $CaCl_2$ freezing point depression data of Haghighi et al. (2008) (Table 3.4; Figure 3.3). Upon close inspection of Figure 3.3, it appears that each subset exhibits downward curvature as the most highly concentrated data points fall below the linear least squares fit line. As the maximum molality investigated decrease, both h and ΔH increase (Table 3.4).

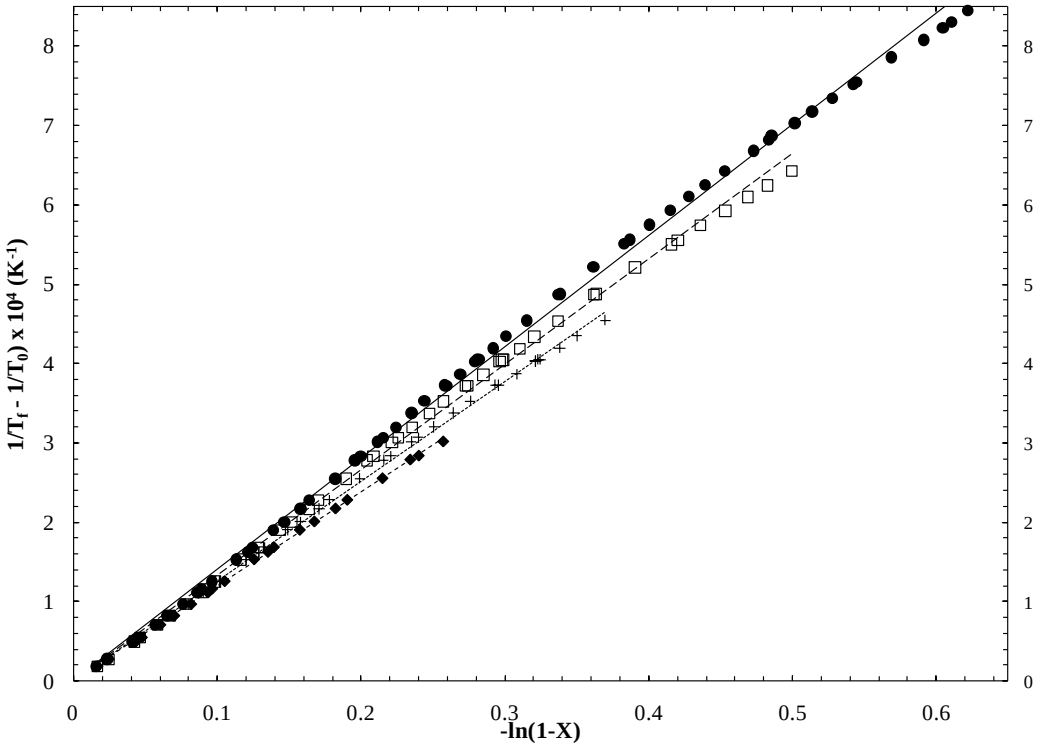

Figure 3.3. Plot of $CaCl_2$ freezing point depression data of Haghighi et al. (2008) as the maximum ion concentration investigated is reduced. Maximum ion concentrations are 11.91m(●), 10.59(□), 8.96(+), 7.17(♦).

Table 3.4 Change in h and ΔH_{fus} for the $CaCl_2$ freezing point depression data of Haghighi et al. (2008) as the maximum ion concentration is reduced.

m (mol ions kg^{-1} H_2O)	ΔT (K)	slope	h	ΔH (kJ mol^{-1})
11.91	51.20	14.01	10.5	5.9
11.24	45.64	13.61	10.8	6.1
10.59	40.80	13.31	11.1	6.2
9.84	35.72	12.96	11.5	6.4
8.96	30.16	12.58	11.9	6.6
8.05	25.25	12.24	12.4	6.8
7.17	20.78	11.88	13.0	7.0
5.95	15.30	11.65	13.6	7.1
4.71	10.98	11.32	14.7	7.3

Intuitively, it makes sense that once the ion is maximally hydrated, as concentration is further increased, h will remain constant or decrease as there will be less solvent molecules available for hydration since some water must remain unbound to act as the solvent (e.g. Nesbitt, 1982). Zavitsas (2001) reported that when NaCl, KCl and $MgCl_2$ freezing point depression data were plotted according to equation 3.10 (T_f^{-1}-T_0^{-1} versus ln(1-X_{sp}), the best fit lines were linear with concentration all the way up to the most highly concentrated solution (eutectic point). Therefore, concentration should not be an issue for NaCl, KCl and $MgCl_2$electrolyte solutions according to Zavitsas (2001). However, for $CaCl_2$ solutions, no consistent molality limit is applied as reported maximum ion molalities are 9.74, 8.55, 7.62, and 6.00 with calculated h = 10.2, 11.3, 12.3, and 13.5 respectively (Zavitsas, 2005). Furthermore, there is no clear indication of what criteria was used in determining linearity. ΔH_{fus} calculated from the slopes of Zavitsas (2001) produce values of 6.4, 6.9, 7.3 kJ mol^{-1} for the latter three respectively which yield an average of 6.9 ± 0.4 kJ mol^{-1}. In order to more fully investigate the effect of concentration, h and ΔH_{fus}(ΔH_{vap}) were determined as before for each dataset of freezing point depression data(boiling point elevation data) from the maximum concentration reported down to the lowest concentration where $\Delta T \geq 4K$. This process was repeated for each electrolyte although negative values of h were allowed in this analysis of the data (Figures 3.4A-D for freezing point depression, Figures 3.5A-D for boiling point elevation). h was also determined as before for each dataset of vapor pressure depression data (Figures 3.6A-H).

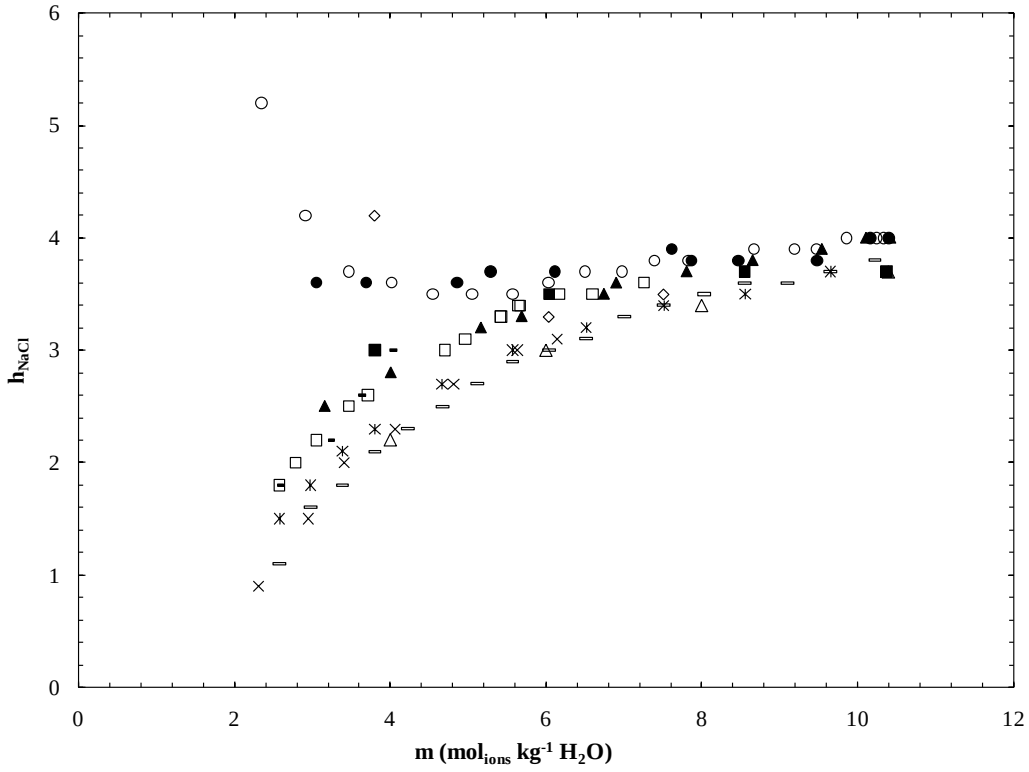

Figure 3.4A. h_{NaCl} as a function of the ion concentration from freezing point depression data of Rodebush (●), Momicchioli et al. (x), Gibbard and Gossman (□), Potter et al. (■), Hall et al. (○), Oakes et al. (▲), Haghighi et al. (♦), Lide (*), Washburn (-).

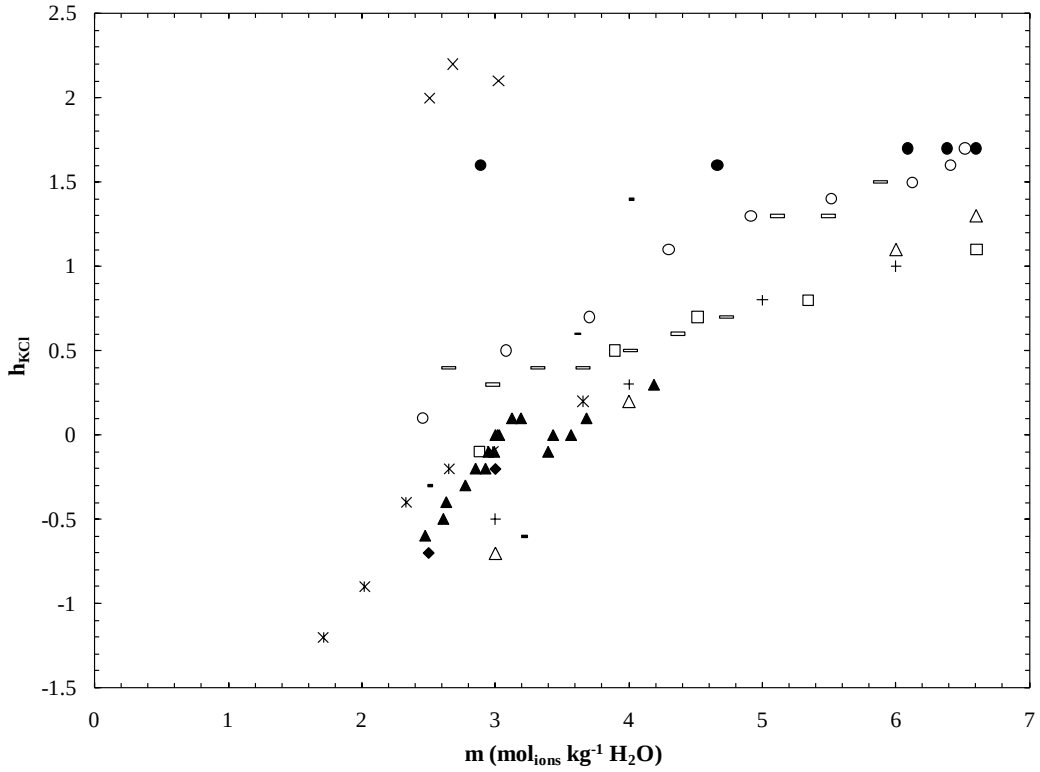

Figure 3.4B. h_{KCl} as a function of the ion concentration from freezing point depression data of for Rodebush (●), Roloff (□),Spencer (♦), Chiorboli et al. (▲), Momicchioli et al. (x), Hall et al. (○), Lide (*), Washburn (-), Forsythe (+).

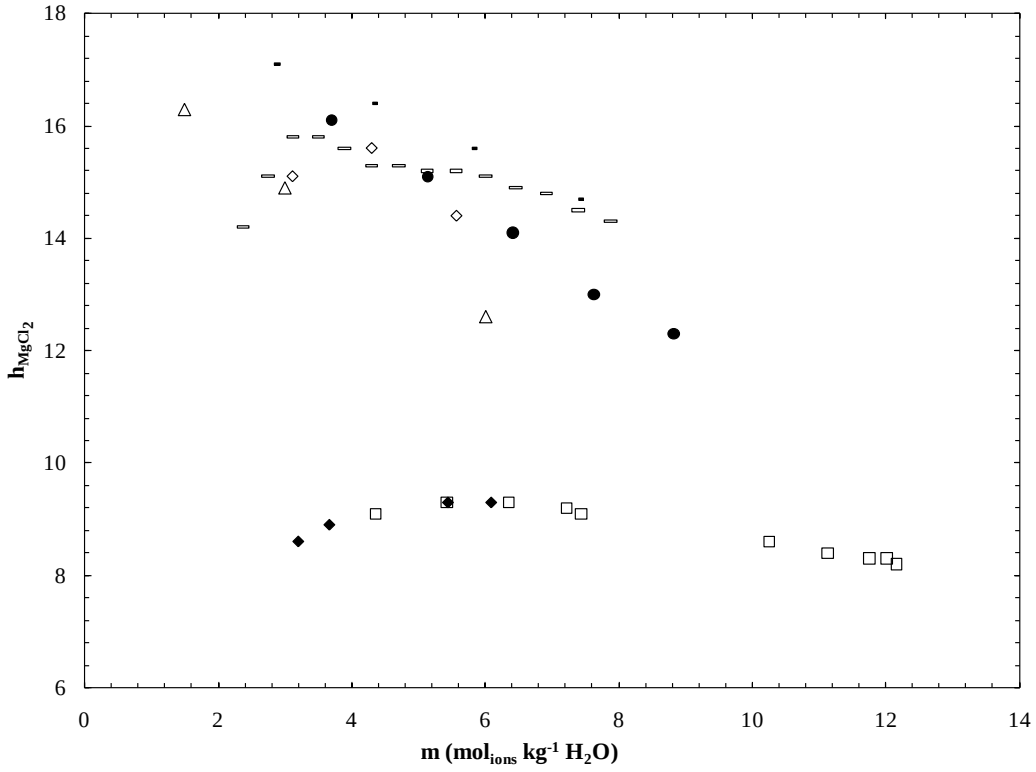

Figure 3.4C. h_{MgCl_2} as a function of the ion concentration from freezing point depression data of for Jones and Bassett (▲), Rodebush (●), Gibbard and Fong (♦), Gibbard and Gossman (□), Haghighi et al. (♦), Washburn (-).

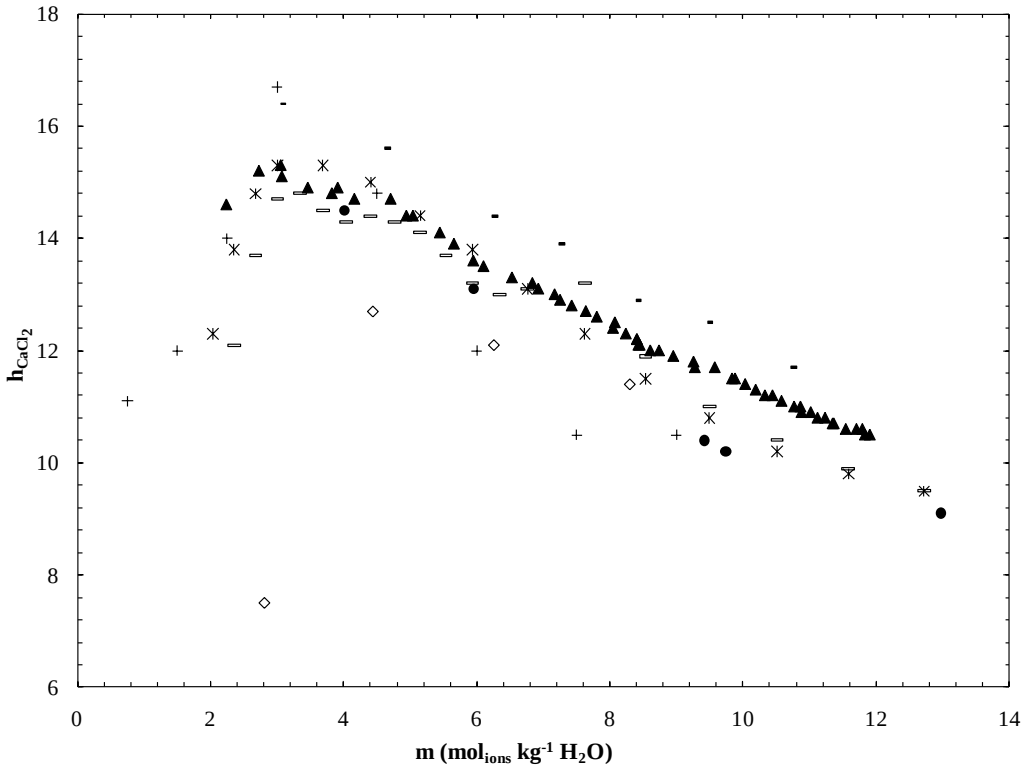

Figure 3.4D. h_{CaCl_2} as a function of the ion concentration from freezing point depression data of for Jones and Bassett (▲), Rodebush (●), Oakes et al. (▲), Haghighi et al. (♦), Lide (*), Washburn (-).

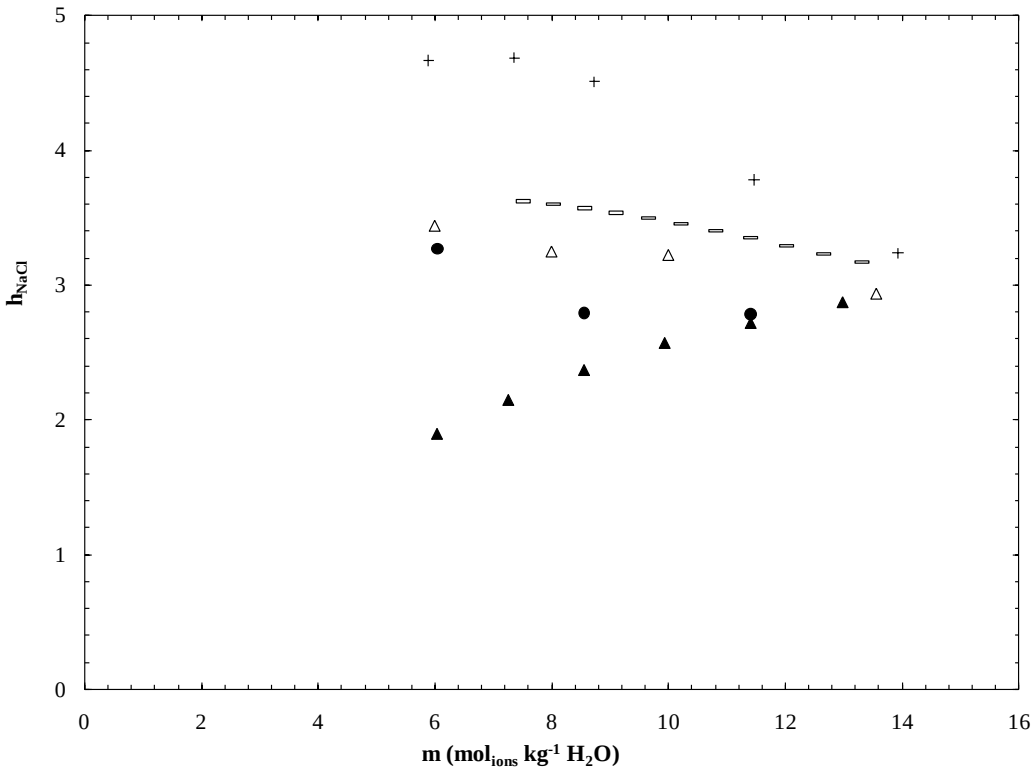

Figure 3.5A. h_{NaCl} a as a function of the ion concentration from boiling point elevation data of Hass (●), Washburn (Δ,▲), Forsythe (+), Zaytsev and Aseyev (-).

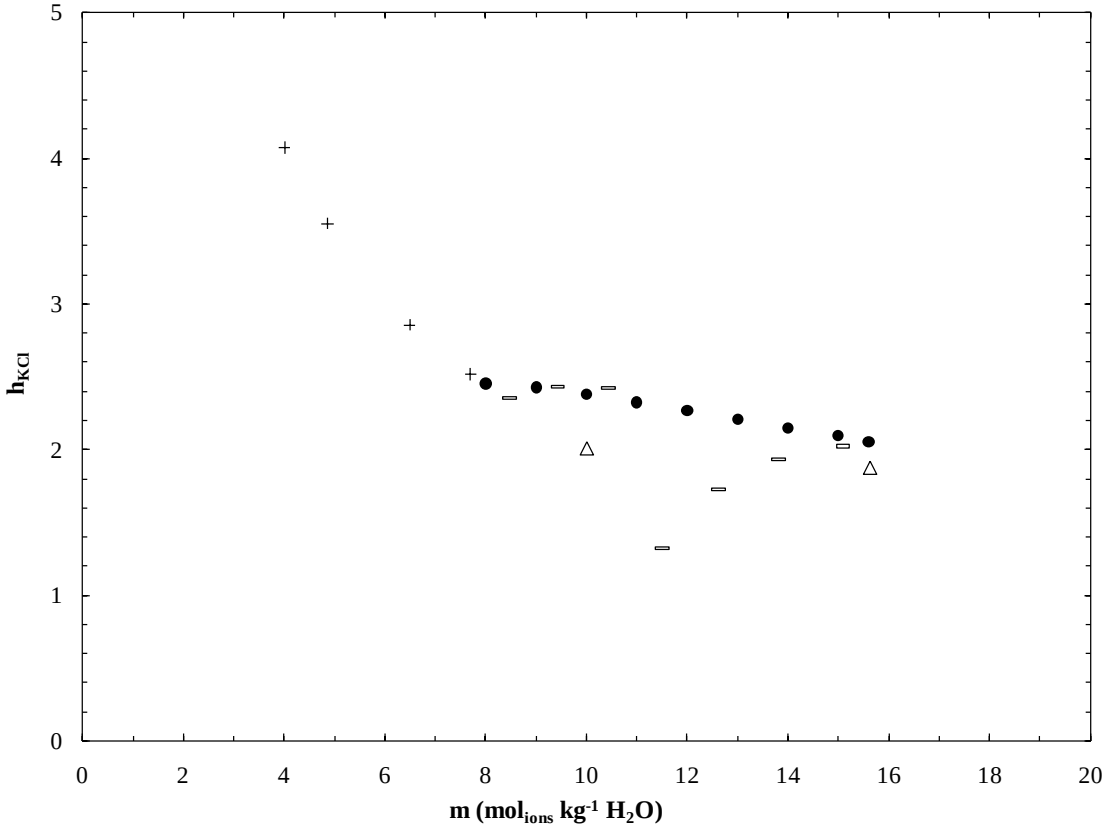

Figure 3.5B. h_{KCl} as a function the ion concentration from boiling point elevation data of Saxton and Smith (●), Washburn (Δ), Forsythe (+), Zaytsev and Aseyev (-).

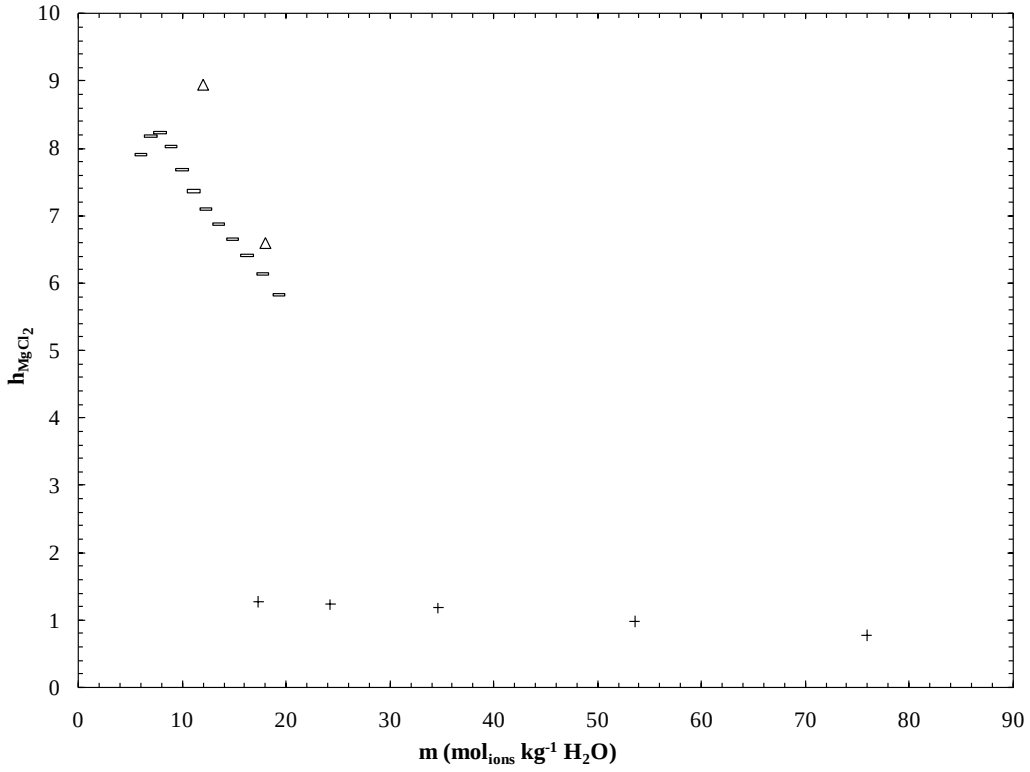

Figure 3.5C. h_{MgCl_2} as a function of the ion concentration from boiling point elevation data of Washburn (Δ), Forsythe (+), Zaytsev and Aseyev (-).

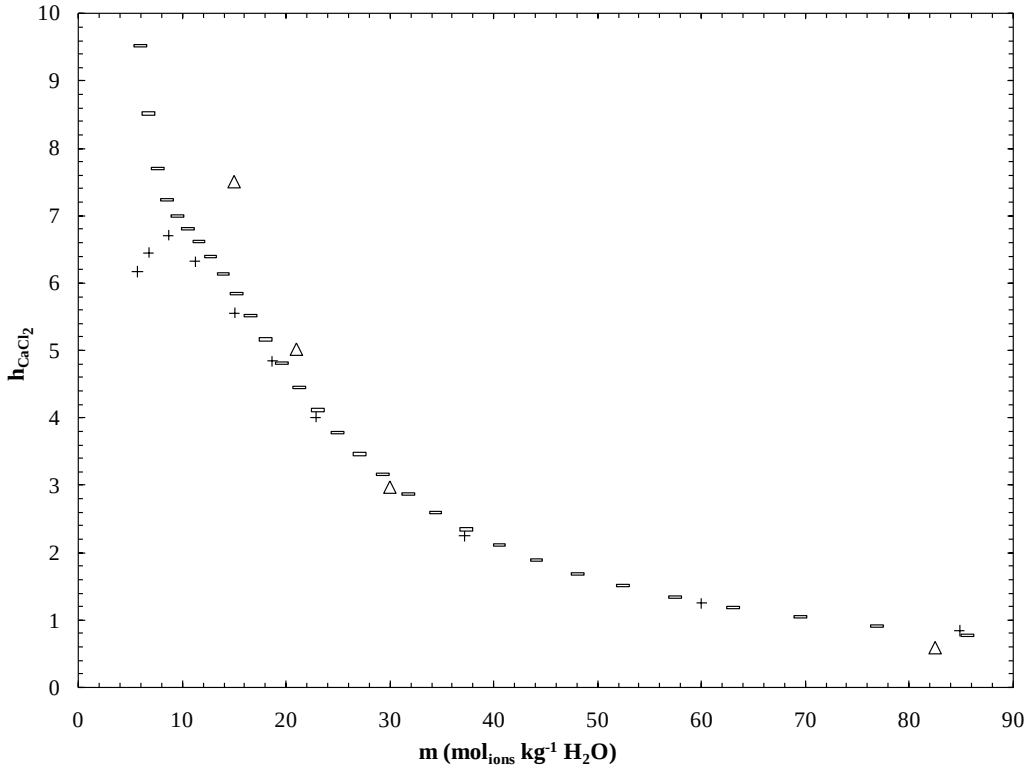

Figure 3.5D. h_{CaCl_2} as a function of the ion concentration from boiling point elevation data of Washburn (Δ), Forsythe (+), Zaytsev and Aseyev (-).

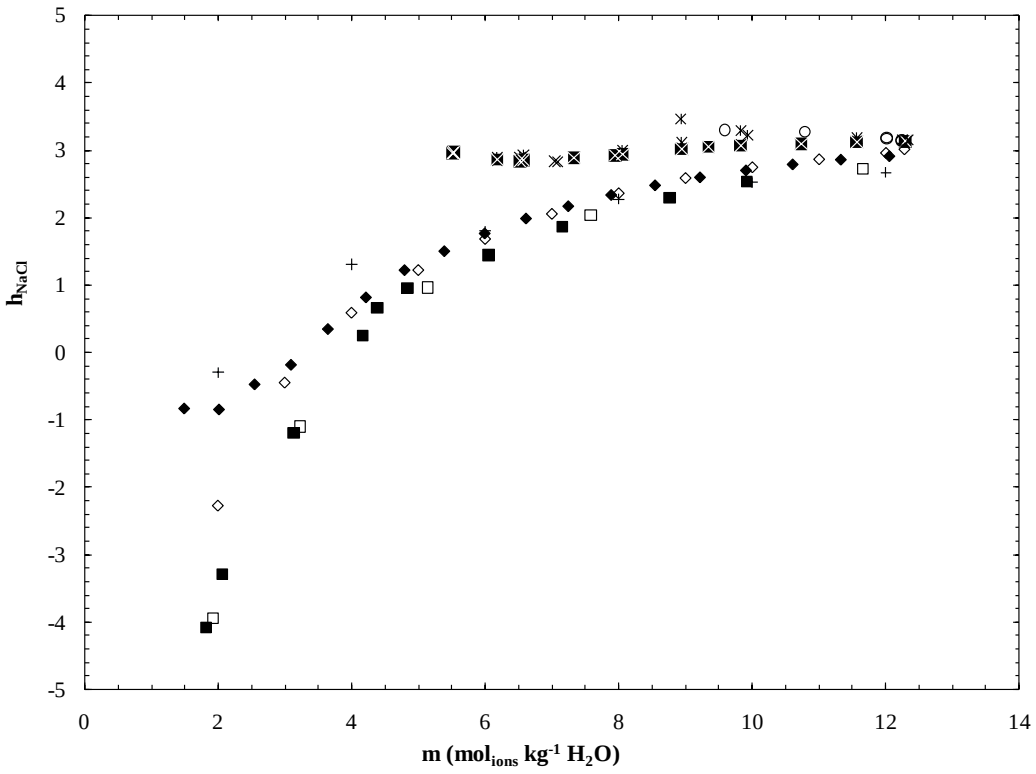

Figure 3.6A. h_{NaCl} a as a function of the ion concentration from vapor pressure depression data of Bousfield and Bousfield (♦), Frazer (20°C = □, 25°C = ■), Pearce and Nelson (◊), Gibson and Adams (○), Olynk and Gordon (20°C = x, 25°C = ■, 30°C = *), Washburn (Δ,▲), Forsythe (+).

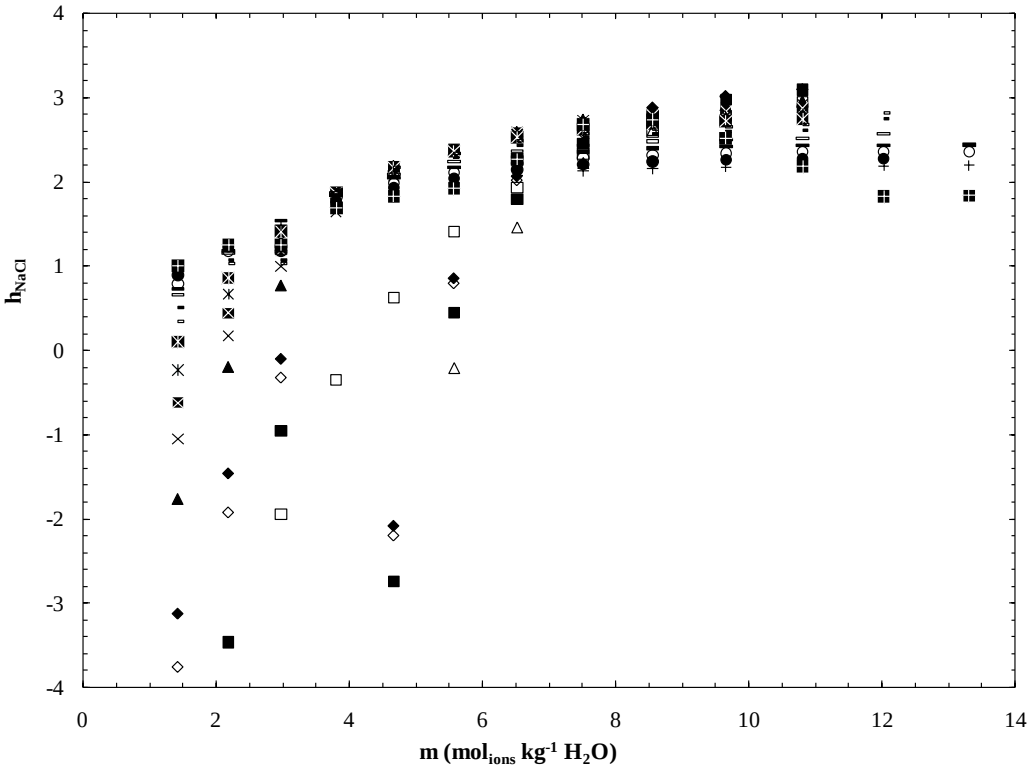

Figure 3.6B. h_{NaCl} a as a function of the ion concentration from vapor pressure depression data of Zaytsev and Aseyev at 5°C (□), 15°C (■), 25°C (◊), 35°C (♦), 45°C (Δ), 55°C (▲), 65°C (x), 75°C (x), 85°C (*), 95°C (*), 105°C (-), 115°C (-), 125°C (-), 135°C (-), 145°C (○), 155°C (●), 165°C (+), 175°C (+).

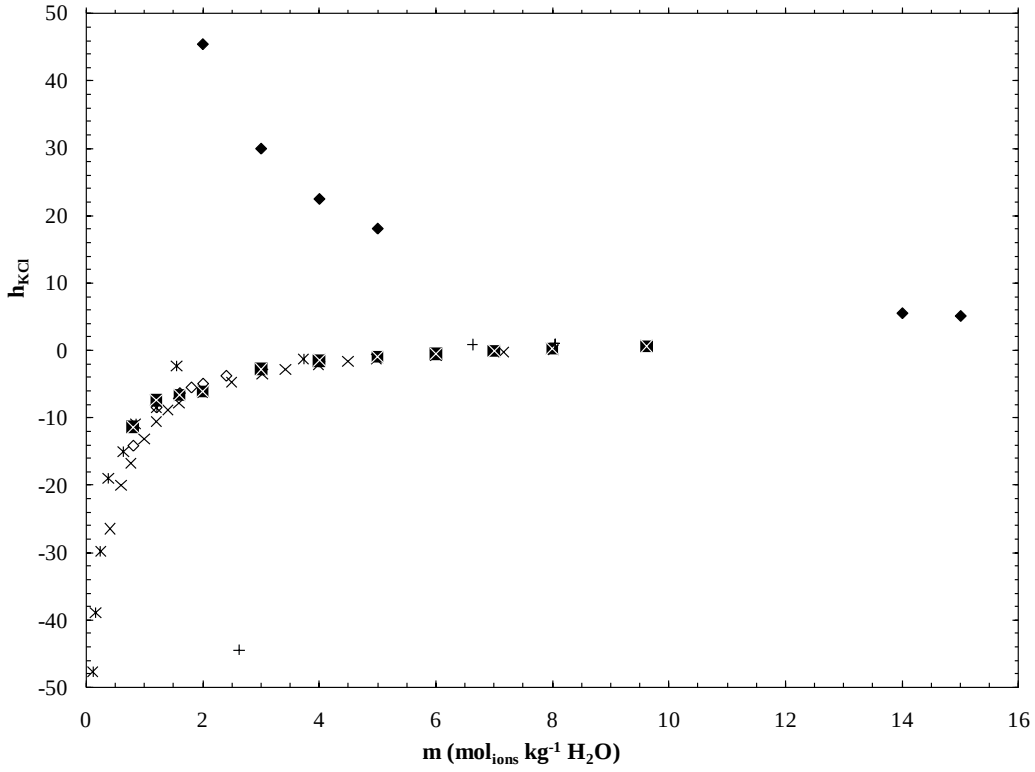

Figure 3.6C. h_{KCl} a as a function of the ion concentration from vapor pressure depression data of Lovelace et al. (◊), Lovelace et al. (X), Brown and Delaney (*), Pearce and Snow (■), Apelblat (+), Washburn (♦)

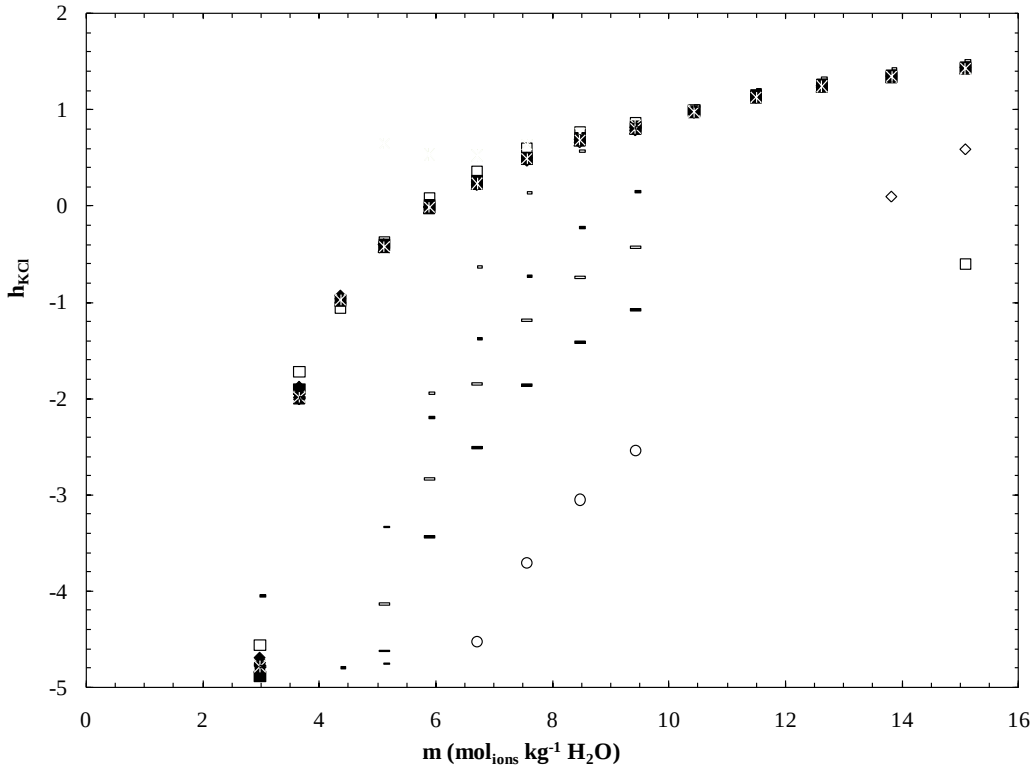

Figure 3.6D. h_{KCl} a as a function of the ion concentration from vapor pressure depression data of Zaytsev and Aseyev at 0°C (□), 10°C (■), 20°C (◊), 30°C (♦), 40°C (Δ), 50°C (▲), 60°C (x), 70°C (x), 80°C (*), 90°C (*), 100°C (-), 150°C (-), 200°C (-), 250°C (-), 300°C (○), 350°C (●)

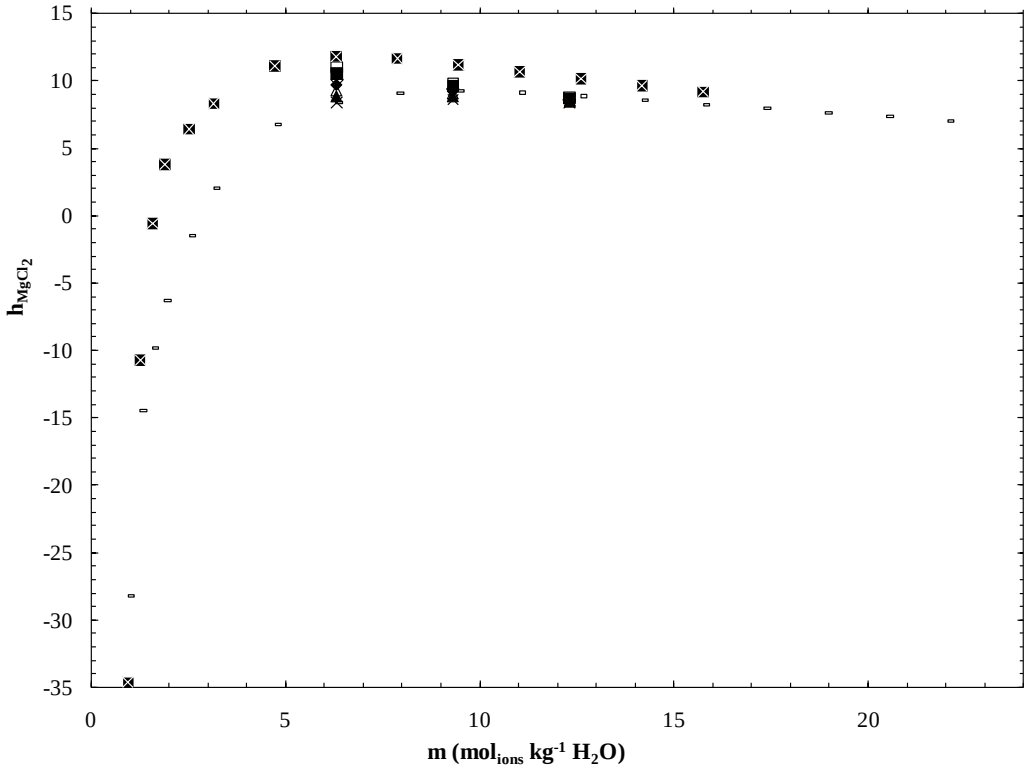

Figure 3.6E. h_{MgCl_2} a as a function of the ion concentration from vapor pressure depression data of Sako et al. at 60°C (□), 70°C (■), 80°C (◊), 90°C (♦), 100°C (Δ), 100°C (▲), 120°C (x) and Washburn for 0°C (x) and 100°C (*).

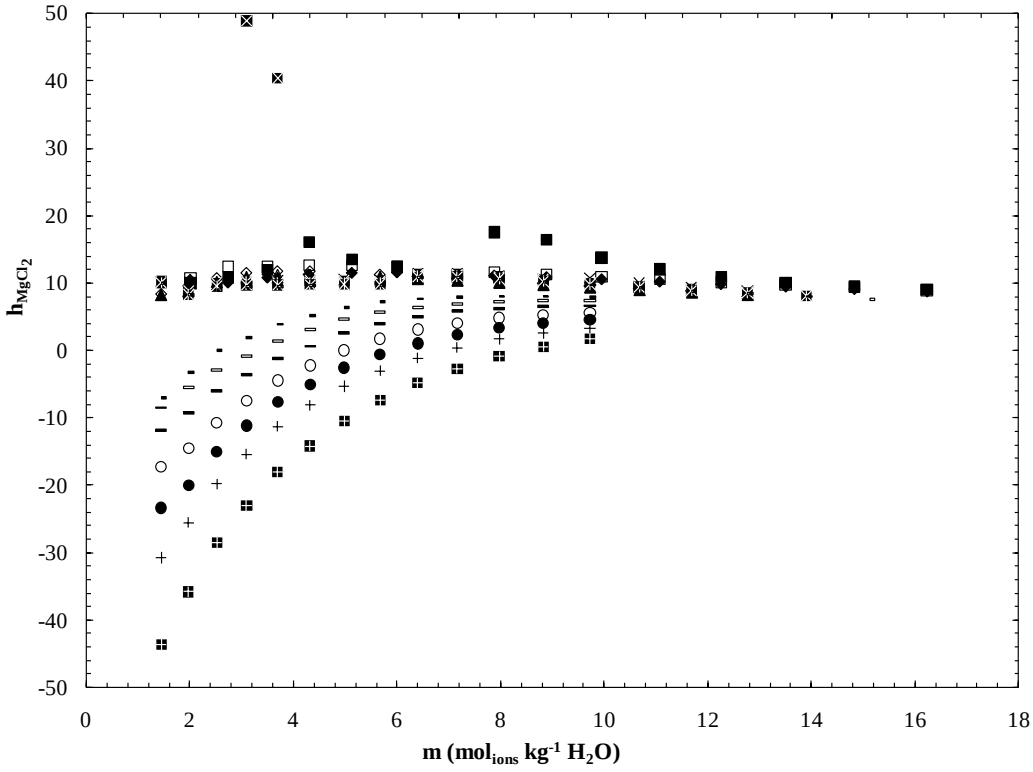

Figure 3.6F. h_{MgCl_2} a as a function of the ion concentration from vapor pressure depression data of Zaytsev and Aseyev at 0°C (□), 10°C (■), 20°C (◊), 30°C (♦), 40°C (Δ), 50°C (▲), 60°C (x), 70°C (x), 80°C (*), 90°C (*), 100°C (-), 125°C (-), 150°C (-), 175°C (-), 200°C (○), 225°C (●), 250°C (+), 275°C (+).

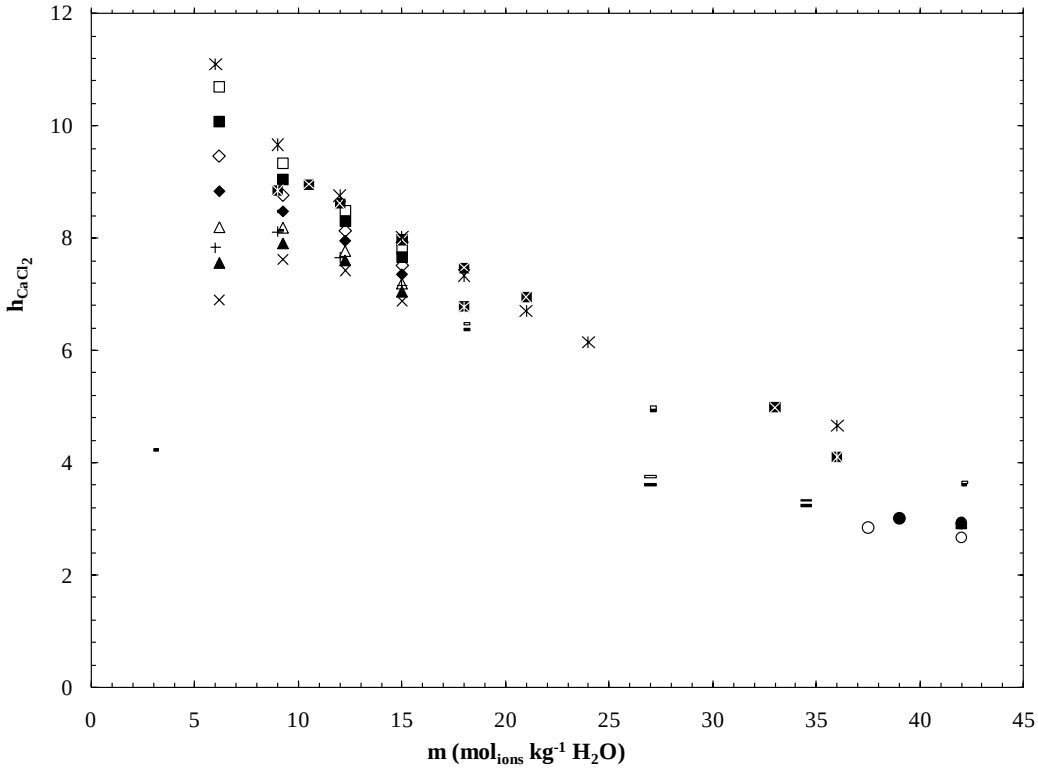

Figure 3.6G. h_{CaCl_2} a as a function of the ion concentration from vapor pressure depression data of Sako et al. at 60°C (□), 70°C (■), 80°C (◊), 90°C (♦), 100°C (Δ), 110°C (▲), 120°C (x); data of Washburn at 0°C (x), 40°C (*), 70°C (*), 90°C (-), 100°C (-), 110°C (-), 120°C (-), 130°C (○), 140°C (●); data of Forsythe at 100°C (+).

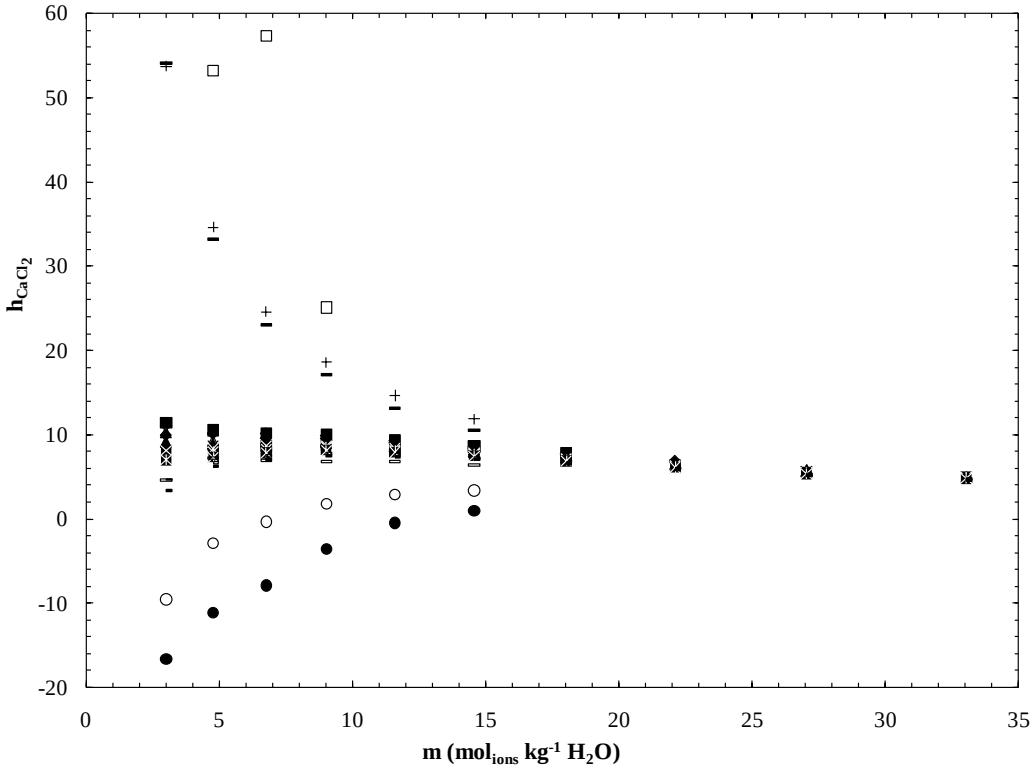

Figure 3.6H. h_{CaCl_2} a as a function of the ion concentration from vapor pressure depression data of Zaytsev and Aseyev at 0°C (□), 0°C (■), 10°C (◊), 20°C (♦), 30°C (Δ), 40°C (▲), 50°C (x), 60°C (x), 70°C (*), 80°C (*), 90°C (-), 100°C (-), 150°C (-), 200°C (-), 250°C (○), 300°C (●), 350°C (+).

For the freezing point depression data, h_{NaCl} decreased with decreasing concentration although there is a divergence in the data sets at ion concentration of ~ 6m (Figure 3.3A). Below this concentration h_{NaCl} appears to increase (Hall et al., 1988; Haghighi et al., 2008), remain constant (Rodebush, 1918) or decrease (Momicchioli et al., 1970; Gibbard and Gossman, 1974; Potter et al., 1978; Oakes et al., 1990; Washburn, 1926; Lide, 2008) depending on the data set investigated. h_{KCl} was also found to

decrease with decreasing concentration with a divergence in the data sets (Figure 3.3B). h_{KCl} appears to remain constant (Rodebush, 1918; Momicchioli et al., 1970) or decrease (Roloff; Spencer, 1932; Hall et al., 1988; Washburn, 1926; Forsythe, 1954; Lide, 2008). Although KCl data produce more consistent results at low concentration, h_{kCl} was found to be negative at ion concentration < 3m which suggests that h_{KCl} may not be accurately determined using this method particularly as the SEHM model of Balomenos et al. (2006) predicts $h_{KCl} \approx 2.3$ at low concentration. The negative h_{kCl} values and the divergence for both electrolytes suggests a need for further experimental work in this area. Overall, for the univalent electrolytes investigated, it appears that h increases with concentration until the eutectic is reached.

As for the divalent cations, there is a large discrepancy in the h_{MgCl_2} data with that of Gibbard and Fong (1972) and Gibbard and Gossman (1974) returning values much lower than the other data sets (Figure 3.3C). The former demonstrate an increase in h_{MgCl_2} as concentration is increased until a maximum is reached, followed by a decrease with further increases in concentration. The data of Haghighi et al. (2008) also appear to follow the same pattern although the data is too sparse to be definitive. The remaining datasets all show an increase in h_{MgCl_2} as concentration is decreased from the eutectic. The h_{CaCl_2} data may be the most robust of the four electrolytes (Figure 3.3D). h_{CaCl_2} appears to increase with ion concentration until a maximum is reached (~3m) and then decreases with ion concentration towards the eutectic. The lack of data, particularly for $MgCl_2$ indicates the need for more research in this area.

From the boiling point elevation data, h_{NaCl} was found to decrease with increasing concentration (Forsythe, 1954; Haas, 1971; Washburn 1926-1930; Zaytsev and Aseyev, 1992) although one dataset (Washburn 1926-1930) shows the inverse. h_{KCl} was also found to generally decrease with increasing concentration (Forsythe, 1954; Saxton and Smith, 1932; Washburn 1926-1930; Zaytsev and Aseyev, 1992). Unlike the analysis of the freezing point depression data, h_{kCl} was not found to be negative. Overall, for the univalent electrolytes investigated, it appears that h decreases with concentration and converge around 3 for NaCl and 2 for KCl. The divalent cations also show a decrease in h with increasing concentration for the analysis of boiling point elevation data. The $CaCl_2$ data generally follow the same pattern and appear to converge around 1 at high concentration. With the exception of the data from Forsythe (1954) which is relatively flat, the $MgCl_2$ data may follow the same pattern as $CaCl_2$ although the data is too sparse to be definitive. The lack of data, particularly for $MgCl_2$ indicates the need for more research in this area.

Similar to the findings for the freezing point depression data, h_{NaCl} was found to decrease (Bousfield and Bousfield, 1923; Forsythe, 1954; Olynk and Gordon, 1943; Pearce and Nelson, 1932; Washburn, 1926-1930) or remain level (Frazer, 1927; Gibson and Adams, 1933) with decreasing concentration for the vapor pressure depression data. Plotting h_{NaCl} as a function of concentration over the temperature range of 5-175°C (Figure 3.6B) shows little variance in h between 6 and 14m with a general decrease below 6m (Zaytsev and Aseyev, 1992). This is quite surprising as Figure 3.6B illustrates that concentration appears to play a larger role in determining h than temperature does.

h_{KCl} was found to decrease with decreasing concentration for all sets of vapor pressure depression data (Lovelace et al., 1916; Lovelace et al., 1921; Brown and Delaney, 1954; Pearce and Snow, 1927; Apelblat, 1998; Zaytsev and Aseyev, 1992) with the exception of Washburn (1926-1930). Furthermore, the hydration number is predicted to be negative for many of the data sets at low concentrations, a finding similar to the freezing point depression results. Over all concentrations and similar temperatures, h_{KCl} was found to be less than h_{NaCl} upon analysis of the vapor pressure depression data.

The vapor pressure depression data demonstrate an increase in h_{MgCl_2} as concentration is increased until a maximum is reached around 6m followed by a decrease with concentration (Sako et al., 1985; Washburn 1926-1930) over the temperature range 0-120°C although negative hydration numbers are predicted for low concentrations. The data of Zaytsev and Aseyev (1992) for temperatures less than 125°C generally return h_{MgCl_2} between 8 and 10. As the temperature is increased from 125°C to 275°C, h_{MgCl_2} decreases with concentration with more negative values at higher temperatures. With the exception of some the data of Zaytsev and Aseyev (1992), h_{CaCl_2} decreases with concentration (Sako et al., 1985; Washburn, 1926-1930; Forsythe, 1954).

Using the hydration numbers (including the negative h_{KCl} values) determined above for each concentration, ΔH was then calculated for each dataset from the maximum concentration down to the lowest concentration where $\Delta T \geq 4K$ for each electrolyte yielding similar results for ΔH_{fusion} (Figures 3.7A-D) and $\Delta H_{vaporization}$ (Figures 3.8A-D).

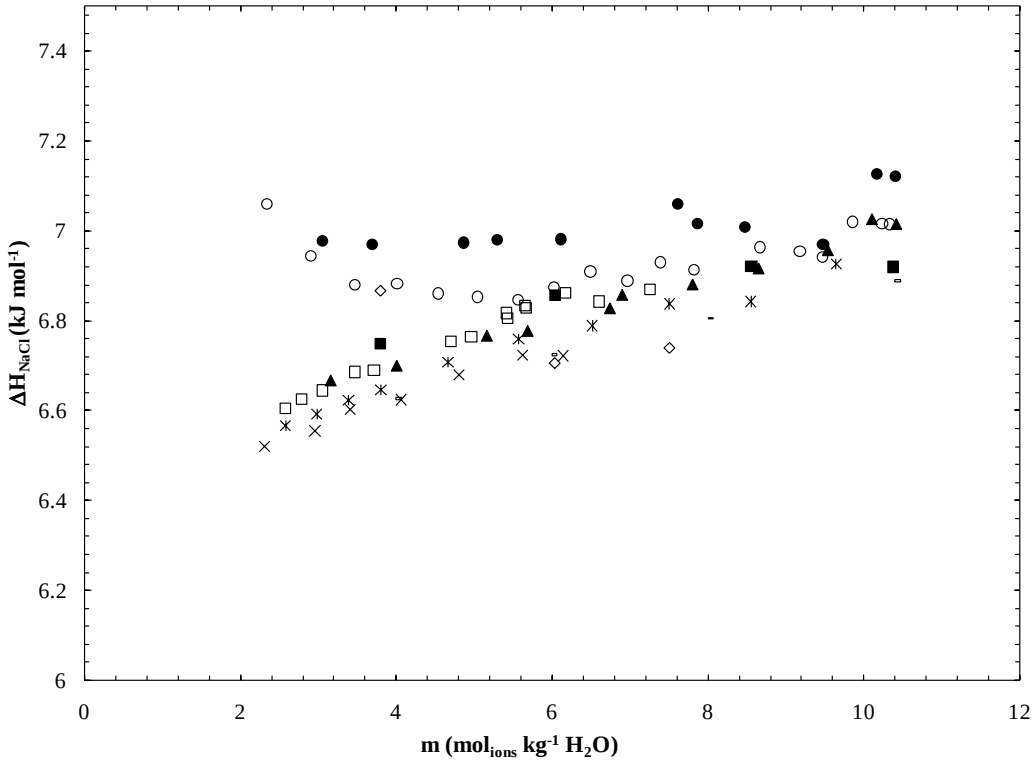

Figure 3.7A. $\Delta H_{fus(NaCl)}$ (kJ mol^{-1}) as a function of the ion concentration for the freezing point depression data of Rodebush (●), Momicchioli et al. (x), Gibbard and Gossman (□), Potter et al. (■), Hall et al. (○), Oakes et al. (▲), Haghighi et al. (♦), Lide (*), Washburn (-).

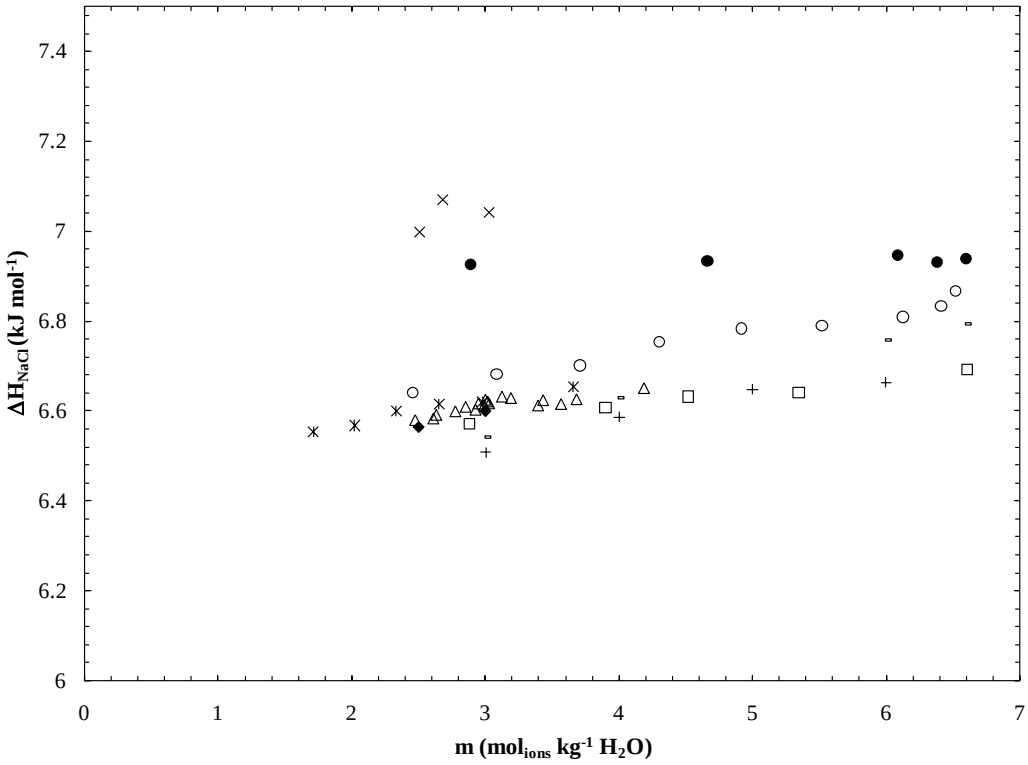

Figure 3.7B. $\Delta H_{fus(KCl)}$ (kJ mol^{-1}) as a function of the ion concentration for the freezing point depression data of Rodebush (●), Roloff (□),Spencer (♦), Chiorboli et al. (▲), Momicchioli et al. (x), Hall et al. (○), Lide (*), Washburn (-), Forsythe (+).

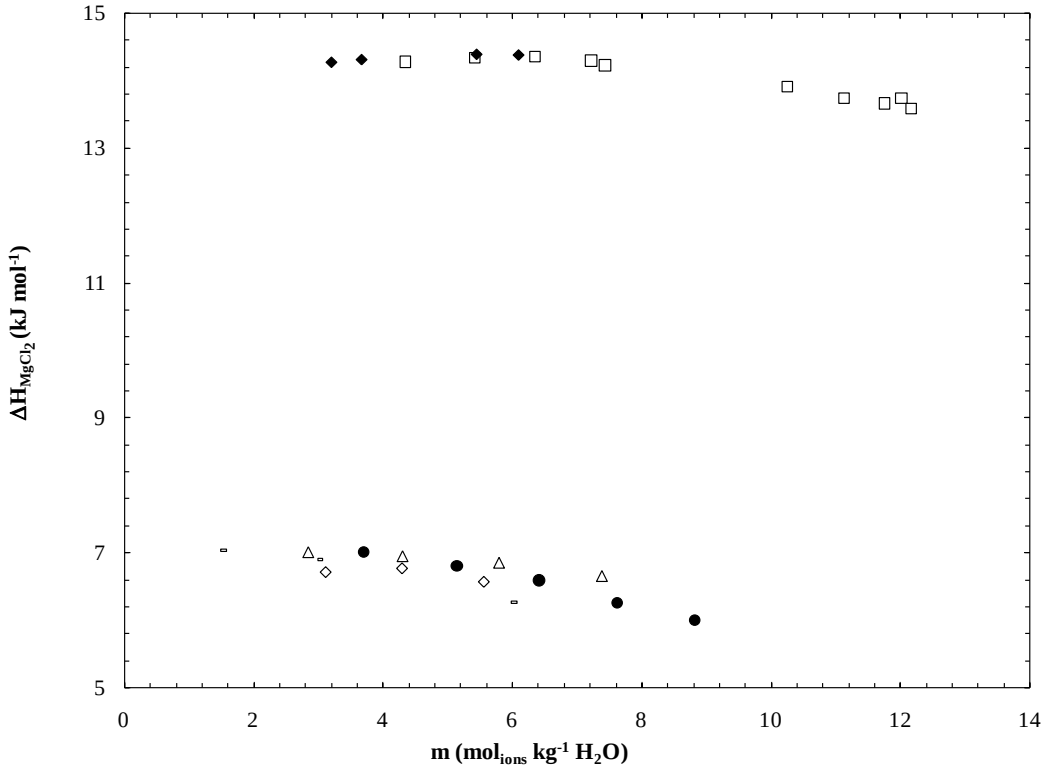

Figure 3.7C. $\Delta H_{fus(MgCl_2)}$ (kJ mol^{-1}) as a function of the ion concentration for the freezing point depression data of Jones and Bassett (▲), Rodebush (●), Gibbard and Fong (♦), Gibbard and Gossman (□), Haghighi et al. (♦), Washburn (-).

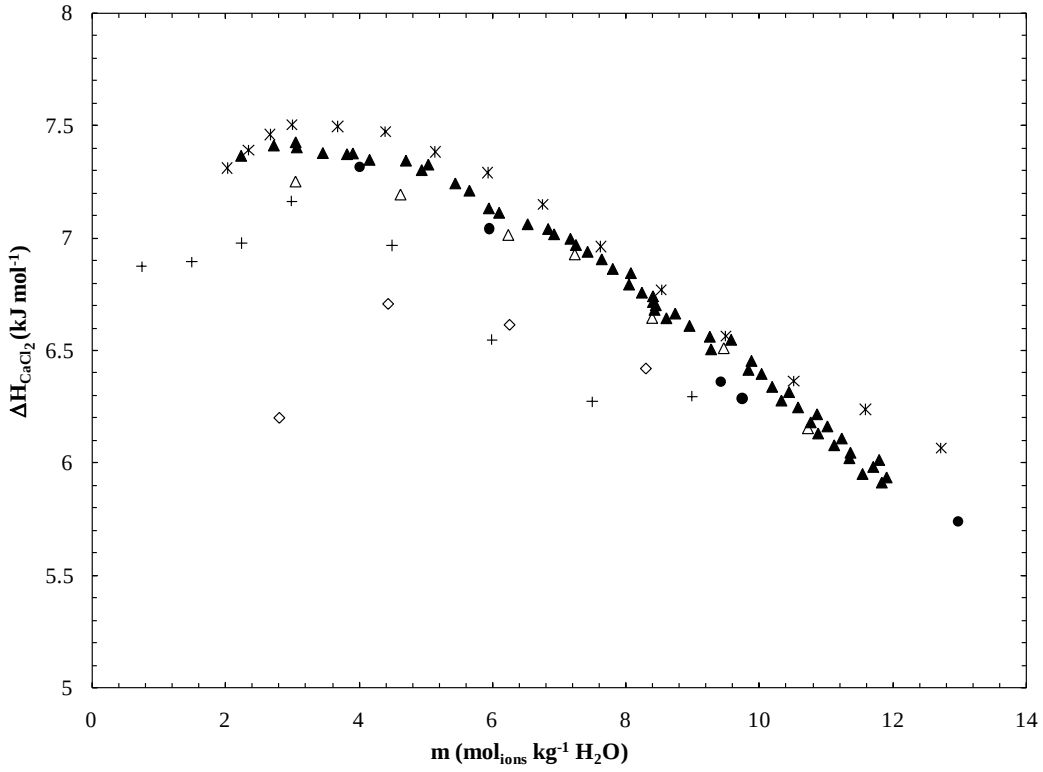

Figure 3.7D. $\Delta H_{fus(CaCl_2)}$ (kJ mol^{-1}) as a function of the ion concentration for the freezing point depression data of Jones and Bassett (▲), Rodebush (●), Oakes et al. (▲), Haghighi et al. (♦), Lide (*), Washburn (-).

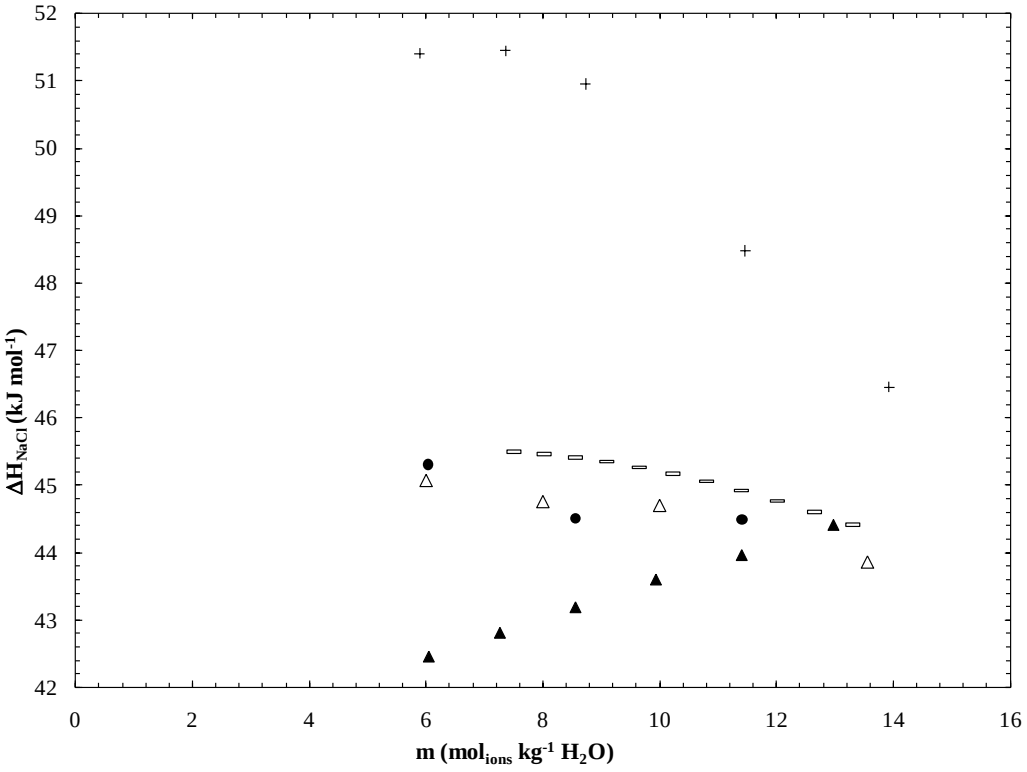

Figure 3.8A. $\Delta H_{vap(NaCl)}$ (kJ mol^{-1}) as a function of the ion concentration for the boiling point elevation data of Hass (●), Washburn (Δ,▲), Forsythe (+), Zaytsev and Aseyev (-).

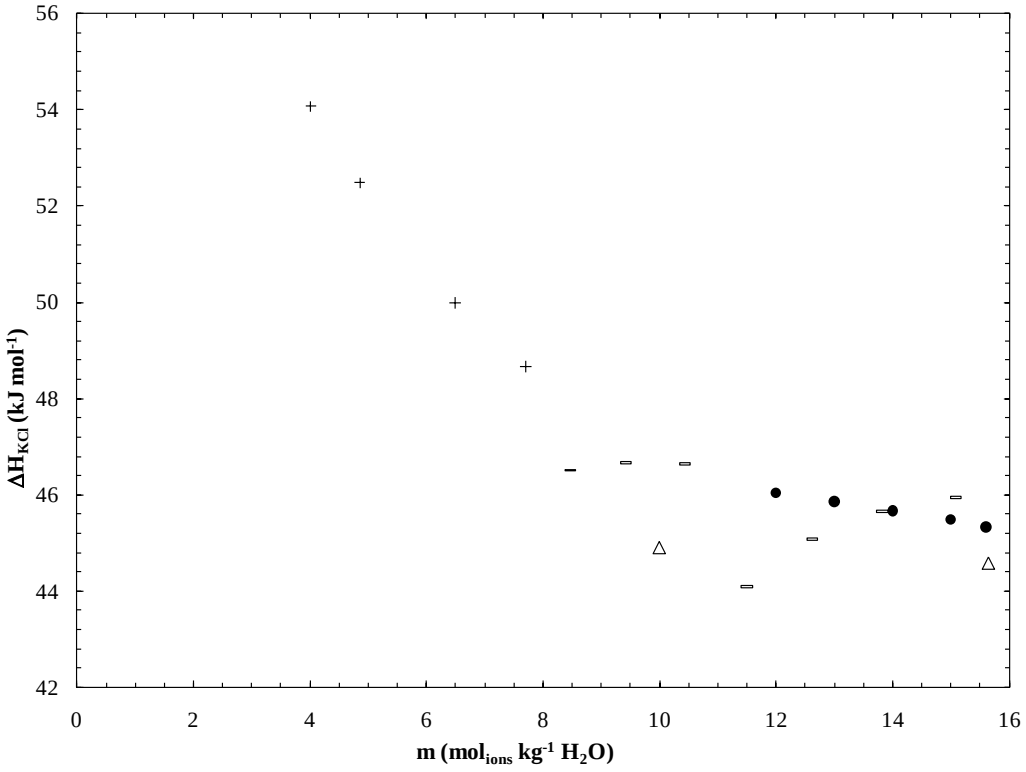

Figure 3.8B. $\Delta H_{vap(KCl)}$ (kJ mol^{-1}) as a function of the ion concentration for the boiling point elevation data of Saxton and Smith (●), Washburn (Δ), Forsythe (+), Zaytsev and Aseyev (-).

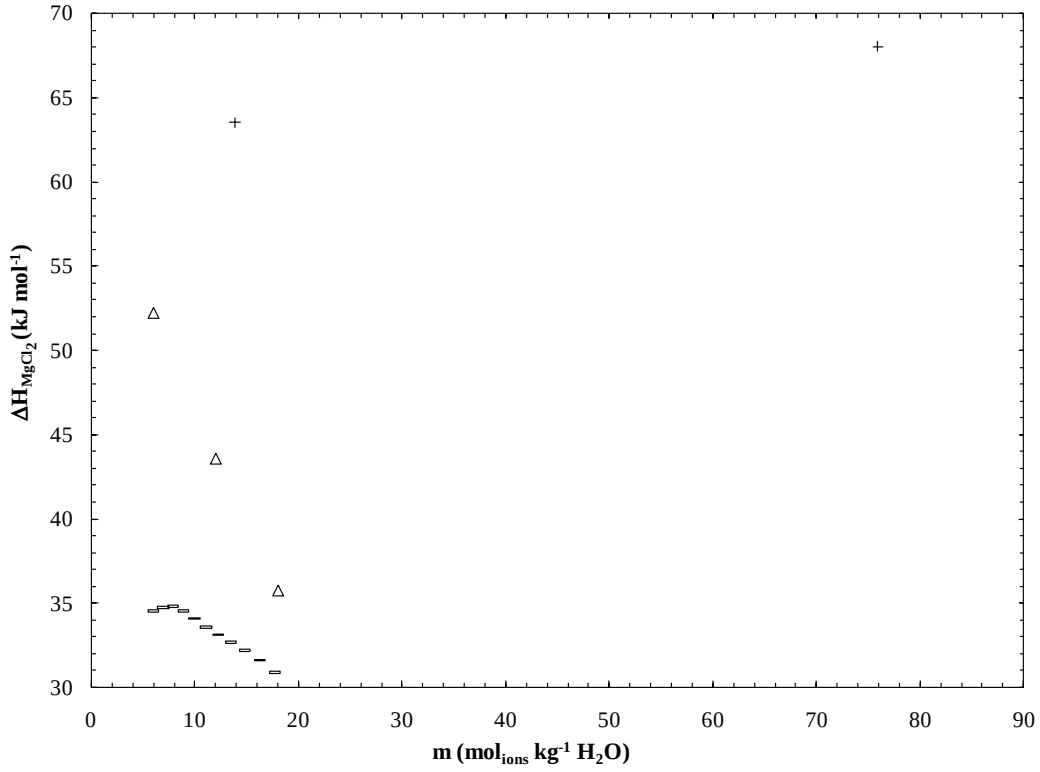

Figure 3.8C. $\Delta H_{vap(MgCl_2)}$ (kJ mol^{-1}) as a function of the ion concentration for the boiling point elevation data of Washburn (Δ), Forsythe (+), Zaytsev and Aseyev (-).

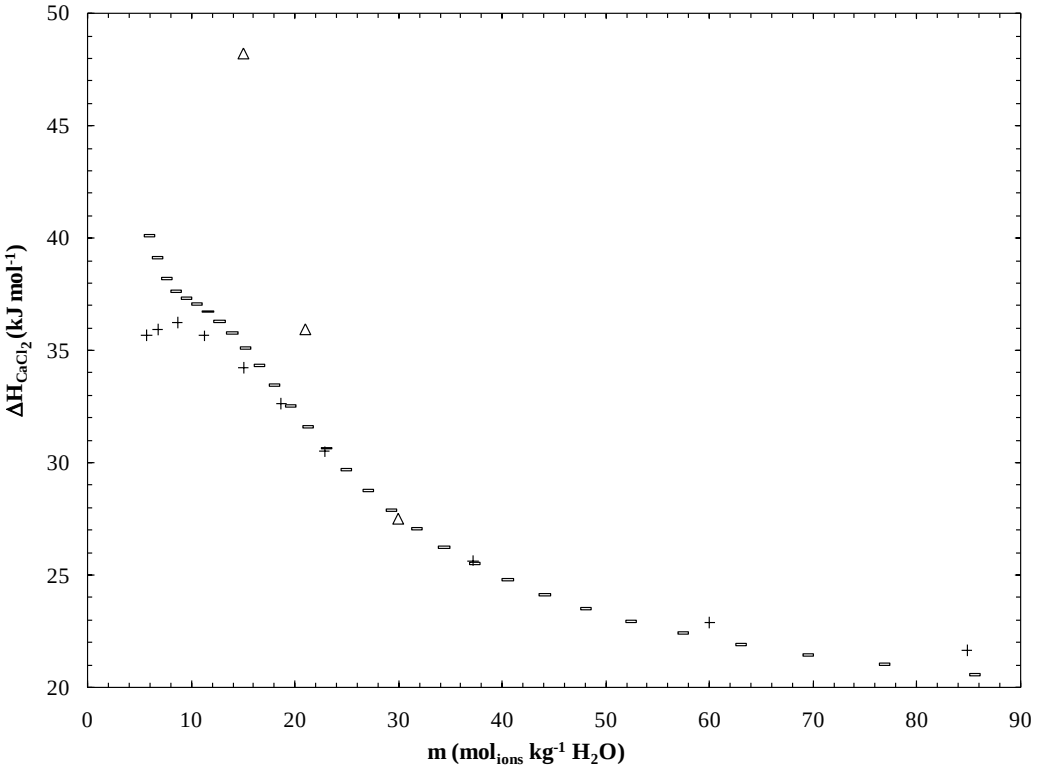

Figure 3.8D. $\Delta H_{vap(CaCl_2)}$ (kJ mol^{-1}) as a function of the ion concentration for the boiling point elevation data of Washburn (Δ), Forsythe (+), Zaytsev and Aseyev (-).

ΔH_{fus} and ΔH_{vap} results for each electrolyte are rather similar to previously discussed hydration data. $\Delta H_{fus(NaCl)}$ was found to decrease with decreasing concentration although there is a divergence in the data sets at ion concentration of ~ 6m (Figure 3.4A). Below this concentration $\Delta H_{fus(NaCl)}$ increases (Hall et al., 1988; Haghighi et al., 2008), remains constant (Rodebush, 1918) or decreases (Momicchioli et al., 1970; Gibbard and Gossman, 1974; Potter et al., 1978; Oakes et al., 1990; Washburn, 1926; Lide, 2008) depending on the dataset. $\Delta H_{fus(KCl)}$ also decreases with decreasing concentration with a divergence in the results from the data sets (Figure 3.4B). $\Delta H_{fus(KCl)}$

appears to remain constant (Rodebush, 1918; Momicchioli et al., 1970) or decrease (Roloff; Spencer, 1932; Hall et al., 1988; Washburn, 1926; Forsythe, 1954; Lide, 2008). For the most part, it appears that ΔH_{fus} decreases with concentration for the univalent electrolytes investigated. Again, there is a large discrepancy in the $MgCl_2$ data with that of Gibbard and Fong (1972) and Gibbard and Gossman (1974) returning ΔH_{fus} values much greater than the other data sets (Figure 3.4C). The former demonstrate an increase in $\Delta H_{fus(MgCl_2)}$ as concentration is increased until a maximum is reached followed by a decrease with concentration. The data of Haghighi et al. (2008) may follow the same pattern although there are only three data points. As with h_{CaCl_2}, $\Delta H_{fus(CaCl_2)}$ appears to increase with ion concentration until a maximum is reached (~3m) and then decreases with ion concentration towards the eutectic. Although it appears that a maximum ΔH_{fus} is reached at a concentration > 0, it is clear that more work needs to be done particularly for $MgCl_2$.

From the boiling point elevation data, $\Delta H_{vap(NaCl)}$ was found to decrease with increasing concentration (Forsythe, 1954; Haas, 1971; Washburn 1926-1930; Zaytsev and Aseyev, 1992) with the exception of one dataset which shows the inverse (Washburn, 1926-1930). $\Delta H_{vap(KCl)}$ was also found to generally decrease with increasing concentration (Forsythe, 1954; Saxton and Smith, 1932; Washburn 1926-1930; Zaytsev and Aseyev, 1992). The divalent cations also show a decrease in ΔH_{vap} with increasing concentration for the analysis of boiling point elevation data with the exception of the data from Forsythe (1954) for the $MgCl_2$ data.

Using a differential scanning calorimeter, Han et al. (2006) found two distinct phase change events, water/ice phase change and eutectic phase change, during the melting of H_2O-NaCl binary mixtures. When normalized to the amount of H_2O participating in the melting of ice, ΔH of the water/ice phase change was found to be approximately 90% of pure water regardless of initial solute concentration. However the normalization was based on weight percent where the fraction of water was defined as:

$$f_{H_2O} = \frac{23 - Wt\%}{23} \tag{3.20}$$

where f_{H2O} is the fraction of water and Wt% is the weight percent of NaCl. Therefore, by their definition, in a saturated solution, $f_{H2O} = 0$, which is physically impossible. Their treatment was performed on the current data although similar results were not obtained as ΔH_{fus} was found to decrease with solute concentration for NaCl solutions. When their data is recalculated as mole fraction, ΔH_{fus} decreases with concentration of the solute (Table 3.5).

Table 3.5 Data of Han et al. (2006).

mass fraction (%, wt/wt)	$L(C_0)$ J/g	f_{H2O}	L_{H2O}	X_{H2O}	L'_{H2O}
0.8	291	0.97	301	0.998	292
4.3	250	0.82	306	0.986	253
8.4	196	0.64	304	0.973	202

This suggests that either there is an error in the calculation of ΔH_{fus} in the present results or that their results were quite fortuitous as $f_{H2O} = 0$ is physically impossible in a saturated solution. Workers investigating sucrose solutions found ΔH_{fus} to vary linearly with concentration (Schawe):

$$\Delta H = (1 - aX_{solute})\Delta H_{fusion} \quad (3.21)$$

where a is a constant for each individual solute. This relationship demonstrates that as solute concentration approaches zero, ΔH_{fus} of the solution should approach that of pure water of 6.00678 kJ mol^{-1} (Feistel and Wagner, 2006). ΔH_{fus} for both univalent electrolytes decrease with concentration although they do not necessarily approach 6 kJ mol^{-1} at infinite dilution. The datasets of NaCl that show a decrease of ΔH_{fus} with concentration yield an intercept of 6.5 kJ mol^{-1} ($R^2 = 0.85$) and those of KCl also give 6.5 kJ mol^{-1} ($R^2 = 0.66$). Below the threshold concentration for the $CaCl_2$ freezing point depression data, ΔH_{fus} may yield similar results although the data below this concentration are too sparse to be meaningful. The same could be expected for boiling point elevation data, that is ΔH_{vap} should approach the value of pure water at 100°C at infinite dilution (at 100°C, $\Delta H_{vap} = 40.657$ kJ mol^{-1} for pure water according to Marsh, 1987). Therefore, ΔH_{vap} was plotted as a function of temperature of solution (Figures 3.9A-D) with results quite similar to that previously determined for concentration. The analysis of boiling point elevation data for both univalent electrolytes return ΔH_{vap} values greater than that of pure water (Marsh, 1987) over all experimental temperatures (Figures 3.9A-B). For the divalent electrolytes, the majority of the calculated results are

below that of pure water (Marsh, 1987) with the exception of some of the data of Washburn (1926-1930). Although calculated values are in reasonable agreement, the apparent lack of convergence at 100°C may raise the question as to the validity of this analysis. According to Marcus (2009), K^+ is a structure breaking ion, both divalent cations, Ca^{2+} and Mg^{2+} are structure making ions and Na^+ is borderline between the two. Although Cl^- is also considered a structure breaking ion (Marcus, 2009), it will be ignored as it is present in all solutions. The present results indicate that KCl solutions have the greatest positive deviation from pure water while NaCl are less positive. That is, ΔH_{vap} is greater in these univalent solutions than for pure water whereas both divalent cation solutions lead to negative deviations from pure water. These results are counter intuitive as it may be assumed that a structure breaking ion would disrupt the hydrogen bonding network of the bulk water making it easier for a molecule of liquid water to be converted to water vapor which would ultimately lead to lower enthalpy values. It may be that since KCl is structure breaking, it does indeed disrupt the hydrogen bonded network of the water molecules leading to an increase in the intensity of the librational band compared to pure water (e.g. James and Frost, 1974; James and Armishaw, 1975). It could be that by disrupting the hydrogen bonding network of the bulk solution, the overall symmetry of the solution is diminished which could be having an effect on the calculated ΔH values.

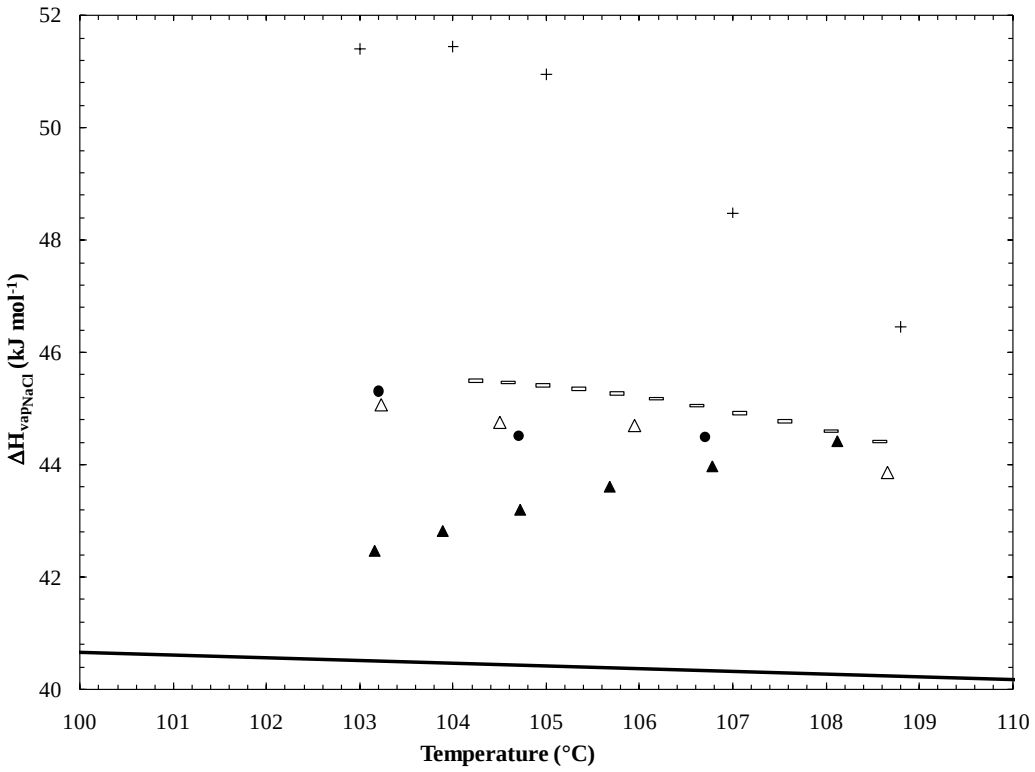

Figure 3.9A. $\Delta H_{vap(NaCl)}$ (kJ mol^{-1}) as a function of temperature for the boiling point elevation data of Hass (●), Washburn (Δ,▲), Forsythe (+), Zaytsev and Aseyev (-) with the solid curve generated from the data of Marsh, 1987.

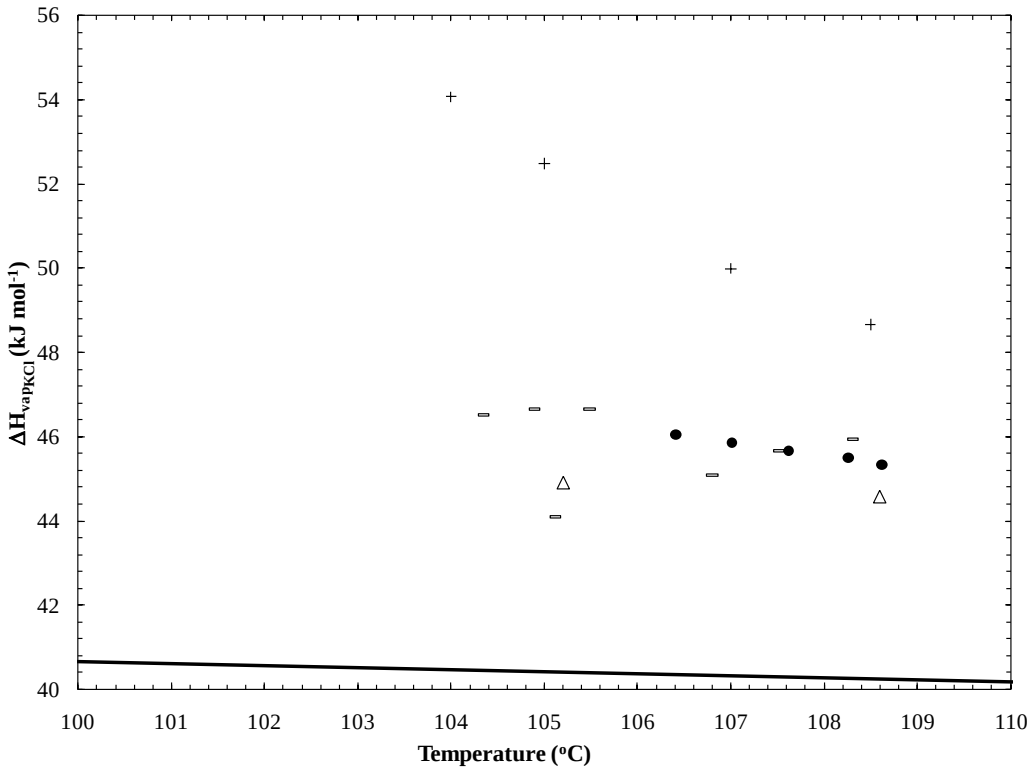

Figure 3.9B. $\Delta H_{vap(KCl)}$ (kJ mol^{-1}) as a function of temperature for the boiling point elevation data of Saxton and Smith (●), Washburn (Δ), Forsythe (+), Zaytsev and Aseyev (-) with the solid curve generated from the data of Marsh, 1987.

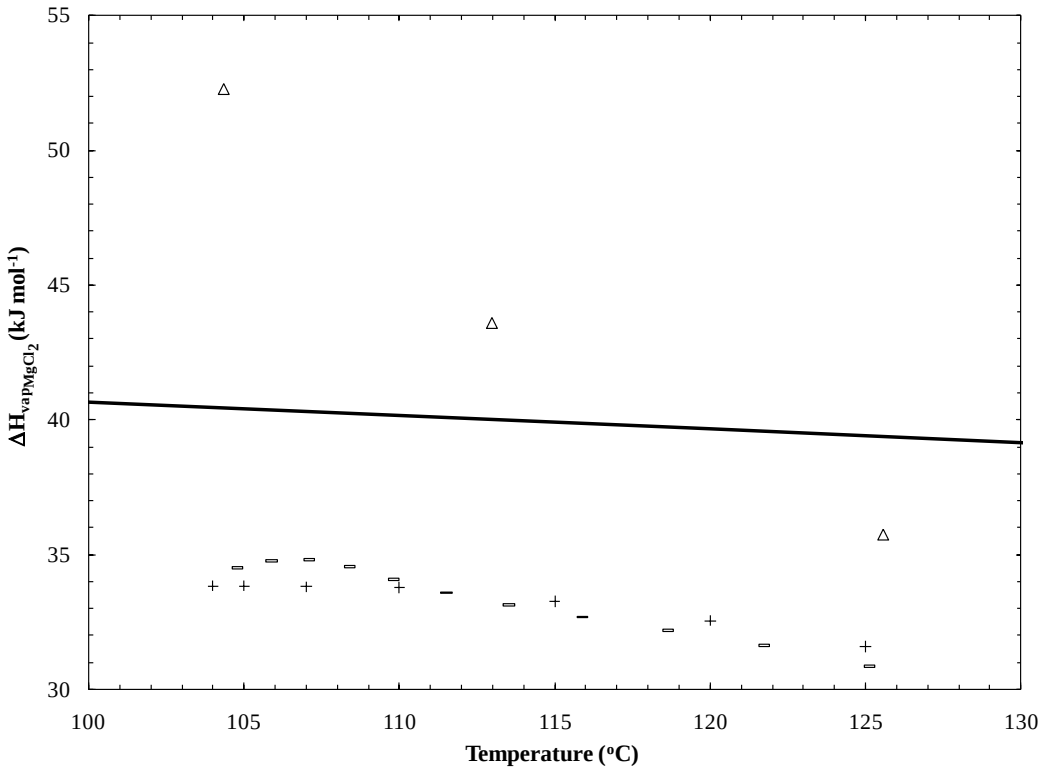

Figure 3.9C. $\Delta H_{vap(MgCl_2)}$ (kJ mol^{-1}) as a function of temperature for the boiling point elevation data of Washburn (Δ), Forsythe (+), Zaytsev and Aseyev (-) with the solid curve generated from the data of Marsh, 1987.

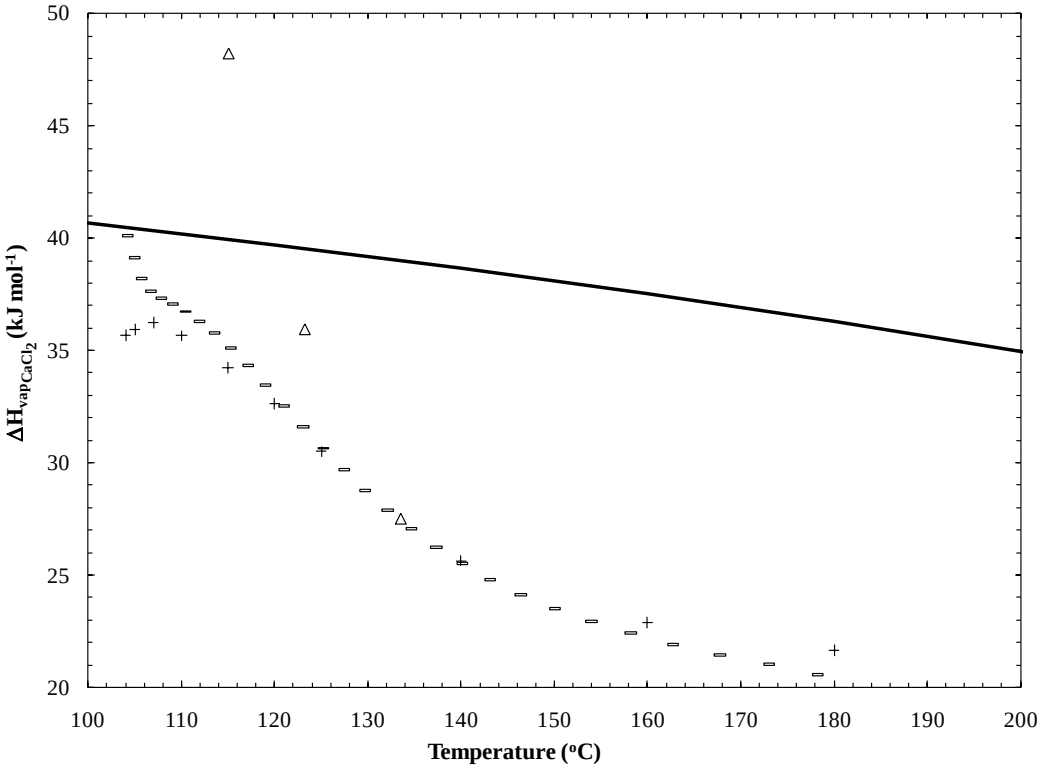

Figure 3.9D. $\Delta H_{vap(CaCl_2)}$ (kJ mol^{-1}) as a function of temperature for the boiling point elevation data of Washburn (Δ), Forsythe (+), Zaytsev and Aseyev (-) with the solid curve generated from the data of Marsh, 1987.

As the figures for h and $\Delta H_{fus/vap}$ appear very similar, $\Delta H_{fus/vap}$ was plotted as a function of h for each electrolyte (Figures 3.10A-D and Figures 3.11A-D). Intuitively, it would make sense that ΔH should be correlated with the number of bound solvent molecules. As more water is available as infinite dilution is approached, one would expect ΔH to approach that of pure water. ΔH does seem to correlate well with h although the relationship for univalent electrolytes appears different than that for divalent chloride salts. $\Delta H_{fus(NaCl)}$ and $\Delta H_{fus(KCl)}$ exhibit upward curvature with h

whereas $\Delta H_{fus(MgCl_2)}$ and $\Delta H_{fus(CaCl_2)}$ exhibit downward curvature with h. For NaCl, as h_{NaCl} approaches 0, $\Delta H_{fus(NaCl)}$ approaches ~ 6.5 kJ mol^{-1} although $MgCl_2$ and $CaCl_2$ give much lower values. From this data, although promising, h does not seem to directly control ΔH_{fus} in simple electrolyte solutions.

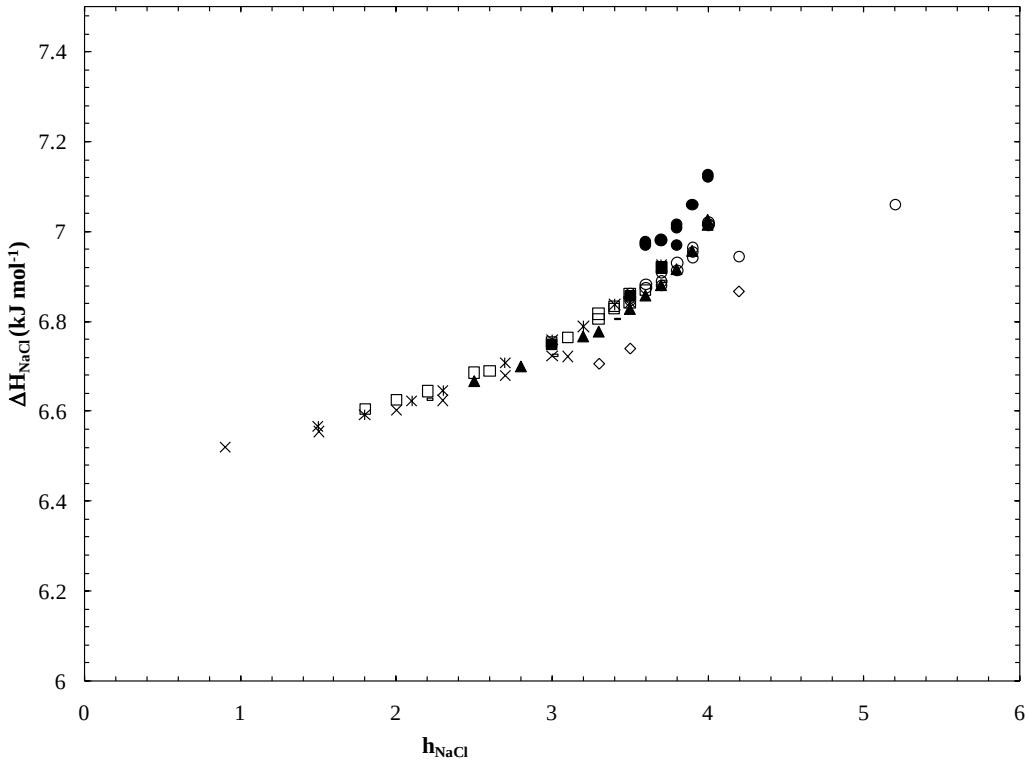

Figure 3.10A. $\Delta H_{fus(NaCl)}$ (kJ mol^{-1}) as a function of h_{NaCl} for Rodebush (●), Momicchioli et al. (x), Gibbard and Gossman (□), Potter et al. (■), Hall et al. (○), Oakes et al. (▲), Haghighi et al. (♦), Lide (*), Washburn (-).

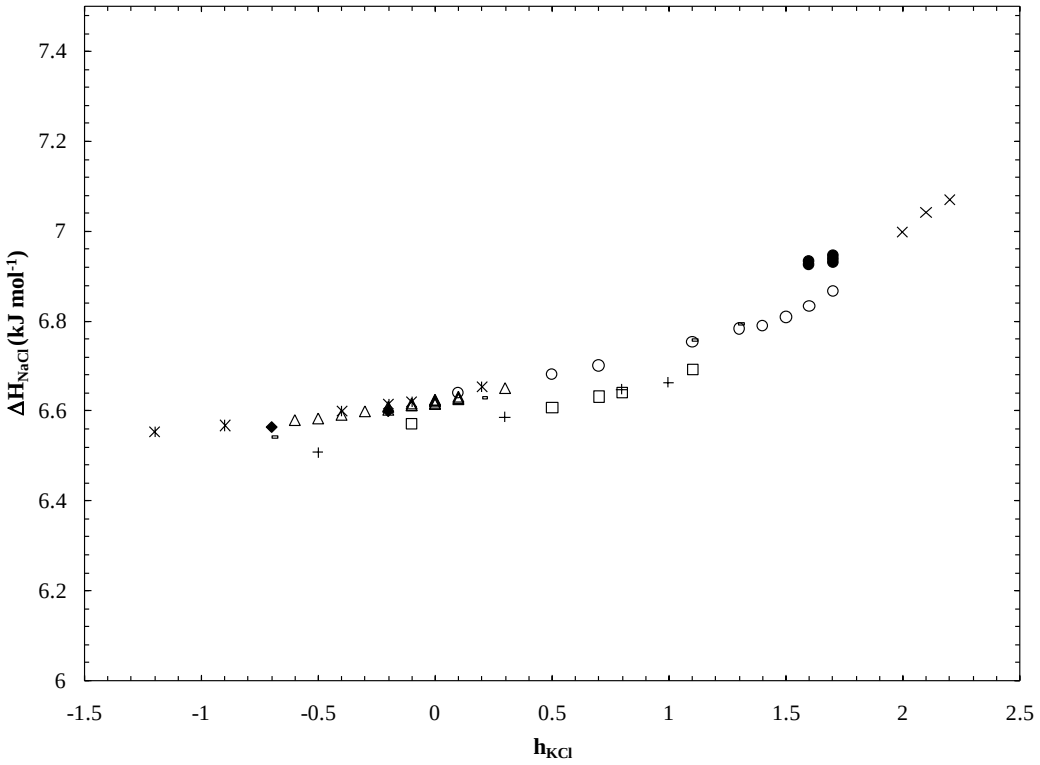

Figure 3.10B. $\Delta H_{fus(KCl)}$ (kJ mol^{-1}) as a function of h_{KCl} for Rodebush (●), Roloff (□),Spencer (♦), Chiorboli et al. (▲), Momicchioli et al. (x), Hall et al. (○), Lide (*), Washburn (-), Forsythe (+).

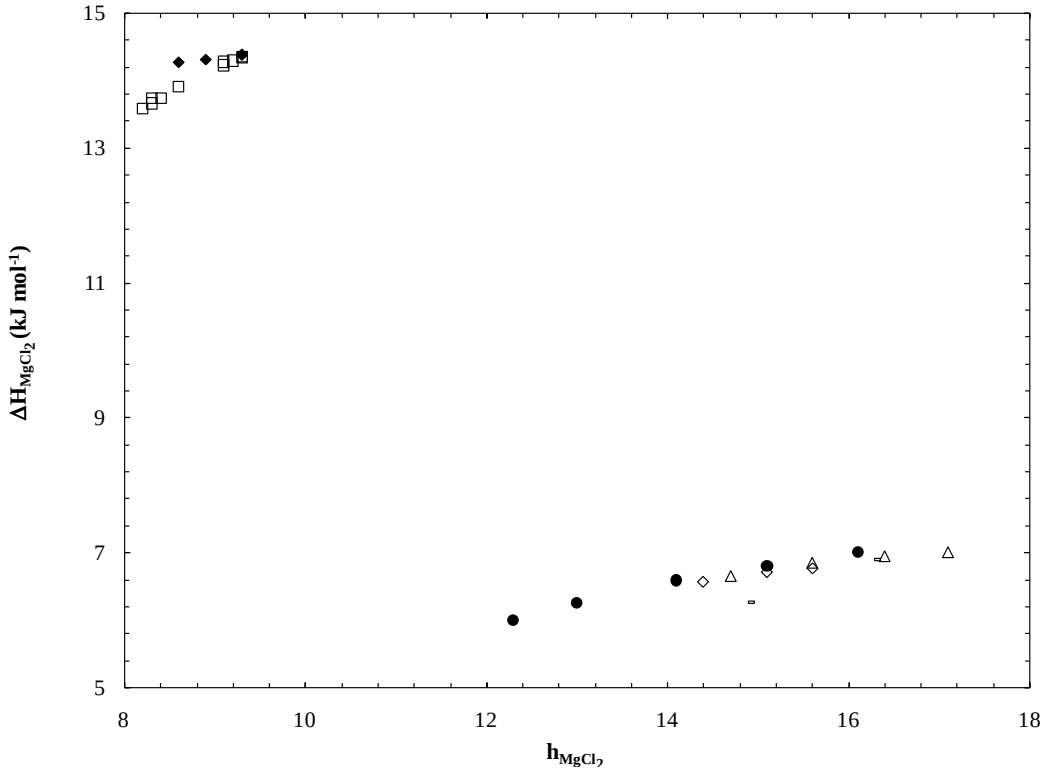

Figure 3.10C. $\Delta H_{fus(MgCl_2)}$ (kJ mol^{-1}) as a function of h_{MgCl_2} for Jones and Bassett (▲), Rodebush (●), Gibbard and Fong (♦), Gibbard and Gossman (□), Haghighi et al. (♦), Washburn (-).

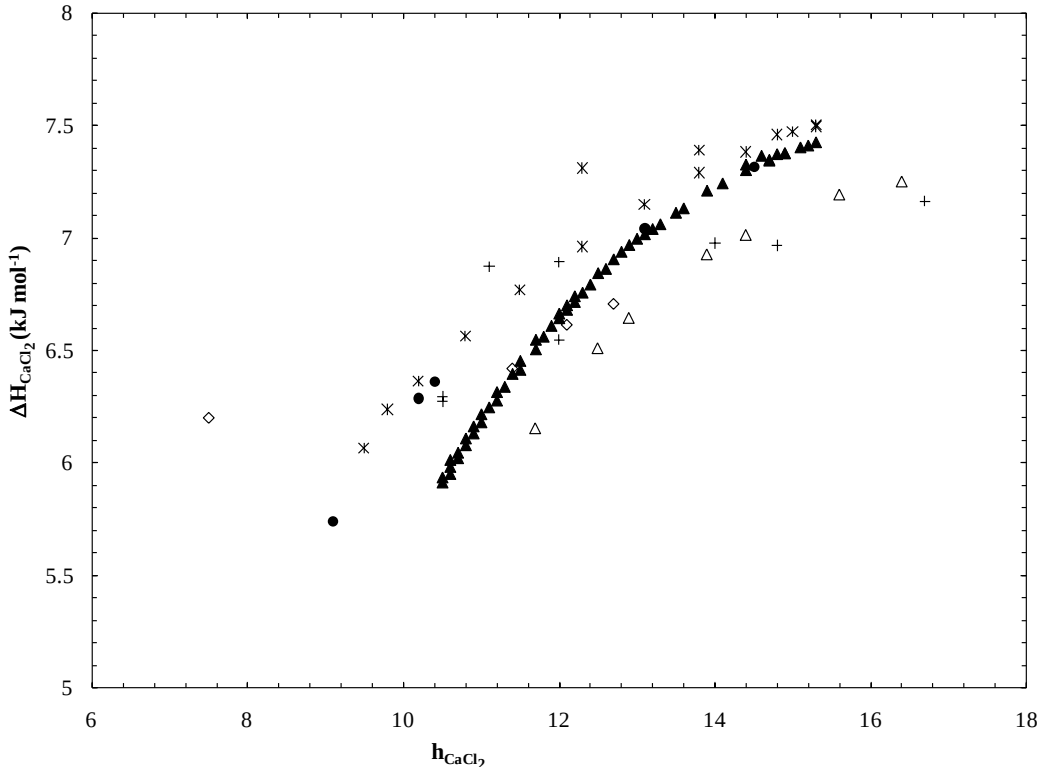

Figure 3.10D. $\Delta H_{fus(CaCl_2)}$ (kJ mol^{-1}) as a function of h_{CaCl_2} for Jones and Bassett (▲), Rodebush (●), Oakes et al. (▲), Haghighi et al. (♦), Lide (*), Washburn (-).

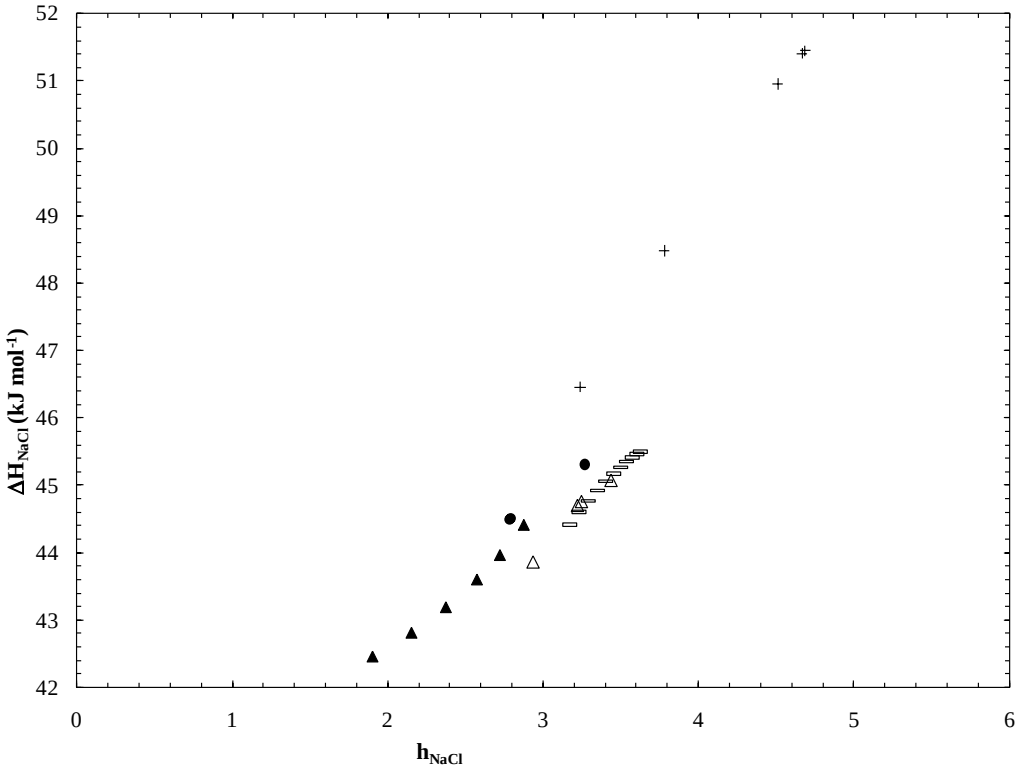

Figure 3.11A. $\Delta H_{vap(NaCl)}$ (kJ mol^{-1}) as a function of h_{NaCl} for Hass (●), Washburn (Δ,▲), Forsythe (+), Zaytsev and Aseyev (-).

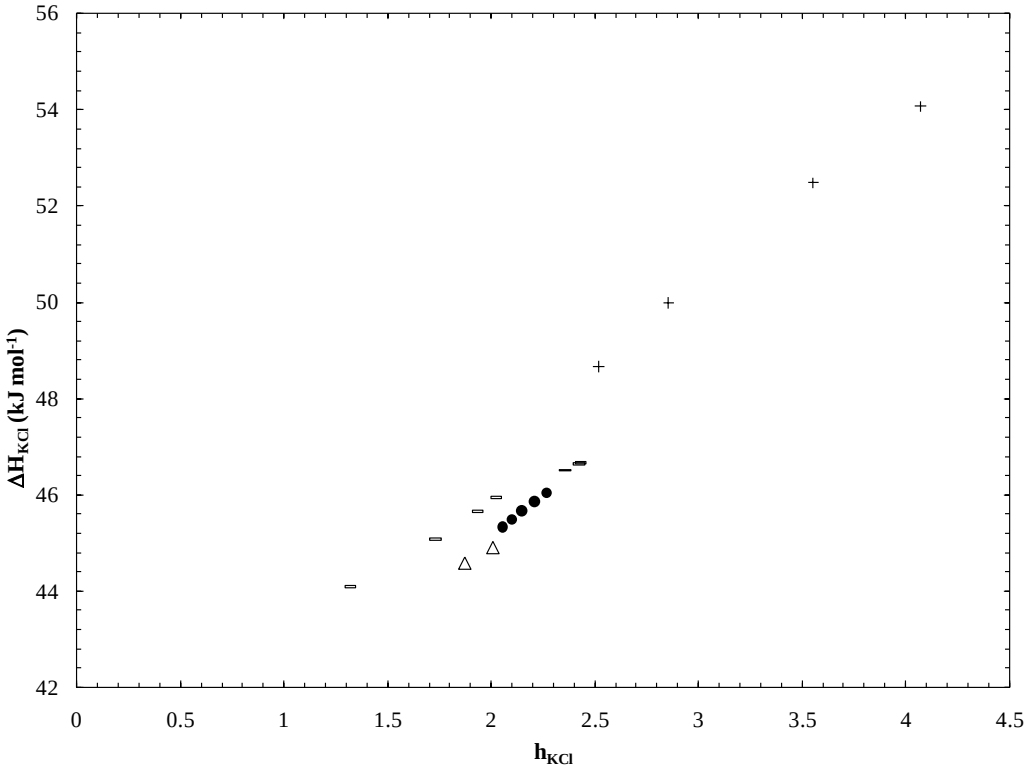

Figure 3.11B. $\Delta H_{vap(KCl)}$ (kJ mol^{-1}) as a function of h_{KCl} for Saxton and Smith (●), Washburn (Δ), Forsythe (+), Zaytsev and Aseyev (-).

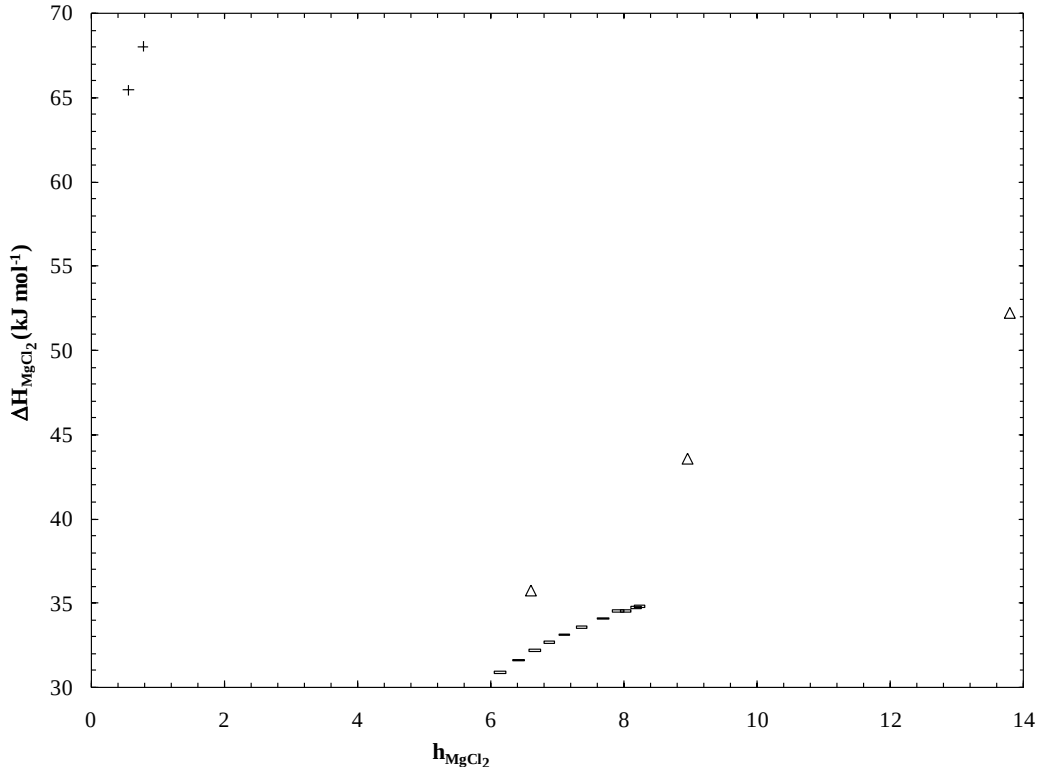

Figure 3.11C. $\Delta H_{vap(MgCl_2)}$ (kJ mol^{-1}) as a function of h_{MgCl_2} for Washburn (Δ), Forsythe (+), Zaytsev and Aseyev (-).

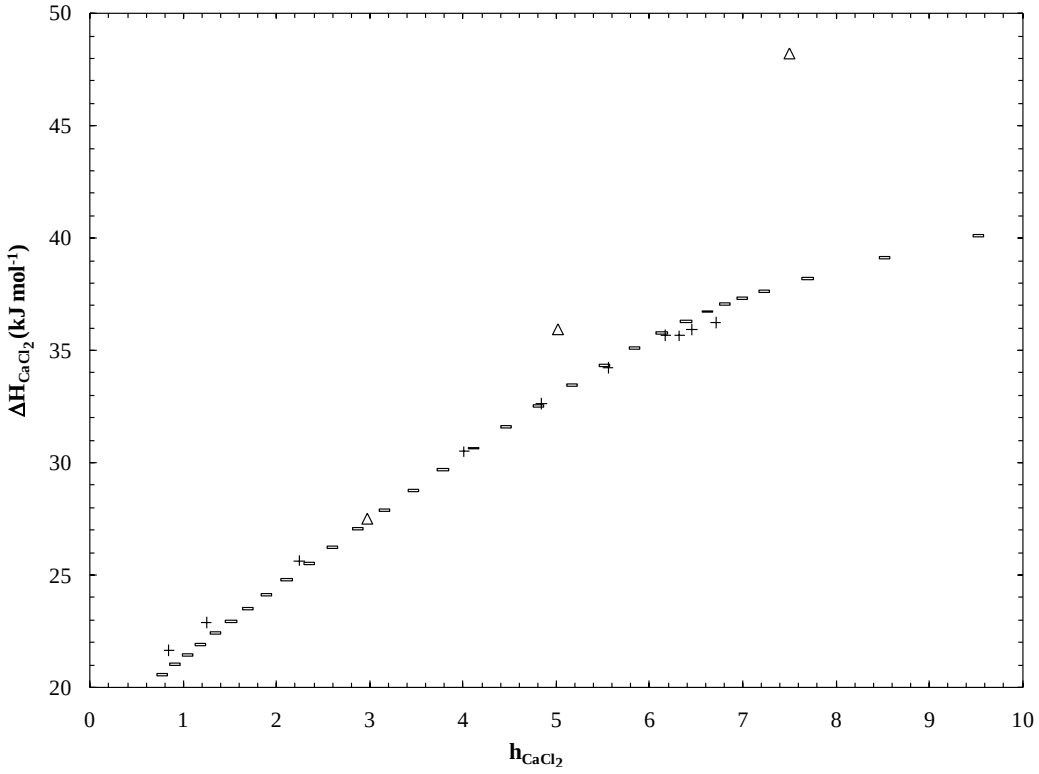

Figure 3.11D. $\Delta H_{vap(CaCl_2)}$ (kJ mol^{-1}) as a function of h_{CaCl_2} for Washburn (Δ), Forsythe (+), Zaytsev and Aseyev (-).

3.8 Predictive Capability of Calculated Hydration Numbers

Despite the uncertainties raised as to the influence temperature and concentration have on h and ΔH, if the previously determined h values are correct, then deviations in ternary solutions should be able to be corrected using these values. To a first approximation, the freezing point depression of a ternary solution can be determined relatively accurately with the assumption that ΔH and h are constant regardless of concentration. Using the previously determined values of h from freezing point

depression data, values may be predicted for ternary mixtures by rearrangement of equation 3.10 yielding rather accurate predictions (Figure 3.12).

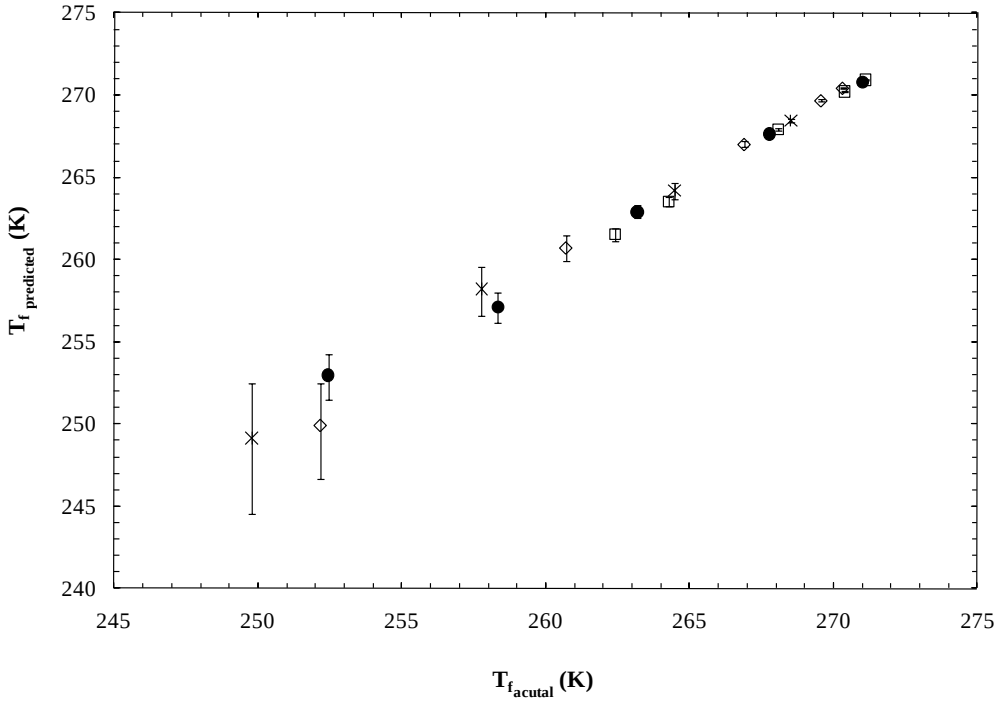

Figure 3.12. Predicted freezing point as a function of the actual freezing point (Haghighi et al., 2008) for ternary systems of H_2O and NaCl, $CaCl_2$ (●); NaCl, KCl (□), $CaCl_2$, KCl (*); $MgCl_2$, NaCl (◊).

Even though the error in the prediction is increased as the freezing point is decreased, the model is able to reasonably predict the freezing point for these ternary systems. Despite the uncertainties in h and ΔH related to concentration and temperature, this provides confidence in using the hydration numbers calculated in the present work. The stepwise multiple regression analysis performed in 2.5.5 can now be

repeated using the newly calculated hydration numbers of $h_{NaCl} = 2.8 \pm 0.9$; $h_{KCl} = 1.2 \pm 1.2$; $h_{MgCl_2} = 9.8 \pm 3.7$; $h_{CaCl_2} = 6.3 \pm 3.3$ determined in the present study. Following the procedure outlined in 2.5.5, a stepwise MR analysis was performed using the statistical software SPSS® v. 16.0 for Windows® in which all possible combinations of independent variables (I, $m_{Ca^{2+}}$, m_{Cl^-}, m_{K^+}, $m_{Mg^{2+}}$, m_{Na^+}, pCO_2, T, $X_{"free" H_2O}$) were considered. All data in the present study as well as data used in the MR model of Gledhill and Morse (2006a) were initially included in the MR analysis. Outliers, KCl 2.0 T55 and NaCl 2.0 T85 were identified as having standardized residuals outside the range of ± 3, and were thus removed from the analysis. A slight positive autocorrelation of the regression was indicated by the calculated Durbin-Watson coefficient (1.591). The t-test statistics were found to be significant (<0.001) and the variance inflation factors (VIF) less than 1.19 for each predictor. Condition indices for collinearity were less than 7 for each predictor with the exception of $m_{Mg^{2+}}$ which was 25. Taken all together, this suggests that severe collinearity was not a factor (Belsley et al., 2005) although there probably is some correlation between $m_{Mg^{2+}}$ and $X_{"free" H_2O}$. Removal of these outliers yielded (adjusted $R^2 = 0.872$, $p < 0.001$) a predictive equation for k:

$$k_{pred} = \beta_0 + \beta_1 T + \beta_2 pCO_2 + \beta_3 X_{"free" H_2O} + \beta_4 m_{Mg^{2+}} \qquad (3.22)$$

where k is the predicted dissolution rate constant, T is the temperature, pCO_2 is the partial pressure of carbon dioxide, $X_{"free" H_2O}$ is the mole fraction of free water, $m_{Mg^{2+}}$ is the magnesium molality and β_i is the coefficient of the i^{th} term. β values (unstandardized coefficients) for predicting k are provided (Table 3.6). As the units of the predictors are

different, standardized coefficients are typically used to determine the relative importance of the individual predictors on the dependent variable and are provided (Table 3.6). Using the standardized coefficients for the direct comparison of the predictors, indicate the relative effects on k are $pCO_2 > T > X_{"free" H_2O} >> m_{Mg^{2+}}$. However, it should be noted that there is some debate as to the usefulness of standardized coefficients (e.g. Bring, 1994; Kim and Ferree, 1981; Kim and Mueller, 1976) so the true relative importance of these variables may be different although it is clear that each has a direct impact on the observed rate. Using the larger hydration numbers determined by Zavitsas (2001, 2005), no cation dependency was found (equation 2.12) whereas a slight dependency on $m_{Mg^{2+}}$ was found in this treatment. Given the well-known inhibitory effect of Mg^{2+} on calcite dissolution, it is not surprising to find that Mg^{2+} has an inhibitory effect on the dissolution kinetics of calcite. Furthermore, the adjusted R^2 value (0.872) is greater in this treatment than previously determined (0.862). As a majority of the data analyzed (both from the present study and that of Gledhill and Morse, 2006a) was obtained at 25 °C and two of the elevated temperatures were found to be outliers, the MR analysis was performed again using only data obtained at 25 °C. This analysis also revealed a small dependence on Mg^{2+} (adjusted $R^2 = 0.889$, $p < 0.001$)

$$k_{pred_{25°C}} = \beta_0 + \beta_1 T + \beta_2 pCO_2 + \beta_3 X_{"free"H_2O} + \beta_4 m_{Mg^{2+}} \quad (3.23)$$

where the variables are the same as before and the T term being neglected as it is incorporated into the constant. Both unstandardized and standardized β values are

provided (Table 3.6) which indicate the relative effects on k are $pCO_2 \approx X_{\text{"free"}H_2O} >> m_{Mg^{2+}}$. It is not surprising to find that Mg^{2+} has an inhibitory effect on the dissolution kinetics of calcite but demonstrates the need to obtain more data both in the presence and absence of Mg^{2+} as well as other inhibitors at elevated temperatures to improve the robustness of the model. The agreement of the present MR model results and that carried out previously suggests that the absolute value of the hydration number may not be as important as the relative number. When normalized to the Mg^{2+} hydration number, the present results agree well with Zavitsas (2001, 2005) for the univalent cations although not as well for Ca^{2+} (Table 3.7). A comparison of the present MR model results (equation 3.22, 3.23) with that of Gledhill and Morse (equation 7, 2006a) suggests that when $X_{\text{"free"}H_2O}$ is used in lieu of I, then molalities may be used instead of activities, thereby simplifying the calculation. More importantly, the comparison demonstrates the significant influence $X_{\text{"free"}H_2O}$ has on k. However, more data will need to be obtained, particularly at elevated temperatures, to determine if $X_{\text{"free"}H_2O}$ and molalities, along with pCO_2 and T are sufficient in determining k in solutions containing inhibitory ions or if activities will ultimately need to be considered.

Table 3.6. The coefficients derived from the MR analysis

Predictor	Coefficient	Unstandardized	Standardized	Unstandardized	Standardized
constant	β_0	-205.45		-149.33	
T (°C)	β_1	57.14	0.48		
$p\,CO_2$ (atm)	β_2	219.06	0.56	58.58	0.57
$X_{"free"H2O}$	β_3	1.4	0.43	194.11	0.56
m_{Mg2+}	β_4	-143.47	-0.14	-143.08	-0.16

Table 3.7. Hydration numbers normalized to h_{Mg2+}

	Zavitsas (2001, 2005)		Present Results	
	h_X / h_{Mg2+}	+/-	h_X / h_{Mg2+}	+/-
Na	0.30	0.20	0.29	0.50
K	0.13	0.33	0.12	1.07
Ca	0.92	0.17	0.64	0.65

3.9 Future Direction

The number of water molecules associated with a specific ion in solution may be expected to be primarily dependent on its charge density. However the present study is too limited to make any definitive conclusions as only two univalent and two divalent cations were investigated. The results of Zavitsas (2001) coupled with ionic radii as presented by Marcus (1988) hints that h may indeed be a function of the charge density (Figure 3.13) although much more work needs to be done.

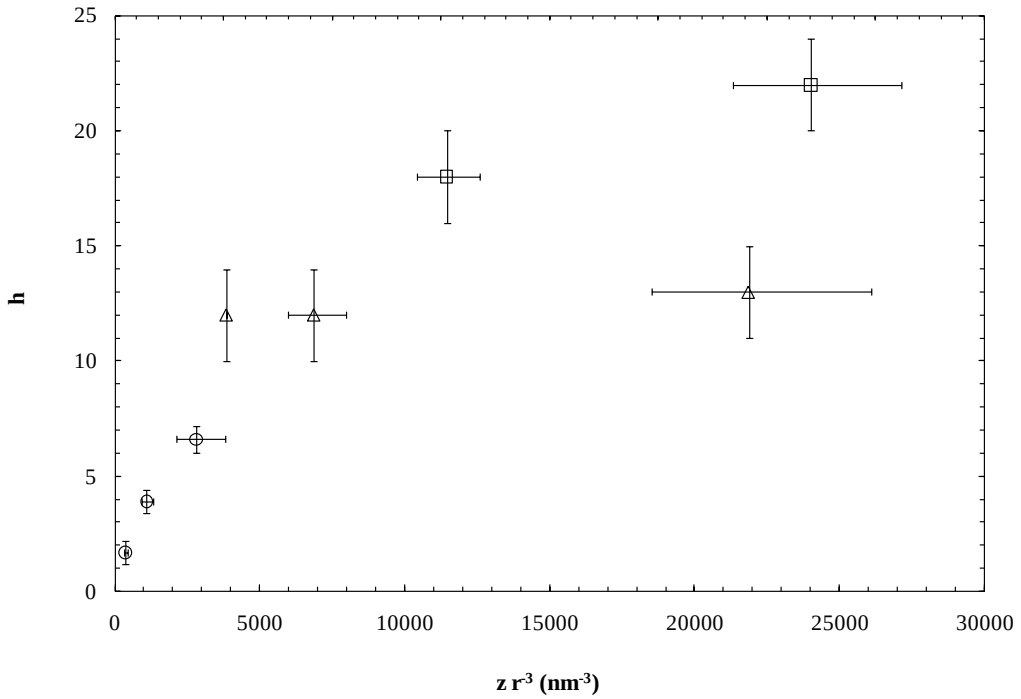

Figure 3.13. Hydration number as a function of charge density for Li^+, Na^+, K^+ (○), Mg^{2+}, Ca^{2+}, Sr^{2+}, (Δ), Al^{3+}, Fe^{3+} (□) with radius of ion given by Marcus (1988)

As there is some discrepancy in hydration numbers calculated from the three colligative property data sets utilized in the present analysis, future experimental work should investigate the feasibility of obtaining osmotic pressure data. Combining the data of Smith (1932) and Smith and Hirtle (1932), consistent values of h_{NaCl} are returned over the temperature range 60-100°C with a decrease with concentration (Figure 3.14) similar to the majority of the freezing point depression data. Osmotic pressure data is useful as small concentrations still produce observable (measureable) differences and that there is

no separate temperature dependent value (with the exception of h) to solve for as there is for freezing point depression (ΔH_{fus}) and boiling point elevation (ΔH_{vap}) data.

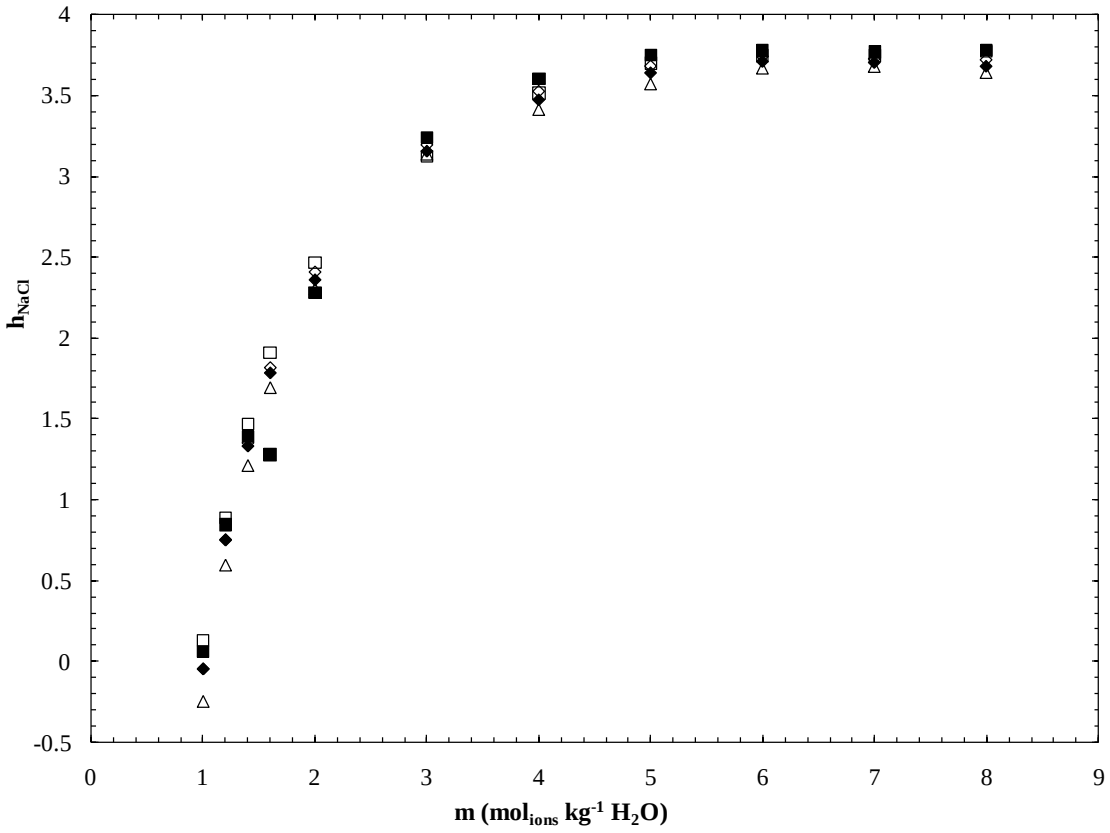

Figure 3.14 h_{NaCl} as a function of ion concentration from the combined osmotic pressure data of Smith (1932) and Smith and Hirtle (1932) at 60°C (□), 70°C (■), 80°C (◊), 90°C (♦), 100°C (Δ).

A variety of semi-empirical models and derivatives have been developed for the prediction of thermodynamic properties in electrolyte solutions such as the Bromley model (1973), ion interaction model of Pitzer (1973), hydration theory of Robinson and Stokes (1973) nonrandom two-liquid (NRTL) model (Chen et al., 1982; Chen et al.,

1986). The Pitzer equations may be the most well-known (e.g. Perez-Villasenor et al., 2003; Ge and Wang, 2009) and are based on a virial expansion of the excess Gibbs energy as a function of the molalities of all of the ionic species present with the empirical parameters typically determined from experimental data. The present results suggest that a much simpler correlation model may be useful to predict colligative properties of mixed electrolyte solutions where the mole fraction of solute must be corrected for bound solvent molecules.

3.10. Conclusions

Hydration numbers of simple electrolytes were determined using colligative property data correcting for bound waters according to the methodology of Zavitsas (2001; 2005). Freezing point depression, boiling point elevation, and vapor pressure depression data sets were all investigated. The freezing point depression datasets of Gibbard and Fong (1972) and Gibbard and Gossman (1974) appear to be anomalous as disparate h and ΔH_{fus} values were found compared to the other datasets and thus were not included in the analysis of h. Hydration numbers determined from freezing point depression data of independent papers were found to be $h_{NaCl} = 3.6 \pm 0.6$; $h_{KCl} = 1.1 \pm 0.7$; $h_{MgCl_2} = 14.6 \pm 1.8$; $h_{CaCl_2} = 11.6 \pm 2.2$ when data was analyzed up to and including the eutectic point. Analysis of boiling point elevation data yield $h_{NaCl} = 3.1 \pm 0.2$; $h_{KCl} = 2.1 \pm 0.3$; $h_{MgCl_2} = 4.3 \pm 3.3$; $h_{CaCl_2} = 6.7 \pm 0.1$. Hydration numbers determined from vapor pressure depression measurements of independent papers give $h_{NaCl} = 3.0 \pm 0.2$; $h_{KCl} = -0.3 \pm 1.2$; $h_{MgCl_2} = 8.6 \pm 0.1$; $h_{CaCl_2} = 7.3 \pm 0.3$. The ΔH results demonstrate the

need for calorimeter research of simple electrolyte solutions to determine if ΔH does approach that of pure water at infinite dilution of solute (i.e. pure solvent). Although there is some uncertainty to these values, as evidenced in comparing hydration numbers calculated using freezing point depression data with that determined from boiling point elevation data, it appears that over the range from freezing point of the most concentrated solution to the boiling point, $h_{NaCl} = 2.8 \pm 0.9$; $h_{KCl} = 1.2 \pm 1.2$; $h_{MgCl_2} = 9.8 \pm 3.7$; $h_{CaCl_2} = 6.3 \pm 3.3$. Finally, these findings suggest that solute bound solvent molecules must be accounted for when determining "true" mole fraction of solute particles in aqueous systems which has implications for a wide variety of scientific fields with an aqueous phase present.

4. CALCITE PRECIPITATION KINETICS IN SALINE WATERS

The effect of ionic strength (I), pCO_2, and temperature on the precipitation rate of calcite was investigated in magnesium-free, phosphate-free, low calcium ($m_{Ca^{2+}} \approx 0.02$ molal) simple KCl and NaCl solutions in a series of classical free drift experiments. Rates were modeled using the general and Davies and Jones rate equations yielding similar results. Reaction orders were found to typically range between 0.8 and 2.5 for both rate equations regardless of electrolyte. For both solutions, rate constants were found to range between $10^{0.8}$ and $10^{1.7}$ mmole m^{-2} hr^{-1} (general rate equation) and $10^{1.5}$ and $10^{2.2}$ mmole m^{-2} hr^{-1} (Davies and Jones rate equation). Under the experimental conditions employed and the resultant precision (~20-25%), I and pCO_2 do not have a significant influence on the precipitation rate of calcite. However, I may enhance carbonate growth overall as calcite dissolution has been shown to be strongly inhibited by I (Finneran and Morse, submitted) with implications for CO_2 mitigation strategies. Precipitation rates increased with temperature although Arrhenius plots yield a broad range of activation energies ($E_a \approx 15 – 28$ kJ mol^{-1}, $R^2 = 0.7232$) which are less than previously reported values for precipitation (e.g. Takasaki et al., 1994 report $E_a \sim 46 \pm 4$ kJ mol^{-1}). The relatively low calculated activation energies coupled with the precision of the results suggest the possibility of surface nucleation in the present results.

4.1. Introduction

Mitigation strategies for anthropogenically produced carbon dioxide (CO_2) typically fall into three broad categories: geological storage, ocean storage, and mineral carbonation (for recent overviews, see volume 217, issues 3-4 (2005) of Chemical Geology and volume 4, issue 5 (2008) of Elements). Geological storage encompasses those strategies in which CO_2 is injected into porous rock formations (see review of Benson and Cole, 2008) exemplified by Statoil's Sleipner project (e.g. Kongsjorden et al., 1997; Torp and Gale, 2003). CO_2 injection into the ocean at moderate depths (typically 1km or greater) is generally referred to as ocean storage (see review of Adams and Caldeira, 2008). Finally, mineral carbonation strategies involve the reaction of CO_2 with calcium and/or magnesium containing silicate minerals forming stable carbonate minerals such as calcite or magnesite (see review of Oelkers et al., 2008).

Although all strategies are promising, several industrial-scale geological storage programs are currently underway, illustrating the feasibility of this type of mitigation. However, even though Statoil has successfully captured CO_2 for over a decade in this manner, the reactivity of reservoir minerals, particularly calcite, with high CO_2 concentrations in solutions of elevated ionic strength relative to seawater (brines) remain limited. Little work has been published on calcite dissolution (Finneran and Morse, submitted; Gledhill and Morse, 2006a) or precipitation rates (Zhang and Dawe, 1998) from solutions with $I > 1$. Zhang and Dawe (1998) concluded that in high salinity waters the precipitation rate of calcite is dependent on $\sqrt{I}$ in a closed system pH-free-drift precipitation experiment when modeled using the Davies and Jones rate equation:

$$R_{DJ} = k\left(\sqrt{\Omega} - 1\right)^{n} \quad (4.1)$$

where R_{DJ} is the Davies and Jones precipitation rate normalized to the reacting surface area, k is the precipitation rate constant that is dependent on temperature and overall solution composition, Ω is the saturation state and n is the reaction order. In using an open system pH-free-drift method to measure calcite dissolution in geologically relevant Na-Ca-Mg-Cl synthetic brines, Gledhill and Morse (2006a) found dissolution rates to be composition dependent assuming a first order reaction using the general dissolution rate equation (Berner and Morse, 1974; Sjöberg, 1978):

$$R_{gen} = k(1 - \Omega)^{n} \quad (4.2)$$

where R_{gen} is the general dissolution rate normalized to the reacting surface area, k is the dissolution rate constant that is dependent on temperature and overall solution composition, Ω is the saturation state and n is the reaction order. Furthermore, Gledhill and Morse (2006a) found that k could be estimated from a multiple regression model and the moderate inhibitory effect of I was reported to be approximately equivalent (in standardized coefficients) and opposite in nature, to the effect of pCO_2.

The observation of Gledhill and Morse (2006a) of the influence of I was further investigated in a series of classical free-drift pH experiments that were conducted in magnesium-free, phosphate-free, low calcium (~0.01 molal) simple electrolyte solutions in order to further elucidate the specific effect that I has on the dissolution kinetics of calcite (Finneran and Morse, submitted). Both KCl and NaCl solutions were investigated because KCl is not believed to strongly interact with carbonic acid system

components (Davis and Oliver, 1972; Frantz, 1998; Oliver and Davis, 1973). Finneran and Morse (2009) proposed that the dissolution rate of calcite was dependent on the amount of free water in both electrolyte solutions. As the salt content increased, the amount of free water available to hydrate (and ultimately dissolve) the calcite surface ions decreased, thereby depressing the rate of dissolution. As a complement to that study, the same methodology was employed in the present manuscript to investigate the influence of I on the precipitation kinetics of calcite in similar, albeit supersaturated, solutions.

4.2. Materials and methods

A schematic diagram of the experimental system is shown in Figure 4.1. Commercially purified high grade CO_2 and ultra-high purity N2 were precisely controlled using dual MKS® Type 1479A Mass-Flo® mass-flow controllers that were controlled by a computer running LabVIEW® software. Both gases flowed individually through NO-OX® tubing into a vigorously stirred ~230 mL water jacketed humidifier containing deionized MilliQ® (18.2 MΩ) water thoroughly mixing the humidified gases. The mixed gas outflow then flowed (2 L min^{-1}) through NO-OX® tubing into a ~100 mL water jacketed vessel containing a solution of known alkalinity. The temperature and pH of the solution was monitored with an Orion ATC probe and Orion Ross combination electrode

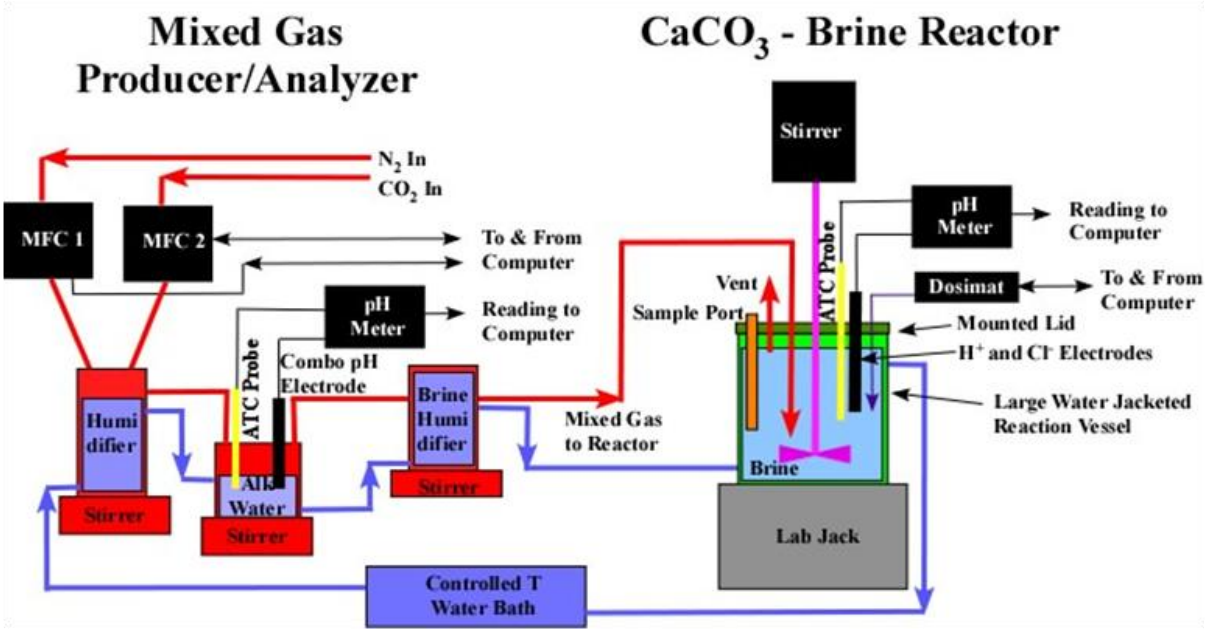

Figure 4.1. Schematic diagram of the experimental pH free drift reactor system used in this study.

coupled to an Orion 720A potentiometer. These measurements allowed for the separate determination of the partial pressure of CO_2 in the mixed gas to be compared with the flow set by the mass-flow controllers. The gas outflow then passed through NO-OX® tubing into a stirred ~230 mL water jacketed humidifier containing water of the same I as the solution being investigated. The mixed gas outflow then encountered a "T" thereby creating two (2) gas outflows through NO-OX® tubing, which were placed at the bottom of the approximately 2 L water jacketed reaction vessel. Gas dispersion tubing was not used as it has been shown that calcite can be caught in the sintered glass which

also can exhibit "memory" effects from slow exchange with liquid in the micropores (Morse and Berner, 1972).

The solution was well stirred at a constant rate (500 rpm) using an electronically controlled IKA Works overhead stirrer to prevent the grinding action a magnetic stirrer may provide while ensuring suspension of the solid in solution as well as thorough mixing of the gas and solution. The temperature of all vessels was held constant (±0.1 °C) using a Neslab constant temperature bath controlled by a computer running LabVIEW® software. Temperature of the solution in the reaction vessel was measured with an Orion ATC probe coupled to an Orion 720A potentiometer. Electrode potential (electromotive force) was measured using a Ross® H+ selective electrode referenced to a Single Refex® solid-state reference electrode thereby avoiding a porous liquid-junction (Knauss et al., 1990). The voltage of the solution was converted to a "Pitzer scale" pH for rate determination following the methodology of Gledhill and Morse (2006a). Total alkalinity (TA) and total CO_2 (DIC) were used to calculate the pH and pCO_2 in solution serving as a check on the internal consistency of the system.

Concentrated stock solutions of ACS reagent grade KCl, NaCl, and $CaCl_2 \cdot 2H_2O$ were synthesized and passed through individual columns of reagent grade calcium carbonate powder and filtered to remove any "foreign" surface active ions (e.g. phosphate and metals) that may have been present at trace levels. Experimental solutions were prepared gravimetrically on the molal scale (m) from these separate concentrated stock solutions and diluted with deionized MilliQ® (18.2MΩ) water for the

appropriate concentration. The initial salt concentrations were verified by analytical determination of calcium and chloride concentrations.

The experimental solution was added to the reaction vessel and allowed to equilibrate with the constant temperature bath and mixed gas bubbling through the solution. The initial calcite saturation state was set by the addition of a concentrated potassium or sodium (depending on supporting electrolyte used) carbonate solution. Once the solution had equilibrated, several aliquots were withdrawn for analysis (TA, Ca^{2+}, Cl^-, DIC) of the initial state. Experimental solutions were reacted with crushed rhombic Iceland spar calcite from Creel, Chihuahua, Mexico that had been obtained from Ward's Scientific Inc. (Rochester, NY). Large calcite pieces were manually crushed with mortar and pestle, wet sieved, sonicated, re-sieved, and finally dried for 48 hours. The resultant 32–63 μm size fraction was estimated to have a specific surface area of 0.042 $m^2\ g^{-1}$ from a geometric determination using scanning electron micrograph (SEM) imaging. The mineralogy was verified by powder X-ray diffraction as being >99% calcite. Reagent grade calcite powder was not used as the powder coated the electrodes during preliminary experiments leading to erratic voltage measurements.

TA was determined by a modified Gran-type titration (Gran, 1952) using a Metrohm 755 Dosimat and an Orion 720A pH meter interfaced with a computer controlled by LabVIEW® software as described in Gledhill and Morse (2006a), although six point calibration curves were employed rather than five. Titrations were conducted at 25 ± 0.1 °C in a water-jacketed open cell into which CO_2 was continuously bubbled in

a modification (Gledhill and Morse, 2006a) of the open cell titration as described in the Guide to Best Practices for Ocean CO_2 Measurements (Dickson et al., 2007).

DIC was determined according to the method of Dickson and Goyet (2005) with a UIC Incorporated Model 5011 CO_2 coulometer with a typical precision of 1%. The Ca^{2+} concentration was determined by EGTA titration with calcium indicator Cal/Ver II®. Endpoint detection was facilitated using a Brinkmann PC 800 colorimeter interfaced with a computer controlled by LabVIEW® software yielding a precision of 2%. The Cl^- concentration was determined by $AgNO_3$ titration using a Metrohm 755 Dosimat and an Orion silver ion selective electrode, and an Orion 720A pH meter interfaced with a computer controlled by LabVIEW® software with a precision of 1.5%. The concentration of the supporting cation (K^+ or Na^+) was calculated from charge balance.

The pCO_2 in the gas feed was first estimated by the ratio of the CO_2 flow rate to the total gas flow rate of 2 L min^{-1} (flow was balanced with ultra-high purity N_2) and more precisely determined by the pH of the solution of known TA. Three point calibration curves were made using 100% (BOTCO), 10% (Scott Specialty Gases) and 1% (Scott Specialty Gases) CO_2 and solutions of known TA.

Prior to calcite addition, samples were drawn and filtered using an in-line 0.45μm Acrodisk filter for initial solution analysis. Although unnecessary, a filter was employed so that the withdrawal of the initial and final samples was subjected to the same experimental protocol. Experiments were terminated typically after 5 h, at which point changes in solution chemistry were within the measurement precision. Samples

were drawn and filtered using an in-line 0.45 μm Acrodisk filter for final solution analysis.

4.3. Calculations

The precipitation and dissolution of calcite can be written in classic form as:

$$Ca^{2+}{}_{(aq)} + CO_3^{2-}{}_{(aq)} \underset{k_r}{\overset{k_f}{\rightleftharpoons}} CaCO_{3(s)} \tag{4.3}$$

where the forward reaction is precipitation with forward rate constant k_f and dissolution is the reverse reaction with rate constant k_r. In terms of carbonic acid system components, the reaction may be rewritten as:

$$Ca^{2+}{}_{(aq)} + 2HCO_3^-{}_{(aq)} \underset{k_r}{\overset{k_f}{\rightleftharpoons}} CaCO_{3(s)} + H_2O + CO_2 \tag{4.4}$$

and given the definition of TA

$$TA = m_{HCO_3^-} + 2m_{CO_3^-} + m_{OH^-} - m_{H^+} \tag{4.5}$$

it is readily apparent that the precipitation of one mole of calcite consumes two moles of TA. Thus, the precipitation rate may be defined from the time dependent rate of change in TA:

$$R = \frac{dm_{CaCO_{3(s)}}}{dt} = -\frac{dm_{Ca^{2+}{}_{(aq)}}}{dt} = -\frac{dm_{CO_3^{2-}{}_{(aq)}}}{dt} = -\frac{1}{2}\left(\frac{dTA}{dt}\right) \tag{4.6}$$

which must be normalized to both the mass of solvent and surface area of calcite used. Geometric surface area was used as previous studies have shown it to be a better analogue of reactive surface area than BET surface area (e.g. Cubillas et al., 2005a, 2005b; Gledhill and Morse, 2006a; Keir, 1980; Walter, 1985). As pCO_2 was constant throughout each experimental run, the change in pH with time was converted to a change in TA with time in order to determine the rate as outlined by Gledhill and Morse (2006a) using the Pitzer formalism incorporated into the software program EQPITZER (He and Morse, 1993).

The experimental rate data were typically modeled over the range of $3 \geq \Omega \geq 1.1$ using both the general growth and the Davies and Jones rate equations. The lower limit of Ω was chosen as the small voltage change with respect to time and the analytical uncertainty of the final solution chemistry as equilibrium is approached may lead to erratic rate measurements as demonstrated by Gledhill and Morse (2004) for dissolution experiments. Three experimental solutions, KCl 2.0 ($I \approx 2.4$), NaCl 2.0 ($I \approx 2.3$) and NaCl 5.0 ($I \approx 5.8$) were repeated (individual batches of solution) under the same initial conditions (pCO_2 = 1 atm, T = 25 °C, mCa2+ ≈ 0.02 molal) yielding a precision of ~20-25%. The Ca^{2+} concentration used was chosen as it provided a large enough (measureable) change in voltage while remaining close to the concentration found in modern seawater with salinity of 35 ($m_{Ca^{2+}} \approx 0.01$ molal) used in the complementary dissolution study (Finneran and Morse, submitted). Additionally, this low Ca^{2+} concentration does not result in erroneously high calculated saturation states using

EQPITZER (He and Morse, 1993) that calcium rich brines do (Gledhill and Morse, 2006b).

4.4. Results

Initial experimental conditions prior to reaction with calcite and final (steady state) conditions after reaction with calcite are presented in Table 4.1. Linear least squares fits of log-log plots of the precipitation rate as a function of Ω-1 (general) or √Ω-1 (Davies and Jones) typically yielded R^2 values of 0.95 or greater over the saturation range investigated. The experimentally determined rate constant (k) and reaction order (n) for each solution investigated is provided in Table 4.2 for both rate equations. Furthermore, rate constants, assuming first order reaction (n = 1), are also provided for both rate equations in Table 4.2 so that direction comparison of k can be made with those determined in the corresponding dissolution study (Finneran and Morse, submitted) as rates were found to be first order using the general dissolution rate equation. About 55% of the n values fall within ±0.2 of 1 which is within the experimental reproducibility of n values, which differ on average by about 0.5. The reproducibility of log k values was about 0.2 (a factor in k of ~1.6). At constant pCO_2 (1atm), T (25 °C) and initial $m_{Ca^{2+}}$ (~0.02 molal), the influence of I was mixed as n was slightly positively correlated with I ($n_{KCl} = 0.28I + 1.01$, $R^2 = 0.36$; $n_{NaCl} = 0.072I + 0.99$, $R^2 = 0.16$) whereas log k was

Table 4.1. Initial and final experimental conditions.

Experimental ID	Ca^{2+}_i (m)	K^+ (m)	Na^+ (m)	Cl^- (m)	TA_i (eq kg^{-1} H_2O)	pH_i	Ionic Strength (m)	Temperature (°C)	X_{CO2} (atm)	Ca^{2+}_f (m)	TA_f (eq kg^{-1} H_2O)	pH_f
KCl 0.5	0.021	0.52		0.49	0.075	6.45	0.70	25.0	1.0	0.007	0.048	6.25
KCl 1.0	0.022	1.09		1.06	0.081	6.43	1.28	25.0	1.0	0.007	0.050	6.22
KCl 2.0	0.023	2.25		2.22	0.087	6.42	2.45	25.0	1.0	0.007	0.054	6.21
KCl 2.0 rep	0.023	2.24		2.21	0.083	6.40	2.44	25.0	1.0	0.009	0.055	6.22
KCl 3.0	0.023	3.26		3.22	0.088	6.41	3.46	25.0	1.0	0.007	0.046	6.13
NaCl 0.5	0.021		0.48	0.49	0.039	6.18	0.60	25.0	1.0	0.015	0.028	6.03
NaCl 1.0	0.021		1.04	1.05	0.043	6.19	1.17	25.0	1.0	0.016	0.033	6.07
NaCl 2.0	0.023		2.17	2.18	0.046	6.19	2.31	25.0	1.0	0.016	0.034	6.05
NaCl 2.0 rep	0.022		2.20	2.19	0.059	6.29	2.35	25.0	1.0	0.012	0.038	6.11
NaCl 3.0	0.023		3.33	3.33	0.051	6.22	3.47	25.0	1.0	0.013	0.031	6.00
NaCl 4.0	0.022		4.43	4.43	0.048	6.18	4.57	25.0	1.0	0.013	0.029	5.96
NaCl 5.0	0.023		5.65	5.65	0.052	6.20	5.80	25.0	1.0	0.009	0.023	5.84
NaCl 5.0 rep	0.023		5.66	5.65	0.065	6.29	5.83	25.0	1.0	0.007	0.032	5.99
KCl 2.0 T40	0.023	2.21		2.20	0.062	6.39	2.38	40.0	1.0	0.010	0.035	6.15
KCl 2.0 T55	0.023	2.20		2.20	0.044	6.37	2.33	55.0	1.0	0.012	0.022	6.08
KCl 2.0 p06	0.023	2.22		2.21	0.067	6.53	2.39	25.0	0.6	0.009	0.041	6.31
KCl 2.0 p03	0.023	2.20		2.20	0.048	6.68	2.34	25.0	0.3	0.011	0.024	6.39
KCl 2.0 p01	0.023	2.18		2.20	0.031	6.97	2.30	25.0	0.1	0.014	0.013	6.60
NaCl 2.0 T40	0.022		2.17	2.18	0.034	6.17	2.29	40.0	1.0	0.016	0.022	5.99
NaCl 2.0 T55	0.022		2.16	2.18	0.025	6.14	2.26	55.0	1.0	0.017	0.016	5.94
NaCl 2.0 p06	0.022		2.16	2.18	0.036	6.30	2.29	25.0	0.6	0.017	0.025	6.14
NaCl 2.0 p03	0.022		2.15	2.18	0.026	6.46	2.26	25.0	0.3	0.018	0.016	6.25
NaCl 2.0 p01	0.023		2.14	2.18	0.015	6.70	2.24	25.0	0.1	0.020	0.009	6.48
NaCl 5.0 T40	0.022		5.58	5.58	0.046	6.29	5.72	40.0	1.0	0.008	0.019	5.89
NaCl 5.0 T55	0.023		5.64	5.65	0.035	6.29	5.76	55.0	1.0	0.011	0.012	5.82
NaCl 5.0 p06	0.023		5.66	5.66	0.051	6.41	5.80	25.0	0.6	0.009	0.023	6.06
NaCl 5.0 p03	0.023		5.63	5.64	0.036	6.56	5.75	25.0	0.3	0.011	0.012	6.09
NaCl 5.0 p01	0.024		5.62	5.65	0.021	6.79	5.72	25.0	0.1	0.017	0.005	6.22

slightly negatively correlated (log k_{KCl} = -0.069I + 1.38, R^2 = 0.07; log k_{NaCl} = -0.076I + 1.36, R^2 = 0.65) using the general rate equation (Figure 4.2). As results determined using the Davies and Jones rate equation closely resembled that of the general rate equation, only results determined using the general rate equation are shown. At constant I (I ≈ 2.3, 2.4, 5.8), T (25 °C) and initial $m_{Ca^{2+}}$ (~0.02 molal), for the two lower I solutions, n increased with increasing pCO_2 (n_{KCl} = 0.60 pCO_2 + 1.09, R^2 = 0.63; $n_{NaCl\ 2}$ = 0.71 pCO_2 + 0.77, R^2 =0.74) whereas the higher I solution experienced a decrease in n with pCO_2 ($n_{NaCl\ 5}$ = -0.66 pCO_2 + 1.96, R^2 =0.62). Increasing pCO_2 served to increase log k for all three solutions investigated (log k_{KCl} = 0.28 pCO_2 + 0.78, R^2 = 0.41; log $k_{NaCl\ 2}$ = 0.13 pCO_2 + 0.99, R^2 =0.66; log $k_{NaCl\ 5}$ = 0.58 pCO_2 + 0.40, R^2 =0.76) as shown in Figure 4.3. At constant I (I ≈ 2.3, 2.4, 5.8), pCO_2 (1atm), and initial $m_{Ca^{2+}}$ (~0.02 molal), temperature served to decrease n (n_{KCl} = -0.014T + 1.97, R^2 = 0.40; $n_{NaCl\ 2}$ = -0.026T + 2.10, R^2 =0.69; $n_{NaCl\ 5}$ = -0.01T + 1.44, R^2 =0.20) and increase log k (log k_{KCl} = 0.69T + 4.07, R^2 = 0.71; log $k_{NaCl\ 2}$ = 1.33T – 10.64, R^2 =0.99; log k_{NaCl5} = 0.38T + 6.66, R^2 =0.78) for all solutions (Figure 4.4).

Table 4.2. Experimentally determined rate constant and reaction order.

Experimental ID	$R = k(\Omega-1)^n$		$R = k(\sqrt{\Omega} - 1)^n$		$R = k(\Omega-1)$	$R = k(\sqrt{\Omega} - 1)$
	n	log k ($mmol\ m^{-2}\ hr^{-1}$)	n	log k ($mmol\ m^{-2}\ hr^{-1}$)	k ($mmol\ m^{-2}\ hr^{-1}$)	k ($mmol\ m^{-2}\ hr^{-1}$)
KCl 0.5	1.6	1.1	1.9	1.9	24	79
KCl 1.0	0.8	1.7	1.0	2.1	38	136
KCl 2.0	1.4	1.2	1.7	1.9	22	76
KCl 2.0 rep	1.9	0.9	2.3	1.8	24	75
KCl 3.0	2.1	1.3	2.5	2.2	46	144
NaCl 0.5	0.8	1.4	0.9	1.7	20	55
NaCl 1.0	0.9	1.3	1.0	1.6	16	43
NaCl 2.0	1.3	1.1	1.5	1.7	16	44
NaCl 2.0 rep	1.7	1.1	2.0	1.9	23	67
NaCl 3.0	1.0	1.1	1.1	1.6	14	36
NaCl 4.0	1.6	0.9	1.9	1.6	13	40
NaCl 5.0	1.0	1.1	1.1	1.6	14	33
NaCl 5.0 rep	1.5	0.8	1.9	1.5	20	76
KCl 2.0 T40	1.2	1.4	1.6	2.0	41	127
KCl 2.0 T55	1.3	1.5	1.6	2.2	63	179
KCl 2.0 p06	1.5	0.9	1.9	1.6	18	62
KCl 2.0 p03	1.2	1.0	1.4	1.6	14	45
KCl 2.0 p01	1.2	0.7	1.4	1.3	8	27
NaCl 2.0 T40	0.8	1.5	1.0	1.8	40	101
NaCl 2.0 T55	0.8	1.5	0.9	1.8	38	94
NaCl 2.0 p06	1.1	1.1	1.2	1.5	14	41
NaCl 2.0 p03	1.0	1.0	1.2	1.5	10	28
NaCl 2.0 p01	0.9	1.1	0.9	1.4	13	34
NaCl 5.0 T40	0.9	1.4	1.1	1.8	20	72
NaCl 5.0 T55	1.1	1.5	1.2	2.0	28	81
NaCl 5.0 p06	1.7	0.8	2.3	1.6	27	111
NaCl 5.0 p03	1.6	0.6	2.1	1.4	7	35
NaCl 5.0 p01	1.9	0.4	2.4	1.3	11	37

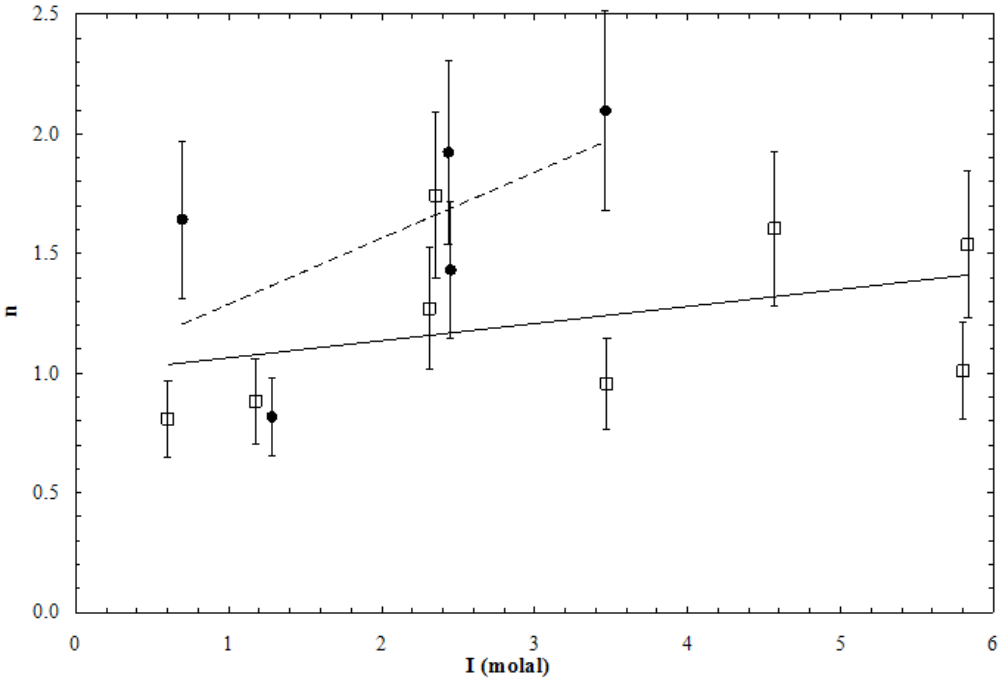

(a)

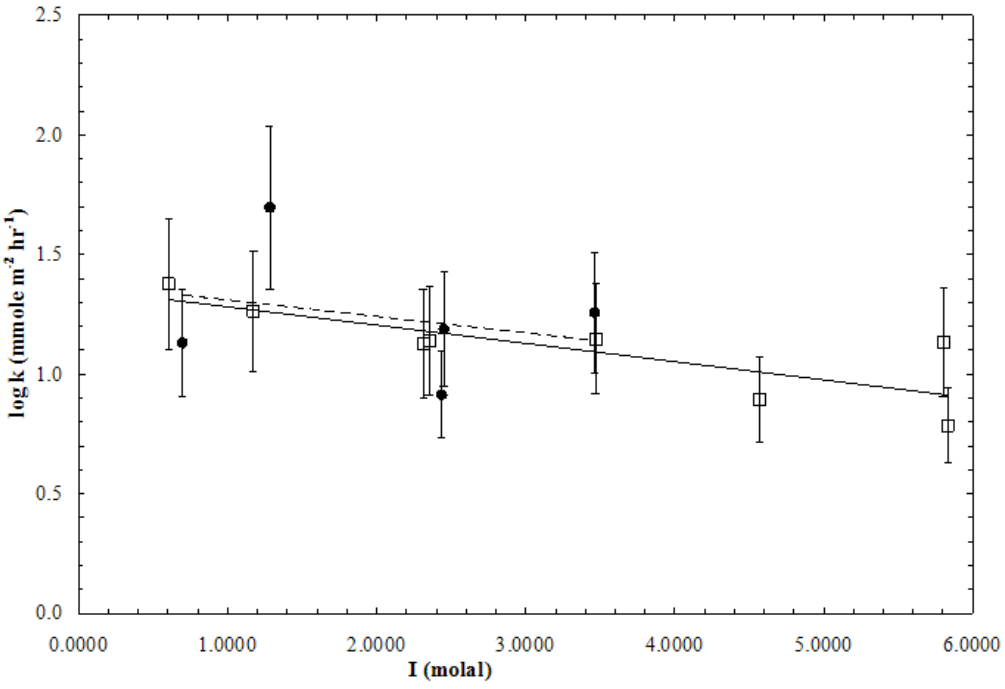

(b)

Figure 4.2. n and log k (mmole m^{-2} hr^{-1}) as a function of I (molal scale) for KCl (●) and NaCl (□).

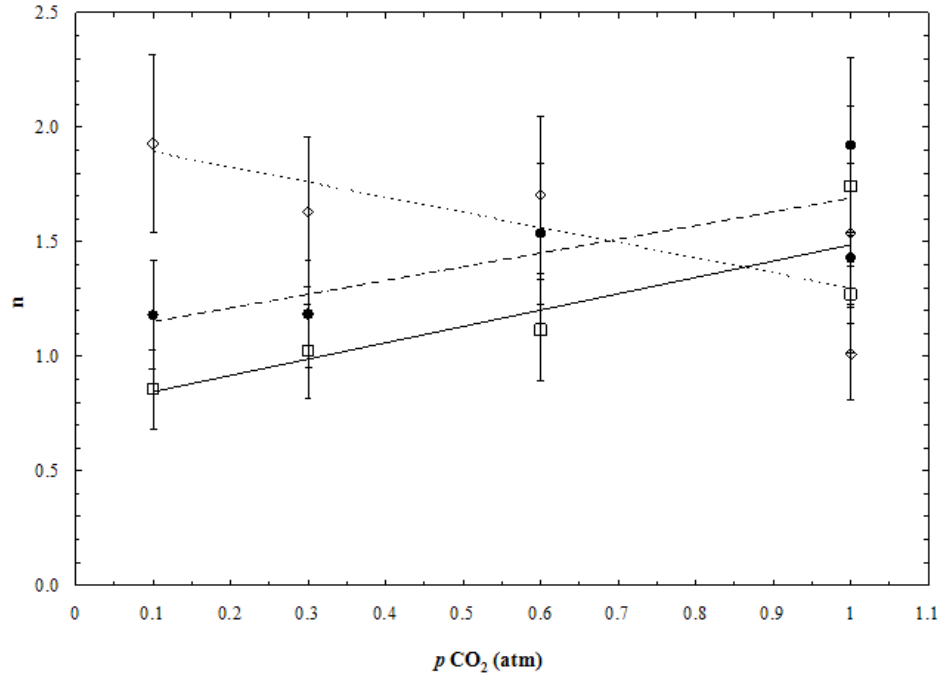

(a)

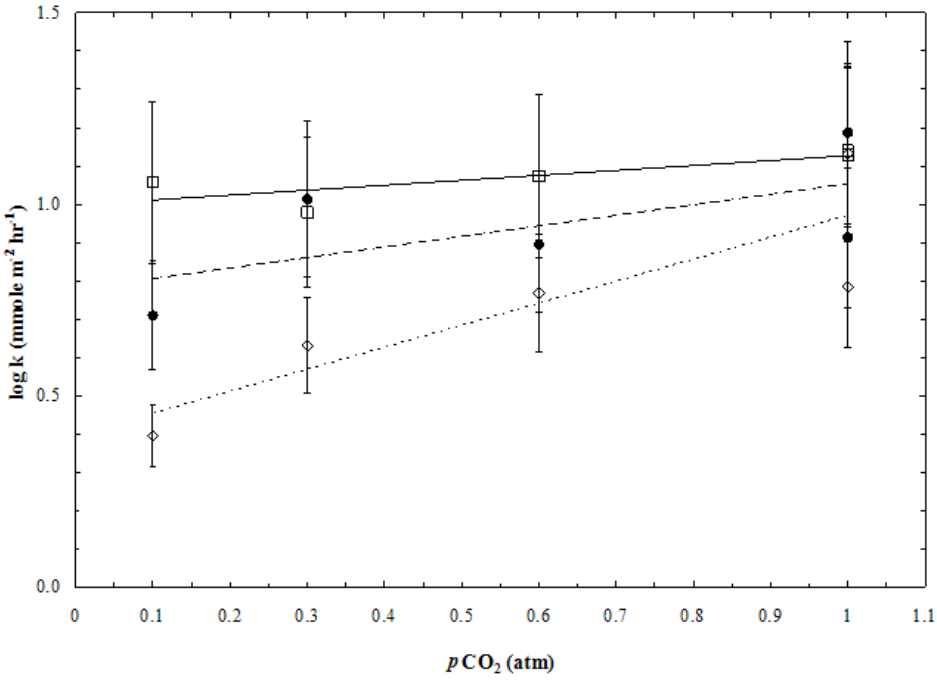

(b)

Figure 4.3. n and log k (mmole m^{-2} hr^{-1}) as a function of pCO_2 (atm) for KCl 2.0 (●), NaCl 2.0 (□) and NaCl 5.0 (◊) solutions.

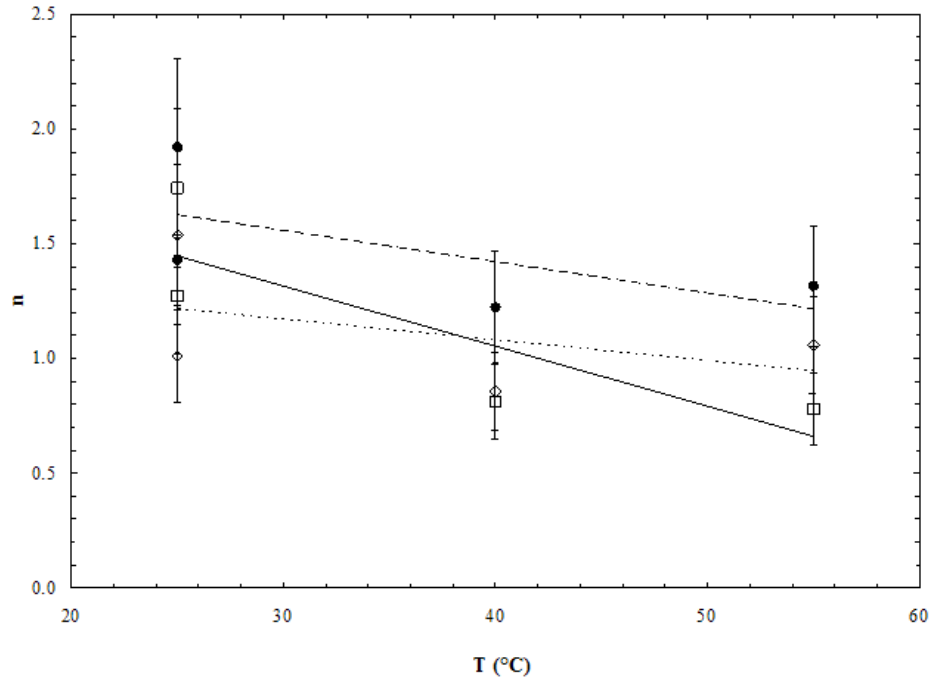

(a)

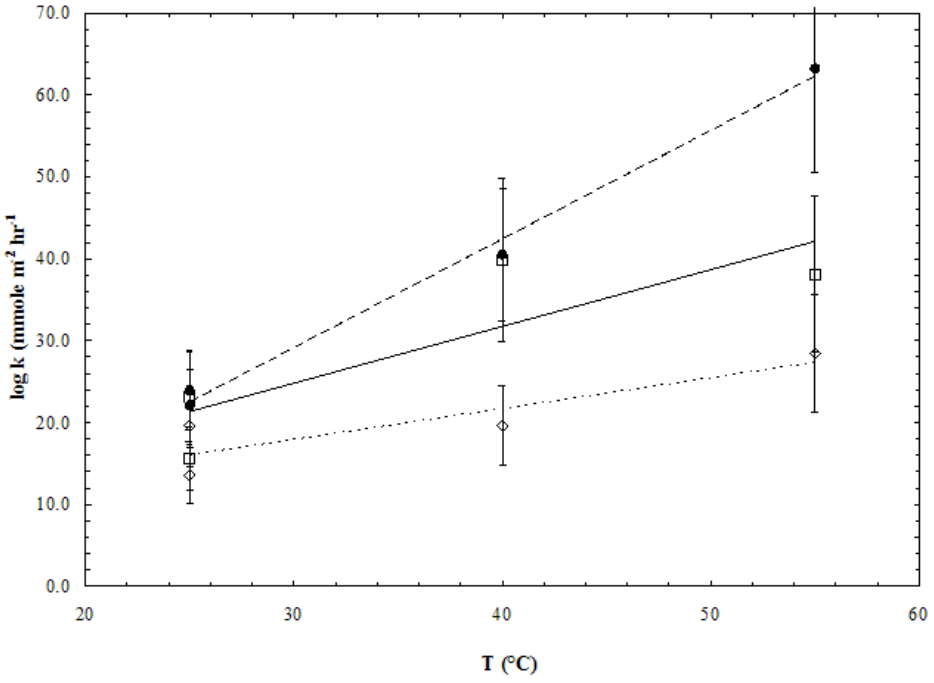

(b)

Figure 4.4. n and log k (mmole m^{-2} hr^{-1}) as a function of T (°C) for KCl 2.0 (●), NaCl 2.0 (□) and NaCl 5.0 (◊) solutions.

4.5. Discussion

At constant pCO_2 (1atm), T (25 °C) and initial $m_{Ca^{2+}}$ (~0.02 molal), increasing I appears to slightly increase n and decrease k using either the general or Davies and Jones rate equation for both electrolyte solutions (Table 4.2). Using the general rate equation, n was found to range between 0.8 – 2.1 and k was found to typically range between $10^{0.8}$ – $10^{1.7}$ with the Davies and Jones rate equation yielding similar results ($0.9 \leq n \leq 2.5$; $10^{1.5} \leq k \leq 10^{2.2}$). The observed narrow reaction order range agrees well with previously reported results (see reviews of Burton, 1993; Morse, 1983; Morse et al., 2007; Plummer et al., 1979) and suggests that the precipitation reaction mechanism(s) is not overly complex under these conditions. If first order kinetics are assumed, k was found to be independent of I using the general ($k_{KCl} = 3.91I + 22.92$, $R^2 = 0.161$; $k_{NaCl} = 0.12I + 16.06$, $R^2 = 0.01$) or Davies and Jones rate equation ($k_{KCl} = 9.27I + 82.83$, $R^2 = 0.08$; $k_{NaCl} = 3.26I + 38.83$, $R^2 = 0.13$) as illustrated by the low R^2 values. k_{KCl} was found to range from 22-46 mmole m^{-2} hr^{-1} and k_{NaCl} = 13-23 mmole m^{-2} hr^{-1} using the general rate equation. The absolute values and ranges of k are smaller than those found in the complementary dissolution study (k_{disKCl} = 78-114; $k_{disNaCl}$ = 23-103 mmole m^{-2} hr^{-1}; Finneran and Morse, submitted) with maximum precipitation values of k being less than or equal to minimum dissolution values of k_{dis}. Absolute values of k for precipitation are about 20-40% that of k_{dis} values which suggests that dissolution of calcite is a faster process under the experimental conditions used in the study. Even with the larger uncertainty of the precipitation results, it is apparent when comparing results that dissolution is more strongly influenced by I than precipitation. Therefore, given the

scatter of the data and the precision of replicates, it appears any influence I has on the precipitation kinetics of calcite under these conditions is minimal. These results combined with the previous dissolution work (Finneran and Morse, submitted) suggest that highly saline aquifers are ideal places for CO_2 sequestration as high I inhibits calcite dissolution with no negative effect on precipitation. Further studies at higher pCO_2 need to be completed to test this hypothesis.

Assuming first order kinetics, k was found to increase with increasing pCO_2 using the general ($k_{KCl} = 15.86\ pCO_2 + 7.64$, $R^2 = 0.95$; $k_{NaCl\ 2} = 8.54\ pCO_2 + 10.14$, $R^2 = 0.53$; $k_{NaCl\ 5} = 8.75\ pCO_2 + 10.32$, $R^2 = 0.229$) or Davies and Jones rate equation ($k_{KCl} = 51.37\ pCO_2 + 26.13$, $R^2 = 0.97$; $k_{NaCl\ 2} = 28.66\ pCO_2 + 25.63$, $R^2 = 0.61$; $k_{NaCl\ 5} = 22.41\ pCO_2 + 44.99$, $R^2 = 0.07$). An increase in pCO_2 from 0.1 to 1 atm almost tripled k in KCl solutions although NaCl solutions did not show the same correlation. In contrast, k_{dis} was found to increase by a factor of 3 – 4 in both KCl and NaCl solutions in the concomitant dissolution study (Finneran and Morse, submitted) with a much larger absolute range of k_{dis} ($21 \leq k_{dis_{KCl}} \leq 87$; $21 \leq k_{dis_{NaCl}} \leq 72$ mmole m^{-2} hr^{-1}) for the two lower I solutions. In comparing the two sets of results, pCO_2 has a larger influence on the dissolution kinetics of calcite than precipitation in NaCl solutions of similar I although results in KCl solutions are similar. However, as I was found to be the dominant influence on calcite dissolution kinetics at high I (Finneran and Morse, submitted), under high pCO_2 conditions which may be expected for CO_2 sequestration, in highly saline aquifers dissolution may be extremely limited.

Finally, temperature was found to increase k for all solutions at constant I, pCO_2, and initial $m_{Ca^{2+}}$, using the general (k_{KCl} = 1.33T - 10.64, R^2 = 0.99; $k_{NaCl\ 2}$ = 0.69T + 4.07, R^2 =0.71; $k_{NaCl\ 5}$ = 0.38T + 6.66, R^2 =0.78) or Davies and Jones rate equation (k_{KCl} = 3.45T – 10.45, R^2 = 0.99; $k_{NaCl\ 2}$ = 1.43T + 24.36, R^2 =0.62; $k_{NaCl\ 5}$ = 0.91T + 32.48, R^2 = 0.36) assuming first order kinetics. k_{dis} was found to approximately double with an increase of 30°C in dissolution work (Finneran and Morse, submitted) with greater absolute k_{dis} values about a factor of three larger than observed precipitation k values for the lower two I solutions. The temperature dependence of the reaction rate is often assumed to follow the classic Arrhenius equation:

$$k = Ae^{-\frac{E_a}{RT}} \tag{4.7}$$

where k is the rate constant, A is the preexponential (or frequency) factor, E_a is the Arrhenius activation energy, R is the gas constant and T is the temperature. Arrhenius plots yield a range of activation energies ($E_{a_{KCl}}$ ~28 ± 7, R^2 = 0.99; $E_{a_{NaCl\ 2}}$ ~21 ± 5, R^2 = 0.70; $E_{a_{NaCl\ 5}}$ ~15 ± 5 kJ mol^{-1}, R^2 = 0.72) which are less than other reported values for precipitation (e.g. Takasaki et al., 1994 report E_a ~ 46 ± 4 kJ mol^{-1}) which may indicate the possibility of surface nucleation in the present results.

Previous laboratory investigations of the effect of I (typically as a function of S) on the precipitation kinetics of calcite have been mixed. Both the nucleation rate of calcite (Bischoff, 1968) and the transformation of aragonite to calcite (Bischoff and Fyfe, 1968) were shown to be proportional to $\sqrt{I}$ in solutions of low I (0–0.05m). Badiozamani et al. (1977) investigated the influence of ionic strength on carbonate

cementation and concluded that increase in S (and thus, I) inhibits nucleation but enhances the crystallization rate of both calcite and aragonite. In contrast, Chen et al. (1979), as reported in Zhong and Mucci (1989), found the addition of NaCl had no impact on the mineralogy, nucleation rate or precipitation rate of Mg-calcite and aragonite in Ca-Mg-Cl-HCO_3 solutions. Kazmlerczak et al. (1982) found that calcite growth rate in $CaC1_2$ solutions was independent of I over the range 0.007-0.20 mol dm^{-3}. Walter (1986) also found that the addition of NaCl to make I of the solution equivalent to that of normal seawater (0.7m) did not significantly change calcite growth rates. Likewise, salinity (and thus, I), over the range S = 5 – 44, was found to have little effect on calcite precipitation rates by Zhong and Mucci (1989). The transformation rate of vaterite to calcite was shown to be proportional to I although the $\Omega_{vaterite}$ of nucleation was independent of I at I > 1 (Morse and Walton, submitted). Reports on the influence of pCO_2 on the precipitation kinetics of calcite have also been mixed. Reddy et al. (1981) found rates were dependent on both pCO_2 and Ω, as rates increased with pCO_2 at low Ω while at high Ω, rates were depressed by increases in pCO_2. Zuddas and Mucci (1994) found n to decrease and k to increase with increases in pCO_2. At low pCO_2 , Lebrón and Suárez (1998) found the precipitation rate of calcite to increase with respect to pCO_2 from ambient pCO_2 to ~0.1 atm.

Zuddas and Mucci (1998) formulated a precipitation rate expression as a function of carbonate ion concentration only and found that as I was varied ($0.1 \leq I \leq 0.93$), both the reaction order with respect to carbonate and the forward reaction rate increased. They suggested this was a result of change in the precipitation mechanism as well as

catalysis provided by the additional electrolyte in a similar fashion to flocculation induced by increasing salt concentration. Furthermore, Zuddas and Mucci (1998) reported that both the reaction order with respect to carbonate and the forward reaction rate increased when the precipitation rates observed by Zhong and Mucci (1989) were expressed as a function of carbonate ion concentration. Therefore, the treatment of Zuddas and Mucci (1998) was applied to the current data although no definitive relationship between I and n or k was found. As bicarbonate would be the dominant species at higher pCO_2, it also was examined as a master variable yielding similar results. Therefore, under the experimental conditions used and the resultant precision of results, expressing observed rates as a function of carbonate or bicarbonate did not improve any correlations between I and n or k than that obtained using the general or Davies and Jones rate equations.

The dehydration of reactants on the surface of a growing crystal is often a rate controlling step in the crystallization processes (e.g. Nancollas and Purdie, 1964) and is an energetic barrier to precipitation (e.g. Arvidson and Mackenzie, 1999; Lippmann, 1973). Therefore, it may be argued that increases in I would increase the precipitation rate as dehydration of the ions being incorporated into the lattice structure should become easier. However, given the many studies cited above in which I does not influence the precipitation rate, I may be a relatively unimportant factor compared to others under the present conditions. For example, Winter and Burton (1992) presented results at the Geological Society of America annual meeting where they found the precipitation rate of calcite to be highly dependent on the ratio of calcium to carbonate

activities ($a_{Ca^{2+}}/a_{CO_3^{2-}}$). More recently, Nehrke et al. (2007) demonstrated the optimum precipitation rate occurs when $[Ca^{2+}] = [CO_3^{2-}]$ and is depressed as the ratio deviates from unity. Figure 5 of their paper suggests that at large deviations from a stoichiometric solution ($[Ca^{2+}] = [CO_3^{2-}]$), the calcite precipitation rate becomes relatively constant. It may be that when $[Ca^{2+}] >> [CO_3^{2-}]$ as in this study and many others, deviations from equivalent concentrations of the incorporated ions overwhelms any influence I, pCO_2 or T may have on the precipitation kinetics thereby accounting for the many works in which I was found to have no influence. Thus, it would be interesting to investigate the influence of I under the experimental conditions employed by Nehrke et al. (2007).

In precipitation experiments, the seed mineral surface area used must be large enough to ensure that spontaneous nucleation does not occur; otherwise calculated growth rates will be erroneously high. Reddy and Gaillard (1981) investigated the influence of calcite seed concentration on the calcite precipitation rate constant and found the rate constant to be independent when the seed concentration was 0.3g L^{-1} or more. However, at lower concentrations the rate constant was greater which they attributed to nucleation (Reddy and Gaillard, 1981). As the surface area of the calcite used in their experiments is different than the one used in the present study, the seed concentrations were converted to solution to solid or volume to surface area (V/A) ratios. According to the work of Reddy and Guillard (1981), the calcite precipitation rate constant is independent of seed concentration at a V/A ratio of ≈ 0.006m or less. Although the V/A ratio (≈ 0.0047m) in the present manuscript should be safely inside

the maximum found by Reddy and Guillard (1981), it may be on the cusp with nucleation contributing to the calculated precipitation rates. Using scanning force microscopy, surface nucleation on calcite has been observed by Dove and Hochella (1993) at very low saturation states ($1.5 \leq \Omega \leq 2.5$) at the early stage of growth on calcite surface. However, they argued that surface nucleation is relatively unimportant as "monolayer growth controls the precipitation process within only 10 min of the start of an experiment" (Dove and Hochella, 1993). However, if surface nucleation continued after growth began, then the calcite surface area would increase at a greater rate than monolayer growth would indicate resulting in erroneously high calculated rates. As noted previously in the methodology section, reagent grade calcite powder was not used as the powder coated the electrodes during preliminary experiments leading to erratic voltage measurements. Although the V/A ratio of the present manuscript is less than the maximum found by Reddy and Guillard (1981), given the possibility of surface nucleation, a lower V/A ratio is strongly encouraged in future work on calcite precipitation kinetics (e.g. the V/A reported by Zhang and Dawe < 0.0006m). Furthermore, given the calculated precision, it is recommended that a chemostat (e.g. Morse, 1974; Mucci and Morse 1983) be employed in future work as well.

4.6. Conclusions

The precipitation rate of calcite in magnesium-free, phosphate-free, low calcium (~0.02 molal) simple electrolyte solutions of either KCl or NaCl was measured in a series of classical free drift experiments. The general and Davies and Jones rate

equations were found to adequately describe the rate data yielding reaction orders typically between 0.8 – 2.5. For both solutions, rate constants were found to range between $10^{0.8}$ and $10^{1.7}$ mmole m^{-2} hr^{-1} (general rate equation) and $10^{1.5}$ and $10^{2.2}$ mmole m^{-2} hr^{-1} (Davies and Jones rate equation). Overall, despite the lower precision (~20-25%) of the present results, if precipitation is assumed to be first order, than in conjunction with previous work (Finneran and Morse, submitted), dissolution has been shown to faster (larger values of k) and to be more strongly influenced by I and pCO_2 than precipitation. As dissolution is strongly inhibited by I (Finneran and Morse, submitted), the results of these two complementary studies suggests that CO_2 mitigation in highly saline aquifers should not experience any deleterious effects under high pCO_2 conditions although further studies are needed. Calculated activation energies are less than others reported in the literature for calcite precipitation which suggests that surface nucleation may have occurred in the present work. In light of this and the relatively poor precision of this research, the use of a smaller V/A ratio as well as a chemostat is encouraged for future work.

5. CONCLUSIONS

There are many components in natural waters that influence the reaction kinetics of calcite. A series of classical free-drift pH experiments were conducted in magnesium-free, phosphate-free, low calcium (~0.01- 0.02 molal) simple electrolyte solutions (KCl, NaCl) in order to investigate the influence of temperature, pCO_2 and ionic strength on both dissolution and precipitation rates of calcite without the influence of other ions.

It was shown (Section 2) that dissolution rates in magnesium-free, phosphate-free, low calcium (~0.01- 0.02 molal) simple electrolyte solutions (KCl, NaCl)can be described using first-order kinetics by the general rate equation: $R = k(1 - \Omega)^n$, where n = 1 (first-order) and k is a function of temperature, partial pressure of CO_2, and I. Rates decreased with increasing I and increased with increasing pCO_2 and temperature, although the influence of pCO_2 and temperature diminished at high I. From the data presented, it is quite clear that the influence of I on the dissolution kinetics of calcite clearly becomes more dominant (compared with pCO_2 and T), as I is increased.

Precipitation rates (Section 4) were modeled using both the general and Davies and Jones rate equations yielding similar results. Reaction orders were found to typically range between 0.8 and 2.5 for both rate equations regardless of electrolyte. For both KCl and NaCl solutions, rate constants were found to range between $10^{0.8}$ and $10^{1.7}$ mmole m^{-2} hr^{-1} (general rate equation) and $10^{1.5}$ and $10^{2.2}$ mmole m^{-2} hr^{-1} (Davies and Jones rate equation). Under the experimental conditions employed and the resultant precision (~20-25%), I and pCO_2 do not have a significant influence on the precipitation

rate of calcite. Precipitation rates increased with temperature although Arrhenius plots yield a broad range of activation energies ($E_a \approx 15 - 28$ kJ mol^{-1}, $R^2 = 0.72$). The relatively low calculated activation energies coupled with the precision of the results suggest the possibility of surface nucleation in the present results. In light of this and the relatively poor precision of this research, the use of a smaller V/A ratio as well as a chemostat is encouraged for future work.

The cation of the supporting electrolyte appears to play a minor role as dissolution rates were found to be faster in KCl than NaCl solutions although rates converged within experimental error as ionic strength approached zero. This led to the most significant finding of Section 2 in that $X_{\text{"free" } H_2O}$ was postulated to play the dominant role in the dissolution kinetics of calcite as water becomes limiting regardless of the temperature (25-55 °C) or the pCO_2 (0.1-1 atm) examined in this study. Furthermore, it was extrapolated that approximately 45-50% $X_{\text{"free"}H_2O}$ represents a critical threshold below which dissolution will not occur (or occur very slowly) in undersaturated solutions which may be related to the transition from a two-dimensional to three-dimensional water layer adsorbed on the calcite surface (see Cardellach et al., 2010 for a discussion of two-dimensional wetting). However, it must be stressed that this hypothesis is the result of extrapolation and clearly needs testing in other simple inert electrolyte solutions before investigating in more complex natural solutions. This suggests that dissolution rates may be controlled in undersaturated solutions by simply modifying the salt content of the solution which may be useful in predicting stability of subsurface CO_2 storage reservoirs.

It was also discovered that the MR model of Gledhill and Morse (2006a) underestimates k at low I or low pCO_2 which illustrates the danger of extrapolating much beyond the experimental domain used in formulating the model. The underestimation of the model at low I suggests that doubly charged cations (e.g. Ca^{2+}, Mg^{2+}) have a greater influence at lower I. At low pCO_2 the MR model of Gledhill and Morse (2006a) completely fails as negative values are predicted for k. In other words, the model predicts precipitation to occur in undersaturated solutions at low pCO_2 conditions. Despite these shortcomings, the MR model did converge at higher I with the experimental NaCl data.

The physical structure of water plays an important role in solution properties even though the surface of pure water is still not completely understood (e.g. Beattie et al., 2009; Buch et al., 2007; Wick and Dang, 2009). As the amount of "free" water was found to play a significant role in the dissolution kinetics of calcite, the analysis of existing colligative property literature data (Section 3) following the methodology of Zavitsas (2001) was conducted in order to elucidate the hydration characteristics of the various cations. The results are surprisingly variable for the various cations with hydration values determined from the analysis of freezing point depression data to be much larger than those determined from the analysis of boiling point elevation data or vapor pressure depression data. Hydration number decreases with temperature and concentration regardless of cation investigated. Although there is some uncertainty to these values, as evidenced in comparing hydration numbers calculated using freezing point depression data with that determined from boiling point elevation data, it appears

that over the range from freezing point of the most concentrated solution to the boiling point, $h_{NaCl} = 2.8 \pm 0.9$; $h_{KCl} = 1.2 \pm 1.2$; $h_{MgCl_2} = 9.8 \pm 3.7$; $h_{CaCl_2} = 6.3 \pm 3.3$. Using these values in the MR analysis of the dissolution data results in a the same predictive equation for k with the inclusion of a Mg^{2+} term:

$$k_{pred} = \beta_0 + \beta_1 T + \beta_2 pCO_2 + \beta_3 X_{"free"H_2O} + \beta_4 m_{Mg^{2+}}$$

where k is the predicted dissolution rate constant, T is the temperature, pCO_2 is the partial pressure of carbon dioxide, $X_{"free"\ H_2O}$ is the mole fraction of free water, $m_{Mg^{2+}}$ is the magnesium molality and β_i is the coefficient of the i^{th} term. A comparison of the present MR model results (equation 3.22, 3.23) with that of Gledhill and Morse (equation 7, 2006a) suggests that when $X_{"free"H_2O}$ is used in lieu of I, then molalities may be used instead of activities, thereby greatly simplifying the calculation in natural complex solutions such as subsurface brines.

Despite the lower precision (~20-25%) of the precipitation results, if precipitation is assumed to be first order, dissolution has been shown to faster (larger absolute values of k) and to be more strongly influenced by I and pCO_2 than precipitation. As dissolution is strongly inhibited by I the results of these two complementary studies suggests that CO_2 mitigation in highly saline aquifers should not experience any deleterious effects under high pCO_2 conditions as any dissolution will occur quite slowly due to the lack of free solvent. Overall, these findings may be useful in understanding and predicting the interaction and reactivity of the host carbonate minerals in subsurface reservoirs to the injection of CO_2 although much work needs to

be completed at elevated temperatures and pressures. Furthermore, it has been shown that the hydration characteristics of ions are quite important to the solution chemistry. The freezing point of ternary solutions were able to be predicted which suggest that a much simpler correlation model may be useful to predict colligative properties of mixed electrolyte solutions where the mole fraction of solute must be corrected for bound solvent molecules.

REFERENCES

Adams, E. E., Caldeira, K., 2008. Ocean storage of CO_2. Elements 4, 319-324.

Akin, G. W., Lagerwerff, J. V., 1965a. Calcium carbonate equilibria in aqueous solutions open to air. I. Solubility of calcite in relation to ionic strength. Geochimica et Cosmochimica Acta 29, 343-352.

Akin, G. W., Lagerwerff, J. V., 1965b. Calcium carbonate equilibria in solutions open to air. II. Enhanced solubility of $CaCO_3$ in presence of Mg^{2+} and SO_4^{2-}. Geochimica et Cosmochimica Acta 29, 353-360.

Alkattan, M., Oelkers, E. H., Dandurand, J. L., Schott, J., 1998. An experimental study of calcite and limestone dissolution rates as a function of pH from 1 to 3 and temperature from 25 to 80 °C. Chemical Geology 151, 199–214.

Al-Abadleh, H. A., Al-Hosney, H. A., Grassian, V. H., 2005. Oxide and carbonate surfaces as environmental interfaces: the importance of water in surface composition and surface reactivity. Journal of Molecular Catalysis A 228, 47-54.

Apelblat, A., 1998. Vapour pressures of $H_2{}^{16}O$ and $H_2{}^{18}O$, and saturated aqueous solutions of KCl from T = 298K to T = 318K by the isoteniscopic method. Journal of Chemical Thermodynamics 30, 1191-1198.

Arakaki, T., Mucci, A., 1995. A continuous and mechanistic representation of calcite reaction-controlled kinetics in dilute solutions at 25 °C and 1 Atm total pressure. Aquatic Geochemistry 5, 225-225.

Arvidson, R. S., Mackenzie, F. T., 1999. The dolomite problem: control of precipitation kinetics by temperature and saturation state. American Journal of Science 299, 257-288.

Badiozamani, K., Mackenzie, F. T., Thorstenson, D. C., 1977. Experimental carbonate cementation: salinity, temperature and vadose-phreatic effects. Journal of Sediment Petrology 47, 529-542.

Bakker, H. J., 2008. Structural dynamics of aqueous salt solutions. Chemical Reviews 108, 1456-1473.

Balomenos, E., Panias, D., Paspaliaris, I., 2006. A semi-empirical hydration model (SEHM) for describing aqueous electrolyte solutions I. Single strong electrolytes at 25 °C. Fluid Phase Equilibria 243, 29-37.

Beattie, J. K., Djerdjev, A. M., Warr, G. G., 2009. The surface of neat water is basic. Faraday Discussions 141, 31-39.

Belsley, D. A., Kuh, E., Welsch, R. E., 2005. Regression diagnostics: identifying influential data and sources of collinearity. John Wiley & Sons, Inc., Hoboken, NJ.

Benson, S. M., Cole, D. R., 2008. CO_2 sequestration in deep sedimentary formations. Elements 4, 325-331.

Berner, R. A., 1967. Comparative dissolution characteristics of carbonate minerals in presence and absence of aqueous magnesium ion. American Journal of Science 265, 45-70.

Berner, R. A., Morse, J. W., 1974. Dissolution kinetics of calcium-carbonate in sea-water .4. Theory of calcite dissolution. American Journal of Science 274, 108-134.

Berner-Kay, E., Berner, R. A., 1987. The global water cycle. Geochemistry and Environment, Prentice Hall, Englewood Cliffs, NJ.

Bischoff, J. L., 1968. Kinetics of calcite nucleation - magnesium ion inhibition and I catalysis. Journal of Geophysical Research 73, 3315-3322.

Bischoff, J. L., Fyfe, W. S., 1968. Catalysis, inhibition, and the calcite-aragonite problem. 1. The aragonite-calcite transformation. American Journal of Science 266, 65-79.

Blandamer, M. J., Engberts. J. B. F. N., Gleeson, P. T., Reis. J. C. R., 2005. Activity of water in aqueous systems; A frequently neglected property. Chemical Society Reviews 34, 440-458.

Bousfield, W. R., Bousfield, C. E., 1923. Vapour pressure and density of sodium chloride solutions. Proceedings of the Royal Society A 103, 429-443.

Bring, J., 1994. How to standardize regression coefficients. The American Statistician 48, 209-213.

Bromley, L. A., 1973. Thermodynamic properties of strong electrolytes in aqueous solutions. American Institute of Chemical Engineers Journal 19, 313 – 320.

Brown O. L. I., Delaney, C. M., 1954. Vapor pressures of aqueous potassium chloride solutions at 25 by means of a new type of differential manometer. The Journal of Physical Chemistry 58, 255-258.

Buch, V., Milet, A., Vacha, R., Jungwirth, P, Devlin, J. P., 2007. Water surface is acidic. Proceedings of the National Academy of Sciences of the United States of America 104, 7342-7347.

Buhmann, D., Dreybrodt, W., 1987. Calcite dissolution kinetics in the system H_2O–CO_2–$CaCO_3$ with participation of foreign ions. Chemical Geology 64, 89–102.

Burgess, J., 1999. Ions in solution: basic principles of chemical interactions. 2nd edition. Ellis Horwood Publishing, Chichester, UK.

Burton, E. A., 1993. Controls on marine carbonate cement mineralogy - review and reassessment. Chemical Geology 105, 163-179.

Burton, W. K., Cabrera, N., Frank, F. C., 1951. The growth of crystals and the equilibrium structure of their surfaces. Philosophical Transactions of the Royal Society of London Series a-Mathematical and Physical Sciences 243, 299-358.

Butler, J. N., Huston, R., 1970. Activity coefficients and ion pairs in the systems sodium chloride-sodium bicarbonate-water and sodium chloride-sodium carbonate-water. Journal of Physical Chemistry 74, 2976-2983.

Busenberg, E., Plummer, L. N., 1985. Kinetic and thermodynamic factors controlling the distribution of SO_4^{2-} and Na^+ in calcites and selected aragonites. Geochimica et Cosmochimica Acta 49, 713-725.

Busenberg, E., Plummer, L.N. 1986. A comparative study of the dissolution and crystal growth kinetics of calcite and aragonite. In: Mumpton, F.A. (Ed.), Studies in Diagenesis., U.S. Geological Survey Bulletin 1578, 99, pp. 139–168.

Capewell, S. G., Hefter, G., May, P. M., 1998. Potentiometric investigation of the weak association of sodium and carbonate ions at 25 °C. Journal of Solution Chemistry 27, 865-877.

Capewell, S. G., Buchner, R., Hefter, G., May, P. M., 1999. Dielectric relaxation of aqueous Na_2CO_3 solutions. Physical Chemistry Chemical Physics 1, 1933-1937.

Cardellach, M., Verdaguer, A., Santiso, J., Fraxedas, J., 2010. Two-dimensional wetting: the role of atomic steps on the nucleation of thin water films on BaF_2 (111) at ambient conditions. Journal of Chemical Physics 132, 234708.

Case, L. C., 1945. Exceptional Silurian Brine near Bay City, Michigan. AAPG Bull.-American Association of Petroleum Geology 29, 567-570.

Charara, M., Lopez, O., Zuddas, P., 2005. A new overall kinetic model describing calcite precipitation from brine-like solutions AGU Fall Meeting Abstract GC13A-1216.

Chen, C., Britt, H. I., Boston, J. F., Evans, L. B., 1982. Local composition model for excess Gibbs energy of electrolyte systems. Part I: single solvent, single completely dissociated electrolyte systems. American Institute of Chemical Engineers Journal 28, 588 – 596.

Chiorboli, P., Momicchioli, F., Grandi, G., 1966. Cryscopical measurements of strong electrolyte solutions. I. The equilibrium method for measuring freezing points with a resistance platinum thermometer. Bollettino scientifico della Facolta di chimica industriale di Bologna 24, 133-153.

Chou, L., Garrels, R. M., Wollast, R., 1988. Comparative study of the dissolution kinetics and mechanisms of carbonates in aqueous solutions. Chemical Geology 70, 77-77.

Conway, B. E., 1981. Ionic hydration in chemistry and biophysics, Studies in physical and theoretical chemistry 12. Elsevier, Amsterdam.

Cubillas, P., Kohler, S., Prieto, M., Causserand, C., Oelkers, E.H., 2005a. How do mineral coatings affect dissolution rates? An experimental study of coupled $CaCO_3$ dissolution-$CdCO_3$ precipitation. Geochimica et Cosmochimica Acta 69, 5459-5476.

Cubillas, P., Kohler, S., Prieto, M., Chairat, C., Oelkers, E.H., 2005b. Experimental determination of the dissolution rates of calcite, aragonite, and bivalves. Chemical Geology 216, 59-77.

Davies, C. W., Jones, A. L., 1955. The precipitation of silver chloride from aqueous solutions .2. Kinetics of growth of seed crystals. Transactions of the Faraday Society 51, 812-817.

Davis, A. R., Oliver B. G., 1972. A vibrational-spectroscopic study of the species present in the CO_2-H_2O System. Journal of Solution Chemistry 1, 329-339.

Davisson, M. L., Criss, R. E., 1996. Na-Ca-Cl relations in basinal fluids. Geochimica et Cosmochimica Acta 60, 2743-2752.

DeKanel, J., Morse, J. W., 1978. Chemistry of ortho-phosphate uptake from seawater on to calcite and aragonite. Geochimica et Cosmochimica Acta 42, 1335-1340.

de Leeuw, N. H., Parker, S. C, 1997. Atomistic simulation of the effect of molecular adsorption of water on the surface structure and energies of calcite surfaces. Journal of Chemical Society, Faraday Transactions I 93, 467-475.

Dickson, A. G., Goyet, C., 2005. Handbook of methods for the analysis of the various parameters of the carbon dioxide system in sea water. Version 2.

Dickson, A.G., Sabine, C.L. and Christian, J.R. (Eds.) 2007. Guide to best practices for ocean CO_2 measurements. PICES Special Publication 3, 191 pp. ("Guide" in one PDF file).

Di Leo, J. M, Marañón, J., 2005. Hydration and diffusion of cations in nanopores. Journal of Molecular Structure THEOCHEM 729, 53-57

Driesner, T., Seward, T. M., Tironi, I. G., 1998. Molecular dynamics simulation study of ionic hydration and ion association in dilute and 1 molal aqueous sodium chloride solutions from ambient to supercritical conditions. Geochimica et Cosmochimica Acta 62, 3095-3107.

Dove, P. M., Hocehlla, M. F., 1993. Calcite precipitation mechanisms and inhibition by orthophosphate: in situ observations by scanning force microscopy. Geochimica et Cosmochimica Acta 57, 705-714.

Dougherty, R. C., Howard, L. N., 1998. Equilibrium structural model of liquid water: evidence from heat capacity, spectra, density, and other properties. Journal of Chemical Physics 109, 7379-7393.

Du, H., Rasaiah, J. C., Miller, J. D., 2007. Structural and dynamic properties of concentrated alkali halide solutions: a molecular dynamics simulation study. Journal of Physical Chemistry B 111, 209-217.

Feistel, R., Wagner, W., 2006. A new equation of state for H_2O in ice. Journal of Physical Chemistry Reference Data 35, 1021-1047.

Finneran, D. W., Morse, J. W., 2009. Calcite dissolution kinetics in saline waters. Chemical Geology 268, 137-146.

Forsythe, W. E., 1954. Smithsonian Physical Tables. Smithsonian Institution Press, Washington DC..

Frantz, J. D., 1998. Raman spectra of potassium carbonate and bicarbonate aqueous fluids at elevated temperatures and pressures: comparison with theoretical simulations. Chemical Geology 152, 211-225.

Frazer J. C. W., Lovelace, B. F., 1914. Studies of the vapor pressure of solutions. A static method for the determination of the difference between the vapor pressure of solution and that of solvent. Journal of the American Chemical Society 36, 2439-2449.

Frazer, J. C. W., 1927. The direct measurement of osmotic pressure. Contemporary developments in chemistry; lectures delivered at Columbia University in the special course in chemistry given in the summer session of 1927. Columbia University, New York, NY.

Fullerton, G. D., Keener, C. R., Cameron I. L., 1994. Correction for solute/solvent interaction extends accurate freezing point depression theory to high

concentration range. Journal of Biochemical and Biophysical Methods 29, 217-235.

Garrels, R. M., Thompson, M. E., 1962. Chemical model for sea water at 25°C and one atmosphere total pressure. American Journal of Science 260, 57-66.

Ge X., Wang, X., 2009. Estimation of freezing point depression boiling point elevation, and vaporization enthalpies of electrolyte solutions. Industrial and Engineering Chemistry Research 48, 2229-2235.

Gibbard, H. F. Jr., Fong, S. L., 1972. Freezing points of aqueous two-salt mixtures of sodium, magnesium, calcium and barium chlorides, 163rd National Meeting, American Chemical Society, Boston, MA., April, 1972.

Gibbard, H. F. Jr., Fong, S-L., 1975. Freezing points and related properties of electrolyte solutions. III. The systems NaCl-$CaCl_2$-H_2O and NaCl-$BaCl_2$-H_2O. Journal of Solution Chemistry 4, 863-872.

Gibbard, H. F. Jr., Gossmann, A. F., 1974. Freezing points of electrolyte mixtures. I. Mixtures of sodium chloride and magnesium chloride in water. Journal of Solution Chemistry 3, 385-393.

Gibson R. E., Adams, L H., 1933. Changes of chemical potential in concentrated solutions of certain salts. Journal of the American Chemical Society 55, 2679-2695.

Gledhill, D. K., Morse, J. W., 2004. Dissolution kinetics of calcite in NaCl-$CaCl_2$-$MgCl_2$ brines at 25°C and 1 bar pCO_2. Aquatic Geochemistry10, 171-190.

Gledhill, D. K., Morse, J. W., 2006a. Calcite dissolution kinetics in Na-Ca-Mg-Cl brines. Geochimica et Cosmochimica Acta 70, 5802-5813.

Gledhill, D. K., Morse, J. W., 2006b. Calcite solubility in Na-Ca-Mg-Cl brines. Chemical Geology 233, 249-256.

Gozalpour, F., Ren, S. R., Tohidi, B., 2005. CO_2 EOR and storage in oil reservoirs. Oil Gas Sci. Technol. 60, 537-546.

Gran, G., 1952. Determination of the equivalence point in potentiometric titrations Part II. The Analyst 77, 661-671.

Gutjahr, A., Dabringhaus, H., Lacmann, R., 1996a. Studies of the growth and dissolution kinetics of the $CaCO_3$ polymorphs calcite and aragonite. 1. Growth and dissolution rates in water. Journal of Crystal Growth 158, 296-309.

Gutjahr, A., Dabringhaus, H., Lacmann, R., 1996b. Studies of the growth and dissolution kinetics of the $CaCO_3$ polymorphs calcite and aragonite. 2. The influence of divalent cation additives on the growth and dissolution rates. Journal of Crystal Growth 158, 310-315.

Han, B., Choi, J. H., Dantzig, J. A., Bischof, J. C., 2006. A quantitative analysis on latent heat of an aqueous binary mixture. Cryobiology 52, 146-151.

Hass, J. L., 1971. The effect of salinity on the maximum thermal gradient of a hydrothermal system at hydrostatic pressure. Economic Geology 66, 940-946.

Haghighi, H., Chapoy, A., Tohidi, B., 2008. Freezing point depression of electrolyte solutions: experimental measurements and modeling using the cubic-plus-

association equation of state. Industrial and Engineering Chemistry Research 47, 3983-3989.

Hales, B, Emerson, S., 1997. Evidence in support of first-order dissolution kinetics of calcite in seawater. Earth and Planetary Science Letters 148, 317-327.

Hall, D. L., Sterner, S. M., Bodnar, R. J., 1988. Freezing point depression of NaCl-KCl-H_2O solutions. Economic Geology 83, 197-202.

Hamer, W. J., Wu, Y.-C., 1972. Osmotic coefficients and mean activity coefficients of univalent electrolytes in water at 25°C. Journal of Physical Chemistry Ref. Data 1, 1047-1100.

Hanor, J. S., 1987. Kilometer-scale thermohaline overturn of pore waters in the Louisiana Gulf-Coast. Nature 327, 501-503.

Hanor, J. S., 1994. Physical and chemical controls on the composition of waters in sedimentary basins. Marine and Petroleum Geology 11, 31-45.

Hausner D. B., Reeder, R. J., Strongin, D. R., 2007. Humidity-induced restructuring of the calcite surface and the effect of divalent heavy metals. Journal of Colloid and Interface Science 305, 101-110.

He, S. L., Morse, J. W., 1993. The carbonic-acid system and calcite solubility in aqueous Na-K-Ca-Mg-Cl-SO_4 Solutions from 0 to 90 °C. Geochimica et Cosmochimica Acta 57, 3533-3554.

James, D. W., Armishaw, R. F., 1975. Structure of aqueous solutions: infrared spectra of the water librational mode in solutions of monovalent halides. Aust. Journal of Chemistry 28, 1179-1186.

James, D. W., Armishaw, R. F., Frost, R. L, 1976. Structure of aqueous solutions. Librational band studies of hydrophobic and hydrophilic effects in solutions of electrolytes and nonelectrolytes. The Journal of Physical Chemistry 80, 1346-1350.

James, D. W., Frost, R. L., 1974. Structure of aqueous solutions. Structure making and structure breaking in solutions of sucrose and urea. The Journal of Physical Chemistry 78, 1754-1755.

Jeschke, A. A., Dreybrodt, W., 2002. Pitfalls in the determination of empirical dissolution rate equations of minerals from experimental data and a way out: an iterative procedure to find valid rate equations, applied to Ca-carbonates and -sulphates. Chemical Geology 192, 183-194.

Jones H. C., Bassett, H. P., 1905. The approximate composition of the hydrates formed by certain electrolytes in aqueous solutions at different concentrations. American Chemical Journal 33, 534-586.

Kazmlerczak, T.F., Tomson, M.B., Nancollas, G. H., 1982. Crystal growth of calcium carbonate – A controlled composition kinetic study. Journal of Physical Chemistry 86, 103-107.

Kendall, T. A., Martin, S. T., 2005. Mobile ions on carbonate surfaces. Geochimica et Cosmochimica Acta 69, 3257-3263.

Kendall, T. A., Martin, S. T., 2007. Water-induced reconstruction that affects mobile ions on the surface of calcite. Journal of Physical Chemistry A 111, 505-514.

Keir, R. S., 1980. The dissolution kinetics of biogenic calcium carbonates in seawater. Geochimica et Cosmochimica Acta 44, 241-252.

Kerisit S., Parker, S. C., 2004. Free energy of adsorption of water and calcium on the {101"4"¯} calcite surface. Chemical Communications 1, 52-53.

Kim, J-O., Ferree, G., 1981. Standardization in causal analysis. Sociological Methods and Research 10, 187-210.

Kim, J-O, Mueller, C. W., 1976. Standardized and unstandardized coefficients in casual analysis: an expository note. Sociological Methods Research 4, 423-438.

Kharaka, Y. K., Hanor, J. S., 2004. Deep fluids in the continents. I. Sedimentary basins. In: Holland, H. D., Turerkian, K. K. (Eds.), Treatise of Geochemistry. Elsevier-Pergamon, Oxford.

Kowacz, M., Putnis, A., 2008. The effect of specific background electrolytes on water structure and solute hydration: consequences for crystal dissolution and growth. Geochimica et Cosmochimica Acta 72, 4476-4487.

Knauss, K. G., Wolery, T. J., Jackson, K. J., 1990. A new approach to measuring pH in brines and other concentrated electrolytes. Geochimica et Cosmochimica Acta 54, 1519-1523.

Kongsjorden, H., Karstad, O, Torp, T. A., 1997. Saline aquifer storage of carbon dioxides in the Sleipner project. Waste Management 17, 303-308.

Lasaga, A. C., 1998. Kinetic theory in the earth sciences. Princeton series in geochemistry;. Princeton University Press, Princeton, NJ.

Lasaga, A.C., Lüttge, A., 2004. Mineralogical approaches to fundamental crystal dissolution kinetics. American Mineralogist 89, 527-540.

Lebrón, I., Suárez, D. L., 1998. Kinetics and mechanisms of precipitation of calcite as affected by PCO2 and organic ligands at 25°C. Geochimica et Cosmochimica Acta 62, 405-416.

Lide, D. R., 2007. CRC handbook of chemistry and physics. Taylor and Francis, Boca Raton, FL.

Lippmann, F., 1973. Sedimentary carbonate minerals. Springer-Verlag, New York, NY.

Lovelace, B. F., Frazer, J. C. W., Miller, E., 1916. Studies of the vapor pressure of solutions. The lowering of the vapor pressure of water produced by dissolved potassium chloride. Journal of the American Chemical Society 38, 515-528.

Lovelace, B. F., Frazer, J. C. W., Sease, V. B., 1921. The lowering of the vapor pressure of water at 20°C produced by dissolved potassium chloride. Journal of the American Chemical Society 43, 102-110.

Lüttge, A., 2006. Crystal dissolution kinetics and Gibbs free energy. Journal of Electron Spectroscopy and Related Phenomena 50, 248-259

MacInnes, D. A., Belcher, D., 1933. The thermodynamic ionization constants of carbonic acid. Journal of the American Chemical Society 55, 2630-2646.

Magini, M, Licheri, G., Paschina, G., Piccaluga, G., Pinna, G., 1988. X-ray diffraction of ions in aqueous solutions: hydration and complex formation. CRC Press, Boca Raton, FL..

Marcus, Y., 1983. Ionic radii in aqueous solutions. Journal of Solution Chemistry 12, 271-275.

Marcus, Y., 1986. Ion solvation. Wiley, Chichester, UK.

Marcus, Y., 1988. Ionic radii in aqueous solutions. Chemical Reviews 88, 1475-1498.

Marcus, Y., 2009. Effect of ions on the structure of water: structure making and breaking. Chemical Reviews 109, 1346-1370.

Marsh, K. N. (Editor), 1987. Recommended reference materials for the realization of physiochemical properties. Blackwell, Oxford.

Max, J., Chapados, C., 2001. IR spectroscopy of aqueous alkali halide solutions: pure salt-solvated water spectra and hydration numbers. Journal of Chemical Physics 115, 2664-2675.

Max, J., Gessinger, V., van Driessche, C., Larouche, P., Chapados, C., 2007. Infrared spectroscopy of aqueous ionic salt solutions at low concentrations. The Journal of Chemical Physics 126, 184507.

Mel'nichenko, N. A., 2007. Hydration numbers of sea water basic ions found by the pulse method of proton NMR. Journal of Structural Chemistry 48, 479-485.

Millero, F. J., 2007. The marine inorganic carbon cycle. Chemical Reviews 107, 308-341.

Millero, F. J., Milne, P. J., Thurmond, V. L., 1984. The solubility of calcite, strontianite and witherite in NaCl Solutions at 25 °C. Geochimica et Cosmochimica Acta 48, 1141-1143.

Momicchioli F., Devoto, O., Grandi, G., Cocco., G., 1970. Thermodynamic properties of concentrated solutions of strong electrolytes I. Activity coefficients of water from freezing-point depressions for alkali chlorides. Berichte der Bunsen-Gesellschaft 74, 59-66.

Morse, J. W., 1974. Dissolution kinetics of calcium carbonate in sea water. III. A new method for the study of carbonate reaction kinetics. American Journal of Science 274, 97-107.

Morse, J. W., 1983. The kinetics of calcium carbonate dissolution and precipitation. In: Reeder, R. J. (Ed.), Carbonates: Mineralogy and Chemistry. Mineralogical Society of America.

Morse, J. W., Arvidson, R. S., 2002. The dissolution kinetics of major sedimentary carbonate minerals. Earth-Science. Reviews. 58, 51-84.

Morse, J. W., Arvidson, R. S., Lüttge, A., 2007. Calcium carbonate formation and dissolution. Chemical Reviews 107, 342-381.

Morse, J. W., Berner, R. A., 1972. Dissolution kinetics of calcium-carbonate in sea-water. II. kinetic origin for lysocline. American Journal of Science 272, 840-851.

Morse, J. W., Hanor, J. S., He, S., 1997. The role of mixing and migration of basinal waters in carbonate mineral mass transport. In: Monannes, I. P., Gregg, J. M., Shelton, K. L. (Eds.), Basinwide Fluid Flow and Associated Diagenetic Patterns: Integrated Petrologic, Geochemical and Hydrological Considerations, SEPM Special Publication No. 57, SEPM, Tulsa, OK, p 41-52.

Morse, J. W., Mackenzie, F. T., 1990. Geochemistry of sedimentary carbonates. Elsevier, Amsterdam.

Morse, J. W., Walton, K., submitted. Vaterite formation and transformation to calcite in aqueous solutions with widely varying ionic strength. Unpublished Manuscript. Department of Oceanography, Texas A&M University, College Station, TX.

Mucci, A., 1986. Growth kinetics and composition of magnesian calcite overgrowths precipitated from seawater: quantitative influence of orthophosphate ions. Geochimica et Cosmochimica Acta 50, 2255-2265.

Mucci, A., Morse, J. W., 1983. The incorporation of Mg^{2+} and Sr^{2+} into calcite overgrowths: influences of growth rate and solution composition. Geochimica et Cosmochimica Acta 47, 217-233.

Mucci, A., Morse, J. W., Kaminsky, M. S., 1985. Auger-spectroscopy analysis of magnesian calcite overgrowths precipitated from seawater and solutions of similar composition. American Journal of Science 285, 289-305.

Muller, P., 1994, 66, 1077. Glossary of terms used in physical organic chemistry (IUPAC Recommendations 1994). Pure and Applied Chemistry 66, 1077.

Nancollas, G. H., Purdie, N., 1964. The kinetics of crystal growth. Quarterly Reviews Chemical Society 18, 1-20.

Nancollas, G. H., Reddy, M. M., 1971. Crystallization of calcium carbonate. II.. Calcite growth mechanism. J. Colloid Interface Sci. 37, 824-830.

Nehrke, G., Reichart, G. J., Van Cappellen, P., Meile, C., Bijma, J., 2007. Dependence of calcite growth rate and Sr partitioning on solution stoichiometry: non-Kossel crystal growth. Geochimica et Cosmochimica Acta 71, 2240-2249.

Nesbitt, H. W., 1982. The Stokes and Robinson hydration theory: a modification with application to concentrated electrolyte solutions. Journal of Solution Chemistry 11, 415-422.

Oakes C. S., Bodnar, R. J., Simonson, J. M., 1990. The system NaCl-$CaCl_2$-H_2O. I. The ice liquidus at 1 atm total pressure. Geochimica et Cosmochimica Acta 54, 603-610.

Oelkers, E. H., Gislason, S. R., Matter, J., 2008. Mineral carbonation of CO_2. Elements 4, 333-337.

Ohtaki, H., Radnai, T., 1993. Structure and dynamics of hydrated ions. Chemical Reviews 93, 1157-1204.

Oliver, B. G., Davis, A. R., 1973. Vibrational spectroscopic studies of aqueous alkali metal bicarbonate and carbonate solutions. Canadian Journal of Chemistry 51, 698-702.

Olynyk, P., Gordon, A. R., 1943. The vapor pressure of aqueous solutions of sodium chloride at 20, 25, and 30 for concentration from 2 molal to saturation. Journal of the American Chemical Society 65, 224-226.

Osakai, T., Ogata, A., Ebina, K., 1997. Hydration of ions in organic solvent and its significance in the Gibbs Energy of ion transfer between two immiscible liquids. Journal of Physical Chemistry B 101, 8341–8348.

Pearce, J., N., Nelson, A. F., 1932. The vapor pressures of aqueous solutions of lithium nitrate and the activity coefficients of some alkali salts in solutions of high concentration at 25°. Journal of the American Chemical Society. 54, 3544–3555.

Pearce, J. N., Snow, R. D., 1927. An improved dynamic method for measuring vapor pressures. The Journal of Physical Chemistry 31, 231-245.

Pérez-Villaseñor, F., Iglesias-Silva, G. A., 2003. Prediction of osmotic and activity coefficients using a modified Pitzer equation for multicomponent strong electrolyte systems at 298 K. Industrial and Engineering Chemistry Research 42, 1087–1092.

Pitzer, K. S., 1973. Thermodynamics of electrolytes. I. Theoretical basis and general equations. The Journal of Physical Chemistry 77, 268–277.

Plummer, L. N., Wigley, T. M. L., Parkhurst, D. L., 1978. Kinetics of calcite dissolution in CO_2-water systems at 5-60 °C and 0.0-1.0 Atm CO_2. American Journal of Science 278, 179-216.

Plummer, L. N., Wigley, T. M. L., Parkhurst, D. L., 1979. Critical review of the kinetics of calcite dissolution and precipitation. In: Jenne, E. A. (Ed.), Chemical Modeling – Speciation Sorption and Kinetics in Aqueous Systems, American Chemical Society, Washington DC.

Pokrovsky, O. S., Golubev, S. V., Schott, J., 2005. Dissolution kinetics of calcite, dolomite and magnesite at 25 °C and 0 to 50 atm pCO2. Chemical Geology 217, 239-255.

Pokrovsky, O. S., Schott, J., Mielczarski, J. A., 2002. Surface speciation of dolomite and calcite in aqueous solutions. In: Hubbard, A. (Ed.), Encyclopedia of Surface and Colloid Science, Marcel Dekker, Inc. New York, NY..

Potter, R. W., II, Clynne, M. A., Brown, D. L., 1978. Freezing point depression of aqueous sodium chloride solutions. Economic Geology 73, 284-285.

Price, W. E., Mills, R., Woolf, L. A., 1996. Use of experimental diffusion coefficients to probe solute−solute and solute−solvent interactions in electrolyte solutions. The Journal of Physical Chemistry 100, 1406–1410.

Pytkowicz R. M., Hawley, J. E., 1974. Bicarbonate and carbonate ion-pairs and a model of seawater at 25°C. Limnology and Oceanography 19, 223-234.

Ramaniah, L. M., Bernasconi, M., Parrinello, M., 1999. Ab initio molecular-dynamics simulation of K^+ solvation in water. Journal of Chemical Physics 113, 9149-9161.

Reddy, M. M., Gaillard, W. D., 1981. Kinetics of calcium carbonate (calcite)-seeded crystallization: influence of solid/solution ratio on the reaction rate constant. Journal of Colloid and Interface Science, 80, 171-178.

Reddy, M. M., Plummer, L. N., Busenberg, E., 1981. Crystal growth of calcite from calcium bicarbonate solutions at constant PCO_2 and 25°C: a test of a calcite dissolution model. Geochimica et Cosmochimica Acta 45, 1281-1289.

Riahi, K., Rubin, E. S., Schrattenholzer, L., 2004. Prospects for carbon capture and sequestration technologies assuming their technological learning. Energy 29, 1309-1318.

Rivett, A. C. D., 1912. Neutralsalzwirkung auf die gefrierpunkte von mischungen in wässeriger lösung. Zeitschrift fur Physikalische Chemie 80, 537-563.

Rodebush, W. H., 1918. The freezing points of concentrated solutions and the free energy of solution of salts. Journal of the American Chemical Society 40, 1204-1213.

Sako, T., Hakuta, T., Yoshitome, H., 1985. Vapor pressures of binary (water-hydrogen chloride, -magnesium chloride, and -calcium chloride) and ternary (water-magnesium chloride-calcium chloride) aqueous solutions. Journal of Chemical and Engineering Data 30, 224-228.

Salem, M.R., 1994. Dissolution of calcite crystals in the presence of some metal ions. Journal of Materials Science 29, 6463–6467.

Saxton, B., Smith, R. P., 1932. The activity coefficient of potassium chloride in aqueous solution from boiling point data. Journal of the American Chemical Society 54, 2626-2636.

Scatchard, G., 1925. The activities of strong electrolytes. II. A revision of the activity coefficients of potassium, sodium, and lithium chlorides, and potassium hydroxide. Journal of the American Chemical Society 47, 648-661.

Scatchard, G., Prentiss, S. S., 1933. The freezing points of aqueous solutions. IV. Potassium, sodium and lithium chlorides and bromides. Journal of the American Chemical Society 55, 4355-4362.

Schawe, J. E. K., 2006. A quantitative DSC analysis of the metastable phase behavior of the sucrose-water system. Thermochimica Acta 45, 115-125.

Schmalz, R. F., 1967. Kinetics and diagenesis of carbonate sediments. Journal of Sedimentary Petrology 37, 60-67.

Schmid, R., Miah, A. M., Sapunov, V. N., 2000. A new table of the thermodynamic quantities of ionic hydration: value and some applications (enthalpy-entropy compensation and Born radii). Physical Chemistry Chemical Physics 2, 97-102.

Sjöberg, E. L., 1978. Kinetics and mechanism of calcite dissolution in aqueous solutions at low temperatures. Stockholm Contributions Geology. 32, 1–96.

Sjöberg, L., Rickard, D. T., 1983. Studies of calcite dissolution reactions: a report of work between 1979-1982. Department of Geology, Stockholm University, Stockholm.

Sjöberg, L., Rickard, D. T., 1985. The effect of added dissolved calcium on calcite dissolution kinetics in aqueous solutions at 25 C. Chemical Geology 49, 405-413.

Sluiter, C. H., 1914. De invloed der hydratatie en der afwikingen van de ideale gaswetten in waterige zoutoplossingen op het stol- en kookpunt. Verslagen der Afdeeling Natuurk 23, 920-930.

Smith, R. P., 1933. The activity coefficient of potassium chloride in aqueous solutions at 0C from electromotive force and freezing point data. Journal of the American Chemical Society 55, 3279-3282.

Smith, R. P., Hirtle, D. S., 1939. The boiling point elevation. III. Sodium chloride 1.0 to 4.0 M and 60 to 100. Journal of the American Chemical Society 61, 1123-1126.

Soper, A., K., 2000. Probing the structure of water around biological molecules: concepts, constructs and consequences. Physica B: Condensed Matter 276-278, 12-16.

Soper, A. K., Weckström, K., 2006. Ion salvation and water structure in potassium halide aqueous solutions. Biophysical Chemistry 124, 180-191.

Spencer, H. M., 1932. The activity coefficients of potassium chloride. An application of the extended Debye-Huckel theory to interpretation of freezing point measurements. Journal of the American Chemical Society 54, 4490-4497.

Stipp, S. L. S., 1999. Toward a conceptual model of the calcite surface: hydration, hydrolysis, and surface potential. Geochimica et Cosmochimica Acta 63, 3121-3131.

Stipp, S. L. S, Eggleston C. M., Nielsen, B. S., 1994. Calcite surface-structure observed at microtopographic and molecular scales with atomic-force microscopy (AFM). Geochimica et Cosmochimica Acta 58, 3023-3033

Stipp, S. L. S., Gutmannsbauer, W. Lehmann, T., 1996. The dynamic nature of calcite surfaces in air. American Mineralogist 81, 1-8.

Stokes, R.H., Robinson, R.A., 1948. Ionic hydration and activity in electrolyte solutions. Journal of the American Chemical Society 70, 1870-1878.

Stokes, R.H., Robinson, R.A., 1973. Solvation equilibria in very concentrated electrolyte solutions. Journal of Solution Chemistry 2, 173-191.

Takasaki, S., Parsiegla, K. I., Katz, J. L., 1994. Calcite growth and the inhibiting effect of iron(III). Journal of Crystal Growth. 143, 261-268.

Terjesen, S. G., Erga, O., Thorsen, G., Ve, A., 1961. Phase boundary processes as rate determining steps in reactions between solids and liquids - the inhibitory action of metal ions on the formation of calcium bicarbonate by the reaction of calcite with aqueous carbon dioxide Chem. Eng. Sci. 14, 277-289.

Torp, T. A., Gale, J., 2003. Demonstrating storage of CO_2 in geological reservoirs: the Sleipner and SACS projects. In: Gale, J., Kaya, Y. (Eds.), Proceedings of the 6th International Conference on Greenhouse Gas Control Technologies. Pergamon, Amsterdam.

UNESCO, 1981a. Background papers and supporting data on the practical salinity scale, 1978. UNESCO, Paris.

UNESCO, 1981b. The practical salinity scale 1978 and the international equation of state of seawater 1980 : tenth report of the Joint Panel on Oceanographic Tables and Standards (JPOTS), Sidney, Canada, 1-5 September 1980. UNESCO, Paris.

Van Cappellen, P., Charlet, L., Stumm, W., Wersin, P., 1993. A surface complexation model of the carbonate mineral-aqueous solution interface. Geochimica et Cosmochimica Acta 57, 3505-3518.

Vilcu, R., Stanciu, F., 1965. Differential cryoscopy in ternary system. Revue Roumaine de Chimie 10, 499-506.

Villegas-Jiménez, A., Mucci, A., Whitehead, M. A., 2009. Theoretical insights into the hydrated(10.4) calcite surface: structure, energetic, and bonding relationships. Langmuir 25, 6813-6824.

Voormeij, D. A., Simandl, G. J., 2004. Geological, ocean, and mineral CO_2 sequestration options: a technical review. Geoscience Canada 31, 11-22.

Walter, L. M., 1985. Relative reactivity of skeletal carbonates during dissolution: implications for diagenesis. In: Schneidermann, N., Harris, P. M. (Eds.), Carbonate Cements, SEPM Special Publication 37, 3-16.

Walter, L. M., 1986. Relative efficiency of carbonate dissolution and precipitation during diagenesis: a progress report on the role of solution chemistry. In: Gaustier, D. L. (Ed.), Roles of Organic Matter in Sediment Diagenesis, SEPM Special Publication 38, 1-11.

Washburn, E. W., 1926-1930. International Critical Tables of Numerical Data, Physics, Chemistry and Technology. National Research Council. USA.

Weyl, P. K., 1958. The solution kinetics of calcite. Journal of Geology 66, 163-176.

White, C. M., Strazisar, B. R., Granite, E. J., Hoffman, J. S., and Pennline, H. W., 2003. Separation and capture of CO_2 from large stationary sources and sequestration in geological formations - coal beds and deep saline aquifers. J. Air Waste Manage. Assoc. 53, 645-715.

Wick, C. D., Dang, L. X., 2009. Investigating hydroxide anion interfacial activity by classical and multistate empirical valence bond molecular dynamics simulations. Journal of Physical Chemistry A 113, 6356-6364.

Wilson, T. P., Long, D. T., 1993. Geochemistry and Isotope Chemistry of Ca-Na-Cl Brines in Silurian Strata, Michigan Basin, USA. Applied Geochemistry 8, 507-524.

Winter, D. J., Burton, E. A., 1992. Experimental investigation aCa/aCO_3 ratio on the kinetics of calcite precipitation: implication for the rate equation and trace element incorporation. Geological Society of America Abstracts with Programs 24.

Wolf, M., Breitkopf, O., Puk, R., 1989. Solubility of calcite in different electrolytes at temperatures between 10-60 °C and at CO_2 partial pressures of about 1 KPa. Chemical Geology 76, 291-301.

Wollast, R., 1989. Modeling of the deposition of carbonates in the system $MgCO_3$-$CaCO_3$-Fe CO_3 during evaporation of a semi-enclosed basin. Abstracts of Papers of the American Chemical Society 198, 16-GEOC.

Yamasaki, A., 2003. An overview of CO_2 mitigation options for global warming - Emphasizing CO_2 sequestration options. Journal of Chemical Engineering of Japan 36, 361-375.

Zavitsas, A.A., 2001. Properties of water solutions of electrolytes and nonelectrolytes. Journal of Physical Chemistry B 105, 7805-7817.

Zavitsas, A.A., 2005. Aqueous solutions of calcium ions: hydration numbers and the effect of temperature. Journal of Physical Chemistry B 109, 20636-20640

Zaytsev I. D., Aseyev, G. G., 1992. Properties of aqueous solutions of electrolytes. CRC Press, Boca Raton, FL. Translated by M. A. Lazarev, V. A. Sorochenko.

Zhang, Y. P., Dawe, R., 1998. The kinetics of calcite precipitation from a high salinity water. Applied Geochemistry 13, 177-184.

Zhong, S. J., Mucci, A., 1989. Calcite and aragonite precipitation from seawater solutions of various salinities - precipitation rates and overgrowth compositions. Chemical Geology 78, 283-299.

Zuddas, P., Mucci, A., 1994. Kinetics of calcite precipitation from seawater. I. A classical chemical kinetics description for strong electrolyte solutions Geochimica et Cosmochimica Acta 58, 4353-4362.

Zuddas, P., Mucci, A., 1998. Kinetics of calcite precipitation from seawater. II. The influence of the I. Geochimica et Cosmochimica Acta 62, 757-766.

VITA

Name:	David Wallace Finneran
Address:	Department of Oceanography Texas A&M University MS 3146 College Station, TX 77843-3146
Email Address:	finneran@ocean.tamu.edu
Education:	B.Sci., Chemistry, University of Delaware, 2002 M.Sci., Chemistry, University of Delaware, 2004 Ph.D., Oceanography, Texas A&M University, 2010